

This file is part of the following work:

**Tamanna, Nafisa (2020) *Use of waste glass as aggregate and cement replacement in concrete*. PhD Thesis, James Cook University.**

Access to this file is available from:

<https://doi.org/10.25903/nft4%2D8q67>

© 2020 Nafisa Tamanna.

The author has certified to JCU that they have made a reasonable effort to gain permission and acknowledge the owners of any third party copyright material included in this document. If you believe that this is not the case, please email

[researchonline@jcu.edu.au](mailto:researchonline@jcu.edu.au)

# **Use of Waste Glass as Aggregate and Cement Replacement in Concrete**

**Thesis submitted by**

**Nafisa Tamanna**

**Bachelor of Science in Civil Engineering**

**(Rajshahi University of Engineering and Technology, Bangladesh)**

**Master of Science in Civil Engineering**

**(University Malaysia Sarawak, Malaysia)**

**April 2020**

**For the degree of Doctor of Philosophy (PhD)**

**In the college of Science and Engineering**

**James Cook University**



## **Acknowledgment**

First and foremost, I am profoundly thankful to almighty Allah for giving me the strength, blessings and the patience to complete this research work successfully.

I thank my primary supervisor, Associate Professor Rabin Tuladhar, for his continuous support, fruitful guidance and insightful discussions throughout this research. I am grateful to him for his supervision and expert engineering intuition, as well as encouragement in the completion of this thesis.

I thank my secondary supervisor, Associate Professor Nagaratnam Sivakugan, for his editorial advice and co-authoring of my journal articles. Thanks are also extended to Dr George Vamvounis for his valuable time and allowing me to use his laboratory for thermogravimetric analysis.

I thank Pioneer North Queensland (PNQ) and Cairns Regional Council for providing recycled glass sand and other materials throughout the study, and I thank Nathan Avosa, Joshua Flanders, Dustin Peacocke, Joshua Lancini and Brendan Hall for their support during experiments.

My sincere appreciation goes to Mr Shaun Robinson, Mr Troy Poole, Mrs Ruilan Liu and Dr Shane Askew for their assistance regarding sample preparation and laboratory testing, also to Ms Melissa Norton and other administrative staff members at the College of Science and Engineering, James Cook University (JCU), for their sincere and wholehearted support.

I acknowledge the Advanced Analytical Centre at JCU for permitting access to X-ray diffraction, scanning electron microscopy and energy-dispersive spectroscopy. I thank ALS Minerals and Geochemistry, Townsville, for the pulverisation of crushed glass into powder form.

I am indebted to the Graduate Research School and College of Science and Engineering, JCU, Townsville, for the opportunity and financial assistance for the duration of my research.

My thanks are also extended to the Bangladeshi community here in Townsville for accepting me as a family member. I also thank my fellow researchers and friends for making my stay in Townsville smooth and enjoyable.

Lastly, but certainly not least, I owe much especially to my beloved parents, husband, and all my family members for their unconditional support, encouragement and sacrifices throughout my academic endeavours.

## **Statement of the contribution of others**

### **Editorial assistance and contribution to co-authored publications**

Associate Professor Rabin Tuladhar

Associate Professor Nagaratnam Sivakugan

### **Scholarship**

James Cook University Postgraduate Research Scholarship (JCUPRS)

### **Research Funding**

Postgraduate research and conference grants (2017 and 2018) from College of Science and Engineering, James Cook University.

Doctoral Completion Grant (2019) from College of Science and Engineering, James Cook University.

### **Materials Support**

Pioneer North Queensland (PNQ)

Cairn Regional Council

## **Abstract**

Over a million tonnes of glass waste is generated in Australia every year. However, due to the low market value of recycled glass and high transport cost, almost 60% of glass waste is sent to landfill or stockpiled in warehouses around the country. Besides the presence of contaminants such as plastic caps, metals, and paper, inconsistency in the chemical composition of different type of glasses, as well as difficulty in sorting different coloured glasses, make the recycling process difficult. Use of waste glass in concrete and mortar has been tried in the past few years to replace coarse aggregate, sand and cement. Several researchers have studied the use of waste glass larger than 4.75 *mm* as coarse aggregate replacement in concrete since the 1960s.

Use of coarse glass aggregate reduced compressive strength as content increased, and mixed results were reported on the effect of glass aggregates on the workability of concrete due to the flat, smooth and elongated nature of glass particles. Furthermore, alkali-silica reaction (ASR) has been another major issue encountered while using waste glass as coarse aggregate replacement in concrete. As deleterious cracks were noticed with the use of coarse glass aggregate, several studies have been conducted to investigate the potential of using recycled crushed glass as a fine aggregate replacement. However, mixed outcomes are reported on the mechanical and durability properties of hardened concrete with the change in glass size. Moreover, when the glass is smaller, a pozzolanic reaction can occur between glass particles and calcium hydroxide instead of a deleterious ASR reaction. Being amorphous and having prominent quantities of silica, crushed glass shows pozzolanic properties. Pozzolanic properties of glass powder was reported to increase with reduced particle size and resulted in a delayed strength gain of concrete.

This research introduces a sustainable way of recycling glass waste as a partial sand and cement replacement in concrete. A mixed-coloured soda-lime glass was supplied by Cairns Regional

Council in Queensland; Australia was used in this study to produce concrete with a target characteristic strength of 32 *MPa*. Chemical composition and physical properties of glass were evaluated to determine its suitability for use in concrete. A series of tests was conducted to determine the fresh and hardened properties of concrete, including its durability characteristics to verify the performance of concrete using recycled waste glass sand (RGS) and recycled glass powder (RGP) in concrete. Concrete produced by replacing natural river sand with 20%, 40% and 60% of RGS showed a significant improvement in strength. RGS concrete also showed improved resistance to chloride ion penetration. RGS addition also significantly reduced expansion caused by the alkali-silica reaction.

Concrete with RGP as a partial cement replacement in concrete showed an improvement in strength over time, like fly ash. Using RGP significantly improved resistance against chloride penetration with increasing glass powder content. Furthermore, RGP also met the relative strength as per Australian Standard requirement to be considered as a supplementary cementitious material. Microstructural analysis was carried out to evaluate the pozzolanic properties of RGP. The test results showed that pozzolanic material does not show its effects early and hence becomes more prominent later.

The environmental benefits of using recycled glass to produce 1  $m^3$  concrete were assessed in the Australian context. The use of RGS in concrete as a sand substitute did not have a high environmental footprint. However, global warming effects was reduced consequently, as a part of cement was replaced by RGP. RGS concrete and RGP concrete can reduce ozone layer depletion up to 14% and 22%, respectively. Compared with conventional concrete, both RGS and RGP concrete have significant influences on reducing the environmental impact caused by concrete production.

A footpath 108 *m* long and 2 *m* wide was cast at Progress Road, White Rock State School in Cairns, Queensland, to demonstrate the use of RGS in concrete as coarse sand replacement. Concrete with 40% RGS achieved the characteristic strength of 32 *MPa* at 28 days. The footpath has been used successfully for a year.

The successful application of using recycled glass in concrete can reduce sand dredging and reduce cement production along with the reduction of glass waste going into landfill sites

## Table of Contents

Acknowledgment.....	ii
Statement of the contributions of others.....	iv
Abstract.....	v
Table of Contents.....	viii
List of Tables.....	xiv
List of Figures.....	xvi
Nomenclature.....	xxii
<b>Chapter 1: Introduction.....</b>	<b>1</b>
1.1 Background.....	1
1.2 Research objectives.....	5
1.3 Thesis organisation.....	6
<b>Chapter 2: A review of the use of waste glass as aggregate and cement replacement in concrete.....</b>	<b>8</b>
2.1 Overview of construction materials.....	8
2.1.1 Concrete.....	8
2.1.2 Aggregates.....	9
2.1.2.1 Manufactured sand.....	9
2.1.3 Cement.....	10
2.1.3.1 Supplementary cementitious materials.....	11
2.1.4 Waste glass.....	14
2.1.4.1 Waste glass recycling rate.....	14
2.2 Waste glass as construction material.....	18
2.2.1 Waste glass as coarse aggregate replacement.....	18

2.2.1.1 Fresh properties of concrete.....	18
2.2.1.2 Mechanical strength of concrete.....	20
2.2.1.3 Alkali-silica reaction and ASR mechanism.....	21
2.2.2 Waste glass as fine aggregate.....	24
2.2.2.1 Fresh concrete properties.....	24
2.2.2.2 Mechanical strength.....	27
2.2.2.3. Durability of concrete.....	35
2.2.3 Waste glass as cement replacement.....	44
2.2.3.1 Fresh properties.....	44
2.2.3.2 Mechanical strength.....	47
2.2.3.3 Concrete durability.....	49
2.3 Life cycle assessment.....	60
2.3.1 Goal and scope definition.....	62
2.3.2 Life cycle inventory analysis (LCI).....	62
2.3.3 Life cycle impact assessment (LCIA).....	63
2.3.4 Interpretation of results.....	63
2.3.5 Environmental life cycle assessment of concrete.....	63
2.3.5.1 Cement production and life cycle assessment of cement.....	64
2.3.5.2 Life cycle assessment of aggregate.....	67
2.4 Summary.....	68
<b>Chapter 3: Performance of recycled waste glass sand as partial replacement of sand in concrete.....</b>	<b>70</b>
3.1 Experimental procedures.....	70
3.1.1 Materials.....	70
3.1.2 Production of recycled crushed glass.....	71

3.1.3 Concrete mix design.....	73
3.1.4 Experimental methods.....	74
3.2 Results and discussion.....	83
3.2.1 Characterisation of crushed glass sand as aggregate.....	83
3.2.1.1 Particle size distribution.....	83
3.2.1.2 Detection of sugar.....	84
3.2.2 Fresh properties of concrete.....	85
3.2.2.1 Slump test.....	85
3.2.2.2 Density of concrete.....	86
3.2.3 Mechanical properties of concrete.....	86
3.2.3.1 Compressive strength of concrete.....	86
3.2.3.2 Flexural and tensile strength of concrete.....	88
3.2.4 Durability of concrete.....	89
3.2.4.1 Rapid chloride penetration test.....	89
3.2.4.2 Alkali-silica reaction test.....	91
3.3 Conclusion.....	93
<b>Chapter 4: Sustainable use of recycled glass powder as cement replacement in concrete...</b>	<b>95</b>
4.1 Experimental programs.....	95
4.1.1 Material.....	95
4.1.2 Mix proportion and sample preparation.....	96
4.1.3 Test methods.....	98
4.2 Results and discussion.....	101
4.2.1 Characterisation of materials.....	101
4.2.2 Fresh concrete properties.....	105
4.2.2.1 Slump test.....	105

4.2.2.2 Density.....	106
4.2.3 Hardened concrete properties.....	107
4.2.3.1 Variation of compressive strength.....	107
4.2.3.2 Flexural and tensile strength of concrete.....	108
4.2.3.3 Rapid chloride permeability test (RCPT).....	109
4.2.3.4. Relative water requirement.....	110
4.2.3.5 Relative strength.....	111
4.3 Conclusions.....	112
<b>Chapter 5: Microstructure analysis of recycled glass sand and recycled glass powder.....</b>	<b>114</b>
5.1 Experimental procedure.....	114
5.1.1 Materials.....	114
5.1.2 Mix Design.....	115
5.1.3 Experimental methods.....	117
5.1.3.1 Thermogravimetric analysis.....	117
5.1.3.2 Scanning electron microscope (SEM).....	119
5.1.3.3 X-ray diffraction (XRD).....	121
5.2 Results and discussion.....	122
5.2.1 Microstructure of alkali-silica reaction for RGS mix.....	122
5.2.1.1 Thermogravimetric analysis.....	122
5.2.1.2 Scanning electron microscope.....	123
5.2.2 Microstructure of glass powder for RGP paste.....	127
5.2.2.1 Thermogravimetric analysis.....	127
5.2.2.2 X-ray diffraction (XRD) results for RGP paste specimens.....	129
5.2.2.3 Scanning electron microscope results for RGP samples .....	132
5.2.2.4 Energy-dispersive spectroscopy (EDS) results from RGP paste specimens.....	137

5.3 Conclusion.....	140
<b>Chapter 6: Environmental benefits of using recycled glass in concrete.....</b>	<b>142</b>
6.1 Methodology.....	142
6.1.1 Goal, functional unit and system boundaries.....	143
6.1.1.1 Goal and functional unit.....	143
6.1.1.2 System boundaries.....	144
6.1.2 Life cycle inventory.....	147
6.1.3 Life cycle impact assessment.....	147
6.1.4 Sensitivity and uncertainty analysis .....	148
6.2 Results and discussion .....	148
6.2.1 Recycled glass sand (RGS) as sand replacement.....	148
6.2.1.1 Sensitivity analysis of RGS.....	152
6.2.1.2 Uncertainty analysis of RGS.....	158
6.2.2 Recycled glass powder (RGP) as cement replacement.....	160
6.2.2.1 Sensitivity analysis of RGP.....	165
6.2.2.2 Uncertainty analysis of RGP.....	171
6.3 Conclusion.....	173
<b>Chapter 7: Application of recycled waste glass sand in concrete footpath.....</b>	<b>175</b>
7.1 Concrete footpath.....	175
7.2 Concrete casting.....	177
7.3 Results and discussion.....	182
7.3.1 Slump test.....	182
7.3.2 Compressive strength.....	183
7.4 Conclusion.....	184
<b>Chapter 8: Conclusions and recommendations.....</b>	<b>185</b>

8.1 Conclusions.....	185
8.2 Recommendations.....	188
References.....	190

## List of Tables

Table 2.1 Chemical composition of cement, fly ash, slag, silica fume and glass powder (Avosa, 2016; Amin and Abu el-hassan, 2015).....	13
Table 2.2 Chemical composition of soda-lime glass (Shi and Zheng, 2007).....	14
Table 2.3 Glass waste production and recycling in USA, 2010 (Environmental Protection Agency, 2010).....	16
Table 2.4 Glass recycling rates in Australia (NRRS, 2017).....	17
Table 2.5 Compressive strength of recycled glass sand in concrete.....	30
Table 2.6 Overview of rapid chloride penetration test of glass sand concrete as aggregate replacement.....	42
Table 2.7 Influence of different parameters on rapid chloride penetration test.....	51
Table 2.8 Summary of CO <sub>2</sub> emissions (Flower and Sanjayan, 2007).....	65
Table 2.9 Life-cycle environmental impacts of conventional and glass powder concrete (Jiang et al, 2014).....	67
Table 2.10 Emission and energy consumption to produce 1 metric tonne of crushed glacier rock with rock crusher (Landfield and Karra, 2000).....	68
Table 3.1 Properties of natural aggregate supplied by Pioneer North Queensland.....	71
Table 3.2 Materials content for 1m <sup>3</sup> of concrete mixture.....	76
Table 3.3 Chloride ion penetrability based on charge passed (ASTMC1202, 2012).....	81
Table 3.4 Mix design of mortar mixes for three ASR prism bars (AS1141.60.1, 2014).....	82
Table 3.5 Grading requirements of glass sand as manufactured fine aggregate.....	82
Table 3.6 Aggregate reactivity classification based on AS 1141.60.1 (AS1141.60.1, 2014).....	84

Table 3.7 Test program with relevant standards.....	84
Table 3.8 Slump and density of control concrete, concrete with RGS.....	88
Table 3.9 Percentage of indirect tensile strength to compressive strength at 28 days.....	91
Table 4.1 Materials content for 1 $m^3$ of concrete mix.....	97
Table 4.2 Mix proportion of mortar for three prism bars of 40 x 40 x 160 $mm$ (AS3583.6, 2018).....	98
Table 4.3 Chemical and physical characteristics of cement, fly ash and RGP.....	102
Table 4.4 Slump and density of control, RGP and fly ash concrete.....	106
Table 4.5 Relative water requirement of RGP.....	111
Table 5.1 Mix design of cement paste for cylinder of 50 $mm$ diameter and 35 $mm$ height.....	115
Table 5.2 Average atomic composition of mortar samples measured by EDS.....	116
Table 5.3 Elemental analysis of spectrum.....	121
Table 5.4 Average atomic composition of mortar samples measured by EDS.....	127
Table 6.1 Travel distance for each material.....	145
Table 7.1 Materials content for 1 $m^3$ of concrete mixture used in field trials.....	176
Table 7.2 Slump test results of control concrete and concrete using RGS.....	183

## List of Figures

Figure 2.1 Typical components of concrete.....	9
Figure 2.2 Bohle quarry crusher dust waste (Gersekowski, 2014).....	10
Figure 2.3 Cement, fly ash, silica fume and ground granulated blast-furnace slag (Forum, 2017).....	13
Figure 2.4 Accumulation of glass bottles (Boehlke, 2018).....	16
Figure 2.5 Slump of concrete mixtures containing fine glass powder, coarse glass powder and fine-coarse glass powder (Terro, 2006) .....	20
Figure 2.6 Unit weight of concrete mixtures containing glass powder as cement replacement and aggregate replacement (Afshinnia and Rangaraju, 2016).....	20
Figure 2.7 Silica tetrahedron.....	22
Figure 2.8 ASR expansion of mortar bar for different ages (Shayan and Xu, 2004).....	24
Figure 2.9 Decreasing ratios in fresh density (Ismail and Al-Hashmi, 2009).....	26
Figure 2.10 Compressive strength of glass sand for 7 and 28 days (Pereira de Oliveira et al., 2008).....	28
Figure 2.11 Scanning electron microscope of clear glass (Du and Tan, 2013).....	34
Figure 2.12 Effect of particle size on ASR expansion (Du and Tan, 2014b).....	35
Figure 2.13 ASR expansion of waste glass (Ismail and Al-Hashmi, 2009).....	37
Figure 2.14 Expansion of mortar bar with (a) brown glass (b) green glass (Park and Lee, 2004).....	38
Figure 2.15 Slump of concretes with glass powder as cement replacement (Khatib et al., 2012).....	45
Figure 2.16 Compressive strength test result glass powder (Nassar and Soroushian, 2012).....	48

Figure 2.17 Mortar bar expansion versus time for samples containing glass powder as a cement replacement (Afshinnia and Rangaraju, 2015).....	53
Figure 2.18 ASR expansion of mortar bar containing glass sludge and fly ash (Kim et al., 2015).....	54
Figure 2.19 ASR expansion of waste glass sand concrete with 60% slag replacing cement (Du and Tan, 2014a).....	56
Figure 2.20 Strength activity index of mortar cubes containing 70 $\mu m$ glass powder (Afshinnia and Rangaraju, 2015b).....	57
Figure 2.21 Calcium hydroxide content of paste modified with glass powder (Aliabdo et al., 2016).....	59
Figure 2.22 Life cycle assessment, considering whole life cycle phases.....	61
Figure 2.23 Life cycle assessment phases (Vieira et al., 2016).....	63
Figure 3.1 Recyclable glass items after sorting procedures.....	72
Figure 3.2 Glass crushing machine (a) imploder, (b) shearing unit, and (c) sanding unit....	72
Figure 3.3 Fine glass sand (3 mm) used as a partial coarse sand replacement.....	73
Figure 3.4 (a) Copper (II) sulphate pentahydrate crystals and colourless solution of aqueous potassium sodium tartrate, (b) Fehling's solution.....	75
Figure 3.5 (a) Compressive strength, (b) tensile strength, and (c) flexural strength set up...	77
Figure 3.6 (a) Specimens coated with epoxy, (b) vacuum saturation conditioning, and (c) RCPT cells set up.....	79
Figure 3.7 (a) Mortar bar prism moulds with gauge stud, and (b) ASR comparator readings.....	81
Figure 3.8 Particle size distribution curves of natural coarse sand, and crushed glass sand...	84
Figure 3.9 Procedures to determine the presence or absence of sugar in aggregate.....	85
Figure 3.10 Compressive strength development of concrete with RGS.....	88

Figure 3.12 Flexural and tensile strength of concrete with RGS.....	89
Figure 3.13 RCPT results of concrete with river sand and RGS at 28 days and 56 days.....	90
Figure 3.14 ASR expansion of mortar with crushed glass.....	92
Figure 3.15 SEM of crushed glass sand particle.....	93
Figure 4.1 (a) Crushed glass (3 mm size) at MRF site, (b) glass powder (45 $\mu$ m size).....	96
Figure 4.2 (a) X-ray fluorescence (XRF), (b) particle size analyser, (c) scanning electron microscope, and (d) X-ray diffraction analyser.....	99
Figure 4.3 (a) Flow table, (b) Prismatic mould of 40 x 40 x 160 mm.....	101
Figure 4.4 CaO-Al <sub>2</sub> O <sub>3</sub> -SiO <sub>2</sub> ternary diagram of cement, fly ash, and glass powder.....	103
Figure 4.5 Cumulative particle size distribution curve of cement, fly ash, and glass powder.....	104
Figure 4.6 Scanning electron microscope of (a) cement, (b) RGP, and (c) fly ash.....	104
Figure 4.7 XRD pattern for cement, and RGP.....	105
Figure 4.8 Compressive strength of concrete with RGP, and fly ash blend.....	107
Figure 4.9 Flexural strength of concrete with RGP and fly ash blend.....	109
Figure 4.10 RCPT results of concrete at 28 days and 56 days.....	110
Figure 4.11 Strength of RGP mortar relative to control mortar at 28 days.....	112
Figure 5.1 Hardened cement sample.....	116
Figure 5.2 SEM samples in isopropanol .....	117
Figure 5.3 Thermal analyser SDT 650.....	119
Figure 5.4 Alumina crucible.....	119
Figure 5.5 (a) Carbon coater, (b) polished samples.....	120
Figure 5.6 SEM image and corresponding EDS analysis.....	121
Figure 5.7 Calcium hydroxide content in mortar bar (ASR) at 21 days.....	123
Figure 5.8 SEM of ASR control mortar sample.....	124

Figure 5.9 SEM of (a) 40 RGS and (b) 60 RGS ASR mortar sample.....	125
Figure 5.10 Si/Ca vs Al/Ca ratio in control and 20 RGS (ASR) mortar.....	126
Figure 5.11 Si/Ca vs Al/Ca ratio in 40 RGS and 60 RGS (ASR) mortar.....	126
Figure 5.12 Calcium hydroxide content cement paste and RGP paste.....	128
Figure 5.13 XRD pattern of control cement paste at 1, 7, 28, 56 and 90 days.....	130
Figure 5.14 XRD pattern of 10 RGP and 20 RGP cement paste at 1, 7, 28, 56 and 90 days.....	131
Figure 5.15 XRD pattern of 30 RGP and 40 RGP cement paste at 1, 7, 28, 56 and 90 days.....	132
Figure 5.16 SEM image of control cement paste at 90 days.....	133
Figure 5.17 SEM image of 10 RGP cement paste at 90 days.....	134
Figure 5.18 SEM image of 20 RGP cement paste at 90 days.....	135
Figure 5.19 SEM image of 30 RGP cement paste at 90 days.....	136
Figure 5.20 SEM image of 40 RGP cement paste at 90 days.....	136
Figure 5.21 2 D scatter plot of EDS analyses of control cement paste at 90 days.....	138
Figure 5.22 2 D scatter plot of EDS analyses of 10 RGP and 20 RGP cement paste at 90 days.....	139
Figure 5.23 2 D scatter plot of EDS analyses of 30 RGP and 40 RGP cement paste at 90 days.....	140
Figure 6.1 System boundaries of conventional concrete.....	145
Figure 6.2 System boundaries of concrete modified with RGS as sand replacement.....	146
Figure 6.3 System boundaries of concrete modified with RGP as cement replacement.....	147
Figure 6.4 Life cycle impact categories associated with 1 m <sup>3</sup> RGS concrete.....	150
Figure 6.5 Major damage categories for 1 m <sup>3</sup> concrete.....	151
Figure 6.6 Relative change of global warming for control concrete.....	153
Figure 6.7 Relative change of global warming for control concrete.....	153

Figure 6.8 Relative change of ozone depletion for control concrete.....	154
Figure 6.9 Relative change of ozone depletion for 60 RGS concrete.....	155
Figure 6.10 Relative change of eutrophication for control concrete.....	156
Figure 6.11 Relative change of eutrophication for 60 RGS concrete.....	156
Figure 6.12 Relative change of fossil fuel for control concrete.....	157
Figure 6.13 Relative change of fossil fuel for 60 RGS concrete.....	158
Figure 6.14 Uncertainty analysis of 1 m <sup>3</sup> control concrete (A) minus 1 m <sup>3</sup> 20 RGS concrete (B).....	159
Figure 6.15 Uncertainty analysis of 1 m <sup>3</sup> control concrete (A) minus 1 m <sup>3</sup> 40 RGS concrete (B).....	160
Figure 6.16 Uncertainty analysis of 1 m <sup>3</sup> control concrete (A) minus 1 m <sup>3</sup> 60 RGS concrete (B).....	160
Figure 6.17 Life cycle impact categories associated with 1 m <sup>3</sup> RGP concrete.....	161
Figure 6.18 Global warming potential of concrete with RGP.....	162
Figure 6.19 Ozone depletion of concrete with RGP.....	163
Figure 6.20 Eutrophication of concrete with RGP.....	164
Figure 6.21 Land and water use of concrete with RGP.....	165
Figure 6.22 Relative change of global warming for control concrete.....	166
Figure 6.23 Relative change of global warming for 30 RGP concrete.....	167
Figure 6.24 Relative change of ozone depletion for control concrete.....	167
Figure 6.25 Relative change of ozone depletion for 30 RGP concrete.....	168
Figure 6.26 Relative change of eutrophication for control concrete.....	168
Figure 6.27 Relative change of eutrophication for 30 RGP concrete.....	169
Figure 6.28 Relative change of land use for control concrete.....	169
Figure 6.29 Relative change of land use for 30 RGP concrete.....	170

Figure 6.30 Relative change of water use for control concrete.....	170
Figure 6.31 Relative change of water use for 30 RGP concrete.....	171
Figure 6.32 Uncertainty analysis of 1 m <sup>3</sup> control concrete (cement) (A) minus 1 m <sup>3</sup> 10 RGP concrete (B).....	172
Figure 6.33 Uncertainty analysis of 1 m <sup>3</sup> control concrete (cement) (A) minus 1 m <sup>3</sup> 20 RGP concrete (B).....	172
Figure 6.34 Uncertainty analysis of 1 m <sup>3</sup> control concrete (cement) (A) minus 1 m <sup>3</sup> 30 RGP concrete (B).....	173
Figure 7.1 Crushed glass (3 mm size) at MRF site, Cairns.....	176
Figure 7.2 Reinforcing mesh for concrete footpath.....	177
Figure 7.3 Form work and reinforcement arrangement prior to concrete pour.....	178
Figure 7.4 Ready mix concrete pouring.....	179
Figure 7.5 Fresh concrete for compressive strength.....	179
Figure 7.6 Screeding of the concrete mix.....	180
Figure 7.7 Expansion joint.....	180
Figure 7.8 Curing of freshly placed concrete.....	181
Figure 7.9 Footpath in the fresh stage.....	181
Figure 7.10 RGS 40 – TMR concrete footpath.....	182
Figure 7.11 Slump test.....	183
Figure 7.12 Compressive strength of control concrete and concrete using RGS.....	184

## **Nomenclature**

<b>AS</b>	Australian standard
<b>ASR</b>	Alkali-silica reaction
<b>ASTM</b>	American society for testing and materials
<b>BSE</b>	Backscattered electrons
<b>C-A-S-H</b>	Calcium aluminium silicate hydrates
<b>CCAA</b>	Cement Concrete Aggregate Australia
<b>C-S-H</b>	Calcium silicate hydrate
<b>EDS</b>	Energy-dispersive X-ray spectroscopy
<b>FNQROC</b>	Far North Queensland Regional Organisation of Councils
<b>ISO</b>	International Organization for Standardization
<b>ITZ</b>	Interfacial transition zone
<b>JCU</b>	James Cook University
<b>LCA</b>	Life cycle assessment
<b>LCI</b>	Life cycle inventory data
<b>LCIA</b>	Life cycle impact assessment
<b>MRF</b>	Materials Recovery Facility
<b>NZS</b>	New Zealand Standards
<b>PNQ</b>	Pioneer North Queensland
<b>PSD</b>	Particle size distribution
<b>RCPT</b>	Rapid chloride penetration test
<b>RGP</b>	Recycled glass sand
<b>RGS</b>	Recycled glass powder
<b>TMR</b>	Department of Transport and Main Roads
<b>TGA</b>	Thermogravimetric analysis

<b>SCM</b>	Supplementary cementitious material
<b>SE</b>	Secondary electrons
<b>SEM</b>	Scanning electron microscope
<b>XRD</b>	X-ray diffraction analysis
<b>XRF</b>	X-ray fluorescence

# Chapter 1: Introduction

## 1.1 Background

The construction sector experiences a growing demand for concrete due to rapid infrastructure development. Growing infrastructure development consumes concrete about 25 million cubic metres of concrete each year in Australia (Tamanna et al., 2017) which leads to massive extraction of natural resources such as natural aggregates. Sand and gravel are the most extracted natural resources in the world corresponding to 79% or 28.6 gigatonnes per year in 2010 (Torres et al., 2017). Natural river sand has been used as a fine aggregate in concrete construction for several decades. In spite of the abundance of sand on the earth's surface, it is a finite natural resource that can soon be depleted. Excessive extraction of sand not only results in sand scarcity but also harms marine ecosystems, water supply and turbidity, marine food sources and climate. Excessive dredging for sand can aggravate damage due to flood, tsunami and storm surge because of erosion of shoreline and riverbanks. It also affects ground water supplies as a result of lowering the water table and saltwater intrusion, and causes damage to river embankments, bridge piers, and civil infrastructure (Torres et al., 2017).

On the other hand, the concrete manufacturing process produces substantial environmental impacts, mainly due to the carbon footprint associated with the cement manufacturing process. Cement, a key ingredient in concrete, is very energy-intensive to produce and is responsible for about 85% of the total embodied energy of concrete (Sivakugan et al., 2017). About 60% of the total CO<sub>2</sub> associated with the cement manufacturing process is emitted during the calcination of limestone (CaCO<sub>3</sub>), and the remaining 40% of the emissions comes from burning fossil fuel to generate energy during the cement manufacturing process. Cement production accounts for more than 8% of global CO<sub>2</sub> emissions (Andrew, 2018). One tonne of cement production releases approximately one tonne of CO<sub>2</sub> into the atmosphere (Sprince et al., 2011).

Concrete industries around the world have long been using supplementary cementitious materials such as fly ash, silica fume, and natural pozzolans as a partial cement replacement in concrete (Sivakugan et al., 2017). Recently, researchers have also tried using other recycled materials, for instance, recycled glass powder (RGP) as a cement replacement in concrete (Afshinnia and Rangaraju, 2016; Islam et al., 2017; Kamali and Ghahremaninezhad, 2015; Soliman and Tagnit-Hamou, 2016; Rahma et al., 2017).

Glass is widely used as a packaging material throughout the world. This material was discovered more than 5000 years ago and has been produced for several applications since then. Glass is known as a 100% recyclable material and can be recycled repeatedly without degradation in quality (Sobolev et al., 2007). However, presence of contaminants such as a plastic cap, metals, paper, and inconsistency in the chemical composition of different type of glasses, as well as difficulty in sorting different coloured glasses, make the recycling process difficult (Afshinnia and Rangaraju, 2016). Furthermore, in Australian context, the lack of local recycling plants coupled with high transportation costs makes the recycling process expensive.

Use of waste glass in concrete and mortar has been tried in the past few years as a partial replacement of coarse aggregate, sand and cement. Several researchers have studied the use of waste glass larger than 4.75 *mm* as a coarse aggregate replacement in concrete since the 1960s. Use of coarse glass aggregate decreased compressive strength with the increase in glass content, and mixed results were reported on the effect of glass aggregates on the workability of concrete (Schmidt and Saia, 1963; Johnston, 1974; Topçu and Canbaz, 2004; Terro, 2006; Yu, 2016; Pauzi et al., 2019). Flat, smooth and elongated glass particles resulted in low strength and workability of concrete. Furthermore, the alkali-silica reaction (ASR) is another major issue encountered while using waste glass as coarse aggregate replacement in concrete. ASR occurs between amorphous silica in glass and alkali in cement producing expansive alkali-silica gel. In the presence of moisture, alkali-silica gel produced can absorb moisture from

surroundings and expand inside the microcracks in aggregates. ASR expansion leads to cracking in the concrete (Du and Tan, 2014b), which makes the concrete more vulnerable to chloride attack. Cracking in concrete due to ASR expansion was found more pronounced when glass particle sizes greater than 19 mm were used in concrete (Johnston, 1974). Excessive cracking was also found in the study of using different forms of glass as coarse aggregate with cement (Pike and Hubbard, 1957). ASR expansion was found to be closely related to the proportion of glass particles in the mix. For instance, a study by Shayan and Xu (2004) found that the use of coarse glass aggregate greater than 30% resulted in an increase in ASR even with low alkali cement.

As deleterious cracks were noticed with the use of coarse glass aggregate, several studies have been conducted to investigate the potential of using recycled crushed glass as a fine aggregate replacement (Ashish, 2018; Sharifi et al., 2013; Du and Tan, 2013; De Castro and De Brito, 2013). Glass sand concrete improved fresh concrete properties due to the smooth surface and relatively low water absorption properties of glass (Zhao et al., 2013). However, mixed outcomes have been reported on the mechanical and durability properties of hardened concrete with the change in glass size (Malik et al., 2013; Ali and Al-Tersawy, 2012; Du and Tan, 2013). Minor cracks can form at the edge of glass aggregates during crushing operations. In the presence of moisture, ASR expansion gels may form on the cracked surface of aggregates leading to ASR cracking of concrete (Du and Tan, 2014b). An increase in glass content as sand replacement was also found to increase ASR expansion (Ling and Poon, 2011; Taha and Nounu, 2009; Limbachiya, 2009; Yuksel et al., 2013; Degirmenci et al., 2011; Topçu and Canbaz, 2004; Du and Tan, 2013; Lam et al., 2007; Ling and Poon, 2012). Degirmenci et al. (2011) reported that concrete with 100% replacement of natural sand with recycled crushed glass exceeded the 0.10% ASR expansion limit at 21 days, which is considered potentially deleterious expansion. ASR expansion was found to increase with the increase in glass sand

size (Du and Tan, 2013; Lee et al., 2011). The minimum and maximum expansion occurred at glass particle size 0.150 mm and 2.36 mm, respectively. When glass is smaller, a pozzolanic reaction can occur between glass particles and calcium hydroxide instead of a deleterious ASR reaction.

Glass is amorphous and has prominent quantities of silica, and hence, finely ground crushed glass shows pozzolanic properties (Tamanna et al., 2016; Tamanna et al., 2017; Tamanna et al., 2018). The pozzolanic properties of glass are found to be influenced by the particle size distribution of glass powder (Shao et al., 2000). The silica (silicate ions) is detached from glass by hydroxyl ions in the pore solution and combines with calcium from portlandite to form calcium silicate hydrate. Glass powder with particle size 300  $\mu\text{m}$  or smaller has been reported to reduce ASR expansion in concrete (Vijaykumar et al., 2013). When finer glass particles are used in concrete results in non-expansive pozzolanic reactions, these produce calcium silicate hydrate (C-S-H) with a low calcium-silicate ratio (Rahma et al., 2017). Pozzolanic properties of glass powder are reported to increase with reduced particle size and result in a delayed strength gain of concrete (Shao et al., 2000; Shi et al., 2005; Khmiri et al., 2012; Patil and Sangle, 2013; Nassar and Soroushian, 2011; Gunalaan and Kanapathy, 2013; Vijaykumar et al., 2013; Soliman and Tagnit-Hamou, 2016). The properties of recycled glass, and hence its effects on concrete, depend on the type of waste glass used. The nature of glass reactivity depends on the chemical composition of the raw materials used and differs slightly for each glass type (Vaitkevičius et al., 2014). Borosilicate glass such as pyrex glass were found to be more reactive than soda-lime glass. Borosilicate glass from pharmaceutical containers cullet had a tendency to expand. In addition, the amount of fluorescent lamp glass negatively influences the pozzolanic reaction. The high content of  $\text{Na}_2\text{O}_{\text{eq}} + \text{PbO}$  and the low content of  $\text{CaO} + \text{MgO}$  causes a high degree of sodium dissolution and is involved in gel formation (Bignozzi et al., 2015). The ASR expansion of treated funnel glass was found to be relatively

higher than crushed beverage glass due to the higher solubility of treated funnel glass (Ling and Poon, 2012). A large amount of dissolved glass was available in the solution to form ASR gel (Ling and Poon, 2012; Saccani and Bignozzi, 2010). Using lead glass in cement and concrete can leach out lead into the environment creating serious soil and ground water pollution as it possesses high lead content. For the successful use of recycled glass in concrete for industrial applications, it is therefore important to characterise the physical and chemical properties of the recycled glass collected by local councils. The effects of replacement levels of cement with recycled glass on the strength and durability properties of concrete need to be assessed as well. In this regard, this study investigates the feasibility of using coloured soda-lime glass, collected by Cairns Regional Council in northern Australia, as a partial sand and cement replacement in concrete.

A comprehensive life-cycle assessment (LCA) is essential to get a complete picture of the environmental impacts of concrete production. The comprehensive LCA consists of entire life-cycle phases, including raw material extraction, manufacturing, construction, operation and demolition. It is essential to define aims, function units and system boundaries. This research focuses on the LCA of recycled glass in concrete, which is at present either in landfill, stockpiled in warehouses or illegally dumped. The study addresses the environmental benefits of using mixed-coloured soda-lime glass collected by Cairns Regional Council as a sand and cement substitution in concrete. A cradle to gate life-cycle impact assessment is used, which includes up to the production of 1m<sup>3</sup> concrete. The results are compared with the control concrete.

## **1.2 Research objectives**

This research aims to develop a concrete mix using crushed/ground glass waste as a partial sand/cement replacement. The research aims to produce concrete with a characteristics mean

strength of 32 *MPa*. The study has been conducted in collaboration with Cairns Regional Council, James Cook University (JCU) and Pioneer North Queensland Concrete (PNQ). The main objectives are:

1. To investigate the chemical composition and physical properties of glass to determine its suitability for use in concrete;
2. To develop optimum concrete mixes with waste glass as a sand and cement substitute and to verify the performance of concrete against all relevant Australian design standards;
3. To quantify the pozzolanic properties of recycled crushed glass and to evaluate any detrimental effects of crushed glass in concrete and suggest preventive measures to overcome those limitations;
4. To trial the use of concrete with crushed glass in field applications and to quantify the environmental benefits of using waste glass in concrete through a comprehensive LCA.

### **1.3 Thesis organisation**

This thesis consists of eight chapters.

**Chapter 1** introduces the background of using waste glass in concrete research and provides the aims and objectives of this research.

**Chapter 2** presents the overview of construction materials, recent literature on the use of recycled glass in concrete as sand and cement substitute, and an environmental life-cycle assessment of concrete.

**Chapter 3** describes the use of mixed-coloured soda-lime glass supplied by Cairns Regional Council as a sand replacement in concrete. The impacts on workability, compressive strength, tensile strength and flexural strength are presented. The durability of concrete with RGS was

also analysed by a rapid chloride penetration test (RCPT) and an alkali-silica reaction (ASR) test.

**Chapter 4** details the use of crushed RGP as a partial cement replacement in concrete. The effects of glass powder on compressive, flexural and tensile strength of concrete are evaluated. Tests on the relative strength of mortar are carried out to assess the reactivity of glass powder as a supplementary cementitious material. Concrete resistance against chloride ion ingress is determined using a rapid chloride penetration test (RCPT).

**Chapter 5** investigates the microstructure of mortar and cement paste containing glass sand and glass powder, respectively. The influence on using recycled glass in mortar and cement paste is evaluated using thermogravimetric analysis, X-ray diffraction, scanning electron microscopy and energy-dispersive spectroscopy.

**Chapter 6** addresses the environmental benefits of using recycled glass to produce 1m<sup>3</sup> of concrete. This study is based on the Australian context, such as water use, material consumption, fuel consumption, greenhouse gas emission (CO<sub>2</sub> equivalent), ozone layer depletion (CFC equivalent) and eutrophication (PO<sub>4</sub> equivalent).

**Chapter 7** demonstrates the use of RGS as a coarse sand replacement in a concrete footpath. Concrete mix design is developed for the various ratios of glass sand to use in the footpath.

**Chapter 8** presents concluding remarks based on the outcomes and recommendations for further development.

## **Chapter 2: A review of the use of waste glass as an aggregate and cement replacement in concrete**

### **2.1 Overview of construction materials**

The construction sector is one of the most dynamic and fastest growing industries in the world. The demand for the construction industry is increasing day by day due to urbanisation and growth of the world's population. Concrete, a primary building construction material, is used in almost all kinds of infrastructure because of its availability, workability and durability properties.

#### **2.1.1 Concrete**

Concrete is one of the most widely used construction materials in the world. It is the second-most consumed material by humankind, second only to water. About 30 billion tonnes of concrete were consumed globally in 2006, compared with 2 billion tonnes in 1950 (World Business Council for Sustainable Development, 2006). In 2013, more than 25 million cubic metres of concrete were poured in Australia (Ilangovana et al., 2008). Traditionally, concrete is produced by mixing binding materials, aggregates and water. Cement is the most important binding material in concrete construction. Concrete mixture is 10-15% cement and 15-20% water. Aggregates cover 60-75% of the total volume of concrete. Typical components of concrete are shown in Figure 2.1.

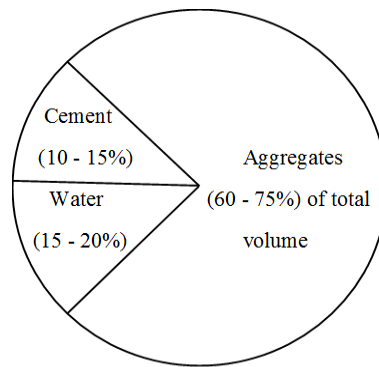


**Figure 2.1 Typical components of concrete**

Concrete has many excellent properties that make it so versatile. It has inherent sustainability benefits such as being relatively cheap and it provides a safe and healthy living environment. However, from an environmental perspective, there are aspects of concrete which can be improved to reduce its carbon footprint. With the sheer volume of concrete used around the world, it is essential to assess and improve its sustainability performance.

### **2.1.2 Aggregates**

Aggregates are inert and granular materials. They offer dimensional stability, stiffness, and most importantly contribute to the strength of concrete structures. Aggregates can broadly be divided into two types: coarse and fine. Coarse aggregates are generally larger than 4.5mm, whereas fine aggregates are smaller than 4.5 mm (Vieira et al., 2016). Fine aggregates are used to fill the voids between coarse aggregates. Crushed rock, gravel or screenings are widely used as coarse aggregates. Fine sand, coarse sand and crusher fines are broadly used as fine aggregates.

A large amount of natural sand is consumed as fine aggregate by concrete industries. Excessive use of natural sand results in depletion of natural resources and also it can lead to other problems such as erosion of riverbanks and sinking of bridge piers. Recycled aggregate and manufactured sand are thus attracting interest as a natural sand replacement in concrete.

### **2.1.2.1 Manufactured sand**

Manufactured sand or crusher dust (Figure 2.2) obtained as a by-product of crushing rocks, can be used as a replacement for natural sand. These are generally known as manufactured sands. Use of manufactured sand reduces overuse of natural sand. The difference between natural sand and manufactured sand lies in its physical and mineralogical properties. The use of crusher dust as a durable building material has been widely accepted in industrialised nations such as Australia, Germany and France (Ilangovana et al., 2008). The shape and texture of crusher dust depend on the type of crusher, reduction ratio and the parent rock (Pilegis et al., 2016).

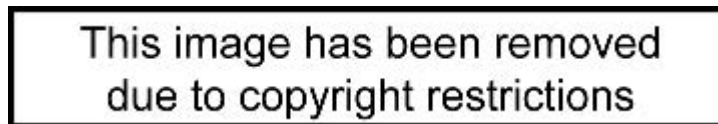


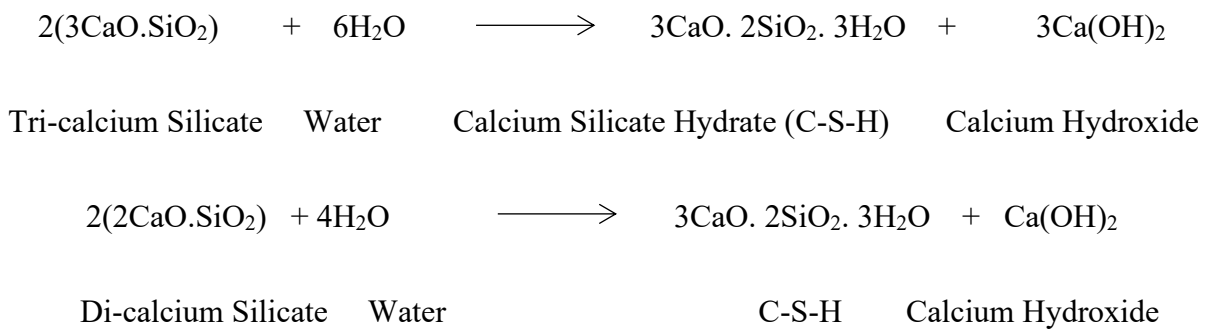
**Figure 2.2 Bohle quarry crusher dust waste (Gersekowski, 2014)**

The particle size distribution, physical and chemical properties of crusher dust should conform to the requirements of Cement Concrete & Aggregates Australia (CCAA). Crusher dust exhibits higher angularity which requires more water to achieve equal workability compared with concrete and natural sand (Pilegis et al., 2016).

### **2.1.3 Cement**

Cement is the key ingredient of concrete. Cement binds coarse and fine aggregates together with the help of water. Cement fills up the void in the fine aggregates and gives strength to the concrete. The main compounds of cement are tri-calcium silicate ( $3\text{CaO}\cdot\text{SiO}_2$ ), di-calcium

silicate ( $2\text{CaO}\cdot\text{SiO}_2$ ), tri-calcium aluminate ( $3\text{CaO}\cdot\text{Al}_2\text{O}_3$ ) and tetra-calcium alumina-ferrite ( $4\text{CaO}\cdot\text{Al}_2\text{O}_3\cdot\text{Fe}_2\text{O}_3$ ). Tri-calcium silicate ( $\text{C}_3\text{S}$ ) hydrates and sets instantaneously and is responsible for gaining early strength (Lea and Hewlett, 1998; Tylor, 1997; Yilmaz and Olgun, 2008). Di-calcium silicate ( $\text{C}_2\text{S}$ ) reacts slowly with water and is responsible for the long-term strength of concrete. Typical Portland cement contains 50%  $\text{C}_3\text{S}$  and 25%  $\text{C}_2\text{S}$ . The main reactions during the hydration of cement are given below.



Calcium silicate hydrate (C-S-H) and calcium hydroxide ( $\text{Ca}(\text{OH})_2$ ) are the main products of cement hydration. Formation of C-S-H gel is the principal source of concrete strength.  $\text{Ca}(\text{OH})_2$  is comparatively weak and brittle. It does not act as a binder but combines with carbon dioxide to form soluble salt (Al-Zubaidi and Tabbakh, 2016).

Cement manufacturing is an energy-intensive process.  $\text{CO}_2$  is emitted during the calcination of limestone ( $\text{CaCO}_3$ ) and it accounts for 60% of total  $\text{CO}_2$  emissions from the cement manufacturing process. Another 40% of emissions comes from burning fossil fuel to generate energy during the cement manufacturing process. Production of one tonne of cement has been shown to release one tonne of  $\text{CO}_2$  into the atmosphere (Sprince et al., 2011). One viable option to reduce the carbon footprint of concrete is to partially replace cement in concrete with supplementary cementitious materials.

### 2.1.3.1 Supplementary cementitious materials

Supplementary cementitious materials (SCMs) are pozzolanic materials that can contribute to the properties of hardened concrete. The use of SCMs in concrete has been developing in North America since the 1970s. SCMs are the by-product of other industries or natural pozzolans and they can be used to partially replace cement in concrete. Typical SCMs used in concrete industry are fly ash, silica fume and ground granulated blast-furnace slag (Figure 2.3). Pozzolans are siliceous and aluminous materials that possess little or no cementitious value. However, they are in finely ground form, and in the presence of water react chemically with  $\text{Ca(OH)}_2$  at ordinary temperatures to form compounds possessing cementitious properties (Mehta, 1987).

Fly ash is a by-product of coal-fired thermal power generation plants (Thomas, 2007). Fly ash is a fine grey powder and its particles are spherical. Fly ash is silicate glass containing silica, aluminium, iron, calcium, magnesium, sodium, potassium and carbon. Fly ash exhibits pozzolanic properties and reacts with  $\text{Ca(OH)}_2$  to form cementitious compounds. Fly ash is generally used as a partial replacement of 15-25% of cement in concrete (Thomas, 2007).

Silica fume, also called micro silica, is a by-product of electric arc furnaces used in the production of silicon or ferrosilicon alloy (Cement Concrete & Aggregates Australia, 2010). It is grey and consists of very fine particles. Due to its high silica content, it acts as a pozzolanic material. Silica fume is a highly reactive pozzolanic material and it reacts chemically with the  $\text{Ca(OH)}_2$  in the cement paste, producing C-S-H.

This image has been removed  
due to copyright restrictions

**Figure 2.3 Cement, fly ash, silica fume and ground granulated blast-furnace slag**  
(Forum, 2017)

Slag cement, also referred to as ground granular blast-furnace slag (GGBS), is a by-product of the iron and steel industries. GGBS can be used as a cement substitute at a replacement level of up to 50% (Suresh and Nagaraju, 2015). It consists of calcium-bearing silicates and aluminosilicates.

Apart from these widely accepted SCMs, recent researchers have assessed the pozzolanic properties of waste glass powder and studied its performance as a pozzolanic material (Shao et al., 2000; Nassar and Soroushian, 2011; Du and Gao, 2014). The chemical compositions of cement, fly ash, slag, silica fume and waste glass powder are tabulated in Table 2.1.

**Table 2.1 Chemical composition of cement, fly ash, slag, silica fume and glass powder**  
(Avosa, 2016; Amin and Abu el-hassan, 2015)

Chemical Composition	Cement	Fly Ash	Slag	Silica Fume	Glass Powder
SiO <sub>2</sub>	18.99	56.86	36.02	96	72.02
Na <sub>2</sub> O	0.16	1.02	0.67	0.45	12.85
CaO	63.94	4.08	38.84	1.20	11.25

Al <sub>2</sub> O <sub>3</sub>	4.99	21.62	15.56	1.10	1.47
MgO	0.78	4.12	4.05	0.18	0.57
Fe <sub>2</sub> O <sub>3</sub>	3.22	6.88	0.84	1.45	0.57
K <sub>2</sub> O	0.35	1.97	0.82	1.20	0.35
SO <sub>3</sub>	2.26	0.63	0.33	0.25	0.12

### 2.1.4 Waste glass

Modern lifestyle is implausible without glass for its versatile applications. Glass was discovered more than 5000 years ago in Mesopotamia and has been produced for various applications since then. Based on the chemical composition, glass is produced in several forms such as: soda-lime glass (containers, sheet, float, tempered ovenware and light bulbs); lead glass (neon tubing, colour TV funnels, electronic parts and optical dense flint); borosilicate glass (chemical apparatus, pharmaceutical and tungsten sealing); and aluminosilicate glass (combustion tubes, fibreglass and resistor substrates) (Jani et al., 2014). Soda-lime glass is the dominant type of glass used for glass containers and windowpanes. Recent research has shown that soda-lime glass powder has pozzolanic properties, hence waste soda-lime glass powder can be used in cementitious materials. The chemical composition of soda-lime glass is listed in Table 2.2. Soda-lime glass accounts for about 90% of manufactured glass (Shi and Zheng, 2007).

**Table 2.2 Chemical composition of soda-lime glass (Shi and Zheng, 2007)**

Soda-lime glass	SiO <sub>2</sub>	CaO	Na <sub>2</sub> O	Al <sub>2</sub> O <sub>3</sub>	K <sub>2</sub> O	MgO
Containers	66-75	6-12	12-16	0.7-7	0.1-3	0.1-5
Sheet	71-73	8-10	12-15	0.5-1.5		1.5-3.5
Float	73-74	8.7-8.9	13.5-15		0.2	3.6-3.8

Light bulbs	73	5	17	1	4
Tempered ovenware	75	9.5	14	1.5	

#### 2.1.4.1 Waste glass recycling rate

Glass is known as a 100% recyclable material and can be recycled repeatedly without degradation in quality (Sobolev et al., 2007). Recycling of waste glass started around the 1970s and since then, waste glass has been collected for recycling around the world, through the rate of recycling differs in different countries. The low value of recycled glass and co-mingling of different coloured glasses at the source, as well as difficulty in removing other contaminants such as soil, metals, paper and chemical residues from the waste glass stream, often makes recycling waste glass challenging (Afshinnia and Rangaraju, 2016). In 2014, approximately 300 tonnes per day of waste glass were disposed at landfills in Hong Kong. The recovery rate of waste glass was not more than 10% due to its low commercial value and the absence of a glass manufacturing industry in Hong Kong (Lu et al., 2017). An accumulation of glass bottles and crushed mixed glass is shown in Figure 2.4.

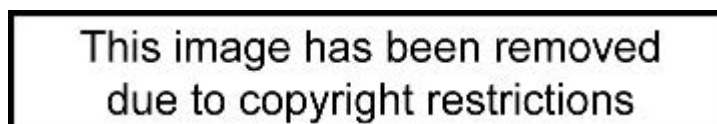


**Figure 2.4 Accumulation of glass bottles (Boehlke, 2018)**

In Singapore, 72,800 tonnes of waste glass was produced in 2011 but merely 29% of the total collected waste glass was recycled. The recycling rate fell to 20% in 2016. That year, 72,300 tonnes of waste glass was produced, of which 57,600 tonnes were disposed of National Environmental Agency (2017). According to the Environmental Protection Agency, the United States produced 11.5 million tonnes of waste glass in 2013, of which only 26% was recovered for recycling (Environmental Protection Agency, 2015). Although recycling of glass increased from 0.75 million tonnes in 1980 to more than 3 million tonnes in 2013, almost 74% of waste glass, predominantly soda-lime glass from container bottles, were disposed of in landfills. Table 2.3 shows waste glass production and recycling rates in the US in 2010. Based on 2010 glass generation rates, 11,530-kilotonnes of waste glass were produced in the US, out of which only 27.1% was recycled.

**Table 2.3 Glass waste production and recycling in US, 2010 (Environmental Protection Agency, 2010)**

Product Category	Generation (Thousands of Tonnes)	Recovery (Thousands of Tonnes)	Recovery (% of Generation)
Durable goods	2170	Neg.	Neg.
(Containers and packaging)			
Beer and soft drink bottles	5670	2350	41.4
Wine and liquor bottles	1700	420	24.7
Other bottles and jars	1990	360	18.1
Total glass containers	9360	3130	33.4

Total glass	11530	3130	27.1
-------------	-------	------	------

Neg.= less than 5000 tonnes or 0.05%

In Australia, glass consumption has been increasing at an average annual rate of 6.7% since 2010-11. The recycling rate of glass was 49%, 46%, 44%, 47% and 42% in fiscal years 2010-11, 2011-12, 2012-13, 2013-14 and 2014-15, respectively (Table 2.4) (NRRS, 2017). In 2014-2015, the glass recycling rate declined from 47% to 42%, but consumption increased. Although approximately 257,000 tonnes of waste glass are generated each year in Victoria, only 124,000 tonnes or 48% are recycled into glass cullet for glass manufacturing (Victoria, 2014).

**Table 2.4 Glass recycling rates in Australia (NRRS, 2017)**

Financial Year	Total Consumption (kt)	Total Recycled (kt)	Recycling Rate (%)
2010-2011	1054	520	49
2011-2012	1210	552	46
2012-2013	1248	552	44
2013-2014	1259	597	47
2014-2015	1364	564	42

In Queensland's context, the recycling rate of waste glass was in the range of 25-35% in 2006 (EPA, 2006). Queensland has no levy and total landfill costs in Queensland are as low as \$30/t. Due to the low cost of landfilling in Queensland, 477,000 tonnes and 398,000 tonnes of glass waste were transported for disposal from New South Wales and Victoria to Queensland, respectively (Ritchie, 2016) . At the local council level, Cairns Regional Council collects around 5000 tonnes of glass waste annually. Approximately 45-50% of glass collected by Cairns Regional Council is recovered and recycled in different forms. However, recyclable glass materials need to be transported from Cairns to Brisbane for further recycling. Low

market value and high transport costs have prompted the Council to look into more sustainable options to use recycled glass locally. Furthermore, the remaining glass waste in the form of glass fines (around 2600 tonnes) cannot be recycled and is sent to landfill (Tamanna et al., 2017; CRC, 2016).

## **2.2 Waste glass as construction material**

Glass is a non-biodegradable material. It takes a long time to break down naturally. The waste glass that cannot be recycled is sent to landfill, creating environmental problems. One viable option to recycle a large amount of glass waste instead of it going to landfill is to use it in the construction industry. Several researchers have studied the use of recycled crushed glass in concrete as either aggregate (both coarse and fine aggregate) or as a cement replacement, with mixed success. Most of these studies are limited to laboratory tests, and few have studied the use of recycled glass in actual field applications.

### **2.2.1 Waste glass as coarse aggregate replacement**

Many researchers have studied the use of waste glass as a coarse aggregate replacement in concrete since the 1960s. Schmidt and Saia (1963) studied the use of glass chips to produce exposed aggregate for architectural applications. Several other researchers have studied the fresh and hardened properties of concrete using waste glass (Johnston, 1974; Polley et al., 1998; Topçu and Canbaz, 2004; Terro, 2006; Yu, 2016).

#### **2.2.1.1 Fresh properties of concrete**

##### **(a) Slump test**

Slump is a primary measure indicating the workability of concrete. The effect of using waste glass on the workability of concrete as coarse aggregate replacement was found to be negligible (Topçu and Canbaz, 2004). However, slump decreased with higher percentages of coarse

aggregate replacement (Topçu and Canbaz, 2004; Kisacik, 2002; Afshinnia and Rangaraju, 2016). This decrease might be due to the poor geometry of waste glass. In contrast, an increase in slump was observed with a higher percentage of coarse glass and fine-coarse glass (Figure 2.5). The increase in slump was due to the lower specific surface area and smooth surface of glass aggregates. Smooth surface attributed to the poorer cohesion and lower inter-particle friction between the cement paste and glass aggregates. Flow properties of the concrete mixture enhanced due to the impermeable nature of waste glass. A similar trend was reported by Topçu and Canbaz (2004).

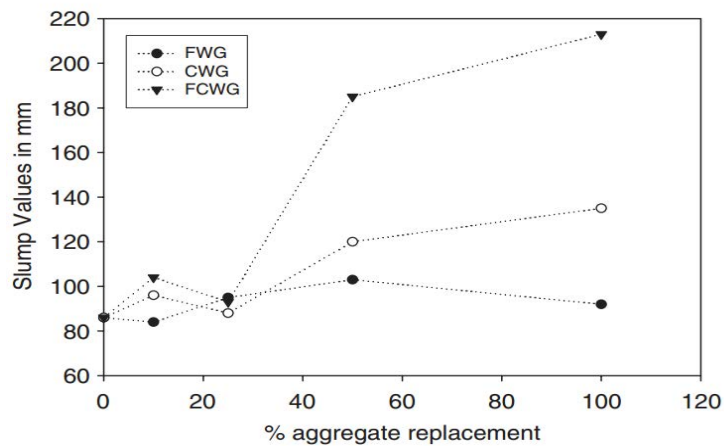


**Figure 2.5 Slump of concrete mixtures containing fine glass powder, coarse glass powder and fine-coarse glass powder (Terro, 2006)**

### **(b) Unit weight**

The unit weight of concrete containing waste glass was found to be less than a control mixture (Terro, 2006; Kisacik, 2002; Afshinnia and Rangaraju, 2016) (Figure 2.6). This was attributed to the lower specific gravity of waste glass compared with typical crushed stones.

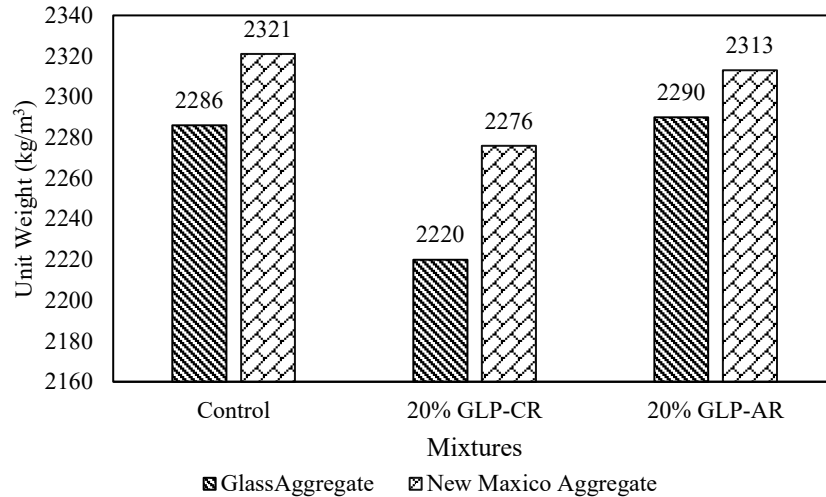


**Figure 2.6 Unit weight of concrete mixtures containing glass powder as cement replacement and aggregate replacement (Afshinnia and Rangaraju, 2016)**

### **(c) Air content**

The inclusion of crushed glass as coarse aggregate in concrete resulted in a slightly higher air content compared with concrete with mineral aggregate (Afshinnia and Rangaraju, 2016). A higher level of trapped air was noticed in the mixture due to the elongated and flat nature of crushed glass. In contrast, a reduction in air content was observed with a high content of waste glass addition in concrete (Topçu and Canbaz, 2004). The reason for this reduction was the poor geometry of waste glass. Furthermore, lower air content with a high proportion of waste glass reduced the porosity between waste glass and cement paste.

#### **2.2.1.2 Mechanical strength of concrete**

The compressive strength of concrete was noticed to decrease with an increase in the amount of waste glass as coarse aggregate replacement (Topçu and Canbaz, 2004; Terro, 2006; Yu, 2016; Kisacik, 2002; Afshinnia and Rangaraju, 2016). Reduction in strength was due to the flat surface and elongated shape of waste glass. Coarse glass particles might weaken the concrete structure by failure of the aggregate particles because of its high friability (Polley et al., 1998).

Concrete with 10 mm glass particles was found to increase in compressive strength at 28 days compared with concrete with 16 mm glass particles. However, Yu (2016) showed that concrete with both glass particles (10 mm and 16 mm) was unable to reach the equal compressive strength of the control concrete at 28 days. In contrast, Shayan and Xu (2004) indicated that compressive strength results easily met and exceeded the target of 32 MPa concrete, while having a large amount of waste glass. This result was found to be due to the addition of fly ash with cement as a binder and superplasticiser as chemical admixtures.

Like compressive strength results, flexural strength was found to decrease with increased waste glass content in concrete (Topçu and Canbaz, 2004; Kisacik, 2002; Afshinnia and Rangaraju, 2016). However, Yu (2016) reported that the flexural strength increment was found to be up to 16.3% when small size waste glass was used with coarse steel slag.

### 2.2.1.3 Alkali-silica reaction and ASR mechanism

Alkali-Silica Reaction (ASR), well-known as “concrete cancer”, is a detrimental chemical reaction in concrete. ASR gradually occurs between the reactive silica of aggregate and alkalis in the pore solution of concrete (Saha et al., 2018). Cement and/or cementitious material is the main source of alkali present in concrete. Alkali also may be available in aggregates, pozzolans and adjacent surroundings used to produce concrete. Three components are responsible for ASR formation: high alkali content, availability of reactive aggregate and sufficient quantity of moisture.

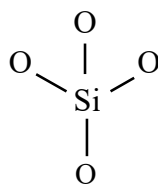


Figure 2.7 Silica tetrahedron



The swelling of alkali-silica gel generates an internal pressure. If the internal pressure surpasses the tensile strength of the specimen, severe cracks will form around the reactive aggregates (Du and Tan, 2014b) and cause detrimental damage to concrete.

ASR can occur in concrete when waste glass is used as coarse aggregates because of large glass particle size. Cracks in coarse glass particles exhibit more reaction and higher expansion (Du and Tan, 2014b). Johnston (1974) showed that the use of waste glass as coarse aggregate with particle size greater than 19mm resulted in concrete cracking. This tendency was also found in a study using different forms of glass as an aggregate with cement by Pike & Hubbard (1957). Use of excessive silica content in concrete mixture also causes ASR expansion. Shayan and Xu (2004) indicated that the use of waste glass up to 30% replacement in concrete caused less harmful effects with low alkali content of concrete (Figure 2.8). Dosage greater than 30% resulted in an increase in ASR. The ASR rate reduced with the decrease of waste glass content (Topçu and Canbaz, 2004; Yu, 2016). Therefore, the tendency of ASR expansion can be reduced by using low alkali cement, appropriate glass content and fine glass particles as sand replacement.

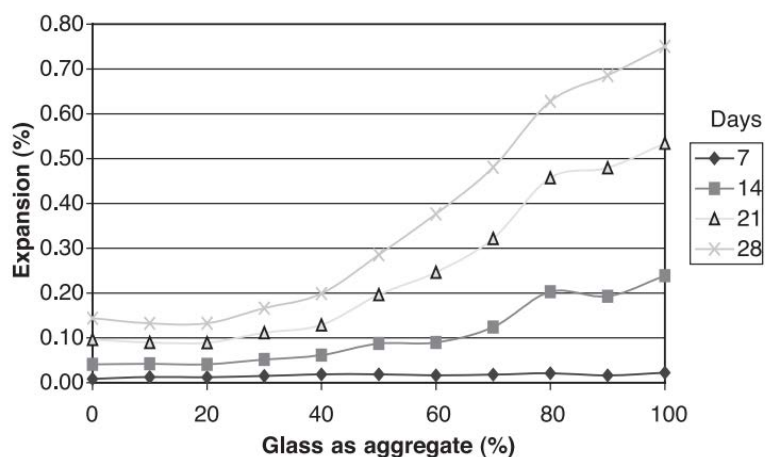


Figure 2.8 ASR expansion of mortar bar for different ages (Shayan and Xu, 2004)

## 2.2.2 Waste glass as fine aggregate

Several studies have been carried out using waste glass as fine aggregate in concrete with mixed outcomes. As the use of waste glass as coarse aggregate does not provide significant results, investigations are undertaken into fine aggregate replacement.

### **2.2.2.1 Fresh concrete properties**

#### **(a) Slump test**

Some variations in published experimental results have been found regarding fresh concrete properties with waste glass as a fine aggregate replacement. A reduction in slump was obtained with an increase in waste glass content (Pereira de Oliveira et al., 2008; Ismail and Al-Hashmi, 2009; Park and Lee, 2004; Chen et al., 2006; Limbachiya, 2009; Topçu and Canbaz, 2004). This reduction was found because of angular glass particles and the reduction of equivalent fineness modulus (Pereira de Oliveira et al., 2008). Angular waste glass particles reduce the cement paste availability, and consequently, the fluidity of the mixes (Adaway and Wang, 2015). Smooth surfaces, harsh texture, sharp edges, as well as consistency in fine glass particles and plastic properties of concrete with waste glass sand, could be affected negatively. A reduction in slump value was also found due to a high proportion of waste glass in concrete (Limbachiya, 2009). However, a slight increase in slump value was noticed where coarse particles were used with an increase in replacement level (De Castro and De Brito, 2013). Researchers Pereira de Oliveira et al. (2008) used a high range of water reducer to get similar workability as a control mixture.

Opposite results regarding slump were reported by many other researchers (Malik et al., 2013; Hunag et al., 2015; Wang et al., 2016; Borhan, 2012; Taha and Nounu, 2008; Terro, 2006). Mardani-Aghabaglou et al. (2015) observed a slight increase in slump with an increase in substitution level. Due to higher compactness of concrete granular skeleton, a higher slump value was found at higher glass replacement levels. The glass grains are finer than natural sand

and able to fill the void of coarse aggregate (Sharifi et al., 2013). Hunag et al. (2015) described the reason behind increasing slump as waste glass increased in mixtures. Waste glass consists of irregular lamellar particles with edges and corners which interact with each other. Although individual particles hardly move, the addition of moisture lubricates the particles and results in an increased slump (Hunag et al., 2015). Less water absorption and the smooth surface of glass sand improved the workability of the concrete mixture (Sharifi et al., 2013; Malik et al., 2013). The poorer cohesion between the waste glass and cement paste also caused an increment in slump value (Yu, 2016).

### **(b) Fresh density**

The fresh density of concrete was found to decrease with an increase in the amount of waste glass as fine aggregate replacement (Adaway and Wang, 2015; Hunag et al., 2015; Du and Tan, 2014a; Ismail and Al-Hashmi, 2009; Topçu and Canbaz, 2004; De Castro and De Brito, 2013) (Figure 2.9). Due to the lower particle density of glass compared with natural sand, the fresh density of concrete was found to be reduced as the glass was incorporated in the concrete mixture. The increment of water-to-cement ratio in the mix also resulted in lower density (Du and Tan, 2014a). The addition of water caused an increase in the volume of voids; hence, higher porosity and lower fresh density (De Castro and De Brito, 2013).

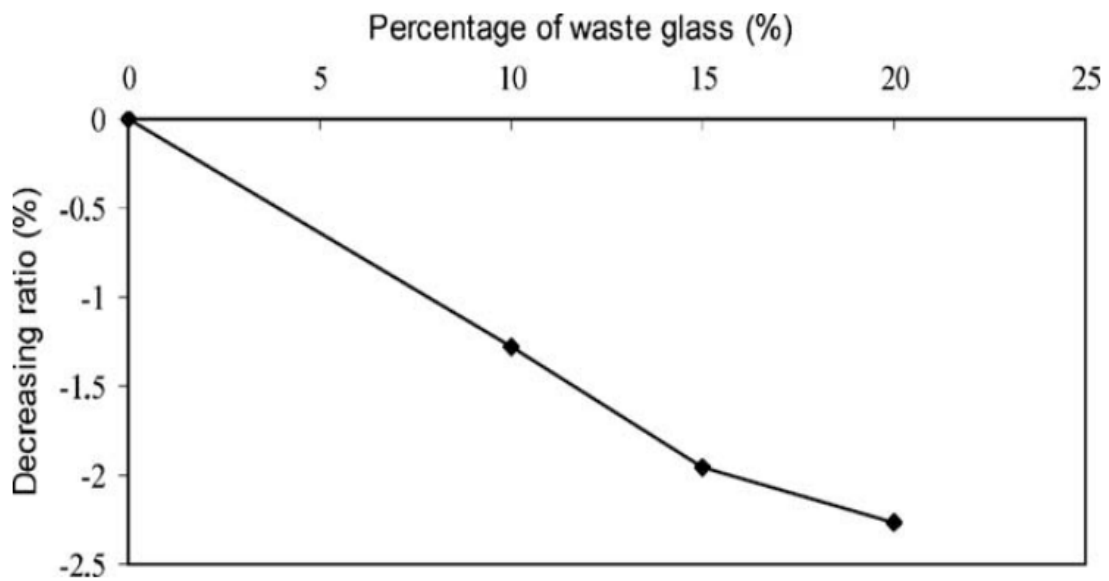


**Figure 2.9 Decreasing ratios in fresh density (Ismail and Al-Hashmi, 2009)**

### **(c) Hardened density**

The dry density of concrete was also noticed to decrease with increasing waste glass sand content as a fine aggregate replacement (Al-qatan et al., 2011; Adaway and Wang, 2015; Topçu and Canbaz, 2004; Ismail and Al-Hashmi, 2009). The lighter specific gravity of glass aggregate led to a reduction in dry density. In contrast, Ling and Poon (2012) found an increase in dry density with increasing glass content. This higher density attributed to the relatively high specific gravity of lead present in the funnel glass. Another study Yu (2016) found that the use of steel slag as aggregate increased the concrete density. However, the addition of waste glass to steel slag concrete could limit the density of concrete.

### **(d) Air content**

Air content was noticed to be lower with a lower glass content (Du and Tan, 2014a). The smooth surface resulted in less retention of air voids. However, more irregular shaped glass

particles compared with natural sand resulted in large retention of air voids; hence, higher air content. A gradual increase in air content was found with higher glass content.

### **(e) Setting time**

The addition of waste glass sand as a sand replacement reduced setting time (Wang et al., 2016). Setting time increased as the glass sand content increased in the mixture and was found to be prolonged as glass sand is water repellent and cannot undergo a polyreaction with slag and OH<sup>-</sup> ions.

## **2.2.2.2 Mechanical strength**

### **(a) Compressive strength**

Several studies have been carried out to investigate the compressive strength of concrete with the addition of crushed glass as fine aggregate. A gradual increase in compressive strength was found when recycled glass sand (RGS) was used (Pereira de Oliveira et al., 2008; Ismail and Al-Hashmi, 2009; Du and Tan, 2014a; Wang et al., 2016; Batayneh et al., 2007) (Figure 2.10). The increasing trend was witnessed along with the inclusion of RGS until the optimum percentage, i.e., maximum compressive strength and thereafter decreasing (Polley et al., 1998; Al-qatan et al., 2011; Dumitru et al., 2010; Gautam, 2012; Malik et al., 2013; Tejaswi et al., 2015; Adaway and Wang, 2015; Hunag et al., 2015). The reduction in strength at higher percentages can be due to inadequate cement paste available in the mixture to assist bonding within the concrete which consequently forms microscopic voids (Adaway and Wang, 2015).

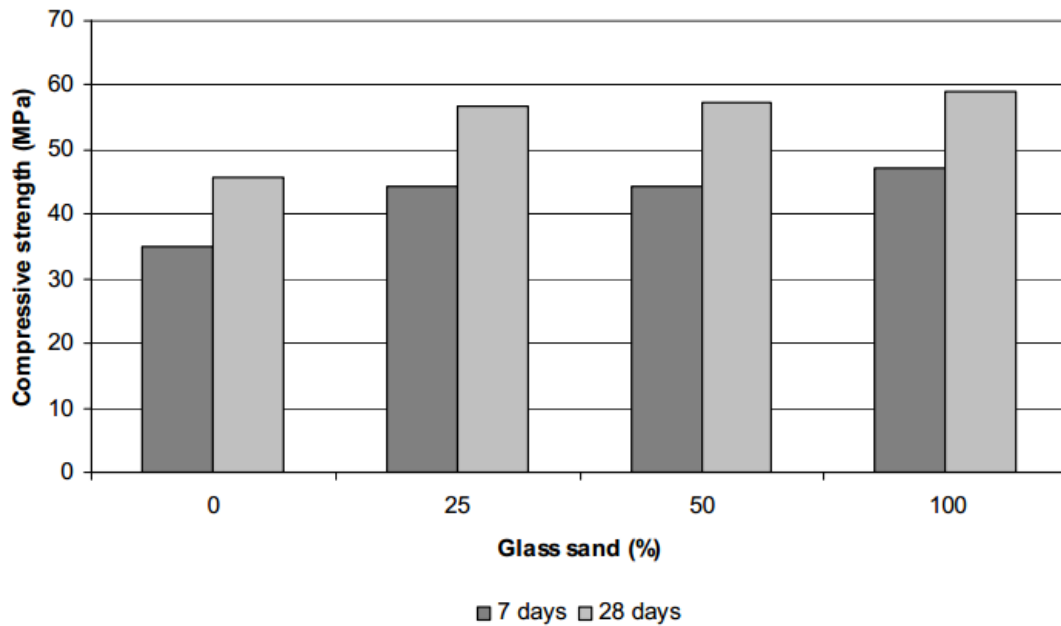


**Figure 2.10 Compressive strength of glass sand for 7 and 28 days (Pereira de Oliveira et al., 2008)**

In contrast, some researchers observed a decrease in compressive strength with the increase in RGS (De Castro and De Brito, 2013; Mardani-Aghabaglou et al., 2015; Sharifi et al., 2013). This reduction is because of higher friability, lower density and higher surface smoothness. Researchers reported comparable strength to the reference concrete up to a certain percentage and following that, decreased strength with increased glass percentage (Terro, 2006; Taha and Nounu, 2008; Limbachiya, 2009). Shayan and Xu (2006) found that crushed glass met the target strength criteria. However, he did not suggest the mix when alkali content is high in the concrete mix because of detrimental alkali-aggregate reaction expansion. Afshinnia and Rangaraju (2016) investigated the combined effect of coarse crushed glass sand (80%) and fine crushed glass sand (20%), and found significant improvement compared to control concrete. In contrast, a downgrade trend was observed in an investigation conducted by (Shayan and Xu, 2004) when fine, and coarse crushed glass ratio was 50:50.

Besides replacement ratio, curing time also has a great impact on compressive strength. Chen et al. (2006) found significantly improved compressive strength even after 91 days compared with control concrete, and more prominent at 365 days. This increasing trend was also supported by (Taha and Nounu, 2009; Ismail and Al-Hashmi, 2009; Du and Tan, 2014a; Metwally, 2007). The pozzolanic reaction that occurred between cement paste and crushed glass sand could improve the microstructure at the interface transition zone in later age. Lee et al. (2013) investigated the effect of glass particle size and found that when glass particle size was 2.36 mm and 1.18 mm, compressive strength reduced at 28 days. Waste glass with particle size less than 600µm exhibited an increase in compressive strength at 28 days. However, no remarkable difference was found in strength depending on the effect of the colour of the glass (Chen et al., 2006).

A reduction was found in the compressive strength when crushed glass was used as sand replacement in mortar (Corinaldesi et al., 2016; Ling and Poon, 2012; Ling et al., 2011). On the other hand, Corinaldesi et al. (2005) demonstrated strong compressive strength using a mixture with higher water-cement ratios. Table 2.5 shows the comparative compressive strength of RGS in concrete.

**Table 2.5 Compressive strength of recycled glass sand in concrete**

Ref.	Percentage	Percentage (optimum)	Curing period (Days)	Strength Effect
(Polley et al., 1998)	10%, 20%, 30%, 40%, 50%, 60%, 70%, 80%, 90%	20%	28, 365	Satisfactory up to optimum percentage
(Wang et al., 2016)	10%, 20%	20%	3, 7, 28	Increasing

(Ismail and Al-Hashmi, 2009)	10%, 15%, 20%	20%	3, 7, 14, 28	Increasing
(Adaway and Wang, 2015)	10%, 20%, 30%, 40%	30%	7, 28	Increasing until optimum, then decreasing
(Hunag et al., 2015)	5%, 10%	5%	7, 28, 56, 91	Increasing until optimum, then decreasing
(Gautam, 2012)	10%, 20%, 30%, 40%, 50%	10%	7, 28	Increasing until optimum, then decreasing
(Malik et al., 2013)	10%, 20%, 30%, 40%	20%	7, 28	Increasing until optimum, then decreasing
(Dumitru et al., 2010)	30%, 45%, 60%	45%	1, 7, 28, 56, 90	Increasing until optimum, then decreasing
(Wang et al., 2014)	30%, 45%, 60%	60%	7, 28, 90	Increasing
(De Castro and De Brito, 2013)	5%, 10%, 15%, 20%			Decreasing
(Mardani-Aghabaglou et al., 2015)	10%, 20%, 30%, 40%, 50%, 60%		28	Decreasing
(Sharifi et al., 2013)	10%, 20%, 30%, 40%, 50%		1,7,14,28	Negligible Decreasing
(Terro, 2006)	10%, 25%, 50%, 100%	10%		Comparable, then decreasing
(Limbachiya, 2009)	5%, 10%, 15%, 20%, 30%, 50%	20%	28	Comparable, then decreasing
(Tejaswi et al., 2015)	10%, 20%, 30%, 40%, 50%	20%	3, 7, 28	Increasing until optimum, then decreasing

(Shayan and Xu, 2004)	50% (coarse sand) + 50% (fine sand)		7, 28	Decreasing
(Afshinnia and Rangaraju, 2016)	80% (coarse sand) + 20% (fine sand)		28	Increasing
(Al-qatan et al., 2011)	25%, 50%, 75%, 100%	50%	3,7	Increasing until optimum, then decreasing
(Taha and Nounu, 2008)	50%, 100%		28	Negligible Decreasing
(Pereira de Oliveira et al., 2008)	25%, 50%, 100%	100%	7, 28	Increasing

## (b) Flexural strength

Researchers had observed that waste glass sand had no significant effect on flexural strength when the waste glass was used as coarse aggregate replacement. Flexural strength was found to decrease, which is inversely proportional to the amount of glass sand used in concrete (Topçu and Canbaz, 2004). A similar trend was found in fine aggregate replacement with waste glass (Taha and Nounu, 2008; Sharifi et al., 2013). Taha and Nounu (2008) drew some conclusions on strength reduction. The inherent plane and smooth surface of large particles may weaken the bond between cement paste and glass particles. Also, inherent cracks in glass particles may tend to make them more breakable in concrete mixtures. Furthermore, contamination such as organic content and foreign materials may degrade with time and form voids in the concrete microstructure. However, Sharifi et al. (2013) found that a small volume of glass addition allowed more adhesion between cement paste and glass. Consequently, it showed higher flexural strength compared to control concrete.

Ismail and Al-Hashmi (2009) found a significant impact on curing time. As recycled glass is a pozzolanic material, it shows a tendency to increase with time and replacement levels up to 20%. Du and Tan (2014a) found that up to 100% replacement ratio, RGS did not reduce concrete strength. On the contrary, it led to an increase in flexural strength with the increase in glass sand content in the concrete, which indicates the more obvious interlocking between glass particles. Angular aggregate can improve strength by internal friction, increased surface area and a higher degree of mechanical interlocking (Kearsley, 2006).

A tendency to decrease was noticed when waste glass was used as sand replacement in mortar due to the weak bond between surface of glass sand and cement paste (Ling et al., 2011; Ling and Poon, 2012; Ismail and Al-Hashmi, 2009; Degirmenci et al., 2011) . However, Ling and Poon (2012) noticed a significant reduction in flexural strength at 90 days due to the retardation effect of lead on the hydration of cement for non-treated funnel glass sand.

### **(c) Tensile strength**

The incorporation of waste glass sand as a sand replacement improved the splitting tensile strength of concrete (Du and Tan, 2014a; Batayneh et al., 2007). A less porous microstructure of cement paste was formed with a low water-cement ratio. The elongated shape of the glass particles might contribute to improve interlocking between glass particles and cement paste. In contrast, a reduction in tensile strength was also found when waste glass was used as a sand replacement (Malik et al., 2013; Taha and Nounu, 2008; Sharifi et al., 2013; Topçu and Canbaz, 2004; Mardani-Aghabaglou et al., 2015; Afshinnia and Rangaraju, 2016; Taha and Nounu, 2009). Waste glass absorbed less water in concrete. It showed an impact on the acute bleeding and segregation on the microstructure properties of concrete (Taha and Nounu, 2008; Taha and Nounu, 2009). The smooth surface of waste glass led to a weak bond in the interfacial transition zone (ITZ), causing a reduction in tensile strength (Mardani-Aghabaglou et al., 2015). Malik

et al. (2013) and Ali and Al-Tersawy (2012) found that the splitting tensile strength decreased with an increase in waste glass content. However, Sharifi et al. (2013) and P.Turgut and Yahlizade (2009) concluded that waste glass was beneficial for lower replacement (i.e. 10% and or 20%) of fine aggregate in concrete. Similar to flexural strength development, waste glass replacement developed a better splitting strength at a longer curing age with improved durability (Wang, 2009).

#### **(d) Modulus of elasticity**

The dynamic modulus of elasticity was observed to decrease with waste glass addition in concrete (Topçu and Canbaz, 2004). Larger size waste glass also caused a reduction in the modulus of elasticity (Yu, 2016). However, Tuncan et al. (2001) found an increased dynamic modulus of electricity with waste glass addition due to the positive effect on the bond properties of finely divided waste glass. Uniformly distributed glass particles might develop interlocking and particle interference. The reduction in cohesion between glass particles and cement paste resulted in an influence on the increased elastic modulus of electricity (Du and Tan, 2014a). The modulus of elasticity was found to increase with increasing concrete age. Reducing the water-to-cement ratio also significantly increased the value of the modulus of elasticity (Yu, 2016).

#### **(e) Ultrasonic-pulse velocity**

Ultrasonic pulse velocity depends on the concrete porosity, aggregate type and ITZ characteristics (Mardani-Aghabaglou et al., 2013). Due to the lower porosity of glass aggregate, ultrasonic pulse velocity was increased (Mardani-Aghabaglou et al., 2015). Wang et al. (2016) also found the ultrasonic pulse velocity of glass sand replacement is higher than control concrete. The ultrasonic pulse velocity increased with glass sand replacement. Large amounts of  $\text{SiO}_2$  and  $\text{Al}_2\text{O}_3$  were present in glass sand which dissolved large amounts of Si and

Al, Si and Al were needed for polyreactions. The addition of glass sand made more densely microstructure; hence, pulse velocity increased. Hunag et al. (2015) described increased ultrasonic pulse velocity with increasing replacement level of waste LCD glass. The unit weight of LCD glass sand was less than that of natural sand. Small particle and large volumes of LCD glass filled the internal voids in concrete effectively.

### 2.2.2.3. Durability of concrete

#### (a) Alkali-silica reaction

Alkali-silica reaction expansion was studied by several researchers with different types of glass and levels of replacement. Glass particle size also has significant impact on alkali-silica reaction. A scanning electron microscope image of glass sand is shown in Figure 2.11.

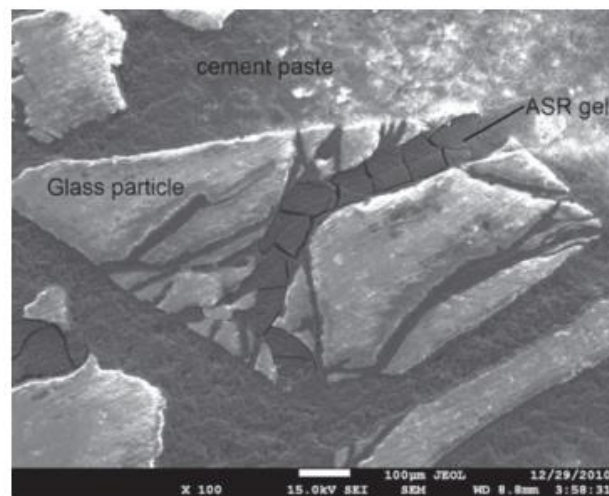


Figure 2.11 Scanning electron microscope image of clear glass (Du and Tan, 2013)

#### *Effect of glass particle size*

The particle size of glass sand is a critical factor influencing the reactivity. No excessive expansion was noticed when the particle size was less than 1 mm, which was an indication of no reaction between glass sand and alkalis in the pore solution (Yuksel et al., 2013). However, glass sand particle size of 0.150 mm to 1.18 mm showed lower expansion, whereas coarser

glass particle size greater than that showed significant expansions (Fischer et al., 2010). ASR did not occur at the aggregate-paste interface (Fischer et al., 2010). ASR expansion occurred in the pre-existing cracks in the interior of glass particles (Afshinnia and Rangaraju, 2015b). The accessibility of cracks reduced and the penetration of pore fluid became more difficult due to lower particle size of glass sand (Afshinnia and Rangaraju, 2015b). ASR expansion was found to be increased continuously with increasing size of glass sand (Lee et al., 2011; Du and Tan, 2013).

The minimum and maximum expansion occurred at 0.150 mm and 2.36 mm, respectively. ASR expansion started decreasing from 2.36 mm to 0.150 mm due to pozzolanic reaction. The pozzolanic reaction occurred between silica in small-particle glass sand and  $\text{Ca}(\text{OH})_2$ , a cement hydration product. The product of pozzolanic reaction does not show swelling in nature due to the low  $\text{SiO}_2/\text{CaO}$  ratio. Internal cracks were more prominent in large particle size, which initiated ASR gel. On the other hand, Du and Tan (2014b) reported that ASR expansion green glass sand increased with the increase in glass sand size up to 1.18 mm and after that (2.36 mm) it reduced. This may be due to the larger surface area of smaller glass sand which occurred ASR most readily and consequently formed more expansion (Figure 2.12).

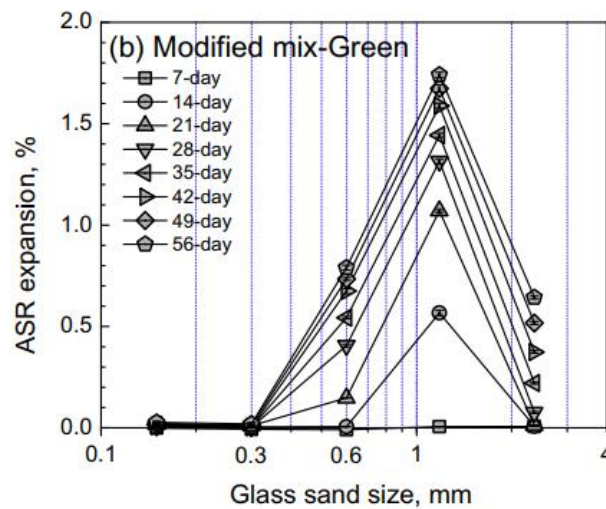
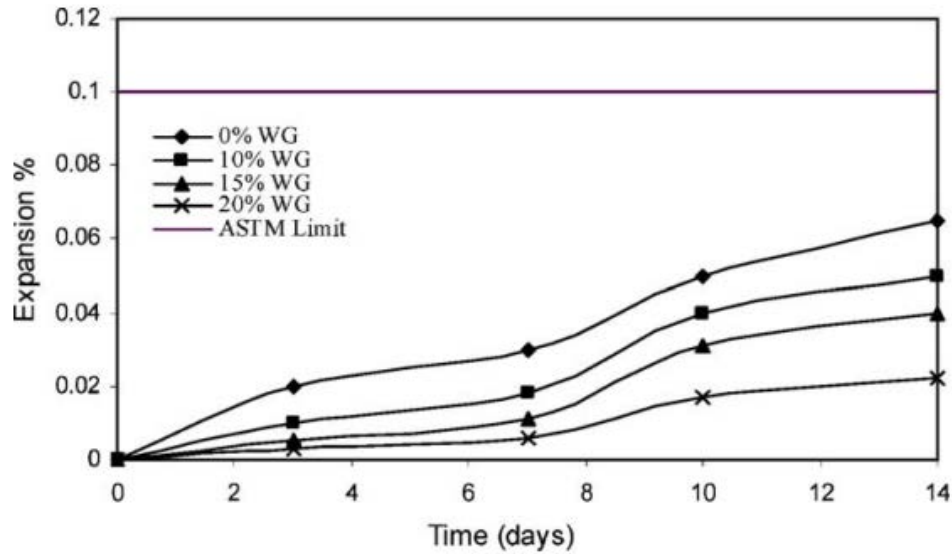


Figure 2.12 Effect of particle size on ASR expansion (Du and Tan, 2014b)

### ***Effect of glass content***

ASR expansion was found to be closely related to the proportion of glass particles in the mixture. An increase in glass content as sand replacement resulted in an increase in ASR expansion (Taha and Nounu, 2009; Ling et al., 2011; Limbachiya, 2009; Yuksel et al., 2013; Degirmenci et al., 2011; Topçu and Canbaz, 2004; Du and Tan, 2013; Lam et al., 2007; Ling and Poon, 2012). Degirmenci et al. (2011) reported that 100% replacement exceeded the 0.10% limit at 21 days which was considered a potentially deleterious expansion. However, ASR expansion was reported to be below 0.1%, which is the boundary for innocuous behaviour, according to ASTM C 1260 specification (Limbachiya, 2009; Shayan and Xu, 2004). Conversely, Chen et al. (2006) reported that E-glass (microscopically thin, transparent coating) content indicated innocuous behaviour and expansion reduced as E-glass content increased. No potentially deleterious expansion was found in the specimen. An increase in E-glass content suppressed ASR expansion due to the pozzolanic effect of fine particles. A clear reduction in the ASR expansion was noticed with the increase in waste glass content (Figure 2.13) (Ismail and Al-Hashmi, 2009; Kim et al., 2015; Aly et al., 2012). This reduction was related to the shortage of available alkali in the cement hydration process due to lime consumption. Similar reasons were also reported in other studies (Chen et al., 2006; Metwally, 2007).



**Figure 2.13 ASR expansion of waste glass (Ismail and Al-Hashmi, 2009)**

Du and Tan (2013) reported that ASR expansion increased substantially with increasing content of glass sand for clear glass sand. A significant micro-crack formed during the crushing process was noticed only in clear glass sand. However, brown and green glass sand was found to be innocuous regardless of the replacement level due to insignificant or absence of micro-cracking. Another study Du and Tan (2014a) found decreased ASR expansion with glass sand content. The calcium ion dissolved from soda-lime glass led to non-swelling ASR gel. Secondary C-S-H gel assisted in developing a densified ITZ microstructure with less porosity.

### ***Effect of glass colour***

The colour of the glass affects alkali-silica reaction (ASR). The green glass showed better resistance to ASR. The presence of chromium oxide ( $\text{Cr}_2\text{O}_3$ ) in green glass resulted in a decrease in the alkali-silica expansion which was added to the glass for greenish hue (Topçu and Canbaz, 2004; Park and Lee, 2004; Jin et al., 2000; Yuksel et al., 2013; Degirmenci et al., 2011; Du and Tan, 2013). Prezzi et al. (1997) noted that the expansion pressure resulting from electrical double-layer repulsion was inversely proportional to the ionic valence. The gel

having  $\text{Cr}^{3+}$  appeared to be less expansive, and the expansion rate decreased with an increase in  $\text{Cr}_2\text{O}_3$  (Jin, 1998). Du and Tan (2013) reported that brown glass sand exhibited less ASR expansion as green glass sand.

In contrast, Dhir et al. (2009) reported that green glass produced a large amount of expansion. They also noted that different coloured glass was not the only influencing factor in ASR expansion. Variations in the manufacturing process would influence the level of internal stress, and consequently, rates of leaching and dissolution of the glass. Dhir et al. (2009) reported that flint glass sand showed the least expansion. Another study Du and Tan (2014b) also found that green glass showed much higher ASR expansion than brown glass in the long term. This finding was also supported by Idir et al. (2010). In general, it took time to show a noticeable expansion. However, Park and Lee (2004) found that brown glass made up of  $\text{Fe}_2\text{O}_3$  showed higher expansion compared with green glass (Figure 2.14). Flint glass sand was found to be more expansive compared with green glass Yuksel et al. (2013).

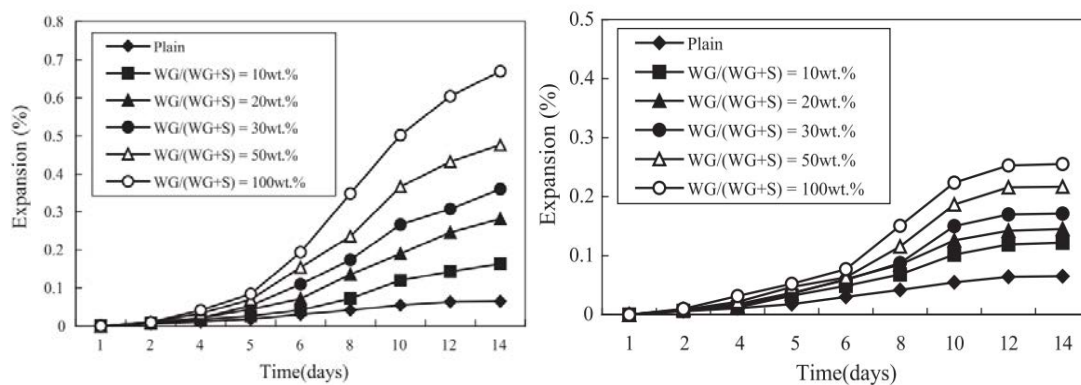


**Figure 2.14 Expansion of mortar bar with (a) brown glass (b) green glass (Park and Lee, 2004)**

White glass sand was found to be the most detrimental colour of aggregate for alkali-silica reaction (Topçu and Canbaz, 2004). According to their study, white glass sand exhibited the most significant expansion. More silicates were found in white glass sand compared with other

coloured glass sand. Degirmenci et al. (2011) reported that white glass exhibited the highest ASR expansion followed by brown glass and green glass, respectively. The mixed-coloured glass sand showed similar ASR expansion as single-coloured green or brown glass (Du and Tan, 2013).

### ***Effect of glass type***

The nature of glass reactivity is an important factor in its beneficial using in concrete (Limbachiya, 2009). E-glass exhibited a reduction in ASR expansion with an increase in E-glass content in the specimen. The equivalent alkali content of E-glass was 0.8, which was much lower than the container glass resulted in a reduction in ASR expansion (Chen et al., 2006). The swelling capacity of the ASR gel depends on its chemical composition, basically on the ratio of  $\text{CaO}/(\text{SiO}_2 + \text{Na}_2\text{O})$  (Corinaldesi et al., 2016). Saccani and Bignozzi (2010) found that soda-lime glass (from beverage containers cullet) showed negligible expansion, while lead silicate glass (from tableware, giftware and home décor items in crystal) exhibited expansion in ASR. Borosilicate glass from pharmaceutical containers cullet showed different behaviour depending on its colour. For example, amber coloured glass hardly exceeded the limit, while uncoloured glass tended to expand.

The ASR expansion of treated funnel glass was relatively higher than crushed beverage glass due to higher solubility of treated funnel glass (Ling and Poon, 2012). A large amount of dissolved glass was available in the solution to form ASR gel (Ling and Poon, 2012; Saccani and Bignozzi, 2010). Aly et al. (2012) found that the hybrid incorporation of waste glass and nano-silica is more efficient than the use of waste glass alone.

### ***Effect of time duration***

Flint and green glass did not show reactivity up to 50% replacement at one year, which was lower than 0.04%. However, a continuous increase in expansion was noticed for flint glass

sand at three years duration with the same replacement level (Yuksel et al., 2013). Another study Du and Tan (2013) reported that brown glass sand exhibited less alkali reactivity in the long term, for instance, at 63 days. However, cracks were observed in the green glass particles at 63 days, while no cracks were noticed at 28 days. Taha and Nounu (2009) found that concrete continued to expand after 52 weeks and was considered a potential risk. However, expansion was within the allowable limit of non-expansive aggregate at 52 weeks. Glass showed a slow and delayed reaction to alkalis (Serpa et al., 2013a).

### **(b) Sorption**

Sorption is an important mode of moisture transport which characterizes the affinity of a porous material to absorb and transmit water by capillarity. Water sorption depends on initial water content, temperature and the nature of material used in concrete. The intrusion of moisture in concrete is one of the most physical phenomena for structures in long-term durability. Moisture movement in concrete over time can damage concrete structures under freeze-thaw attack, sulphate attack and rapid chloride penetration. Moisture transport can occur in three modes: capillary absorption (sorption); diffusion; and permeation (Nassar and Soroushian, 2012). Use of pozzolanic material in concrete can improve structure through the refinement of the pore size, blocking off the consecutive capillary pores and reduction of the pore volume (Basheer et al., 2001).

A reduced sorptivity coefficient was observed when waste glass sand was used as a sand replacement. The favourable effect of waste glass sand grading improved the particles packing and almost certainly reduced the quantity of capillary pores (Pereira de Oliveira et al., 2008). Mohammadinia et al. (2019) found a decrease in capillary rise of water which was mainly due to low water absorption of gravel-sized glass particles.

### **(c) Rapid chloride penetration test**

Waste glass sand also resulted in a reduction of chloride ion penetration (Chen et al., 2006; Du and Tan, 2014a; Wang et al., 2014; Mardani-Aghabaglou et al., 2015). Du and Tan (2014a) observed that concrete with 30% and 45% glass sand showed moderate penetration resistance whereas concrete with 75% glass sand produced low permeable concrete. Chloride resistance tended to improve with an elongated curing age (Du and Tan 2014a) as well as with increased proportion of glass sand in concrete (Du and Tan, 2014a; Mardani-Aghabaglou et al., 2015). However, Chen et al. (2006) reported that concrete with glass sand (particle size greater than 75 $\mu$ m) did not have pozzolanic activity because of its specific surface area and thus did not exhibit a positive influence on concrete. De Castro and De Brito (2013) recapitulated that microstructure of concrete was usually governed by the quality of cement, therefore there was no significant resistance to chloride ion penetration. Nevertheless, Wang et al. (2014) concluded that glass sand concrete governed compact internal structure compared with control concrete and thus exhibited lower/reduced porosity. Consequently, concrete mixed with glass sand can provide better resistance to water erosion.

**Table 2.6 Overview of rapid chloride penetration test of glass sand concrete as aggregate replacement**

Ref	Percentage	W/cm	Size	Curing period (Days)	Penetrability of glass sand concrete
(Du and Tan, 2014)	30%, 45% & 60%	0.49,0.3 8,0.32	ASTM C33	28, 90	Moderate to Low
(Wang et al., 2014)	20%, 40%, 60% & 80%	.485	No 8	28	Moderate to Low
(Chen et al., 2006)	10%, 20%, 30%, 40% & 50%	0.68, 1	>75 $\mu$ m		Very Low

(Mardani-	15%, 30%, 45%,	0.45	ASTM	28	Very Low
Aghabaglou et al., 2015)	60%		C33		

#### **(d) Drying shrinkage**

Drying shrinkage refers to the change in volume during hydration due to the loss of capillary water as concrete ages. It is a phenomenon that causes an increment in tensile stress which may lead to cracking at the edges of the concrete structure. In hardened cement concrete, drying shrinkage is a widespread problem. However, the addition of glass in concrete can abate shrinkage (Dumitru et al., 2010; Hunag et al., 2015). Dumitru et al. (2010) found lower drying shrinkage for concrete using crushed glass as partial sand replacement for both 56 and 90 days. The reduction is noteworthy with the increment of glass sand replacement ratios (Limbachiya, 2009). Besides replacement ratios, w/c ratio is an influencing factor in concrete mixtures. Glass sand concrete with low w/c ratio could reduce drying shrinkage because of higher elastic modulus and negligible water absorption of glass sand (Du and Tan, 2014a). The higher w/c ratio makes the concrete porous and prone to crack.

In contrast, Shayan and Xu (2004) observed that the addition of glass sand (coarse sand 50% and fine sand with different ratios) resulted in an increase in shrinkage compared with reference concrete. However, it was within the margin of 0.075%, specified by Australian Standard AS 3600. Another study Shayan and Xu (2006) showed the same positive trend of shrinkage. De Castro and De Brito (2013) reported that concrete mixed with fine and coarse glass aggregate exhibited lower drying shrinkage compared with concrete with fine sand and concrete with coarse sand separately.

Moreover, drying shrinkage of RGS mortar showed a similar reduction trend compared with RGS concrete (Ling et al., 2011; Ling and Poon, 2013). Ling et al. (2011) showed 100% glass sand replacement produced 17% lower drying shrinkage compared with reference mortar at 112 days. Other substitutions also satisfied the specification of Australian Standard AS 3600 (Ling and Poon, 2013; Tan and Du, 2013). In contrast, Penacho et al. (2014) exhibited the opposite trend: 100% glass sand increased drying shrinkage about 19%. However, Ling and Poon (2011) reported that glass sand mortar could reduce drying shrinkage from 1 to 85 days but the control mortar exhibited the lowest shrinkage beyond 85 to 112 days. Other research Ling and Poon (2012) showed a positive influence of long-term effect on drying shrinkage. Drying shrinkage is found to be reduced due to lower absorption capacity of glass sand in comparison with natural river sand and impermeable properties of glass.

#### **(e) Sulphate attack**

Sulphate attack occurs when sulphate ions come in contact with cement paste in concrete. Sulphate ions penetrate the specimen to form crystals in the pores, and therefore, the weight is increased (Wang et al., 2016). The new crystals occupy space and cause cracks. The addition of E-glass content improved sulphate resistance of concrete (Chen et al., 2006). E-glass addition in concrete caused weight reduction and strength loss due to lower porosity. Ling et al. (2011) concluded that the glass had a higher degree of resistance to acid attack than that of river sand in mortar. Hunag et al. (2015) found glass sand had better resistance to sulphate attack. However, normal-weight concrete was found more effective. Wang et al. (2016) emphasised that glass sand substitution caused better resistance to sulphate attack with a more complete and rapid polymerisation reaction. Thus, glass sand substitution would be beneficial to structures constructed near seawater, wastewater and sulphate soil.

#### **(f) Water absorption**

Water absorption has a significant effect on concrete durability. Concrete with low water absorption can provide better protection to reinforcement within it (Nwaubani and Poutos, 2013). Due to its impermeable nature, the use of waste glass in concrete can reduce the permeability of concrete (Taha and Nounu, 2008). The quantity of absorbed water in concrete was reduced with an increase in recycled glass. Glass has a negligible water absorption nature. Hence, the total demand for water absorption was reduced in concrete with glass sand. Less water demand can hinder the continuity of the microcracks inside the concrete and restrict the movement of ions and moisture inside the concrete (Taha and Nounu, 2008).

As aggregate, rough natural sand shows strong bonding between cement and concrete rather than smooth surface glass aggregate. ASR expansion causes cracks in concrete and this makes the concrete less durable than typical concrete. Small glass size and optimum replacement levels ensure a significant role in ASR expansion as well as strength. However, no concrete conclusion regarding particle size and level of replacement was found when waste glass was used as a fine aggregate replacement in concrete.

## **2.2.3 Waste glass as cement replacement**

### **2.2.3.1 Fresh properties**

#### **(a) Slump test**

##### ***Concrete***

The performance of concrete containing waste glass as partial replacement of cement has been investigated by several researchers (Soliman and Tagnit-Hamou, 2016; Khatib et al., 2012; Aliabdo et al., 2016; Shruthi et al., 2015; Nassar and Soroushian, 2012; Bajad et al., 2011; Nwaubani and Poutos, 2013). A systematic increase in slump was found as glass powder increased in the mixture (Khatib et al., 2012; Kamali and Ghahremaninezhad, 2015; Soliman

and Tagnit-Hamou, 2016; Nassar and Soroushian, 2012) (Figure 2.15). The increase in slump indicated an improvement in workability, and lower water demand of glass powder in concretes (Kamali and Ghahremaninezhad, 2015; Soliman and Tagnit-Hamou, 2016). Three main factors are responsible for the outcomes of concrete workability: geometry; smoothness; and the surface area of glass particles (Afshinnia and Rangaraju, 2016). Due to the smooth surface of glass powder, workability was improved due to the smooth surface of glass powder (Soliman and Tagnit-Hamou, 2016), as the geometry- related issues were insignificant in the case of glass powder (Afshinnia and Rangaraju, 2016). Increasing glass content could be a reason for cement dilution, which tended to reduce the formation of cement hydration products in the initial minutes of mixing. Consequently, less cement hydration caused insufficient products to bridge various particles together (Soliman and Tagnit-Hamou, 2016). In contrast, a slight reduction in slump was noticed with an increase in glass powder content (Shayan and Xu, 2006; Shruthi et al., 2015; Bajad et al., 2011) due to the non-spherical and rough geometry of waste glass powder. The cement content decreased as the quantity of glass powder increased in the mixture. A limited portion of cement was available to provide a lubricating effect in the mix, affecting the workability (Bajad et al., 2011).

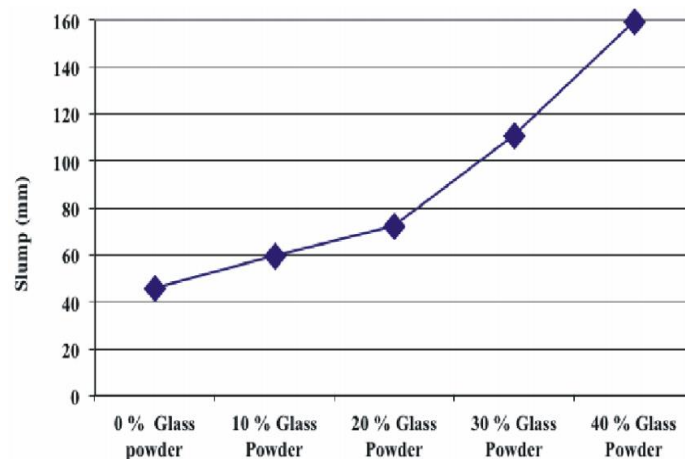


**Figure 2.15 Slump of concretes with glass powder as cement replacement (Khatib et al., 2012)**

## ***Mortar***

A flow table test is a method to determine the workability of mortar. The workability of mortar was found to reduce with an increase in glass powder content (Nwaubani and Poutos, 2013). Reviews Islam et al. (2017) confirmed the increase in workability with glass powder addition. However, a reduction of flow value was observed when fly ash was replaced by glass powder due to coarser particle size and irregular shape of glass powder (Lu and Poon, 2018). Another study Afshinnia and Rangaraju (2015a) observed that the flow behaviour of mortar improved with coarse glass powder (lower surface area) compared with fine glass powder (smooth surfaces with fractured faces). Use of glass cullet improved the workability in mortar because of the inherent smooth surface and negligible water absorption of glass. Cement was needed in reduced amounts to coat the cullet as the large particle size of glass cullet, i.e., smaller surface. High fluidity improved flow due to more available cement paste available in the mixture (Lu and Poon, 2018).

## **(b) Density**

### ***Fresh density***

The fresh density of concrete was reduced as the amount of glass aggregate in concrete increased (Taha and Nounu, 2009; Khatib et al., 2012). This reduced density in concrete was attributed to the lower specific gravity of waste glass (Afshinnia and Rangaraju, 2016; Soliman and Tagnit-Hamou, 2016; Nassar and Soroushian, 2012).

### ***Hardened density***

An increase in bulk density (dry) and bulk density (after immersion) was observed when milled waste glass was used as a partial cement replacement (Nassar and Soroushian, 2012). This increase accelerated the conversion of calcium hydroxide ( $\text{Ca(OH)}_2$ ) to calcium silicate hydrate

(C-S-H) due to the pozzolanic reaction of waste glass powder in concrete. The specific gravity of the resulting C-S-H (2.3-2.6) is somewhat higher than that of  $\text{Ca}(\text{OH})_2$  (2.24) (Nassar and Soroushian, 2012). Besides, the filling effect of microscopic glass powder improved particle packing in concrete (Nassar and Soroushian, 2012; Nwaubani and Poutos, 2013). However, Shayan and Xu (2006) found fluctuating dry densities arose due to lack of full compaction (100%).

### **(c) Air content**

The air content of concrete was affected when glass powder was used as a cement replacement in concrete. Finely ground glass powder showed higher air content compared with control concrete as well as mineral aggregates (Afshinnia and Rangaraju, 2016).

### **(d) Setting time**

Glass powder mortar did not exhibit a significant difference in the initial and final setting time (Kamali and Ghahremaninezhad, 2016). However, a slightly decreasing trend was found in cement paste containing waste glass powder.

## **2.2.3.2 Mechanical strength**

### **(a) Compressive strength**

Strength of concrete with glass powder as cement replacement depends on the particle size of glass powder, amount of glass powder and duration of curing. Concrete with a glass particle size of less than  $90\mu\text{m}$  showed a notable increase in strength at 28 days (Patil and Sangle, 2013; Nwaubani and Poutos, 2013). Strength was found to be equal or even greater to that of control concrete in between 28 and 90 days. Initially, a reduction in strength was observed compared with control concrete (Al-Zubaidi and Tabbakh, 2016; Lee et al., 2013; Khatib et al., 2012; Gunalaan and Kanapathy, 2013). Strength of concrete with glass powder increased with curing

time. Strength development at later curing ages showed a pozzolanic reaction. Several studies found that compressive strength increased gradually until the optimum replacement level and showed a better result than any other replacement (Al-Zubaidi and Tabbakh, 2016; Lee et al., 2013; Khatib et al., 2012; Gunalaan and Kanapathy, 2013; Soliman and Tagnit-Hamou, 2016; Aliabdo et al., 2016; Nwaubani and Poutos, 2013; Du and Gao, 2014; Afshinnia and Rangaraju, 2015b; Patil and Sangle, 2013; Dhirendra et al., 2012) (Figure 2.16). This increase in compressive strength was attributed to the pozzolanic reaction, which can improve the quality of cement matrix in concrete (Bajad et al., 2011). Beyond the optimum replacement level, strength started to decline. A systematic reduction in strength was observed with an increase in glass powder content (Al-Zubaidi and Tabbakh, 2016; Lee et al., 2013; Khatib et al., 2012; Gunalaan and Kanapathy, 2013; Soliman and Tagnit-Hamou, 2016; Aliabdo et al., 2016; Bhat and Rao, 2014). It could be due to an increase in w/c with constant water in the mix. Glass powder does not utilise water for the reaction. Therefore, the compressive strength increased when constant w/c was maintained for all mix (Bhat and Rao, 2014).

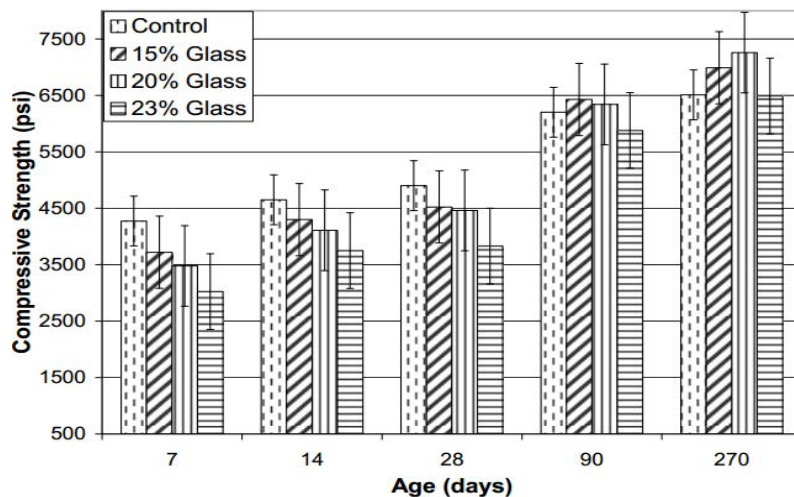


**Figure 2.16 Compressive strength test result glass powder (Nassar and Soroushian, 2012)**

**(b) Flexural strength**

Shayan and Xu (2006) found a reduction in flexural strength when glass powder was used as a cement replacement. Concrete with a mixture of glass powder and glass sand provided the lowest strength. A decrease was noticed in flexural strength compared with control concrete. But the recycled glass had the potential to reach a long-term effect. The long-term effect can be attributed to enhancing the binding qualities of the calcium silicate hydrate, which is formed during the pozzolanic reaction of glass. The pozzolanic reaction improved the interfacial transition zone and refined the capillary pores in concrete microstructure (Nassar and Soroushian, 2011; Nassar and Soroushian, 2012). However, mortars with glass powder demonstrated better strength compared with control concrete when used as a cement replacement (Kamali and Ghahremaninezhad, 2015).

### **(c) Tensile strength**

The increasing trend was observed along with the inclusion of RGP until the optimum percentage, i.e., maximum strength, and after that decreased with an increase in glass powder content (Aliabdo et al., 2016).

### **(d) Ultrasonic pulse velocity**

The ultrasonic pulse velocity was found to be reduced with an increase in glass powder content in concrete as a cement replacement (Khatib et al., 2012).

## **2.2.3.3 Concrete durability**

### **(a) Chloride ion penetration**

The durability of reinforced cement concrete is enormously/extremely dependent on the resistivity to the ingress of chloride ion in the concrete. Chloride ion intrusion in concrete is one of the most natural phenomena for structures which are constructed near a shoreline (Cement Concrete & Aggregate Australia, 2009). However, cement type, replacement ratio,

curing time and w/c ratio have an influence on chloride ion penetration in concrete (Aggarwal and Siddique, 2014). The addition of glass powder in concrete has significant improvements against concrete permeability compared with control concrete. Concrete modified with glass powder caused a reduction in chloride ion penetration. Schwarz et al. (2008) and Nassar and Soroushian (2011) found that an elongated curing time could improve the chloride resistance of concrete. They noted that glass powder concrete enhanced resistance to chloride ion penetration by pore refinement and pore-blocking with the C-S-H gel formation during the pozzolanic reaction. (Nassar and Soroushian, 2012) investigated the rapid chloride penetration test (RCPT) with low w/cm ration and high w/cm ratio. Glass powder concrete did not show much difference, however, a low w/cm ratio showed similar a reduction trend of high w/cm ratio.

Du and Tan (2017) explained the reason behind improved resistance. The resistivity of concrete depended on porosity, pore solution and pore structure. Cement pore solution is made up of hydration products, i.e.,  $\text{Na}^+$ ,  $\text{K}^+$ ,  $\text{Ca}^{2+}$  and  $\text{OH}^-$ . When glass powder was used as a partial cement replacement, these hydration products are consumed to produce C-S-H gels with low Ca/Si ratio. Consequently, the amount of ion is reduced in the pore solution thus enhancing microstructure and reducing the permeability of concrete. Another investigation Carsana et al. (2014) reported that concrete with ground glass exhibited improved chloride ingress similar to fly ash concrete. Shayan and Xu (2006) and Nassar and Soroushian (2012) recommended glass powder as a cement replacement to construct pavements, submarine structural design, and parking areas which are often affected by chloride ions from de-icing salts.

**Table 2.7 Influence of different parameters on rapid chloride penetration test**

Ref	Percentage	W/cm	Size	Curing period (days)	Penetrability of glass powder concrete
(Schwarz et al., 2008)	10%	0.42	-	28, 56, 90	High - moderate – low
(Nassar and Soroushian, 2011)	15%, 20%, 23%	0.45	25 $\mu m$	90, 450	Moderate – low
(Nassar and Soroushian, 2012)	20%	0.38 & 0.50	13 $\mu m$	-	Low (w/cm = 0.38) Moderate ( w/cm =0.50)
(Shayan and Xu, 2006)	20%, 30%	0.49	<10 $\mu m$	220,380	Moderate –Low (20%) Low-Low (30%)
(Carsana et al., 2014)	30%	0.5	400 $m^2/kg$ 600 $m^2/kg$	28	50 42
(Kamali and Ghahremaninezhad, 2015)	5%,10%,15%, 20%	0.5	8.4 $\mu m$	28-56-91	High-Moderate-Moderate (5%) Moderate-Moderate-Low (10%) Moderate-Low-Very Low (15%) Moderate-Low-Very Low (20%)
(Du and Tan, 2017)	15%, 30%,45%, 60%	0.486	ASTM C33		Very low

### (b) Water absorption

It was found that the amount of water absorption was more when recycled glass was used in powder form compared with the conventional control mix (Taha and Nounu, 2009; Nassar and Soroushian, 2012). Water absorption increased with increased glass powder content (Nwaubani and Poutos, 2013). This reduction might be attributed to the pozzolanic reaction of glass

powder, which can refine pore structures and decrease connectivity. However, the pozzolanic reaction would be limited by other cement hydration products, such as portlandite at higher glass powder content (Du and Gao, 2014).

In mortar samples, a reduction in water absorption was noticed except that the brown glass was increased due to increased porosity. The waste glass might have filled the microcracks and the pores in the mortar leading to decreases in voids otherwise occupied with water (Al-Zubaidi and Tabbakh, 2016).

### **(c) Sorption**

Milled waste glass concrete exhibited significant reductions in the rates of absorption and cumulative water sorption (Nassar and Soroushian, 2012; Nassar and Soroushian, 2011; Du and Tan, 2017). Waste glass may be attributed to the availability of more CH at the old ITZ of recycled aggregate to undergo pozzolanic reaction. The formation of additional C-S-H refined the pore microstructure and created a denser and less permeable microstructure (Nassar and Soroushian, 2012). Water sorption reflected the ability of water uptake rate into unsaturated concrete. The resistance against water sorption of waste glass powder concrete was attributed to the reduced size and connectivity of pores in the paste matrix and ITZ. However, Du and Tan (2017) found slightly increased water absorption with increasing glass powder volume, because of lower effective water-to-cement ratio at higher cement replacements rates. Schwarz et al. (2008) noticed high sorptivity at a later age but reduced sorption at an early age.

Mortar with RGP also reduced the rate of water absorption due to accelerated hydration and the creation of more hydration products (Mirzahosseini and Riding, 2014). Glass cullet can fill in higher porosity at later ages as glass cullet reacts slower than cement. Mirzahosseini and Riding (2014) also found green glass had a higher tendency to participate in pozzolanic reactions compared with clear glass. Water absorption of green glass was found to reduce to

some extent more than clear glass. In contrast, due to the similar fineness of glass powder and cement clinker, no influence on sorptivity was reported (Matos and Sousa-Coutinho, 2012).

#### (d) Alkali-silica reaction

Cement, in combination with glass powder, had a low risk of ASR deterioration (Afshinnia and Rangaraju, 2015a) (Figure 2.17). ASR expansion of glass powder was reduced compared with the control mortar bars. Smaller particle sizes offered slightly better results than coarser particles. Cement with 20% glass powder showed a better reduction in ASR expansion than cement with 10% glass powder.

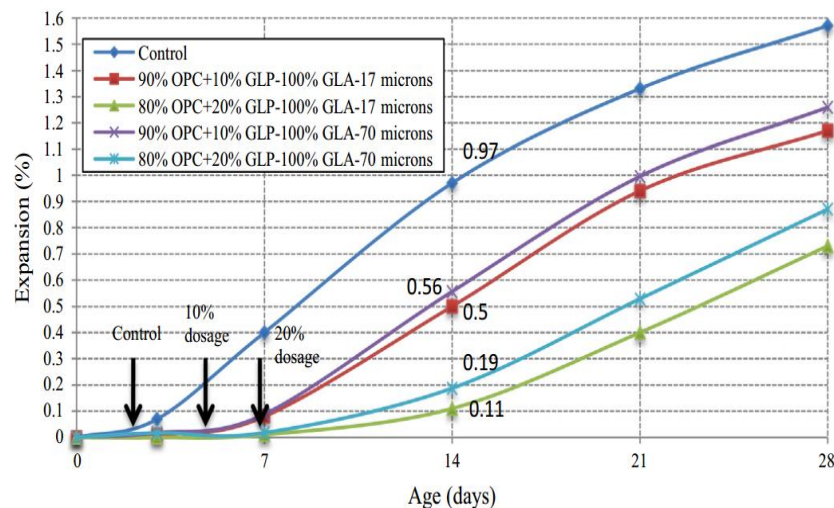


**Figure 2.17 Mortar bar expansion versus time for samples containing glass powder as a cement replacement (Afshinnia and Rangaraju, 2015a)**

The ASR of mixtures with glass powder was noticed to decrease (Kim et al., 2015) by increasing the amount of glass powder as cement replacement (Figure 2.18). The expansion of all mixtures except the control sample was within the permissible limit at 16 days. Kim et al. (2015) concluded that waste glass could reduce ASR expansion as effectively as by fly ash.

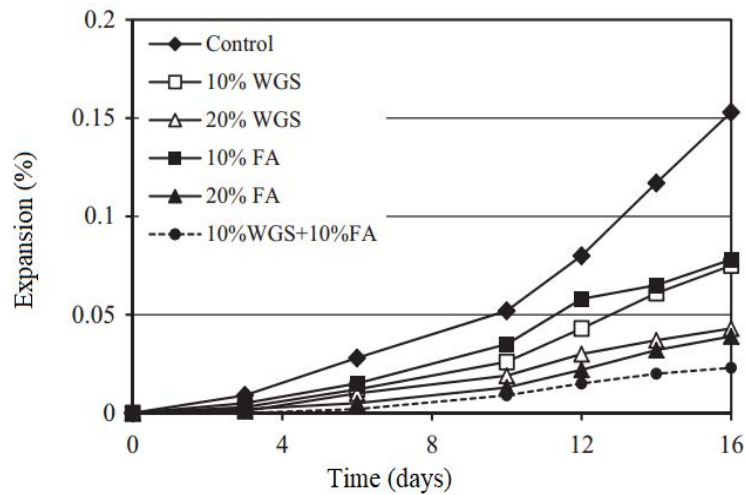


**Figure 2.18 ASR expansion of mortar bar containing glass sludge and fly ash (Kim et al., 2015)**

ASR expansion indicated innocuous behaviour of mortar containing waste glass with a median particle size of  $13 \mu\text{m}$  (Nassar and Soroushian, 2012). According to ASTM C 1260, ASR expansion greater than 0.20% at 16 days indicates deleterious behaviour, while less than 0.10% at 16 days indicates innocuous expansion.

### ***Effect of using supplementary cementitious materials in ASR mitigation method***

Using fly ash together with waste glass sand in the mixture led to a more stable behaviour indicating no deleterious ASR expansion (Pereira de Oliveira et al., 2008; Kim et al., 2015). Topçu and Canbaz (2004) found that use of fly ash or  $\text{Li}_2\text{O}_3$  increased resistance against ASR. Topçu and Canbaz (2004) also described the mechanism of reducing ASR expansion by using fly ash in the mixture. According to their study, the addition of fly ash in the mixture caused a reduction in soluble alkaline concentration and hence decreased the pH of the pore solution. A reduction in pH reduced the reactivity between the alkalis of cement and the silica of aggregate as well. The pozzolanic reaction was formed due to the addition of fly ash and therefore, the permeability of mortar was found to be lower resulting in a reduction in water penetration.

ASR gel was unable to swell due to lack of water penetration and consequently, expansion was prevented. Alkali content of fly ash was reported lower than that of cement. However, Topçu and Canbaz (2004) found  $\text{Li}_2\text{O}_3$  to be a more significant admixture compared with fly ash and that it performed better with elapsed time. Ling et al. (2011) found metakaolin to be an effective suppressor to mitigate ASR expansion. The increase in metakaolin content resulted in a gradual reduction in ASR expansion in the waste glass mortar. On the contrary, Lee et al. (2011) noticed that fly ash was more efficient in reducing ASR expansion compared with metakaolin. However, both fly ash and metakaolin can effectively mitigate ASR expansion due to pozzolanic reaction. This led to the formation of C-S-H that could take up alkalis and subsequently led to the reduction of ASR expansion.

Another study Lam et al. (2007) found that pulverised fuel ash was a better ASR suppressor than metakaolin with the same glass content. Metakaolin was needed at 5% to suppress ASR expansion effectively whereas pulverised fuel ash was needed at only 2.5%. The inclusion of fibre – for instance, steel fibre and polypropylene reinforcing fibre – decreased ASR expansion with an increase in the fibre content (Park and Lee, 2004).

The combination of cement, fly ash or slag cement, and waste glass sand attributed to a lower risk of deleterious ASR expansion (Du and Tan, 2014a). They concluded that the use of fly ash and slag cement reduced the alkalinity of the pore solution and restricted transport properties of the cementitious system due to lower porosity and denser ITZ section. The use of  $\text{Ca}(\text{OH})_2$  to form additional C-S-H led to a pozzolanic reaction instead of forming ASR gel. Addition of ASR suppressors such as slag, metakaolin, glass powder and  $\text{Li}_2\text{O}_3$  improved the mitigating ability to reduce ASR expansion (Taha and Nounu, 2009).

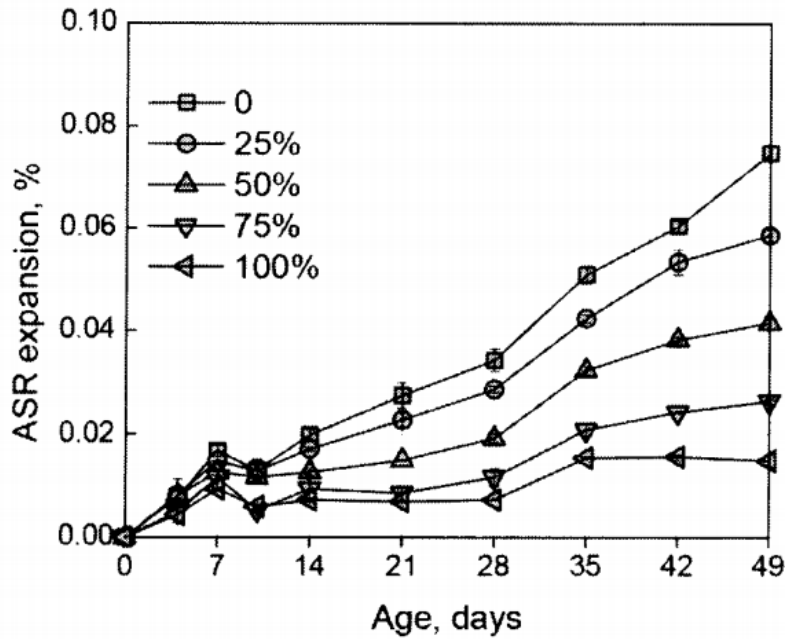


**Figure 2.19 ASR expansion of waste glass sand concrete with 60% slag replacing cement (Du and Tan, 2014a)**

Use of glass powder as an aggregate replacement showed significantly better performance in mitigating ASR expansions, compared with when glass powder was used as a cement replacement material (Afshinnia and Rangaraju, 2015a). The fine glass powders act as sacrificial particles that react with the alkaline pore solution in the matrix and consume available alkalis. Hence, the availability of alkalis reduces for the coarse aggregate to react with and makes them less vulnerable to ASR distress. However, (Schwarz et al., 2008) found that glass powder as a cement replacement material demonstrated the potential to reduce deleterious expansion and this reduction was found to be proportional to the content of glass powder.

### **(e) Pozzolanic reactivity**

#### ***Strength activity index***

The strength activity index is the ratio of a test mortar (containing SCMs) and control mortar (with 100 per cent Portland cement). A strength activity index is required to consider the waste glass powder as a pozzolanic material. According to ASTM C 618/ AS 3582.1, mortar with

supplementary cementitious material (SCM) should gain 75% strength of control mortar (without SCM) to be taken into account as a pozzolanic material at 28 days (ASTMC618, 2014; AS3582.1, 2016). In addition, mortar modified with glass powder should provide at least 85% strength of the control mortar at 90 days, according to EN 450-1 (Standards, 2012). Glass powder fulfils the limits of Class F and Class C pozzolanic materials at both of seven and 28 days according to standard ASTM C 618 (Aliabdo et al., 2016; Ismail and Al-Hashmi, 2009). The particle size of glass powder is an important parameter in characterising its pozzolanic properties (Afshinnia and Rangaraju, 2015a; Carsana et al., 2014). Afshinnia and Rangaraju (2015a) found that smaller particle size glass powder exhibited better pozzolanic behaviour and yielded better compressive strength under ambient curing temperatures than coarser glass powder. However, another study Afshinnia and Rangaraju (2015b) found that an increase in glass powder replacement was affected negatively in the strength activity index, as well as coarser glass particle size (Figure 2.20).

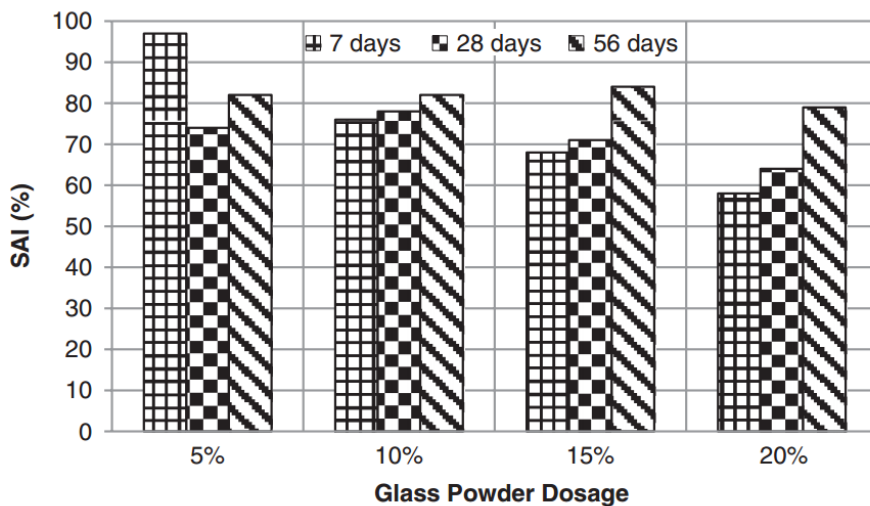


**Figure 2.20 Strength activity index of mortar cubes containing 70  $\mu\text{m}$  glass powder (Afshinnia and Rangaraju, 2015b)**

Mortar with more finely ground glass powder showed a slightly higher index compared with that of mortar with 10% silica fume (Carsana et al., 2014). E-glass particles also play an

important role in the strength activity index. The lower particle size of E-glass satisfied the strength requirement of pozzolanic material as proposed (Chen et al., 2006; Shao et al., 2000). (Bignozzi et al., 2015) conducted an activity index for several types of glass-blend cements including soda-lime glass, crystal glass, funnel glass and fluorescent lamp glass. The pozzolanic behaviour was found to be effective for soda-lime glass and funnel glass, whereas crystal glass showed a lower activity index. Hence, these outcomes clearly illustrated that finely ground glass powder could be considered as an effective pozzolanic material.

### ***Thermogravimetric analysis***

Thermogravimetric analysis (TGA) can be used to quantify the pozzolanic reaction. It can be calculated as a function of increasing temperature (with constant heating rate) or as a function of time (with constant temperature and/or constant mass loss). TGA is conducted to evaluate the  $\text{Ca(OH)}_2$  content of a cement paste having waste glass powder as cement replacement. The presence of  $\text{Ca(OH)}_2$  in cement mix is an indication of cement hydration as  $\text{Ca(OH)}_2$  is one of the products of cement hydration along with calcium silicate hydrate (Kamali and Ghahremaninezhad, 2015). The amount of  $\text{Ca(OH)}_2$  is determined using the mass loss in the TGA plot between 450 °C and 600 °C, which represents the typical temperature range of  $\text{Ca(OH)}_2$  decomposition (Aliabdo et al., 2016). The amount of  $\text{Ca(OH)}_2$  of cement paste increases over time as more cement is hydrated. However, the use of waste glass powder as a cement replacement reduced the amount of  $\text{Ca(OH)}_2$  (Aliabdo et al., 2016; Kamali and Ghahremaninezhad, 2015) (Figure 2.21).

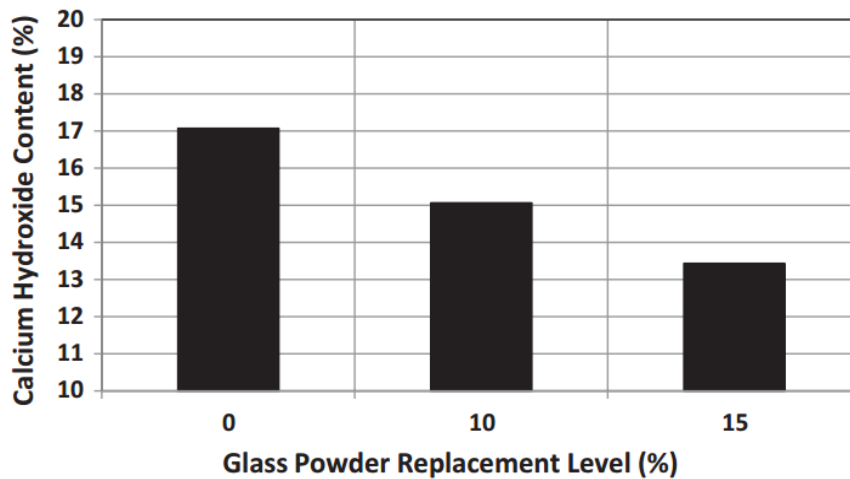


**Figure 2.21 Calcium hydroxide content of paste modified with glass powder (Aliabdo et al., 2016)**

This reduction can be a result of either the decrease in cement content (dilution effect) or the pozzolanic effect of glass powder present in cement paste (Afshinnia and Rangaraju, 2015a). The reduction percentage in  $\text{Ca(OH)}_2$  should be the same if a pozzolanic reaction does not take place (Aliabdo et al., 2016). In a pozzolanic reaction,  $\text{Ca(OH)}_2$  is used to produce additional calcium silicate hydrate and a reduction of  $\text{Ca(OH)}_2$  amounts in the cement paste (Rupasingle et al., 2014; Kamali and Ghahremaninezhad, 2016; Du and Tan, 2017). An increase in calcium silicate hydrate with a decrease in  $\text{Ca(OH)}_2$  also confirmed the increase in compressive strength (Aly et al., 2012). The pozzolanic reaction of waste glass powder as cement replacement was found to be prominent at a later age (Kamali and Ghahremaninezhad, 2016; Mirzahosseini and Riding, 2014). However, Du and Tan (2017) found that  $\text{Ca(OH)}_2$  became insufficient for pozzolanic reaction beyond a replacement of 30%. Coarse glass powder (i.e.,  $70 \mu\text{m}$ ) showed minimal pozzolanic behaviour when used as cement replacement (Afshinnia and Rangaraju, 2015b). Different curing temperatures showed a large impact on the pozzolanic reactivity of glass powder. Mirzahosseini and Riding (2014) confirmed that elevated temperature can accelerate the glass hydration reaction and show significant pozzolanic reaction.

A reduction was noticed in the  $\text{Ca(OH)}_2$  in mortar with waste glass. A hybrid combination of waste glass and nano-silica also showed decrease in  $\text{Ca(OH)}_2$  (Aly et al., 2012). Glass powder mortar with smaller particle size ( $17 \mu\text{m}$ ) exhibited better pozzolanic behaviour compared with the large particle size glass powder ( $70 \mu\text{m}$ ) (Afshinnia and Rangaraju, 2015a).

Waste glass powder can be used as a partial replacement of cement. There are variations in optimum replacement level as well as mix design. Glass powder size is also considered as an inevitable part in ASR expansion as well as strength.

### **2.3 Life cycle assessment**

Life cycle assessment (LCA) is a recognised method of estimating and evaluating the environmental impacts associated with the entire life cycle of a product. A “cradle to grave” LCA approach takes into account all the processes involved in raw materials extraction, raw materials processing, manufacture, distribution, use, repair, maintenance, disposal and recycling (Figure 2.22). In a “cradle-to-gate” approach, on the other hand, only specific stages in the life of a product are investigated. This process involves from raw materials extraction to manufacturing of the product (Figure 2.22). LCA is carried out based on the requirements of the international standards of the ISO 14.040 (Principals of Framework) (ISO14040, 2006) and ISO 14.044 (Requirements and Guidelines) (ISO14044, 2006).

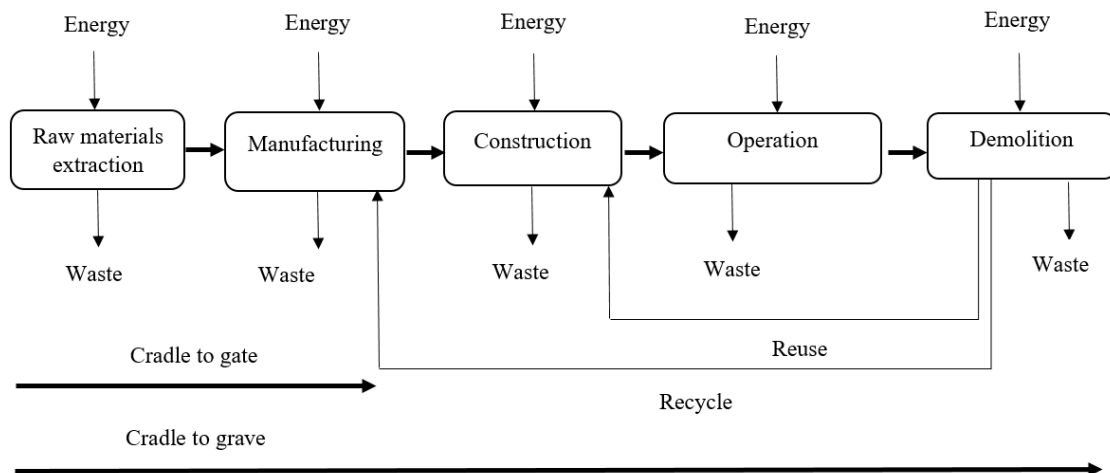


**Figure 2.22 Life cycle assessment, considering whole life cycle phases (Sivakugan et al., 2017)**

ISO 14.040 defines LCA as a methodology for assessing and evaluating the environmental aspects and potential impacts associated with a product by compiling an inventory of relevant inputs and outputs of a product system and interpreting the results of the inventory analysis and impact assessment phases (ISO14040, 2006). According to the ISO standards, the LCA methodology consists of four main analytical phases (Figure 2.23): (a) goal and scope definition; (b) life cycle inventory analysis (LCI); (c) life cycle impact assessment (LCIA); and (d) interpretation of results (Vieira et al., 2016).

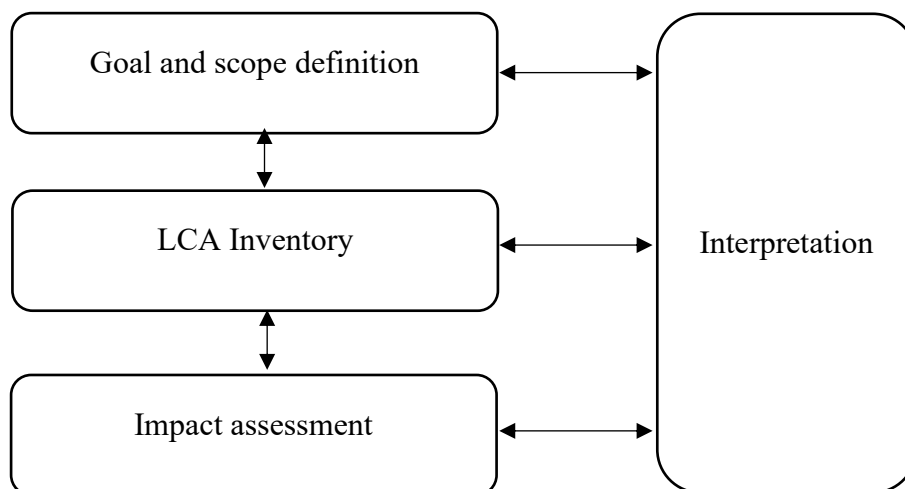


**Figure 2.23 Life cycle assessment phases (Vieira et al., 2016)**

### **2.3.1 Goal and scope definition**

The goal and scope definition is the primary phase of an LCA methodology. This key phase states the context of the study and sets out a specific margin of the environmental impact considerations. According to ISO 14040, the goal of an LCA study states the intended applications, the aims for performing the study, the intended people to whom the outcomes are to be communicated, and where the outcomes are going to be operated (Vieira et al., 2016; Yin, 2015). The goals should be comprehensively defined and compatible with the intended application. It includes technical details: for instance, the functional unit, the system boundaries, the allocation methods, the data quality requirements, any assumptions, limitations and the impact categories (Vieira et al., 2016, Yin, 2015). In this step, the approach should be considered according to the study.

### **2.3.2 Life cycle inventory analysis (LCI)**

The second phase of LCA methodology is inventory analysis and this involves data collection and analysis procedures regarding the production system. Inventory analysis quantifies data for all the relevant inputs and outputs of individual process within the system boundary, including raw material inputs, energy inputs, water inputs, and emissions to air, water and land. The life cycle of a product can be composed of hundreds of unit processes, and the collection of data would be a time-consuming process depending on system boundaries. A flow diagram is developed using data on inputs and outputs. The flow diagram should be as detailed as possible to achieve maximum accuracy. The data collection and data procedure including the validation of collected data and the relating data to unit processes are required to develop the inventory analysis of the product system (Yin, 2015).

### **2.3.3 Life cycle impact assessment (LCIA)**

The LCIA phase aims to evaluate the significance of environmental impacts and estimate resources based on life-cycle inventory results. This phase consists of three compulsory elements: selection of impact categories, category indicators and characterisation models; the classification stage, where the LCI parameters are chosen impact categories; and impact measurements, where the LCI results are characterised as an indicator result (Jiang et al., 2014). The indicator result is the ultimate outcome of a life cycle impact assessment.

### **2.3.4 Interpretation of results**

Interpretation is the final phase of an LCA in which, the outcomes from the inventory analysis and impact assessment are summarised. The aim of this phase is to analyse and deliver results, reach conclusions, explain limitations and provide recommendations based on the findings of the LCA (Jiang et al., 2014). Interpretation also comes up with a clear and complete overview of the LCA results, according to the goal and scope definitions.

### **2.3.5 Environmental life cycle assessment of concrete**

Concrete is the world's most consumed construction material and it is used in almost all kinds of building construction and infrastructure because of its versatility and excellent properties. The consumption of concrete is more than 3.8 tonnes per person on the planet annually (Petek Gursel et al., 2014). The production of concrete is very energy intensive and a source of greenhouse gas emissions. The civil construction industry is responsible for nearly 30% of the world's greenhouse gas emissions (Khasreen et al., 2009). In 2015, carbon emission was 23.1 tonnes CO<sub>2</sub> e- per person in Australia, which was five times higher than the global average (Lawania et al., 2015). It is required to estimate carbon dioxide (CO<sub>2</sub>) emission due to different

components of concrete. The primary components of concrete are cement, water and aggregates. Concrete components are well-known contributors to global warming.

### **2.3.5.1 Cement production and life cycle assessment of cement**

Cement is a binding material in concrete. Cement production was recorded at nearly 0.6 tonnes per capita each year (Jiménez et al., 2015). The cement industry is highly resource intensive and is the leading contributor of the world's greenhouse gas emissions. This industry accounts for about 7% of global emissions of carbon dioxide (Jiménez et al., 2015). Cement production releases CO<sub>2</sub> to the environment both directly and indirectly and is the main cause of global warming. CO<sub>2</sub> is emitted directly during the calcination process in cement production. In the calcination process, limestone (CaCO<sub>3</sub>) decomposes and releases more than 50% of total CO<sub>2</sub> emissions from cement production (Feiz et al., 2015). One study Flower and Sanjayan (2007) found that calcination process released 0.5 tonnes of CO<sub>2</sub> for each tonne of CaO production. The remaining CO<sub>2</sub> emission was from the combustion of fossil fuels used to heat the cement kiln.

Life cycle assessment of the cement production process reported that the amount of CO<sub>2</sub> emitted during the production of cement was in the range of 0.7 tonnes/tonne to 1 tonne/tonne cement (Feiz et al., 2015; Chen et al., 2010; Gartner, 2004). Every tonne of cement production consumed 1.5-1.6 tonnes of raw materials, 120-160 kWh of electrical energy and 3000-4300+ MJ of fuel energy (Hasanbeigi et al., 2010). The amount of CO<sub>2</sub> emissions are shown in Table 8. In the Australian context, the production of 1 tonne of cement released 0.8 tonnes CO<sub>2</sub>. Another study Hasanbeigi et al. (2005) reported that cement production emitted 0.82 tonnes CO<sub>2</sub>/tonne together with the transport of cement to concrete batching plants (Hasanbeigi et al., 2005).

**Table 2.8 Summary of CO<sub>2</sub> emissions (Flower and Sanjayan, 2007)**

Activity	Unit	CO <sub>2</sub> Emission
Cement	t CO <sub>2</sub> -e/tonne	0.8200
Coarse aggregate (Granite)	t CO <sub>2</sub> -e/tonne	0.0459
Coarse aggregate (Basalt)	t CO <sub>2</sub> -e/tonne	0.0357
Fine aggregate	t CO <sub>2</sub> -e/tonne	0.0139
Fly ash	t CO <sub>2</sub> -e/tonne	0.0270
Ground granulated blast furnace slag	t CO <sub>2</sub> -e/tonne	0.1430
Concrete batching	t CO <sub>2</sub> -e/m <sup>3</sup>	0.0033
Concrete transport	t CO <sub>2</sub> -e/ m <sup>3</sup>	0.0094
On site placement activities	t CO <sub>2</sub> -e/ m <sup>3</sup>	0.0090

The use of environmentally friendly material as partial cement replacements in concrete has been increasing attention in reducing greenhouse gas emission. Fly ash is ground granulated blast furnace slag and is widely used as supplementary cementitious materials. These materials can reduce greenhouse gas emission, energy consumption, water use and environmental toxicity. Flower and Sanjayan (2007) investigated the environmental impact of fly ash and ground granulated blast furnace slag and found that the CO<sub>2</sub> emission of fly ash was 0.027 tonnes CO<sub>2</sub>-e/tonne. Fly ash as a cement replacement was capable of reducing 13-15% of CO<sub>2</sub> emissions in concrete mixtures. Furthermore, ground granulated blast furnace slag emitted 0.143 tonnes CO<sub>2</sub>-e/tonne which is 22% less emission than conventional concrete (Flower and Sanjayan, 2007).

Waste glass powder has been recognised as a pozzolanic material to replace cement partially in concrete. Jiang et al. (2014) studied environmental impacts on waste glass containing concrete and found using glass powder as a cement replacement could reduce greenhouse gas emissions by 5%, 10% and 19% for 20 MPa, 30 MPa and 35 MPa concretes. Cumulative

energy demand also showed less energy use relative to conventional concrete. Life cycle environmental impacts on conventional concrete and glass powder concrete are shown in Table 2.9. From that table, it is found that the reduction in life cycle impacts by using glass powder was improving.

**Table 2.9 Life-cycle environmental impacts of conventional and glass powder concrete (Jiang et al., 2014)**

Life-cycle environmental impact	Unit	Conventional concrete			Glass powder concrete		
		20	30	35	20	30	35
		<i>MPa</i>	<i>MPa</i>	<i>MPa</i>	<i>MPa</i>	<i>MPa</i>	<i>MPa</i>
Global warming	kgCO <sub>2</sub> eq	230	290	340	220	260	280
Cumulative energy demand	MJ	1400	1800	2100	1400	1600	1700
Water use	m <sup>3</sup>	9.9	12	13	9.8	11	11
Acidification	H <sup>+</sup> moles eq	40	48	57	40	45	49
Carcinogenic	kg benzene eq	2.4	3.0	3.6	2.3	2.7	3.0
Noncarcinogenic	kg toluene eq	3600	4500	5400	3500	4100	4300
Respiratory effects	kg PM2.5 eq	0.094	0.11	0.13	0.091	0.10	0.11
Eutrophication	kg N eq	0.034	0.042	0.048	0.034	0.038	0.040
Ozone depletion	10 <sup>-6</sup> kg CFC-11 eq	9.0	11	13	8.4	9.7	10
Ecotoxicity	kg2,4-D eq	52	63	73	49	56	58
Smog	Kg NO <sub>x</sub> eq	0.56	0.68	0.78	0.55	0.62	0.66

Cement replacement ratio and strength of concrete are influencing factors on the outcomes of environmental impacts. Moreover, the production process of waste glass concrete would still have some impacts on environment and these need to be considered for further study.

### 2.3.5.2 Life cycle assessment of aggregate

Aggregates are the second major component in concrete production, comprising three-quarters of concrete volume. The use of aggregates is increasing rapidly along with concrete production. In 2013, 150 million tonnes of aggregates were produced in European Union countries (Napolano et al., 2016). Although the use of aggregates in concrete does not have a high environmental footprint as cement, excessive use depletes natural resources. The phases of acquisition and transport also consume energy depending on the transport distances and transport vehicle type (Napolano et al., 2016). Aggregates used in concrete construction are typically categorised as “natural” and “artificial”. Natural aggregates collected from sea or river beds do not require any processing. However, artificial crushed aggregates exploited from rocks and quarries require mechanical crushing. Energy consumption and emission of glacier rock crusher produced by rock crusher are tabulated in Table 10. Flower and Sanjayan (2007) investigated the environmental impact on granite and basalt aggregates and found that the CO<sub>2</sub> emission of granite was 0.0459 tonnes CO<sub>2</sub>-e/tonne. Furthermore, basalt emitted 0.0357 tonnes CO<sub>2</sub>-e/tonne which includes transportation of concrete from the quarry to the concrete batching plants.

**Table 2.10 Emission and energy consumption to produce 1 metric tonne of crushed glacier rock with rock crusher (Landfield and Karra, 2000)**

Emissions	CO <sub>2</sub> , fossil	0.6465 kg/tonne
	NO <sub>x</sub> as NO <sub>2</sub>	0.0021 kg/tonne
	SO <sub>x</sub> as SO <sub>2</sub>	0.0036 kg/tonne
	Particulates (unspecified)	0.0038 kg/tonne
Energy	Total primal energy	9.8192 MJ/tonne

In addition, CO<sub>2</sub> emissions due to concrete sand production and following transportation were 0.0139 tonnes CO<sub>2</sub> -e/tonne. Production of a tonne of fine aggregate emitted less CO<sub>2</sub> -e/tonne compared with the production of a tonne of coarse aggregate (Flower and Sanjayan, 2007). For instance, a tonne of fine aggregate generated 30-40% less CO<sub>2</sub> than coarse aggregate due to lack of crushing steps. On account of this, the use of alternative and recycled construction materials has received growing attention.

## **2.4 Summary**

A number of researchers have studied the use of recycled crushed glass in concrete as aggregate and cement replacement, with mixed success. Several studies have been carried out on reusing waste glass as fine aggregate in concrete since the beginning of the 1980s. However, the mechanical and durability properties of concrete presented inconsistent outcomes that have been reported by various researchers. Inconsistent results were caused by the chemical reaction between reactive silica in glass and alkali in cement during hydration. This alkali-silica reaction (ASR) is deleterious and results in excessive expansion. Expansion causes concrete to crack which is the prime cause of strength reduction. The reactivity of silica glass depends on chemical composition, the type of waste glass, fineness, percentage of replacement and particle size distribution. However, only limited research has been conducted on the pozzolanic effect of glass powder in cement paste. The use of waste glass as a cement substitute will not be fully understood unless the microstructural behaviour of cement paste during hydration is completely studied.

This research focuses on the development of sustainable concrete mix by partially replacing sand and cement with crushed recycled glass. This study also focuses on the quantification of environmental benefits achieved through the alternative use of glass waste. The concrete thus

produced is intended to be used in light-weight concrete works such as footpaths and precast concrete elements such as drainage pits, kerbs and culverts. Being able to recycle a proportion of glass waste into concrete as sand or cement replacement provides a whole new opportunity for recycling glass waste and reduces the amount of waste going to landfill. Furthermore, use of recycled glass in concrete contributes towards sustainable development by reducing the consumption of natural sand and cement.

## Chapter 3: Performance of recycled waste glass sand as partial replacement of sand in concrete

Nafisa Tamanna, Rabin Tuladhar, Nagaratnam Sivakugan. "Performance of recycled waste glass as partial replacement of sand in concrete." *Construction and Building Materials*. Vol. 239, 10 April, 2020.

This chapter studies the use of mixed-coloured soda-lime glass supplied by Cairns Regional Council, Australia, as sand replacement in concrete. In this research, concrete with a target characteristic strength of 32 MPa was produced by replacing natural river sand with 20%, 40%, and 60% of crushed recycled glass sand (RGS) to investigate the effect of replacement levels on fresh and hardened properties of concrete. The impact on workability, compressive strength, tensile strength and flexural strength was evaluated. The durability of concrete with RGS was also analysed by a rapid chloride penetration test (RCPT) and an alkali-silica reaction (ASR) test. The study suggests development and promotion of the use of sustainable concrete mix with recycled glass as a sand replacement at an industrial scale.

### 3.1 Experimental procedures

#### 3.1.1 Materials

General-purpose cement with a specific surface area of 562 m<sup>2</sup>/kg was used throughout the research. The equivalent alkali content ( $\text{Na}_2\text{O}_{\text{eq}} = \text{Na}_2\text{O} + 0.658 \text{K}_2\text{O}$ ) of this cement was calculated to be 0.39% (expressed as low alkali cement, i.e. less than 0.6%). The coarse aggregate used was obtained from Edmonton Quarry, following the grain size requirement specified by AS 2758.1 (AS2758.1, 2014). For fine aggregate, natural coarse sand and fine sand were used with a nominal size of 5 mm and 2 mm, respectively. Coarse and fine sand were

obtained from Barron River and Tableland regions, respectively. The properties of aggregate are tabulated in Table 3.1. SIKARE Retarder was used as an admixture.

**Table 3.1 Properties of natural aggregate supplied by Pioneer North Queensland**

Aggregates	20 mm Coarse aggregate	Coarse sand	Fine sand
Nominal size of sample (mm)	20	5	2
Particle density dry (t/m <sup>3</sup> )	2.68	2.55	2.60
Particle density saturated surface dry (t/m <sup>3</sup> )	2.69	2.58	2.62
Water absorption (%)	0.4	0.9	0.7

### 3.1.2 Production of recycled crushed glass

Mixed-coloured soda-lime glass supplied by the Cairns Regional Council was utilised as a partial coarse sand replacement. Council collects all commingled recyclables from the yellow recycling bins and transports to a materials recovery facility (MRF) unit. All collected recyclable materials, which includes paper, cardboard, plastic bottles, aluminium cans and glass bottles are sorted and large items removed as the stream passes through the conveyor belt. A vibrating conveyor belt separates light items, such as paper, cardboard, etc. Heavy items, for example, plastic bottles, glass bottles and crushed glass are sent to the other conveyor belts where larger contaminants are removed manually. Glass items are then sent to glass crushing facility. Figure 3.1 shows recyclable glass items after sorting procedures.

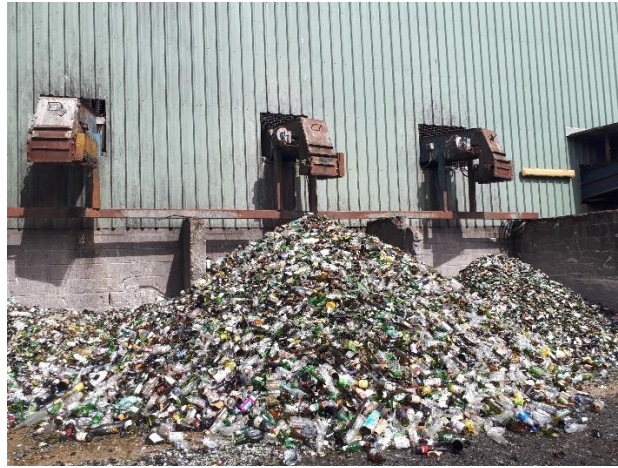


**Figure 3.1 Recyclable glass items after sorting procedures**

Glass crushing is done at three stages: imploder, shearing unit and sanding unit. The imploder has rotating blades to crush glass (Figure 3.2a). After the imploder, glass particles are moved to the shearing unit for further crushing by shearing (Figure 3.2b). Some large glass particles and other impurities are removed before reaching the sanding unit. The rotating grinding shaft of the sanding unit (Figure 3.2c) crushes material to sand fineness. Glass sand particles are dropped into two separate drums through 5 mm (coarse glass) and 3 mm (fine glass) holes. The coarse glass particles of 5 mm in size are then sent to landfill while the fine glass particles are sent to be utilised in construction. In this study, a fine glass of 3 mm (Figure 3.3) was used as received, without any modification (i.e., cleaning or sorting), and tested to meet the requirements of Cement concrete Aggregate Australia (CCAA).



**Figure 3.2 Glass crushing machine (a) imploder (b) shearing unit (c) sanding unit**



**Figure 3.3 Fine glass sand (3 mm) used as a partial coarse sand replacement**

### 3.1.3 Concrete mix design

The concrete mix design used in this study for control specimen closely followed the mix design used by Pioneer North Queensland (PNQ) for their commercial concrete plant (Table 3.2). The mix design was designed for a characteristic strength of 32 MPa at 28 days. Based on the mix design, the target slump value was in the range of 80-100 mm. By trial and error, it was found that 0.53 w/c ratio achieved the targeted slump value. A total of four concrete batches were prepared, including the control concrete without any RGS for comparison purpose. The other three concrete batches corresponded to the replacement of coarse sand with 20%, 40%, and 60% recycled glass sand, noted as 20 RGS, 40 RGS and 60 RGS, respectively.

**Table 3.2 Materials content for 1 m<sup>3</sup> of concrete mixture**

Material	Cement (kg)	Fine Aggregate (kg)		Recycled Glass Sand (kg)	Coarse Aggregate (kg) 20 mm	Water (L)	Plasticizer (mL/100 kg of Cement)
		Fine Sand	Coarse Sand				
Control	336	270	632	-	981	180	400
20 RGS	336	270	505.6	126.4	981	180	400
40 RGS	336	270	379.2	252.8	981	180	400
60 RGS	336	270	252.8	379.2	981	180	400

Four batches of concrete were mixed separately in a pan mixer, according to AS 1012.2 (AS1012.2, 2014). Mixtures were poured into moulds to cast cylinders and beams for compressive, flexural, tensile strength and RCPT. Vibration was applied by a mechanical vibrating table. After casting, all samples in the mould were allowed to set initially for 24 hours. Then, specimens were demoulded and cured for a specific period, for instance, 7, 28, 56 days in water at  $23\pm 2$  °C, according to AS 1012.8.1 (AS1012.8.1, 2014).

### **3.1.4 Experimental methods**

The experimental study included (a) material properties tests – particle size distribution test and sugar content test and (b) fresh concrete properties – slump test and fresh concrete density test (c) hardened concrete properties – compressive, tensile and flexural strength tests. RCPT and ASR tests were also carried out on concrete and mortar specimen, respectively to determine durability properties of concrete.

#### **(a) Material properties test**

##### ***Particle size distribution***

Particle size distribution is a mathematical function that describes the relative amount of particles present according to size. A sieve analysis was conducted to analyse particle size distribution, according to AS 1141.11.1 (AS1141.11.1, 2009).

##### ***Detection of sugar in glass aggregates***

The detection of sugar in aggregate is a qualitative method to determine the presence or absence of sugar. The presence of sugar interferes with the chemical reaction that delays the setting of concrete. This test can directly detect sugar from honey, wine, fruit juices and other sources of glucose. The mixed-coloured glass used in this study was mainly obtained from glass

containers such as beverage bottles and food containers and are prone to sugar contamination. The detection of sugar in RGS was conducted following AS 1141.35 (AS1141.35, 2007). Fehling's reagent was used to detect sugar in the aggregate. Fehling's solution was prepared by mixing equal volumes of the blue aqueous solution of copper (II) sulphate pentahydrate crystals (Figure 3.4a i) and a colourless solution of aqueous potassium sodium tartrate (also known as Rochelle salt) (Figure 3.4a ii) with a strong alkali (commonly sodium hydroxide). The aggregate to be tested was added to Fehling's solution (Figure 3.4b) and the resultant mixture was heated. A reddish-brown precipitate indicates the presence of sugar in aggregate.

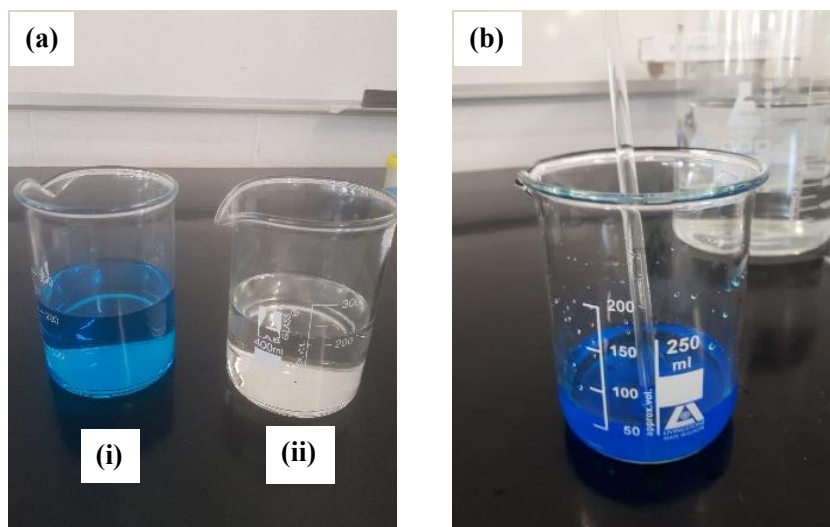


**Figure 3.4 (a) Copper (II) sulphate pentahydrate crystals and colourless solution of aqueous potassium sodium tartrate, (b) Fehling's solution**

### **(b) Fresh concrete properties**

In this research, fresh and hardened concrete properties were also evaluated to investigate the effect of using RGS in concrete as a partial fine aggregate replacement. The properties of fresh concrete were investigated by conducting a slump test and fresh density test.

A conical hollow frustum with a 300 mm height, 200 mm diameter at the bottom and 100 mm diameter at the top was used in the slump test. The cone was placed on a smooth base plate and

filled with fresh concrete in three layers. Each layer was compacted 25 times with a compaction rod to avoid air voids. Excess concrete was taken off from the top surface and levelled with a trowel. The cone was lifted in a vertical direction and the concrete was allowed to subside. The difference between the height of the cone and the subsided concrete is the slump and it is expressed in mm. The slump test was carried out according to AS 1012.3.1 (AS1012.3.1, 2014).

Concrete cylinders were weighted forthwith after casting the moulds (fresh density) and prior testing (hardened density) as per AS 1012.12.1 to assess the density (AS1012.12.1, 2014).

Density was calculated by:

$$\text{Density of concrete} = \frac{\text{Mass of concrete (kg)}}{\text{Volume of concrete (m}^3\text{)}} \quad (3.1)$$

### **(c) Hardened properties**

#### ***Compressive and flexural strength***

Compressive strength, flexural strength and indirect tensile strength tests were conducted to investigate the basic hardened properties according to AS 1012.9 (AS1012.9.1, 2014), AS 1012.11 (AS1012.11, 2014) and AS 1012.10 (AS1012.10, 2000), respectively. A compressive strength test was performed to determine the maximum compressive load that the sample could carry per unit area. Cylinders with 100 mm diameter and 200 mm height were cast for compressive strength following AS 1012.8.1 (AS1012.8.1, 2014). Seven cylinders were cast and cured for each batch. One cylinder was used for the seven days testing and three of each cylinder were used for the 28 and 56-days testing. All cylinders were cured in water until testing commenced. During the compression test, a rubber cap was affixed on the rough end of the cylinder to allow smooth testing surfaces at either end. A steady load of 1.4 kN/sec. was applied to the cylinder until the sample failed per AS 1012.9. The compressive strength was measured by using the formula below and converted into Mega Pascals (MPa).

$$\text{Compressive Strength} = \frac{\text{Ultimate Load at failure (N)}}{\text{Cross Sectional Area (mm}^2\text{)}} \quad (3.2)$$

Flexural strength of a material is its ability to resist deformation under loading. Force was applied to the beam through two supporting rollers (bottom support of 300 mm) and two loading rollers (top supports of 100 mm) (Figure 3.5c). A four-point loading was set up with a loading rate of 0.07 kN/s. A total of seven beams, 100 mm × 100 mm × 360 mm were cast to test flexural strength for 28 days of curing. Flexural strength was calculated by:

$$f_r = \frac{M}{Z} = \frac{PL(1000)}{BD^2} \quad (3.3)$$

$f_r$  = Flexural Strength or Modulus of Rapture, *MPa*

M = Bending Moment at failure of specimen

Z = Section modulus of cross-section

P = Maximum load applied to the specimen, *kN*

L = Length between support rollers, *mm*

B = Width of the specimen, *mm*

D = Height of the specimen, *mm*

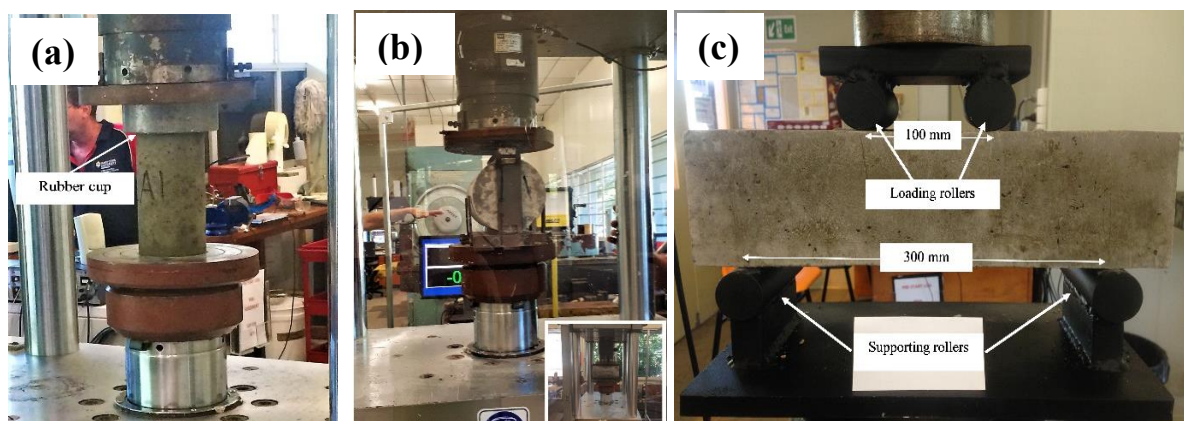


**Figure 3.5 (a) Compressive strength, (b) tensile strength, and (c) flexural strength set up**

### *Tensile strength*

Tensile strength is the highest amount of tensile stress that a material can absorb before failure. Cylinders of 150 *mm* diameter and 300 *mm* height were cast for tensile strength and cured for 28 days. A loading rate of 1.2 *kN/s* was applied for the tensile test and calculated by:

$$T = \frac{2000P}{\pi LD} \quad (3.4)$$

Whereas,

T = Indirect tensile strength, in *MPa*

P = Maximum indirect tensile force indicated by the testing machine, in *KN*

L = Length, in *mm*

D = Diameter, in *mm*

#### **(d) Concrete durability**

##### ***Rapid chloride penetration test***

RCPT was conducted to assess concrete durability, according to ASTM C 1202 (ASTMC1202, 2012). A concrete specimen of 100 *mm* in diameter and 50 *mm* thickness was cut from the 200 *mm* cylinder using a water-cooled diamond saw. The circumference surface of the specimen was coated with epoxy (Figure 3.6a) and placed in a vacuum desiccator in such a manner that both end faces of the specimen remained exposed. The desiccator was sealed properly, and a vacuum pump was used to decrease pressure 50 *mm Hg* within a few minutes. This vacuum condition was maintained for three hours to remove air particles from the pores inside the specimen. De-aerated water was poured into the desiccator to submerge the specimen and soak it for 18±2 hours to fill up the voids with water for vacuum saturation conditioning (Figure 3.6b). The specimen was placed between two cells. One of the cells was filled with a 0.3 *N* sodium hydroxide solution, and other cell was filled with 3% sodium chloride solution (Figure

3.6c). A 60V direct current was applied between two liquid cells for six hours. The total current passing through the specimen was recorded every 30 minutes and calculated by integrating the current with a time equation as per standard, where Q is charge passed (*coulombs*),  $I_0$  is current (*amperes*) immediately after voltage is applied, and  $I_t$  is current (*amperes*) at t minutes after voltage is applied.

$$Q = 900 (I_0 + 2I_{30} + 2I_{60} + \dots + 2I_{300} + 2I_{330} + I_{360}) \quad (3.5)$$

The specimen was categorised based on the amount of total charge passed using the (ASTMC1202, 2012) guideline (Table 3.3). The higher the penetrability shown by the RCPT test shows lower resistance to chloride penetration into concrete and hence the lower durability. Reversely, very low permeability shows higher resistance to chloride ion penetration.

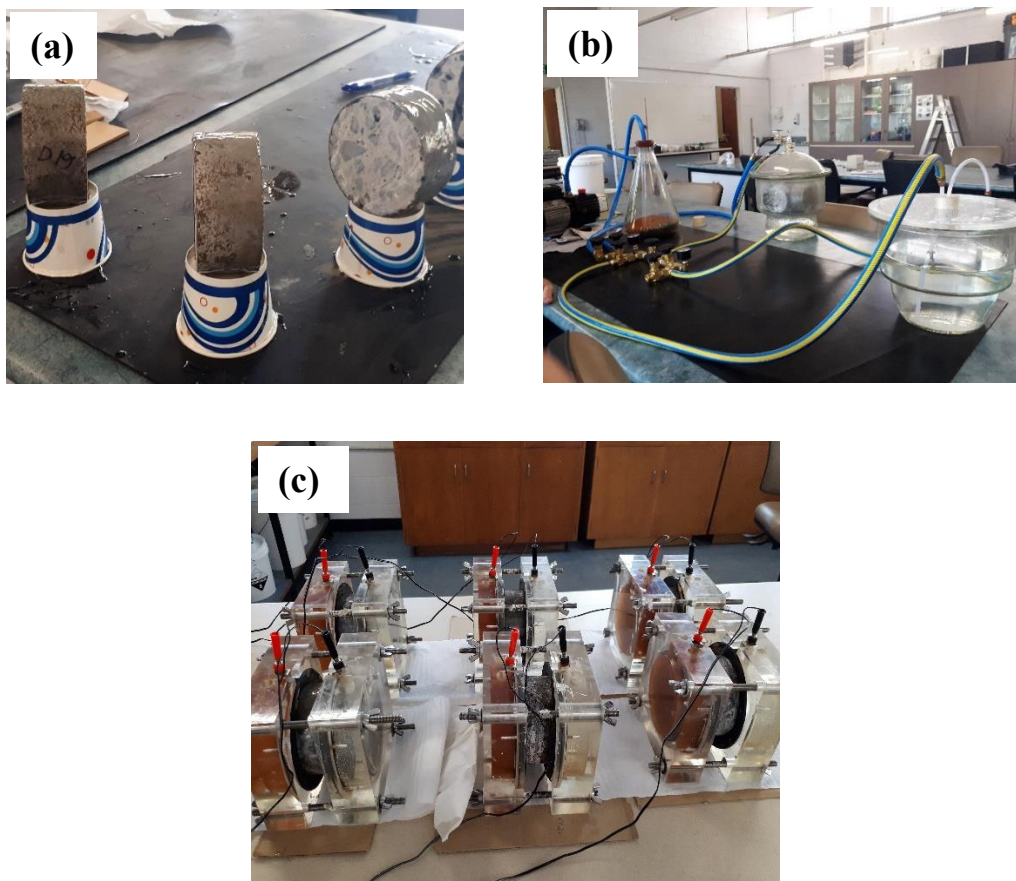


**Figure 3.6 (a) Specimens coated with epoxy, (b) vacuum saturation conditioning and (c) RCPT cells set up**

**Table 3.3 Chloride ion penetrability based on charge passed (ASTMC1202, 2012)**

Charge Passed (coulombs)	Chloride Ion Penetrability
>4000	High
2000-4000	Moderate
1000-2000	Low
100-1000	Very Low
<100	Negligible

***Accelerated mortar bar tests***

An accelerated mortar bar test was conducted on the mortar with and without RGS to determine the potential deleterious alkali-silica reaction as per Australian Standard AS 1141.60.1 (AS1141.60.1, 2014). Two gang prism moulds of size  $25\text{ mm} \times 25\text{ mm} \times 285\text{ mm}$  with a gauge length of  $250\text{ mm}$  were used in this experiment (Figure 3.7a). A gauge stud was attached to each end of the mould to obtain precise comparator readings. Three mortar bars were prepared for each mix according to the proportion specified in AS 1141.60.1 (Table 3.4). In this test, the grading requirements of the manufactured fine aggregate was followed for RGS as tabulated in Table 3.5.

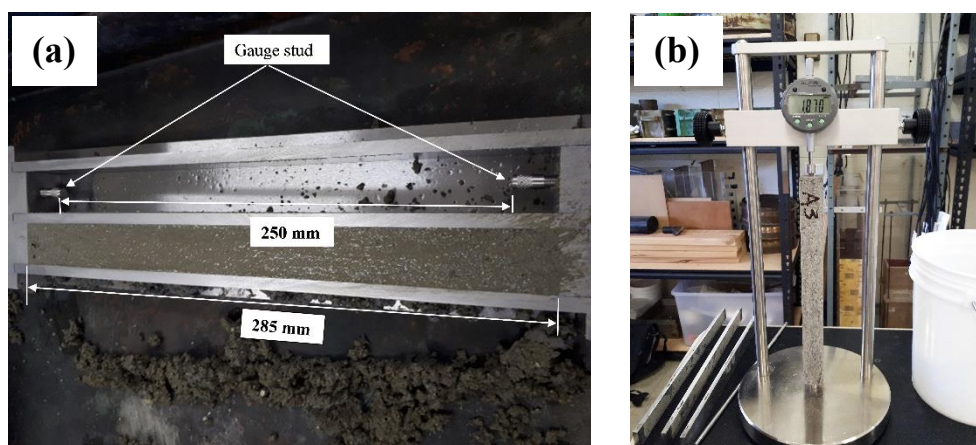


**Figure 3.7 (a) Mortar bar prism moulds with gauge stud and (b) ASR comparator readings**

**Table 3.4 Mix design of mortar mixes for three ASR prism bars (AS1141.60.1, 2014)**

Material	Cement (g)	Sand (g)	Recycled Glass Sand (g)	Water (mL)
Control	440	990	-	206.8
20 RGS	440	792	198	206.8
40 RGS	440	594	396	206.8
60 RGS	440	396	594	206.8

**Table 3.5 Grading requirements of glass sand as manufactured fine aggregate**

Sieve Size, mm		% by mass	20 RGS	40 RGS	60 RGS
Passing	Retained on		(g)	(g)	(g)
4.75	2.36	10	19.8	39.6	59.4
2.36	1.18	25	49.5	99	148.5
1.18	0.600	25	49.5	99	148.5
0.600	0.300	25	49.5	99	148.5
0.300	0.150	15	29.7	59.4	89.1

Moulds were placed in a humidity-controlled storage area of 23<sup>0</sup>C with 95% humidity for the first 24 hours. After demoulding, the initial comparator reading of each specimen was recorded. Samples were placed in a storage container filled with sufficient tap water and stored in a water bath at 80<sup>0</sup>C for the next 24 hours. A zero reading was recorded before placing in a container filled with enough 1mol/L sodium hydroxide. Comparator readings were recorded at 1, 3, 7, 10, 14 and 21 days after the zero reading. The expansion was calculated according to the standard below:

$$E_n = \left( \frac{l_n - l_z}{l_g} \right) * 100 \quad (3.6)$$

Where,

$E_n$  = Expansion of each specimen after a period of n days since the zero reading

$l_n$  = Specimen length after a period of n days since the zero reading

$l_z$  = Specimen length at zero reading

$l_g$  = Effective gauge length of specimen (usually 250 mm)

The average of three samples was taken as the ASR expansion. The reactivity of the aggregate was classified based on ASR expansion value (Table 3.6). All the test programs with the relevant standard are tabulated in Table 3.7.

**Table 3.6 Aggregate reactivity classification based on AS 1141.60.1 (AS1141.60.1, 2014)**

Mean mortar bar expansion (E), %		AS 1141.60.1 aggregate reactivity classification
Duration of specimens in 1mol/L NaOH at 80 °C		
10 days	21 days	
-	$E < 0.10^*$	Non-reactive
$E < 0.10^*$	$0.10^* \leq E < 0.30$	Slowly reactive
$E \geq 0.10^*$	-	Reactive
-	$0.30 \leq E$	Reactive

\*The value for natural fine aggregates is 0.15%

**Table 3.7 Test program with relevant standards**

Tests	Standard	Curing (days)
Particle size distribution	AS 1141.11.1	-
Detection of Sugar	AS 1141.35	-
Slump test	AS 1012.3.1	-

Density of concrete	AS 1012.12.1	7, 28, 56
Compressive strength	AS 1012.8.1	7, 28, 56
Flexural strength	AS 1012.11	28
Tensile strength	AS 1012.10	28
Rapid chloride penetration test (RCPT)	ASTM C1202	28, 56
Alkali-Silica Reaction (ASR)	AS 1141.60.1	1, 3, 7, 10, 14, 21

## 3.2 Results and discussion

### 3.2.1 Characterisation of crushed glass sand as aggregate

#### 3.2.1.1 Particle size distribution

Figure 3.8 shows the particle size distribution of natural coarse sand and RGS, determined by sieve analysis according to AS 1141.11.1 (AS1141.11.1, 2009) with grading limits. Coarse sand and RGS were well graded, however RGS showed slightly coarser distribution compared with natural coarse sand as well as grading limits. Coarse sand presented an homogeneous distribution whereas RGS had particles with a specific size of range predominating. The portion of finer particles in RGS was lower than coarse sand, with the maximum percentage of 44% retained on 1.18mm sieve following 30% retained on 0.600 mm. RGS showed the coarser distribution in the middle of sieves (0.300 mm -1.18 mm) compared with the lower limit which is negligible to be taken into account as fine aggregate in concrete. The angular nature of RGS can provide better bonding with the cement paste in the concrete (An et al., 2017).

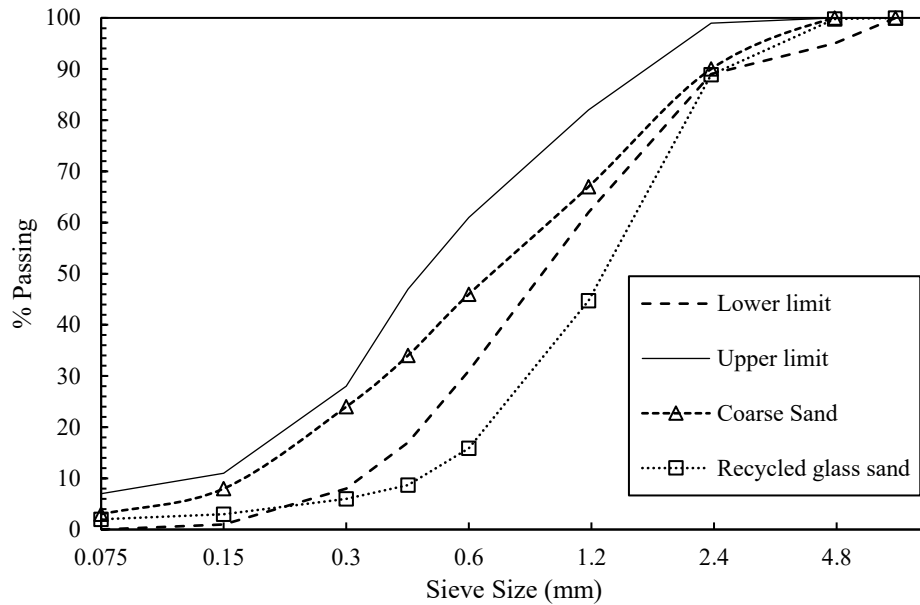


**Figure 3.8 Particle size distribution curves of natural coarse sand and crushed glass sand**

### 3.2.1.2 Detection of sugar

100 g RGS was placed in a 250 mL beaker (Figure 3.9a) and covered with water. Then, 50 mL of 1 N hydrochloric acid was added to the mixture. The mixture was boiled for 5 minutes (Figure 3.9b) and filtered immediately while still hot (Figure 3.9c). As the filtrate was found to be acidic to litmus paper (Figure 3.9d), 5 mL of filtrate was cooled and neutralised with 1 N sodium hydroxide solution (Figure 3.9e). The precipitate was removed by filtration. Finally, 3 mL of Fehling's solution (described in experimental methods) was added into the mixture and heated in a boiling water bath for 5 min. Glass sand did not show reddish-brown precipitate after the addition of Fehling's solution which indicated the absence of sugar (Figure 3.9f). It was inferred from the test that RGS used in this research was free from contamination and therefore suitable to replace sand in concrete. Glass bottles used in this study were mainly used for food and beverages. However, the sugar detection test showed no sign of sugar in the mixed-coloured glass. The possible reason for the absence of sugar can be that the crushed glass was

stored outside at the MRF site in Cairns and the rain over time may have washed sugar content away from the stockpile. This suggests that simple washing of crushed glass can effectively remove any sugar content from the glass.

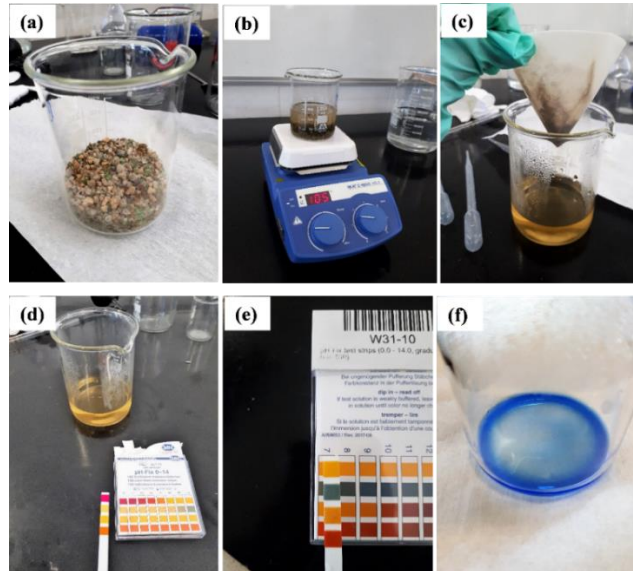


**Figure 3.9 Procedures to determine the presence or absence of sugar in aggregate**

## 3.2.2 Fresh properties of concrete

### 3.2.2.1 Slump test

The slump test was carried out to assess the workability of concrete with RGS and without RGS (Table 3.8). Control concrete showed 90 mm slump, which was in the range of targeted slump of 80-100 mm. However, workability decreased significantly with an increase in the quantity of RGS. This decreasing trend was in agreement with the study by (Adaway and Wang, 2015). The 20 RGS and 40 RGS exhibited similar slump values, nearly 69% and 71% of control concrete, respectively. The 60 RGS showed even less slump compared with any other mixtures, only 46% slump value of control concrete. The shape of the glass sand particles - for instance, sharp edges, and rough texture – resulted in lower fluidity of mixture, and hence

reduced slump was observed. A similar decrease pattern was observed on the flowability of mortar (Tan and Du, 2013).

### 3.2.2.2 Density of concrete

Table 3.8 shows the fresh and hardened density of concrete containing RGS as a fine aggregate replacement. Control concrete exhibited a fresh density of  $2394 \text{ kg/m}^3$  whereas 20 RGS and 40 RGS concrete had a fresh density of  $2377 \text{ kg/m}^3$  and  $2365 \text{ kg/m}^3$ . The density of RGS concrete was very similar to that of the control concrete. The slightly reduced value of density in RGS concrete might be due to the lower specific gravity of RGS compared with sand used in the study. RGS had a specific gravity of 2.42 while sand exhibited 2.62. The dry density of concrete was measured at 7, 28 and 56 days. Control concrete showed a hardened density of  $2406 \text{ kg/m}^3$ ,  $2399 \text{ kg/m}^3$  and  $2396 \text{ kg/m}^3$  at 7, 28 and 56 days, respectively. As can be seen in Table 3.8, the hardened density of RGS concrete was found to be very similar to that of control concrete.

**Table 3.8 Slump and density of control concrete, concrete with RGS**

Sample Name	Slump (mm)	Fresh Density ( $\text{kg/m}^3$ )	Hardened Density ( $\text{kg/m}^3$ )		
			7 days	28 Days	56 Days
Control	90	2394	2406	2399	2396
20 RGS	60	2377	2387	2372	2378
40 RGS	65	2365	2361	2369	2382
60 RGS	40	2350	2358	2356	2361

### 3.2.3 Mechanical properties of concrete

#### 3.2.3.1. Compressive strength of concrete

The compressive strength tests of RGS concrete with various ratios were carried out and compared with concrete without glass sand (control concrete) (Figure 3.10). Control concrete and concrete with 20 RGS achieved design strength as early as in seven days, which was mainly characterised for 28 days. The 20 RGS concrete gained a compressive strength of 34.2 *MPa* at 7 days, which was 5.8% higher than that of the control. As the replacement level increased, the strength slightly decreased. However, 60 RGS concrete achieved a slightly higher compressive strength (2.3%) than 40 RGS concrete at seven days.

All concrete mixtures achieved the characteristic strength of 32 *MPa* at 28 days. The control concrete gained strength of about 38.75 *MPa* at 28 days. The concrete with 20 RGS obtained the highest strength (i.e., 41.40 *MPa*) which was 7% higher than the control concrete at 28 days. The other two fine aggregate replacements (i.e., 40 RGS and 60 RGS) performed favourably with strengths of 86% and 96% of the control concrete, respectively. The increase in strength for the fine aggregate replacement is attributed to the angular nature of the RGS than the naturally rounded sand particles, which has also been proved by other research (Adaway and Wang, 2015). The strength development of concrete depends on the interlocking bond between the cement matrix and glass sand, which is governed by the development of the interfacial transition zone (ITZ).

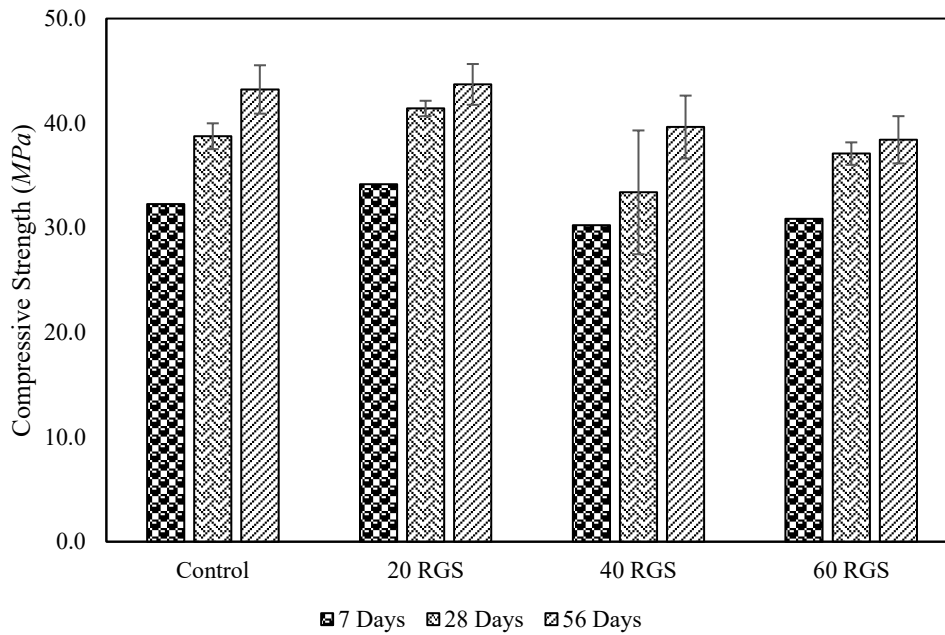


**Figure 3.10 Compressive strength development of concrete with RGS**

The control concrete reached 43.22 MPa of strength, a 34% improvement at 56 days. The 20 RGS concrete achieved the highest compressive strength at 56 days, albeit 1% compared with the control concrete. It was evident that RGS quantity had a slightly negative impact on its strength as glass sand quantity increased. Increased glass sand quantity weakens the mechanical bond inside the concrete microstructure, leading to a decrease in strength of ITZ. The 40 RGS and 60 RGS concrete achieved strengths of 92% and 89%, respectively, compared with control concrete. However, strength development showed a slow increase in strength at 56 days compared with 28 days of strength. The 40 RGS mix increased the most with 31%, followed by 20 RGS with 28% and 60 RGS with 24%.

### 3.2.3.2. Flexural and tensile strength of concrete

Flexural strength and indirect tensile strength tests were conducted on control and RGS concrete at 28 days. There was no significant difference in both flexural and tensile strength for glass sand addition compared to the control concrete (Figure 3.12). Strength results tended to increase with an increase in glass sand quantity. The angular size of glass sand can attribute

to a better interlocking between cement and glass sand. However, a decrease in strength was found for 40 RGS and 60 RGS for flexural and tensile strength, respectively. Reduction in tensile strength of concrete with higher percentage RGS replacement (60%) is in line with the reduction in compressive strength at 60% replacement level. Percentage of indirect tensile strength to compressive strength was in the range of 8-1% (Table 3.9).

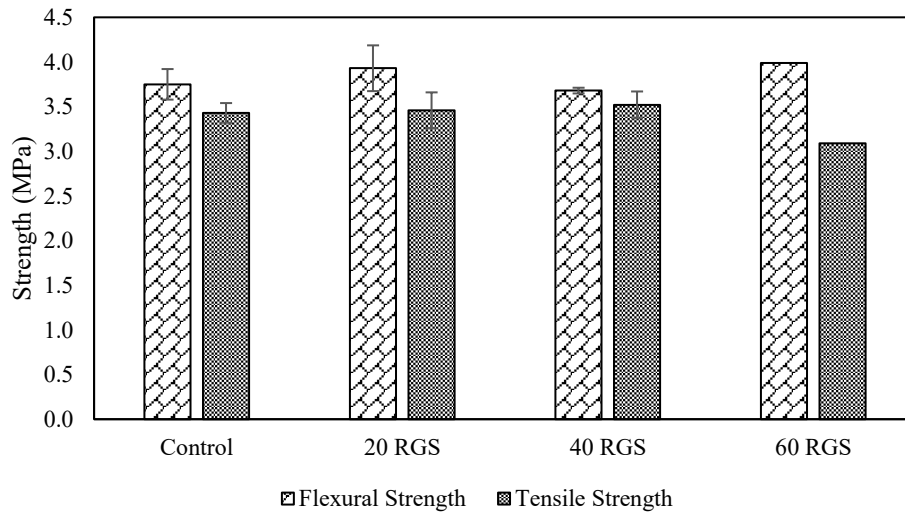


**Figure 3.12 Flexural and tensile strength of concrete with RGS**

**Table 3.9 Percentage of indirect tensile strength to compressive strength at 28 days**

Sample Name	28 days (%)
Control concrete	8.85
20 RGS	8.36
40 RGS	10.54
60 RGS	8.33

### 3.2.4 Durability of concrete

#### 3.2.4.1 Rapid chloride penetration test

Concrete durability depends on its resistance to the ingress of moisture and chloride ions into the concrete. In this research, RCPT was conducted on the concrete cylinder at 28 and 56 days to evaluate the resistance of concrete to chloride ion penetration. Figure 3.13 depicts the average charge passing through the concrete containing river sand (control concrete) and RGS. Results show that control concrete appeared as the most vulnerable to ingress of chloride ion at both curing periods. The charge passed through the control concrete was 5234 *coulombs* at 28 days, which is classified as high permeable concrete according to ASTM C 1202 (ASTMC1202, 2012). As the curing period increases, the RCPT value was noticed to reduce. At 56 days, reduction in chloride ion penetration was seen to be 19% less compared with control concrete at 28 days, but it was still in the high permeable range.

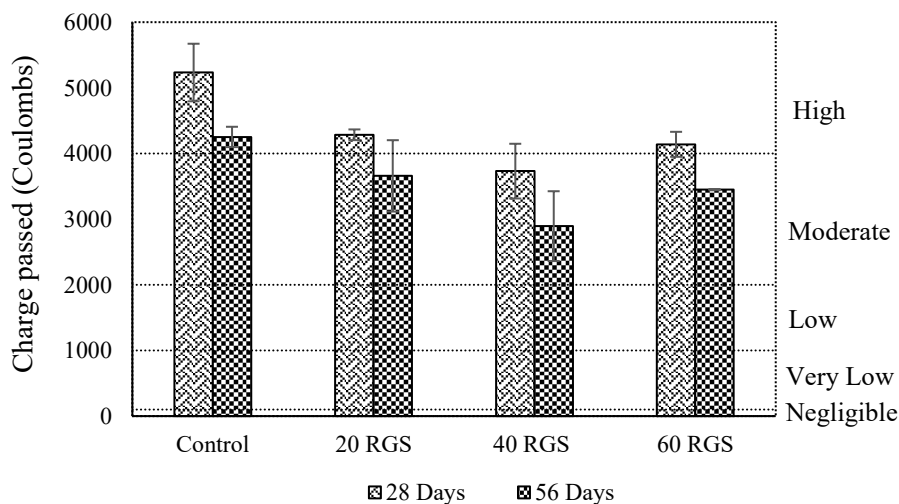


**Figure 3.13 RCPT results of concrete with river sand and RGS at 28 days and 56 days**

Concrete with RGS showed improved resistance to chloride ion penetration. Similar improved resistance was also found in one study (Du and Tan, 2014a). RCPT value for 20 RGS was found 4285 *Coulombs* at 28 days, classified as high permeable concrete. The RCPT value was noticed to decrease at 56 days, and it exhibited moderately permeable concrete. 40 RGS exhibited the highest resistance among other replacements and presented 29% and 32% improvement in chloride resistance compared with control concrete at 28 and 56 days,

respectively. This agrees with the increase in compressive strength of concrete with an increase in RGS replacement levels up to 40%. During the concrete mixing, it was observed that uniform mixing of materials could be achieved for 20 RGS and 40 RGS. However, for the high replacement level of natural sand with glass sand (60 RGS), mixing and finishing of the concrete specimen was relatively difficult. It is observed that up to 40% replacement, the cohesion between the cement and glass sand improved the microstructure of the ITZ, as also noted by others (Du and Tan, 2014a). However, at higher glass sand replacement (60 RGS) the concrete was observed to be more porous due to difficulty in mixing with high glass sand percentage. This has resulted in the increase in charge passing through the 60 RGS specimen in the RCPT test at 28 days, as well as 56 days (Figure 3.13). However, 60 RGS showed 20% and 19% more resistant than that of control concrete at 28 and 56 days, respectively.

#### **3.2.4.2 Alkali-silica reaction test**

The main concern of using RGS as a fine aggregate replacement in concrete is alkali-silica reaction (ASR). The expansions of the mortar bar showed an increasing trend over time (Figure 3.14). However, all mortar bar specimens exhibited expansion less than 0.10% at 21 days which is classified as non-reactive, based on AS 1141.60.1. The highest expansion value of about 0.086% was observed for control mortar bars (with no RGS) at 21 days. It is noticeable that the ASR expansion of RGS mortar was less than that of control mortar bar. The expansion was found to be reduced with an increase in glass sand content from 20-60%. The least ASR expansion was noticed for 40 RGS, followed by 60 RGS at 21 days. Aggregates (both river sand and RGS) were within the non-reactive classification at 21 days, as specified in AS 1141.60.1. However, the addition of RGS in mortar further reduced ASR expansion.

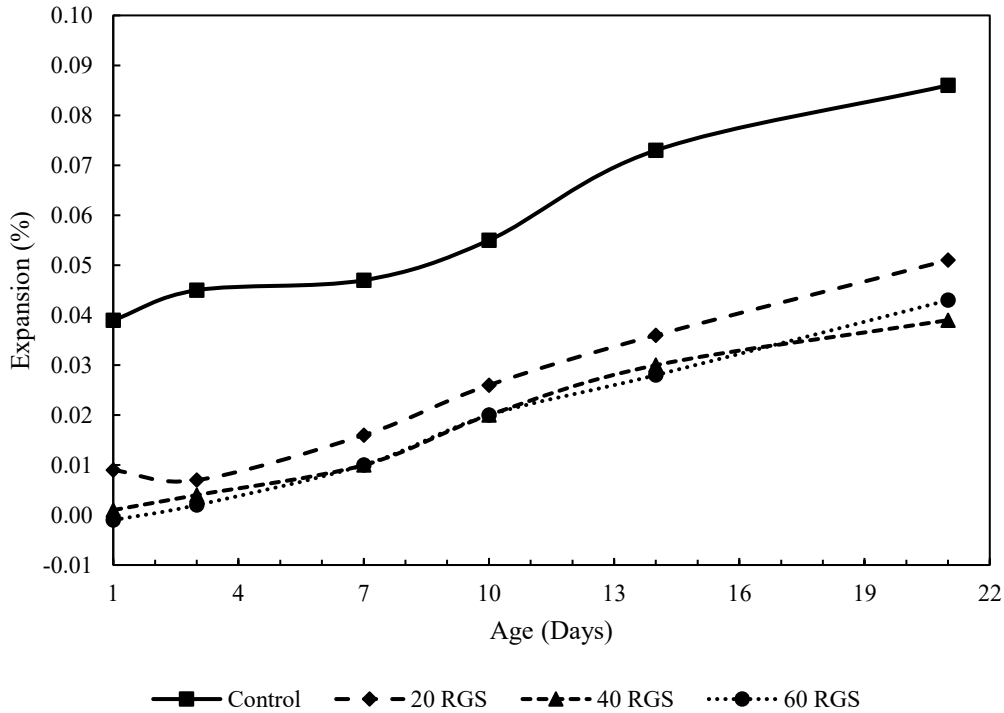


**Figure 3.14 ASR expansion of mortar with crushed glass**

Experiments Fischer et al. (2010) and Du and Tan (2014b) showed that alkali-silica reaction expansion that leads to ASR cracking is induced within the internal cracks of the large soda-lime glass particles rather than at the glass/cement paste interface. Alkali ions can penetrate through the internal cracks in large aggregates that are produced during the crushing process and form ASR gel. However, no cracks were detected on the crushed glass sand surface used in this research because of smaller glass particles (Figure 3.15). Smaller glass particles (less than 4.5 mm) with no surface cracks do not have alkali ions from penetrating into the glass particles forming ASR gel. This resulted in no ASR expansion when smaller size glass particles were used to replace natural sand in concrete. Finer size RGS reacts with portlandite ( $\text{Ca(OH)}_2$ ) and forms secondary calcium silicate hydrate (C-S-H) with a low Ca/Si ratio. Hou et al. (2004) explained that pozzolanic C-S-H is formed in the microstructure as long as  $\text{Ca(OH)}_2$  is present to react with dissolved silica and hinder the formation of expansive ASR gels.

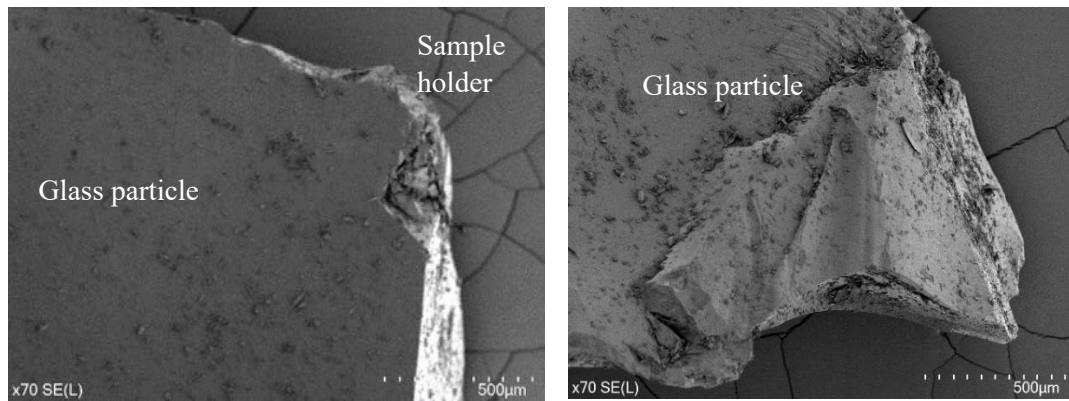


**Figure 3.15 SEM of crushed glass sand particle**

### **3.3 Conclusion**

A series of experiments was conducted to investigate the influence of RGS concerning strength characteristics and durability properties. Addition of RGS had a significant impact on workability due to angular edges and rough texture of the glass sand. Although the fresh density was reduced successively with the increase in glass content, improvement was noticed in the hardened density with curing time. Target compressive strength was being achieved by all concrete mixtures in 28 days and most significantly, in seven days by control concrete and 20 RGS concrete. No adverse reduction in strength was noticed up to 60% replacement of natural sand with RGS. The RGS concrete showed satisfactory tensile and flexural strength results. The latter exhibited a similar propensity to compressive strength. RGS concrete showed enhanced resistance to chloride-ion penetration up to 60% replacement and made concrete less permeable. The addition of recycled glass as coarse sand replacement was also proven to be not detrimental against alkali-silica reaction. Furthermore, the use of RGS to replace natural sand reduces the alkali-silica reaction due to the pozzolanic reaction between finer glass particles and alkali from cement hydration. The results show that recycled crushed glass can be used to replace up to 60% sand in concrete. However, with an increase in replacement rate, workability of concrete can reduce, and measures need to be taken to improve the workability

of concrete by the addition of suitable admixture. The successful application of using RGS in concrete can reduce sand dredging, along with the reduction of glass waste going into landfill sites.

## **Chapter 4: Sustainable use of recycled glass powder as cement replacement in concrete**

Nafisa Tamanna, Rabin Tuladhar. “Sustainable Use of Recycled Glass Powder in as Cement Replacement in Concrete”. *The Open Waste Management Journal*, 2020, 13:1-13.

N. Tamanna, R. Tuladhar, N. Avosa and S. Sivakugan. “The effect of using waste glass powder as cement replacement in concrete.” *Proceedings of the 28<sup>th</sup> Biennial Conference of the Concrete Institute of Australia*, 22-25 October 2017, Adelaide, South Australia.

This chapter presents a sustainable way of using recycled glass powder (RGP) as a cement replacement in concrete. This research was conducted in three phases. The first phase consisted of material characterisation to determine accurate chemical and physical characteristics of recycled crushed glass powder (RGP). The second phase consisted of an experimental investigation on the effects of RGP on fresh concrete properties (slump test, and fresh density test), hardened concrete properties (hardened density test, compressive strength, tensile strength, and flexural strength), and durability of concrete (rapid chloride penetration test). Five concrete mixes were investigated: General Portland (GP) cement concrete (control); fly ash blend (30% fly ash) concrete; and three concrete mixes containing RGP as cement substitution at 10%, 20% and 30% (noted as 10 RGP, 20 RGP and 30 RGP, respectively). The relative strength test of mortar was conducted to assess the reactivity of glass powder with the cement.

### **4.1 Experimental programs**

#### **4.1.1 Material**

General-purpose cement and fly ash blend cement (with 30% fly ash) were used in this research. Coarse aggregate with a nominal size of 20 mm from Edmonton quarry was used in the study. Two different types of fine aggregates used were coarse sand and fine sand obtained from the Barron River and Tableland regions, respectively. In this research, RGP was used in concrete as a partial cement replacement. The mixed soda-lime glass used in this study was collected from the kerb-side domestic waste collection by the Cairns Regional Council.

The 3 mm glass particles (Figure 4.1a) are further pulverised to powder (80% passing through 45 µm sieve) (Figure 4.1b) at ALS Minerals Geochemistry-Townsville Laboratory. At the moment, the council sends 5mm coarse glass particles to be used in road construction as base course and subbase or are sent to landfill. Use of recycled glass powder in concrete as partial cement replacement has the potential to create a high-value market for recycled glass.



**Figure 4.1 (a) Crushed glass (3 mm size) at MRF site, (b) glass powder (45 µm size)**

#### **4.1.2 Mix proportion and sample preparation**

This research was conducted in three phases. The first phase consisted of material characterisation to determine accurate chemical and physical characteristics of RGP. The second phase consisted of an experimental investigation on the effects of RGP on fresh concrete (slump test, and fresh density test), hardened concrete properties (hardened density test, compressive strength, tensile strength, and flexural strength), and durability of concrete (rapid chloride penetration test). Five concrete mixes were investigated: GP cement concrete

(control); fly ash blend (30% fly ash) concrete; and three concrete mixes containing RGP as cement substitution at 10%, 20% and 30% (noted as 10 RGP, 20 RGP and 30 RGP, respectively). To keep the concrete mix industry-relevant, concrete mix supplied by Pioneer North Queensland (PNQ) Concrete (Table 4.1) was used as the control mix in the study. SIKA RE Retarder was used in the mixture as an admixture to retard the setting time of the mixture. Testing was conducted on seven, 28 and 56 days of curing.

**Table 4.1 Materials content for 1 m<sup>3</sup> of concrete mix**

Material	Cement (kg)	Recycled Glass Powder (kg)	Fine Aggregate (kg)		Coarse Aggregate (kg) 20 mm	Water (L)	Admixture (mL/100 kg of Cement)
			Fine Sand	Coarse Sand			
Control	336	-	270	632	981	180	400
10 RGP	302.4	33.6	270	632	981	180	400
20 RGP	268.8	67.2	270	632	981	180	400
30 RGP	235.2	100.8	270	632	981	180	400
Fly Ash Blend (30% fly ash)	336	-	270	632	981	180	400

In the third phase, the relative strength test was conducted according to AS 3583.6 (AS3583.6, 2018) on cement mortar to investigate the potential of RGP as supplementary cementitious material. Five mortar mixes were prepared using standard sand (CEN-NORMSAND DIN EN 196-1). The amount of cement, sand and water was used according to AS 3583.6 (AS3583.6, 2018) (Table 4.2). The quantity of water used in each mix should provide a flow of  $110 \pm 5$  for control mortar, as required by AS 2701(AS2701, 2001).

**Table 4.2 Mix proportion of mortar for three prism bars of 40 x 40 x 160mm (AS3583.6, 2018)**

Material	Cement (g)	RGP (g)	Fine Sand (g)	Water (mL)
Control	450	-	1350	250
10 RGP	405	45	1350	250
20 RGP	360	90	1350	248
30 RGP	315	135	1350	247

Concrete mixing was performed according to AS 1012.2 (AS1012.2, 2014) and prepared for compressive, flexural and indirect tensile strength and RCPT. All moulded samples were then stored for initial setting. Samples were demoulded after 24 hours and cured for a specific period in water, according to AS 1012.8.1 (AS1012.8.1, 2014). Mortar samples were prepared in accordance with AS 2350.12 (AS2350.12, 2006).

### 4.1.3 Test methods

The test methods included (a) chemical composition test- X-ray fluorescence (XRF), particle size distribution test, scanning electron microscope and X-ray diffraction analysis (b) fresh concrete properties – slump test and fresh concrete density test (c) hardened concrete properties – compressive, tensile, flexural strength tests, RCPT. Relative water requirement and relative strength requirement tests were also carried out on mortar specimen.

#### (a) Chemical composition test

The chemical compositions of cement, RGP and fly ash were found by X-ray using ME-XRF26 method (Figure 4.2a). The particle size distributions, including specific surface area, were determined using a laser-based particle size analyser Malvern Mastersizer 2000 (Figure

4.2b). The morphology of materials was performed with a scanning electron microscope (Hitachi SU5000) (Figure 4.2c). The samples were coated with platinum to make them electrically conductive. X-ray diffraction analysis was performed by using a D2 PHASER 2<sup>nd</sup> generation diffractometer (XRD), with a copper anode X-ray tube at 30 kV and 10 mA, between 5° and 70° with a counting time of 160 s, at a step size 0.02 (Figure 4.2d).

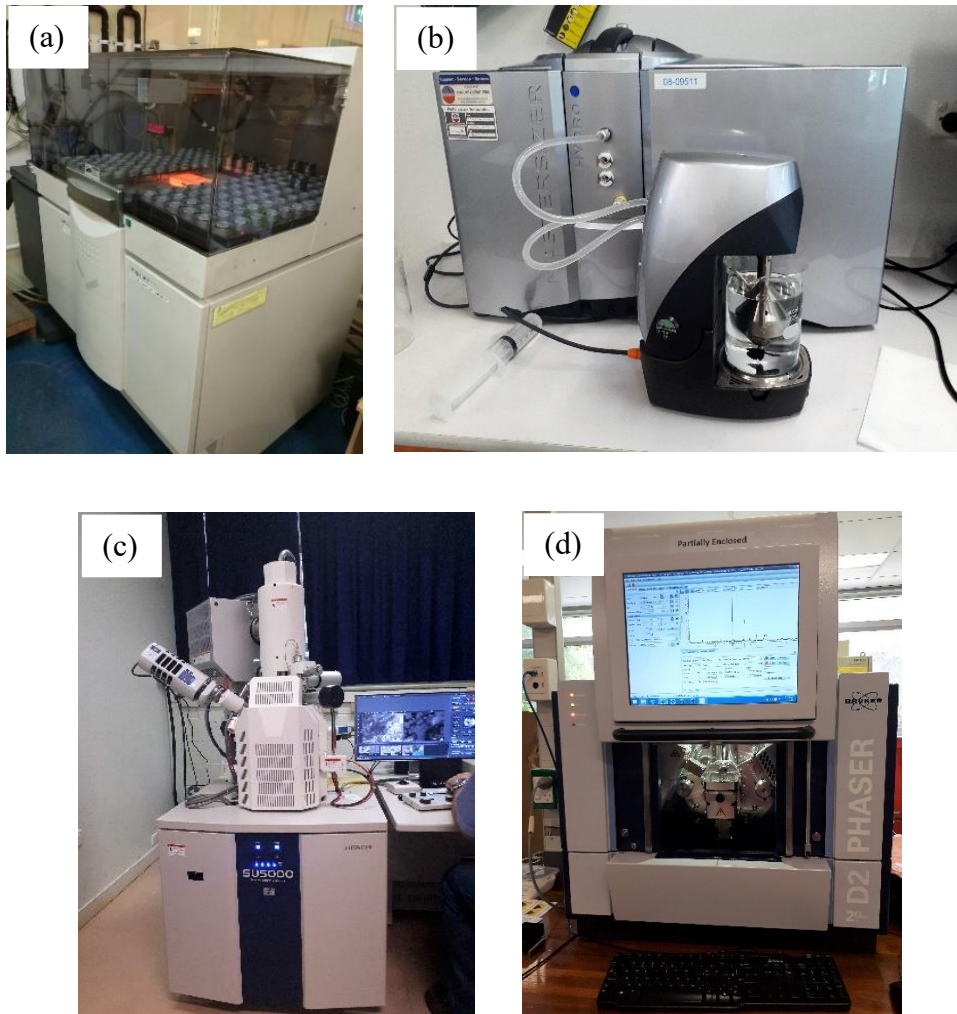


**Figure 4.2 (a) X-ray fluorescence (XRF) (b) particle size analyser (c) scanning electron microscope (d) X-ray diffraction analyser**

### **(b) Fresh concrete properties**

A slump test was conducted to measure the consistency of fresh concrete as per AS 1012.3.1 (AS1012.3.1, 2014). The fresh and hardened density of concrete were calculated after

moulding the cylinders (fresh density) and directly before testing (hardened density), by weighing and measuring samples, according to AS 1012.12.1 (AS1012.12.1, 2014) (Section 3.1.3).

### **(c) Hardened concrete properties**

For a compressive strength test, cylinders with a 100 mm diameter and 200 mm height were prepared according to AS 1012.8.1 (AS1012.8.1, 2014). A total of 32 cylinders were cast and cured. One cylinder was cast for each batch for the seven days test to estimate the early strength gain and three of each cylinder were prepared for the 28 and 56 days. A total of nine cylinders (150 mm diameter and 300 mm height) were prepared for the splitting tensile strength test following AS 1012.8.1 (AS1012.8.1, 2014). Concrete beams of 100 mm × 100 mm × 360 mm were tested on a four-point bending test to determine the flexural strength of concrete at 28 days based on AS 1012.11(AS1012.11, 2014).

### ***Relative water requirement and relative strength***

The test method for relative water requirement determines the amount of water needed for a specified flow. A flow table (Figure 4.3a) was used to determine a flow according to AS 2701 (AS2701, 2001). The flow mould was filled with mortar in a 25 mm thick layer until the mould was full. The mould was lifted away and allowed the flow table to drop 25 times in 15 seconds through 12 mm. The change in diameter of mortar was measured, and the required flow was obtained by trial and error. Relative water requirement was calculated as the ratio of water of test mortar (with supplementary cementitious material, SCM) and control mortar (containing 100% Portland cement). Relative strength index is a test to assess the reactivity of SCMs. It is the ratio of the strength of test mortar (containing SCMs) and control mortar (with 100% Portland cement) expressed as a percentage. According to AS 3582.1 (AS3582.1, 2016), test mortar (SCMs such as fly ash) should gain 75% of control mortar strength to be considered as

a SCMs. AS 2350.12 (AS2350.12, 2006) was followed to prepare control and test mortar (mortar containing 10 RGP, 20 RGP and 30 RGP). Three prismatic specimens  $40\text{ mm} \times 40\text{ mm} \times 160\text{ mm}$  (Figure 4.3b) were cast and cured for 28 days for each batch. Compressive strength of the mortar bars was tested at the loading rate of  $2.4\text{ kN/s}$  until failure according to AS 2350.11 (AS/NZS2350.11, 2006). The relative strength was calculated using Equation 4.1.

$$\text{Relative strength} = \frac{\text{Average compressive strength of test mortar at 28 days (in MPa)}}{\text{Average compressive strength of control mortar at 28 days (in MPa)}} \times 100\% \quad (4.1)$$

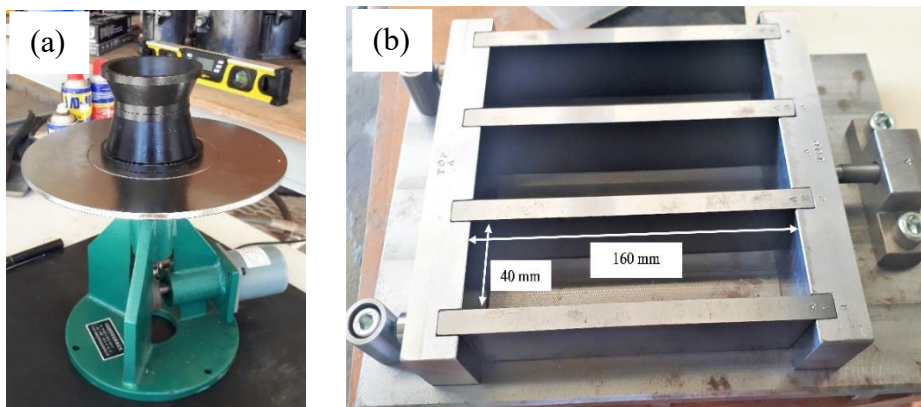


**Figure 4.3 (a) Flow table (b) Prismatic mould of  $40 \times 40 \times 160\text{ mm}$**

### ***Rapid chloride penetration test***

A commonly used method to determine concrete durability is a rapid chloride penetration test (RCPT). Concrete resistivity against chloride ions penetration in concrete was determined using RCPT according to ASTM C 1202-12 (ASTMC1202, 2012) (Section 3.3).

## **4.2 Results and discussion**

### **4.2.1 Characterisation of materials**

The chemical compositions of cement, RGP and fly ash are listed in Table 4.3. RGP had the highest content of silicon dioxide ( $\text{SiO}_2$ ), which is the basic requirement to consider as a pozzolanic material. The  $(\text{SiO}_2 + \text{Al}_2\text{O}_3 + \text{Fe}_2\text{O}_3)$  of RGP was found to be higher than the

minimum requirement of 70%, according to ASTM C 618 (ASTMC618, 2014). (Figure 4.4) shows the location of RGP in the CaO-Al<sub>2</sub>O<sub>3</sub>-SiO<sub>2</sub> ternary diagram, along with Portland cement and fly ash.

The particle size distribution of cement, fly ash, and RGP all showed uniformly graded distribution curves (Figure 4.5). Cement with a specific surface area of 562 m<sup>2</sup>/kg and fly ash having a specific surface area of 342 m<sup>2</sup>/kg showed similar particle size distribution. However, cement exhibited higher specific area due to the angular particle compared with the round-shaped fly ash. On the other hand, RGP showed finer particle size distribution than cement and fly ash with a specific surface area of 1169 m<sup>2</sup>/kg. Table 4.3 shows that the effective size (D<sub>10</sub>, corresponding to 10% finer) of RGP was smaller than that of cement and fly ash. 50% of RGP was found to be smaller than 11.6 μm, whereas 90% of RGP was finer than 51.8 μm. Cement and fly ash had 50% of particles finer than 21.4 μm and 20.1 μm, respectively. D<sub>90</sub> (diameter corresponding to 90% finer) of cement and fly ash particles was greater than RGP.

**Table 4.3 Chemical and physical characteristics of cement, fly ash and RGP**

	Cement	Fly Ash	RGP
Chemical Composition (%)			
SiO <sub>2</sub>	18.99	56.86	72.02
Na <sub>2</sub> O	0.16	1.02	12.85
CaO	63.94	4.08	11.25
Al <sub>2</sub> O <sub>3</sub>	4.99	21.62	1.47
MgO	0.78	4.12	0.57
Fe <sub>2</sub> O <sub>3</sub>	3.22	6.88	0.57
K <sub>2</sub> O	0.35	1.97	0.35
SO <sub>3</sub>	2.26	0.63	0.12
Physical properties			

Specific Surface Area	562	342	1169
( $m^2/kg$ )			
$D_{10}$ ( $\mu m$ )	4.85	4.92	1.90
$D_{50}$ ( $\mu m$ )	21.4	20.1	11.6
$D_{90}$ ( $\mu m$ )	70	75.3	51.8

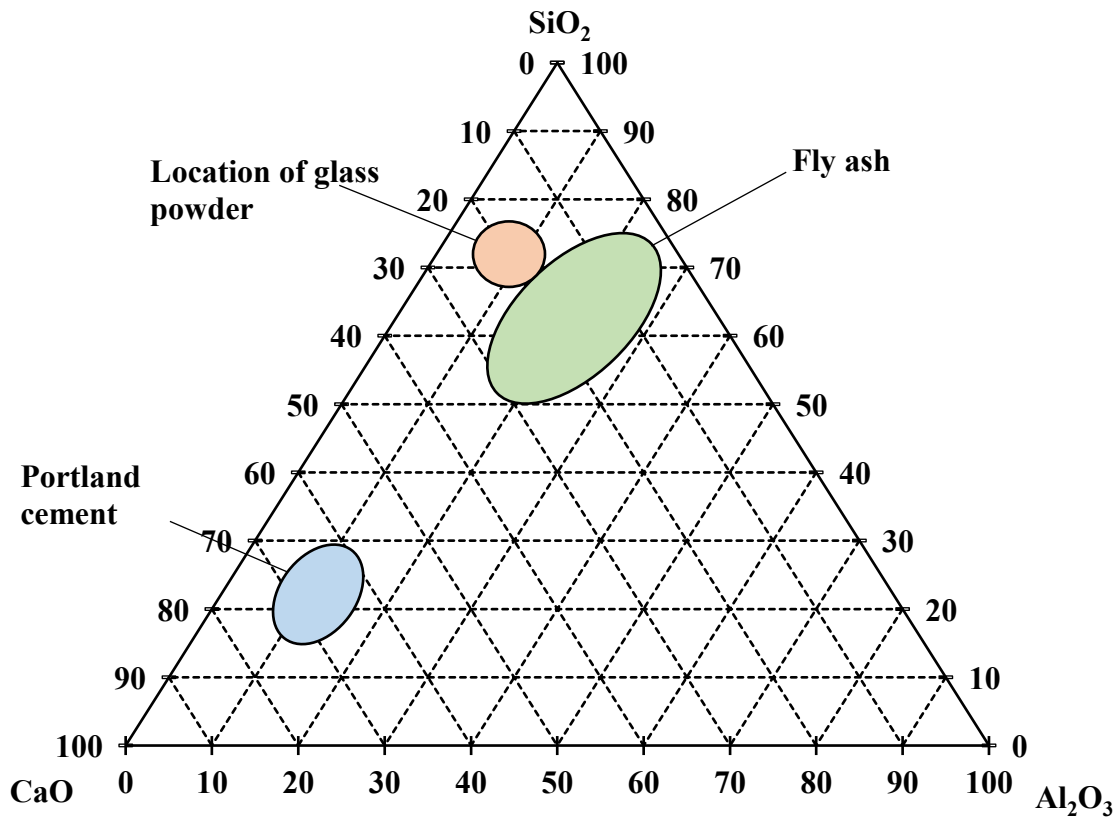
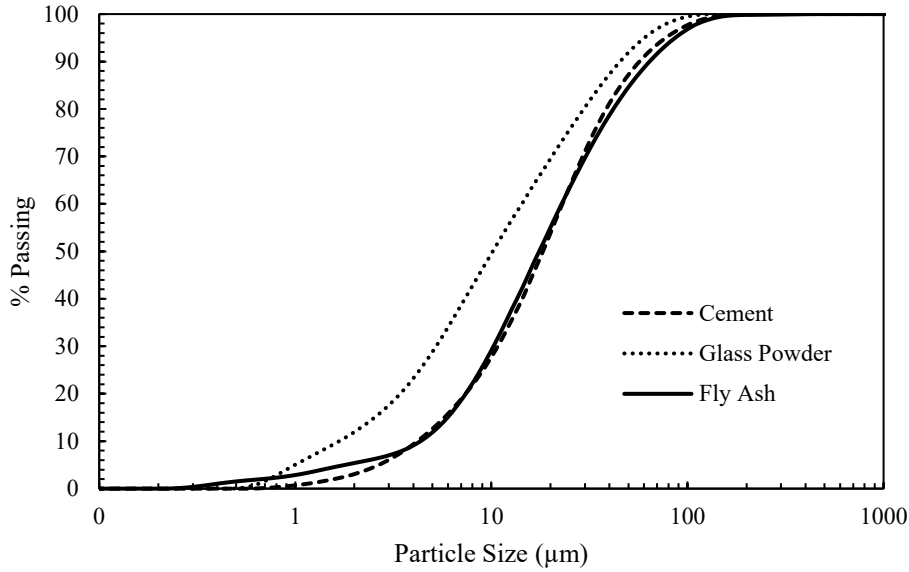
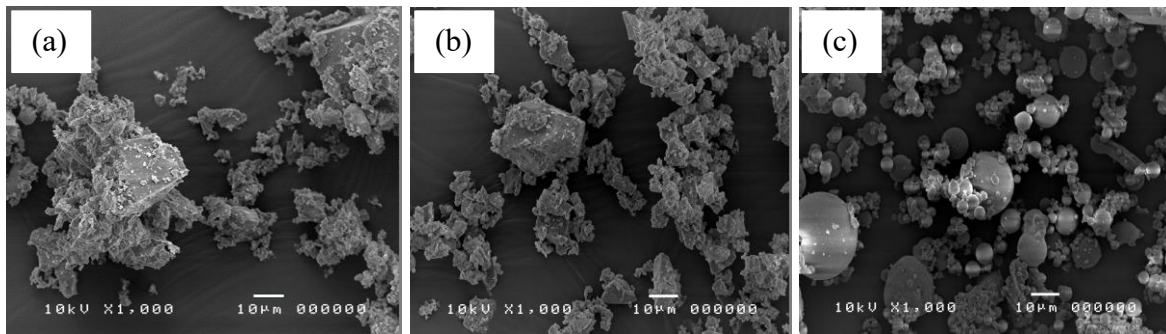


Figure 4.4 CaO-Al<sub>2</sub>O<sub>3</sub>-SiO<sub>2</sub> ternary diagram of cement, fly ash and glass powder



**Figure 4.5 Cumulative particle size distribution curve of cement, fly ash and glass powder**

The microstructures of these three materials are shown in Figure 4.6 using a scanning electron microscope. Cement and RGP showed angular shaped particles with a heterogeneous distribution. RGP consisted of sharp edges particles, whereas fly ash showed spherical shapes.



**Figure 4.6 Scanning electron microscope of (a) cement, (b) RGP, (c) fly ash**

X-ray diffraction analysis was performed to determine the X-ray patterns of cement and RGP (Figure 4.7). X-ray patterns of cement indicated a crystalline phase with a certain peak of major components, for instance, tri-calcium silicate, di-calcium silicate, calcium hydroxide, and calcium silicate hydrate (C-S-H). RGP did not show a clear crystalline peak. In the amorphous

phase, X-rays are scattered in many directions leading to a large hump. RGP showed a large hump between  $15^\circ$  and  $35^\circ$  due to the high silica compositions. It is evident that the RGP is a typical amorphous material as no clear crystalline peak could be noticed.

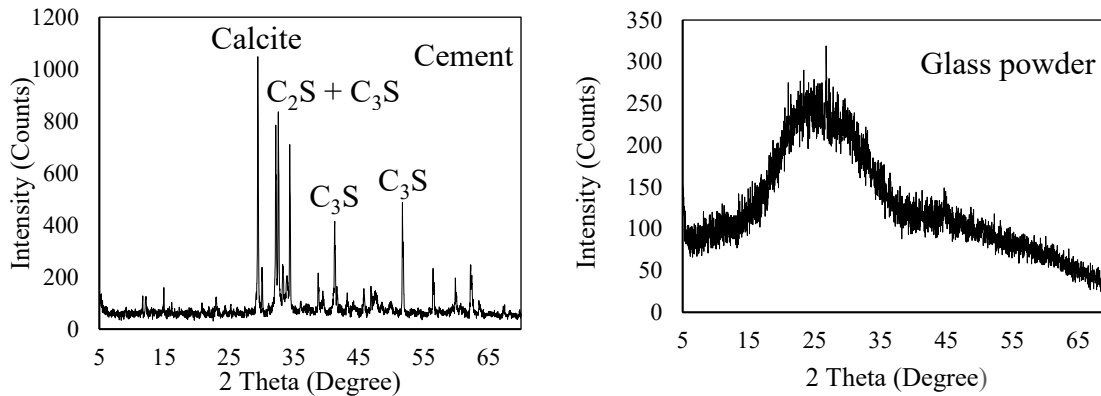


**Figure 4.7 XRD pattern for cement and RGP**

## 4.2.2 Fresh concrete properties

### 4.2.2.1 Slump test

A slump test was conducted to determine the consistency and workability of control concrete, concrete with RGP and fly ash (Table 4.4). The target slump was in a range of 80-100 *mm*. The control concrete, 10 RGP and 20 RGP mixtures achieved the desired slump. However, 30 RGP showed a slump greater than 100 *mm*. The 10 RGP mixture exhibited less slump than that of the control mixture. However, as replacement level increased up to 30 RGP, slump drastically increased due to less water affinity of RGP. The real water-to-cement ratio increased in the mixture as the amount of RGP increased. The presence of more free water led to an increase in slump value. In addition, increasing RGP content could be a reason for cement dilution, which tends to reduce the formation of cement hydration products in the initial minutes of mixing, thereby causing insufficient products to bridge various particles together (Soliman and Tagnit-Hamou, 2016). Fly ash concrete showed less workability with the same amount of water used

in this study compared with control concrete and concrete with RGP. The reduced value of slump in fly ash concrete might be due to the porous nature of fly ash, which can absorb water from the mixture. A similar decrease pattern was observed by Akmal et al. (2017).

#### 4.2.2.2 Density

Table 4.4 shows the fresh density of control concrete was  $2394 \text{ kg/m}^3$ . A slight reduction in fresh density was observed with the addition of RGP due to the lower specific gravity of RGP, which had a specific gravity of 2.09 whereas cement had a specific gravity of 3.03. Fly ash concrete had a fresh density of  $2410 \text{ kg/m}^3$ , which was slightly higher than the control concrete and concrete with RGP. The decrease in hardened density was noticed for the control, 10 RGP and fly ash concrete at seven and 28 days. However, a significant increase in density was seen for the 10 RGP, 20 RGP and 30 RGP, as  $2416 \text{ kg/m}^3$ ,  $2364 \text{ kg/m}^3$  and  $2338 \text{ kg/m}^3$ , respectively, at 56 days. Addition of RGP exhibited an increase in hardened density with time. This can be attributed to the development of additional C-S-H gel which is formed during the pozzolanic reaction of glass with calcium hydroxide. This can improve the interfacial transition zone and refine the capillary pores in the concrete microstructure (Nassar and Soroushian, 2011; Nassar and Soroushian, 2012). Fly ash concrete also supported this phenomenon and showed an increase in density at 56 days.

**Table 4.4 Slump and density of control, RGP and fly ash concrete**

Sample Name	Slump ( <i>mm</i> )	Fresh Density ( $\text{kg/m}^3$ )	Hardened Density ( $\text{kg/m}^3$ )		
			7 days	28 Days	56 Days
Control	90	2394	2406	2399	2396
10 RGP	80	2381	2379	2373	2416
20 RGP	90	2312	2318	2329	2364
30 RGP	120	2254	2230	2250	2338

Fly Ash Blend	70	2410	2394	2376	2393
---------------	----	------	------	------	------

## 4.2.3 Hardened concrete properties

### 4.2.3.1 Variation of compressive strength

The compressive strength for control, RGP and fly ash concrete were tested at seven, 28 and 56 days (Figure 4.8). The control concrete showed better compressive strength than RGP and fly ash blend concrete at early ages (i.e., seven days). Compressive strength of concrete decreased as RGP replacement level increased, 20 RGP and 30 RGP showed 27% and 53% less strength than that of control concrete. RGP concrete had a negative impact on early-age strength due to the delay in pozzolanic reaction.

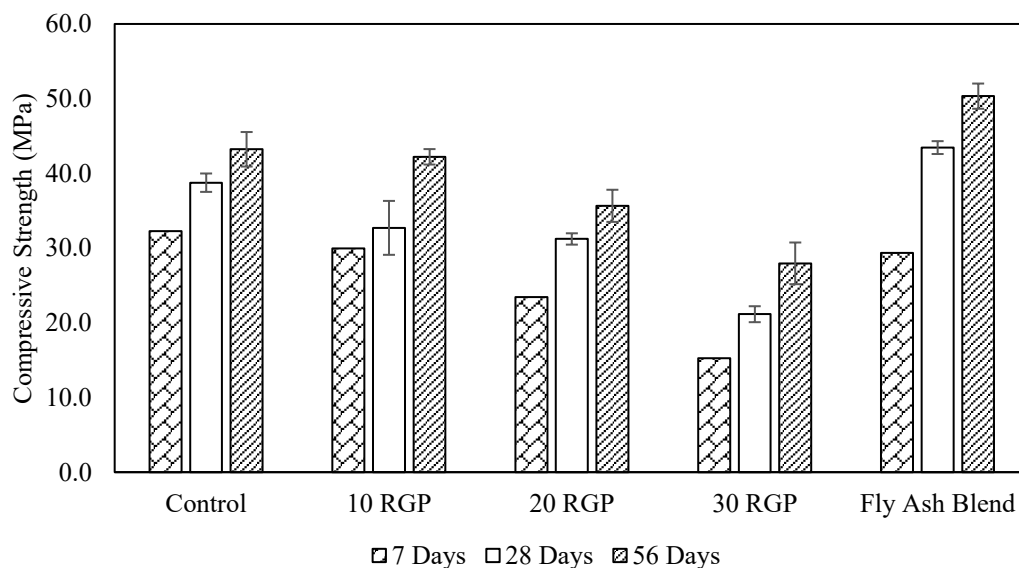


**Figure 4.8 Compressive strength of concrete with RGP and fly ash blend**

All concrete achieved the characteristic strength of 32 MPa at 28 days except 20 RGP (31.2 MPa) and 30 RGP (21.2 MPa). Figure 4.8 shows that fly ash blend concrete produced the highest strength (43.5 MPa) at 28 days. However, 10 RGP and 20 RGP achieved compressive

strength equivalent to 84% and 81% of control concrete. 30 RGP concrete showed lower strength gain than other concrete.

Control concrete achieved a strength of 43.22 *MPa* at 56 days. 10 RGP concrete achieved 96% strength of the control concrete, whereas 20 RGP and 30 RGP concrete obtained 82% and 64%, respectively. Fly ash blend concrete had the maximum strength of 50.34 *MPa* at 56 days. Strength development exhibited a significant increase (41%, 52%, and 83% increase) for 10 RGP, 20 RGP and 30 RGP concrete, respectively at 56 days. RGP and fly ash concrete gained further strength at later ages due to the formation of denser additional C-S-H at 56 days. The failure pattern of control and fly ash blend concrete was usually conic, shear-conic, and shear and less dispersion with large distinct pieces. However, the addition of RGP displayed failure patterns most resembling conic and shear-conic modes and smashed into many pieces.

#### **4.2.3.2 Flexural and tensile strength of concrete**

The flexural and tensile strength tests of the concrete with RGP and fly ash as a partial cement substitute were conducted at 28 days (Figure 4.9). The addition of RGP did not show any significant effects on the flexural strength as all results obtained were within 10% of the control concrete. Recycled glass has the potential to reach a long-term effect. The long-term effect can be attributed to the enhanced binding qualities of the calcium silicate hydrate, which is formed during the pozzolanic reaction of glass with calcium hydroxide. However, tensile strength showed a decreasing trend as the RGP replacement level increased. The percentage of indirect tensile strength to compressive strength was in the range of 8-12%. Fly ash blend concrete exhibited 8% and 25% higher flexural and tensile strength than the control concrete, respectively at 28 days.

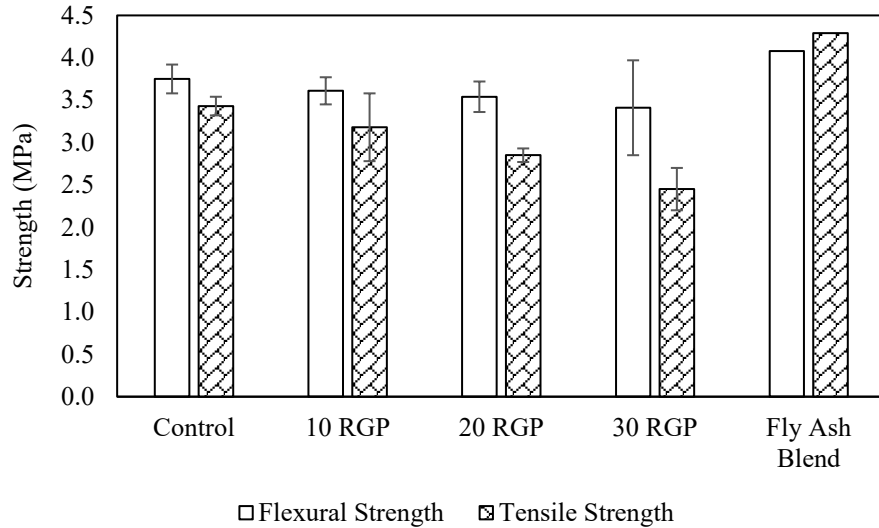


**Figure 4.9 Flexural strength of concrete with RGP and fly ash blend**

#### 4.2.3.3 Rapid chloride permeability test (RCPT)

RCPT was conducted on the concrete cylinder at 28 and 56 days to evaluate the resistance of concrete to chloride ion penetration (Figure 4.10). Control concrete showed the highest chloride penetration value compared with RGP and fly ash concrete both at 28 days and 56 days. The RCPT value of control concrete was 5234 coulombs at 28 days. According to ASTM C 1202, when the amount of charge passed (in coulombs) through the concrete is higher than 4000, the chloride ion permeability is considered as high. RGP and fly ash blend concrete showed lower chloride permeability compared with that of control concrete. The RCPT values of 10 RGP and 20 RGP were 5152 and 4840 coulombs, respectively at 28 days, still classified as highly permeable concrete. As can be seen, RCPT values of 30 RGP and fly ash concrete were found to be 24% and 53% less permeable than that of control concrete which were in between 2000-4000 coulombs range, classified as moderately permeable concrete. A reduction of chloride ion permeability can be attributed to the formation of additional C-S-H gels, which resulted in a reduction in permeability of concrete.

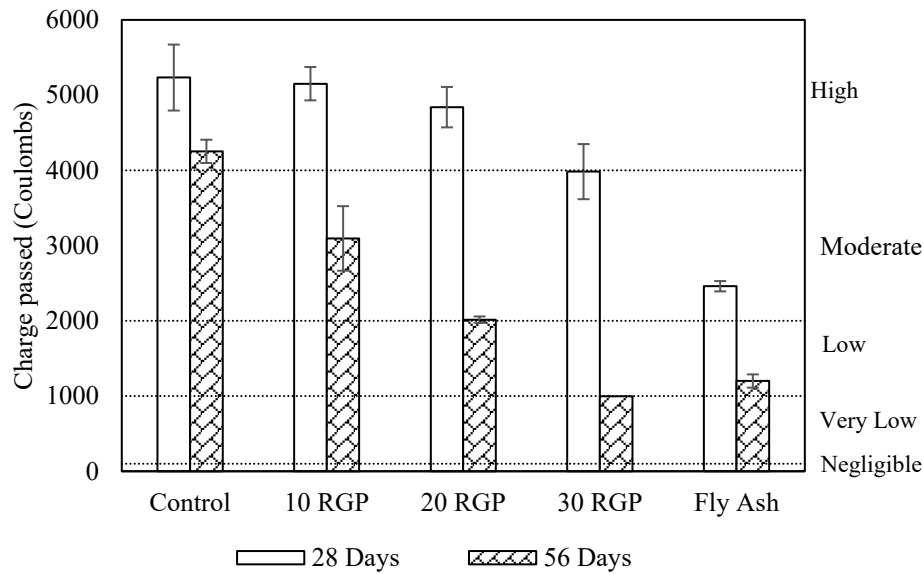


**Figure 4.10 RCPT results of concrete at 28 days and 56 days**

A 19% reduction was noticed for control concrete at 56 days due to further hydration but still exhibited in a high permeable category. A total current passed through all the specimen decreased with increase in curing time. The reduction rate in the permeability of concrete for RGP mixes was even more pronounced at 56 days due to increase in density and due to formation of additional C-S-H gel. Permeability of 10 RGP and 20 RGP concretes was moderate in category whereas 30 RGP showed very low permeable concrete. Fly ash concrete showed moderate to low permeability with an increase in curing time.

#### **4.2.3.4. Relative water requirement**

According to AS 3583.6 (AS3583.6, 2018), the control mortar was prepared by using the amount of water required to give a flow of  $110 \pm 5$ . The test mortar with RGP was required to have sufficient water to achieve a flow within  $\pm 3$  units of control mortar. 250 mL water was required for control mortar to gain a specified flow (Table 4.5). RGP mortar showed flow values within three units of the control mortar. Relative water requirement to control mortar was 100%, 99.2%, and 98.8% for 10 RGP, 20 RGP and 30 RGP, respectively. Water

requirement decreased as the RGP replacement level increased. This trend suggests that RGP does not absorb much water as cement, and hence has a lower water requirement.

**Table 4.5 Relative water requirement of RGP**

Sample	Water Content ( <i>mL</i> )	Flow (%)	Relative water requirement (%)
Control	250	110.9	-
10 RGP	250	112.8	100
20 RGP	248	110.7	99.2
30 RGP	247	109.8	98.8

#### **4.2.3.5 Relative strength**

A compressive strength test of mortar was conducted to assess the relative strength of RGP mortar bars at 28 days. Figure 4.11 shows that 10 RGP mortar gained the highest relative strength, which was about 75% of the control mortar. An increase in glass powder replacement affected negatively in relative strength. The 20 RGP and 30 RGP mortar achieved a relative strength of 61% and 59%, respectively. Relative strength was found to decrease with an increase in RGP quantity, and 40 RGP exhibited the lowest relative strength. The reason behind the reduction of strength in higher percentage might be due to inadequate cement paste available in the mixture to assist bonding within the mix which is consequently forming the microscopic voids (Adaway and Wang, 2015). However, 10 RGP satisfied the requirements of AS 3582.1 (AS3582.1, 2016) to be deliberated as a supplementary cementitious material.

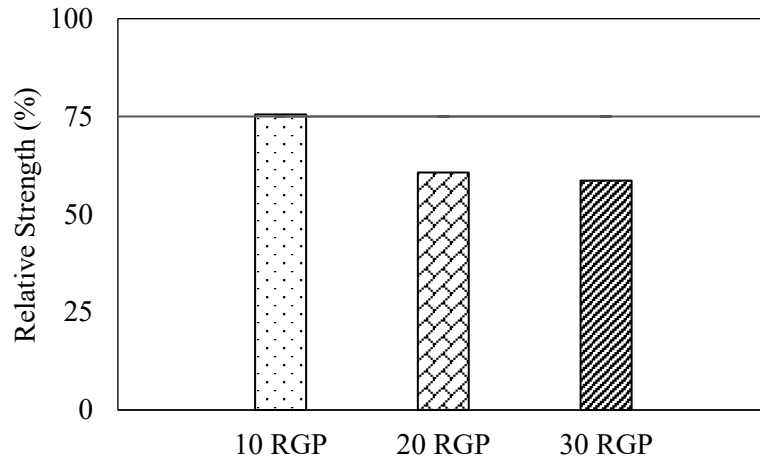


**Figure 4.11 Strength of RGP mortar relative to control mortar at 28 days**

### 4.3 Conclusions

This research studied the use of crushed recycled glass powder as a partial cement replacement in concrete. The recycled glass considered in this study was mixed-coloured soda-lime glass, collected from domestic waste by Cairns Regional Council, Australia. Having less water affinity and smooth surface, RGP improved the workability of concrete. A reduction in fresh density was observed with the addition of RGP due to the lower specific gravity of glass powder. Addition of RGP improved hardened density with curing time even though a decrease was noticed with the increase in RGP replacement level. RGP did not show significant strength gain at an early age due to the delay in pozzolanic reaction. However, 10 RGP concrete achieved the target characteristic strength of 32 MPa at 28 days. RGP showed a substantial strength development at 56 days. The addition of RGP exhibited adequate flexural and tensile strength but a similar downtrend was observed in flexural and tensile strength as compressive strength with the increase in RGP content. RGP concrete exhibited a reduction in permeability due to large specific surface area and production of more C-S-H gel. 10 RGP was found to satisfy the requirement of 75% relative strength requirement as per AS 3582.1 to be considered as supplementary cementitious material. Pozzolanic behaviour was also confirmed by TGA

and SEM analysis from 10 RGP. This research showed that the use of RGP as cement replacement is feasible for replacement levels up to 10%. However, long-term curing and lower particle size distribution are mandatory for successful use of RGP with higher replacement levels without compromising strength. The outcome of this research aims to contribute towards sustainable development by reducing the consumption of cement, as well as the reduction of glass waste going into landfill.

## Chapter 5: Microstructure analysis of recycled glass sand and recycled glass powder

Nafisa Tamanna, Norsuzailina Mohamed Sutan, Rabin Tuladhar, Delsye Teo Ching Lee and Ibrahim Yakub. "Pozzolanic Properties of Glass Powder in Cement Paste". *Journal of Civil Engineering, Science and Technology*. Vol. 7, Issue 2, September 2016.

Nafisa Tamanna, Norsuzailina Mohamed Sutan, Rabin Tuladhar. "The effect of waste glass powder on microstructural behaviour when used as a partial cement replacement". *5<sup>th</sup> International fib Congress*. 7-11 October 2018, Melbourne, VIC Australia.

This research investigates the microstructure of mortar and cement paste containing recycled crushed glass sand and glass powder, respectively. A series of tests was conducted to evaluate the potential of alkali silica reaction (ASR) and pozzolanic reactivity in recycled glass sand (RGS) mortar and recycled glass powder (RGP) cement paste, respectively, including thermogravimetric analysis, X-ray diffraction (XRD), scanning electron microscopy (SEM) and energy-dispersive spectroscopy (EDS). TGA was carried out to quantify hydration product,  $\text{Ca(OH)}_2$  for both RGS mix and RGP pastes. The morphology and chemical composition were analysed for RGS and RGP paste using SEM and EDS, respectively. XRD was conducted to identify the hydration product, calcium hydroxide ( $\text{Ca(OH)}_2$ ) in the cement paste. The mortar was prepared by replacing natural river sand with 20%, 40% and 60% of recycled glass sand, whereas cement paste was produced by replacing General Portland (GP) cement with 10%, 20%, 30% and 40% of recycled glass powder.

### 5.1 Experimental procedure

#### 5.1.1 Materials

Microstructural analysis was carried out for recycled glass sand (RGS) mix and recycled glass powder (RGP) paste. The experimental program consisted of two main phases. In the first phase, microstructure analysis of a mortar bar corresponding to the alkali-silica reaction was conducted to investigate the influence on using RGS in the mortar. The second phase consisted of tests on the microstructure of cement paste containing RGP.

### 5.1.2 Mix Design

#### (a) Mix design for RGS mix

RGS mortar was used to characterize the potential of ASR samples. Mortar sample from accelerated mortar bar test was used for the first phase. The mix design of mortar mixes used for three ASR prism bars are described in Section 3.1.3. RGS mortar bars were prepared for each mix according to the proportion (Table 5.1). Four RGS mixes were investigated: GP mortar with natural sand (Control 0 RGS); and three mixes containing RGS as sand substitution at 20%, 40% and 60% (noted as 20 RGS, 40 RGS and 60 RGS, respectively).

**Table 5.1 Mix design of RGS mix for three ASR prism bars (AS1141.60.1, 2014)**

Material	Cement (g)	Sand (g)	Recycled Glass Sand (g)	Water (mL)
Control (0 RGS)	440	990	-	206.8
20 RGS	440	792	198	206.8
40 RGS	440	594	396	206.8
60 RGS	440	396	594	206.8

#### (b) Mix design for RGP mix

Cement paste was prepared to investigate the effect of using RGP in the microstructure and to evaluate the pozzolanic reactivity of glass powder. Four cement mixes were investigated: GP cement paste (Control 0 RGP); and three mixes containing RGP as cement substitution at 10%,

20% and 30% (noted as 10 RGP, 20 RGP and 30 RGP, respectively). A plastic mould of 50 mm diameter and 35 mm high was used to cast a cement paste sample according to mix design (Table 5.2). The cement paste samples were cured at room temperature.

**Table 5.2 Mix design of cement paste for cylinder of 50 mm diameter and 35 mm height**

Material	Cement (g)	Recycled Glass Powder (g)	Water (mL)
Control (0 RGP)	82	-	41
10 RGP	73.8	8.2	41
20 RGP	65.6	16.4	41
30 RGP	57.4	24.6	41

ASR mortar and cement paste samples were prepared for thermogravimetric analysis (TGA), scanning electron microscopy (SEM) and energy-dispersive X-ray spectroscopy (EDS). X-ray diffraction (XRD) was also carried out for cement paste specimens. The hardened sample was cut into small pieces and crushed to powder using a bevelled-edge chisel (Figure 5.1). For SEM and EDS test, samples were kept in isopropanol (Figure 5.2) for several hours after cutting into small pieces to remove the capillary water from the samples.

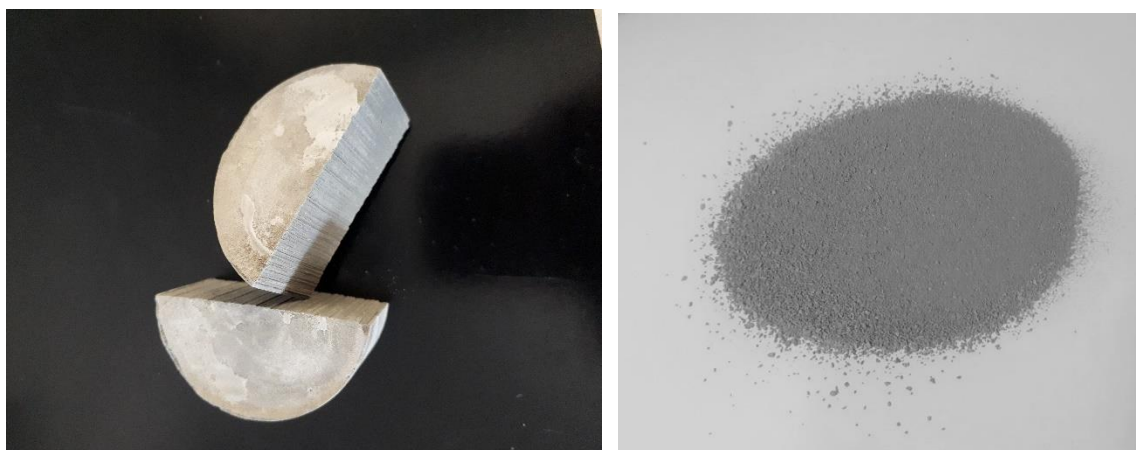


**Figure 5.1 Hardened cement sample**



**Figure 5.2 SEM samples in isopropanol**

### **5.1.3 Experimental methods**

Microstructural analysis was conducted for RGS mix and RGP paste. A series of tests was conducted to evaluate the potential of ASR samples using RGS mix and pozzolanic reactivity of glass powder using RGP paste. Thermogravimetric analysis, scanning electron microscopy and energy-dispersive spectroscopy were carried out for RGS mix. However, for RGP paste, thermogravimetric analysis, X-ray diffraction, scanning electron microscopy and energy-dispersive spectroscopy were conducted.

#### **5.1.3.1 Thermogravimetric analysis**

Thermogravimetric analysis (TGA) is a widely applied technique to determine the change in weight of a sample as a function of temperature (with constant heating rate) or as a function of time (with constant temperature or constant mass loss). TGA is generally used to determine the hydration products present in the cementitious system. In TGA, the sample is gradually heated from room temperature to a specified temperature while the weight loss due to decomposition

of chemical component is recorded along with the temperature. The weight loss over a broad temperature range, from 50 °C to 200 °C, indicates the loss of water from the main hydrate, C-S-H. However, strong overlaps from many of the hydrates – for instance, bound water, ettringite and monosulphate – makes C-S-H quantification difficult. The other hydrate portlandite (Ca(OH)<sub>2</sub>) decomposes to CaO and H<sub>2</sub>O in between 400 °C and 500 °C. The weight loss occurs mainly due to the evaporation of water. The amount of Ca(OH)<sub>2</sub> can be calculated using the following equation:

$$\text{Ca(OH)}_2 (\%) = \text{WL}_{\text{CH}} \times (\text{M}_{\text{CH}} / \text{M}_{\text{W}}) \quad (5.1)$$

Where,

$\text{WL}_{\text{CH}}$  = Percentage weight loss occurred between 400 °C and 600 °C

$\text{M}_{\text{CH}}$  = Molecular weight of calcium hydroxide

$\text{M}_{\text{W}}$  = Molecular weight of water

The amount of Ca(OH)<sub>2</sub> shows the presence of Ca(OH)<sub>2</sub> in cement mix as a by-product of cement hydration. The Ca(OH)<sub>2</sub> quantity increases over time as more cement is hydrated. Amount of Ca(OH)<sub>2</sub> present in the mix can be used to evaluate the pozzolanic effect of glass powder. In a pozzolanic reaction, Ca(OH)<sub>2</sub> is consumed by the pozzolanic reaction to produce additional calcium silicate hydrate (C-S-H). Consequently, a reduction in Ca(OH)<sub>2</sub> is noticed in the cement paste after pozzolanic reaction. Higher amount of Ca(OH)<sub>2</sub> indicates the lower pozzolanic reaction.

TGA was carried out using a Simultaneous Thermal Analyser SDT 650 (Figure 5.3). About 5-10 mg of samples were placed in one alumina crucible (Figure 5.4). Another empty crucible was placed into the heating chamber as a reference and both crucibles were heated from the

same heat source. The specimen was heated from room temperature to 600 °C at the rate of 10 °C per minute in an N<sub>2</sub> atmosphere with a flow rate of 50 ml/min.



**Figure 5.3 Thermal analyser SDT 650**



**Figure 5.4 Alumina crucible**

### **5.1.3.2 Scanning electron microscope (SEM)**

A scanning electron microscope (SEM) is a strong magnification tool that uses a focused beam of electrons to produce images of a sample. The electrons interact with electrons in the sample and generate a variety of signals at the surface of solid specimens. The signals exhibit detailed information about the sample, including chemical composition, morphology and orientation of

materials. Quantitative chemical composition can be obtained through an energy dispersive spectrometer (EDS). In this research, SEM of the control sample and glass sample (sand and powder) was carried out at the advanced analytical centre, JCU, with a scanning electron microscope (Hitachi SU5000). The analysis was performed on a carbon-coated polished surface to get the sample electrically conductive in Figure 5.5. SEM images were taken both in the secondary-electrons (SE) mode, with an acceleration voltage of 15 *kV*, and in the backscattered electrons (BSE) mode, using an accelerating voltage of 25 *kV*.

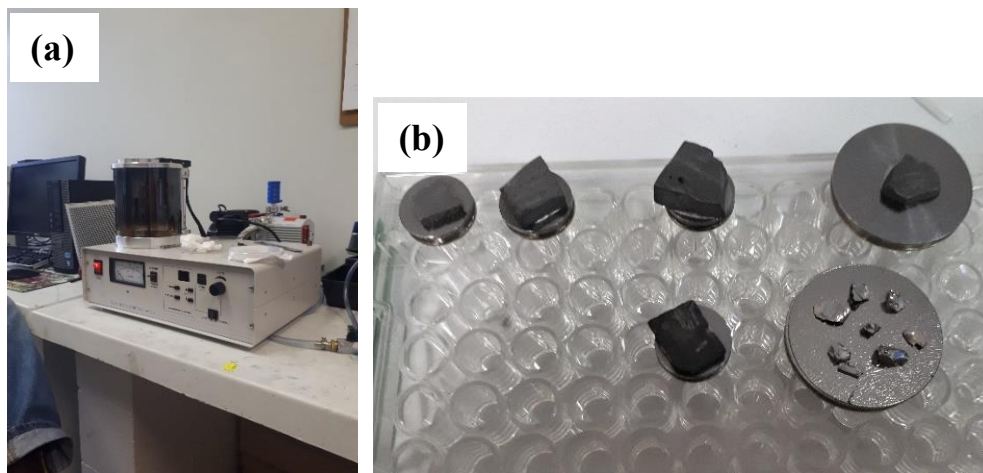


**Figure 5.5 (a) Carbon coater (b) polished samples**

EDS analysis was performed on polished samples in high vacuum conditions. Elements such as, C, O, Na, Mg, Al, Si, S, K, Ca, Fe were selected to get chemical compositions. Point analyses were carried out on a randomly chosen 50 points on the surface of the specimens (RGS mortar mixes and RGP cement pastes) (Figure 5.6). Scatter plot was drawn according to the ratio of element from the spectrum (Table 5.3).

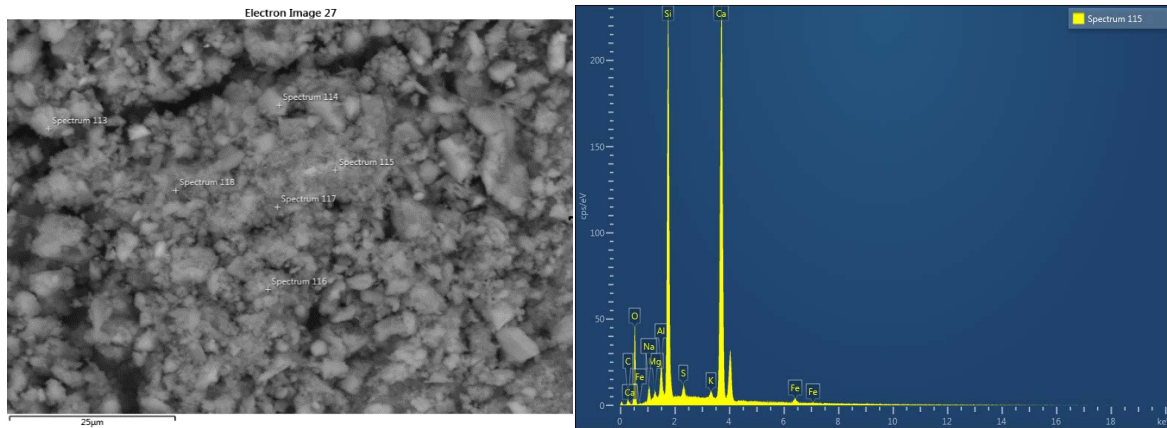


**Figure 5.6 SEM image and corresponding EDS analysis**

**Table 5.3 Elemental analysis of spectrum**

Element	Line Type	Apparent Concentration	k Ratio	Wt%	Standard Label
C	K series	0.51	0.00508	2.88	C Vit
O				43.09	
Na	K series	0.87	0.00368	1.19	Albite
Mg	K series	0.26	0.00171	0.38	MgO
Al	K series	1.22	0.00877	1.56	Al <sub>2</sub> O <sub>3</sub>
Si	K series	14.44	0.11446	16.94	SiO <sub>2</sub>
S	K series	0.52	0.00446	0.63	FeS <sub>2</sub>
K	K series	0.44	0.00374	0.44	KBr
Ca	K series	30.29	0.27066	31.95	Wollastonite
Fe	K series	0.72	0.00721	0.94	Fe
Total:				100	

### 5.1.3. X-ray diffraction (XRD)

XRD is the most prominent analytical method for phase identification of cementitious materials. In XRD, cement samples consist of several dominant major and minor phases. As an amorphous material, glass powder does not show a clear crystalline peak. Instead it shows

a large hump between 15-35 °C due to the high silica composition. Therefore, when glass powder is mixed with cement in cement paste, the diffraction pattern is found from the sum of the diffraction patterns of individual phases. In this study, XRD was conducted to identify the hydration product, calcium hydroxide ( $\text{Ca(OH)}_2$ ) in the cement paste and glass powder modified cement paste. The amorphous silica from glass powder reacts with  $\text{Ca(OH)}_2$  to form further calcium silicate hydrate. Consequently,  $\text{Ca(OH)}_2$  decreases over time, which is attributed to the pozzolanic reaction of glass powder. X-ray diffraction analysis was performed by using a D2 PHASER 2<sup>nd</sup> generation diffractometer (XRD), with a copper anode X-ray tube between 5 °C and 70 °C. The diffractometer operated at 30 *kV* and 10 *mA*, with a counting time of 160 *s*, at a step size of 0.02.

## **5.2 Results and discussion**

### **5.2.1 Microstructure of alkali-silica reaction for RGS mix**

#### **5.2.1.1 Thermogravimetric analysis**

TGA was carried out on RGS specimens (Table 5.1) to investigate the  $\text{Ca(OH)}_2$  content in the accelerated alkali-silica reaction mortar at 21 days. In cement hydration reaction, the amount of  $\text{Ca(OH)}_2$  increases over time as more cement is hydrated. In the presence of glass sand,  $\text{Ca(OH)}_2$  undergoes pozzolanic reaction with glass sand to produce additional C-S-H. Hence, the lower amount of  $\text{Ca(OH)}_2$  in the mix indicates the higher pozzolanic reaction. Control (0 RGS) mortar showed the highest  $\text{Ca(OH)}_2$  content of 2.2% at 21 days (Figure 5.7). The  $\text{Ca(OH)}_2$  content was found to decrease in 20 RGS compared to control mortar. This reduction can be attributed to the consumption of  $\text{Ca(OH)}_2$  in the reaction with glass sand. However, the content of  $\text{Ca(OH)}_2$  for 40 RGS is similar compared to 20 RGS, and is still lower than control mortar. Increase in  $\text{Ca(OH)}_2$  was observed in 60 RGS mortar bar compared with 20 RGS and 40 RGS. The amount of  $\text{Ca(OH)}_2$  was however, still lower compared with the Control (0 RGS)

mortar. This shows that 40% replacement is the optimum replacement rate for the natural sand with RGS. Higher replacement level, impedes the pozzolanic reaction. Lower pozzolanic reaction in 60 RGS can be attributed to inadequate mixing of concrete constituents when higher amount of RGS is used to replace natural sand.

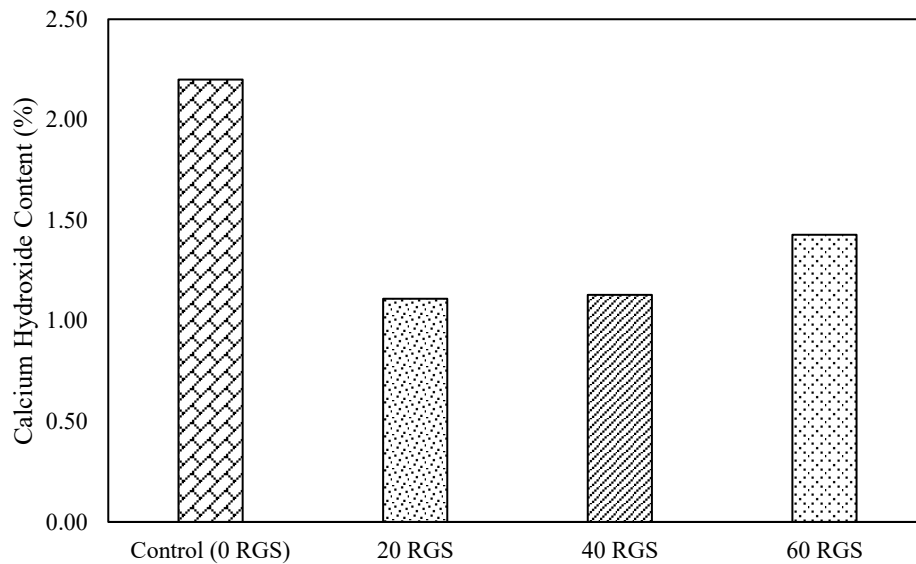


**Figure 5.7 Calcium hydroxide content in mortar bar (ASR) at 21 days**

### **5.2.1.2 Scanning electron microscope**

A SEM test was carried out to exhibit the microstructure of mortar bar obtained from the alkali-silica reaction, which was exposed to 1N NaOH solution for 21 days. The SEM of the control (0 RGS) mortar bar is shown in Figure 5.8. C-S-H was found to form on the top of cracks at higher magnification (x1.3k) (right side). The C-S-H formed on the surface showed dense microstructure in the sample.

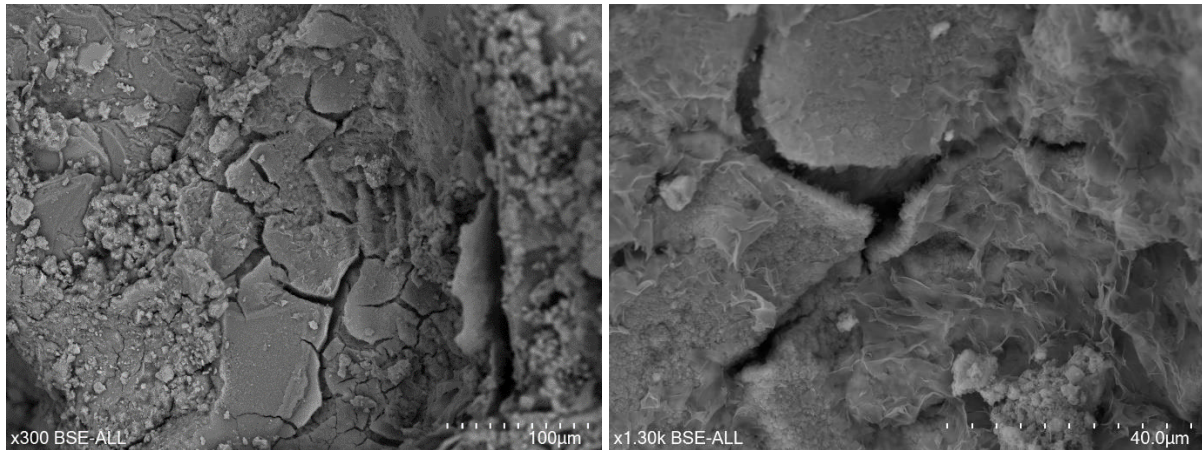


**Figure 5.8 SEM of ASR control (0 RGS) mortar sample**

Fischer et al. (2010) showed that ASR cracking is induced within the internal cracks of the large soda-lime glass particles rather than at the glass cement paste interface. As glass sand used in this research was smaller in size (3 mm), no internal cracks were found at the surface and inside the glass particles (Figure 5.9). However, some partially reacted glass sand particles were found to be covered with the reaction products (Figure 5.9) to produce C-S-H. A significant amount of C-S-H was present in 40 RGS mortar bar samples. Similar to 40 RGS mortar bar samples, no internal crack was noticed in 60 RGS mortar bar samples. This shows no ASR expansion which also agreed with the result from alkali-silica reaction section 3.2.4.2. The formation of ettringite (needle like structures) was observed together with the hydration product. The ASR expansion was not observed in the SEM microstructure for glass sand mortar samples. Finer size RGS reacts with  $\text{Ca(OH)}_2$  and forms secondary C-S-H with a low Ca/Si ratio. However, some negligible cracks were seen in 60 RGS mortar bar sample. These cracks may be due to drying shrinkage during sample preparation (Fischer et al., 2010).

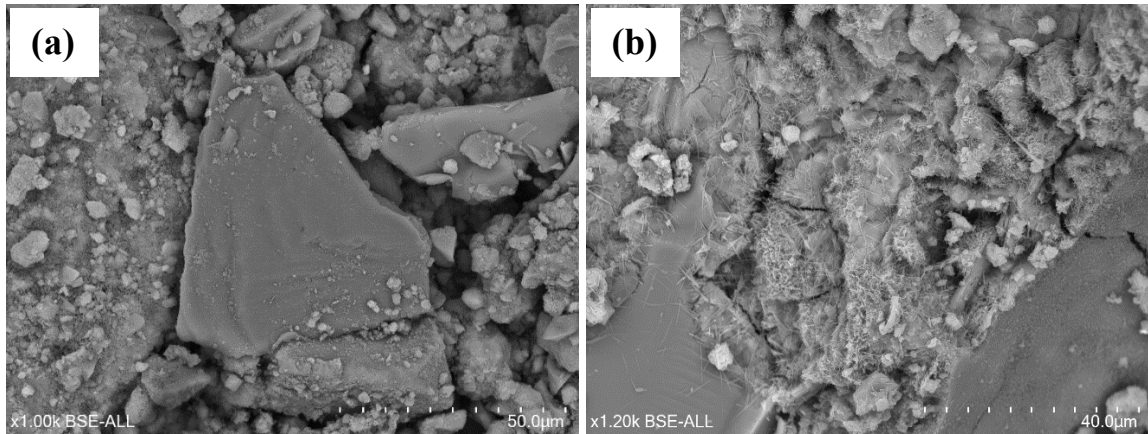


**Figure 5.9 SEM of (a) 40 RGS and (b) 60 RGS ASR mortar sample**

Figures 5.10 and 5.11 show the 2D scatter plot of Si/Ca vs Al/Ca ratios in Control (0 RGS) and glass sand mortar bar (20 RGS, 40 RGS, 60 RGS), samples obtained from ASR tests at 21 days. 2D scatter plot was drawn according to the ratio of silicon dioxide to calcium vs the ratio of aluminium to calcium from the EDS spectrum (Table 5.3). Control (0 RGS) and 20 RGS mortar show similar data clouds in terms of Al-intermixing. However, Al-intermixing, for instance, calcium aluminium silicate hydrate (C-A-S-H) for 20 RGS was found to be predominant within 0.017-0.12. Control (0 RGS) mortar shows the Si/Ca data cloud within 0.1-0.7 whereas the Si/Ca vs Al/Ca ratios for 20 RGS mortar was 0.15-0.67. The Si/Ca ratios were observed to increase (Figure 5.10) as the amount of glass sand increased up to 40% and 60%. 40 RGS and 60 RGS mortar showed Si/Ca ratio within 0.13-1.85 and 0.05-1.9. The increase Si/Ca ratio presented in glass sand mortar showed reduced Ca/Si ratio. With a low Ca/Si ratio, highly reactive glass sand may react with calcium and produce C-S-H (Serpa et al., 2013). Consequently, the reactive alkalis were retained in the form of C-S-H and improved the alkali binding capacity with the addition of glass sand in the mortar (Zapała-Sławeta, 2017). 40 RGS and 60 RGS showed high Si/Ca ratio compared to Control (0 RGS) and 20 RGS. Reversely, in low Ca/Si ratio, finer RGS can react with  $\text{Ca(OH)}_2$  and produce C-S-H at later days.

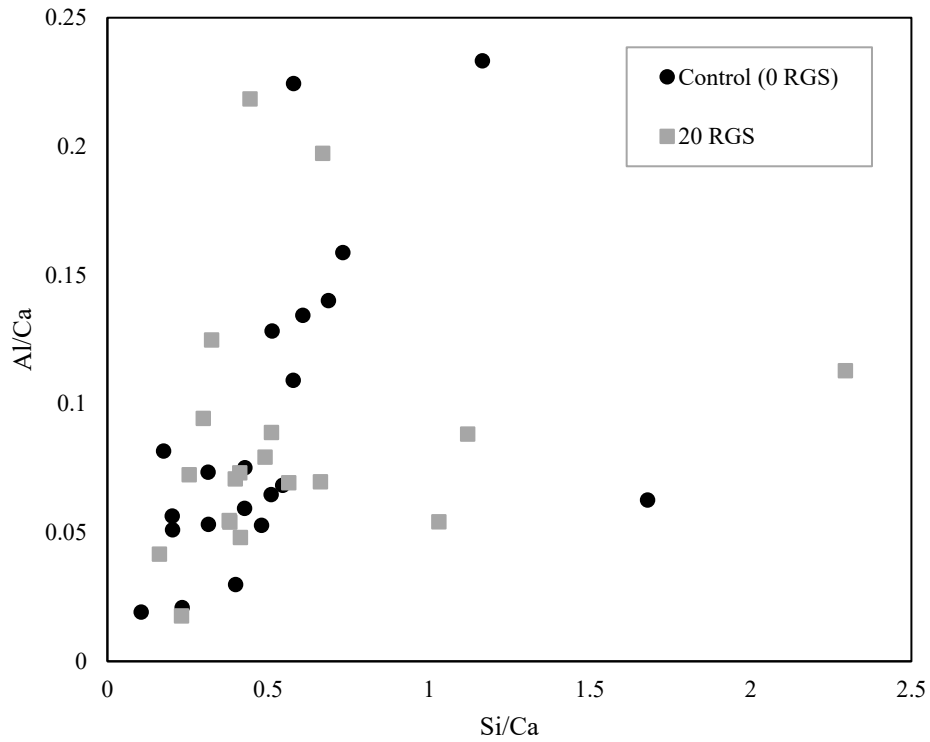


Figure 5.10 Si/Ca vs Al/Ca ratio in Control (0 RGS) and 20 RGS (ASR) mortar

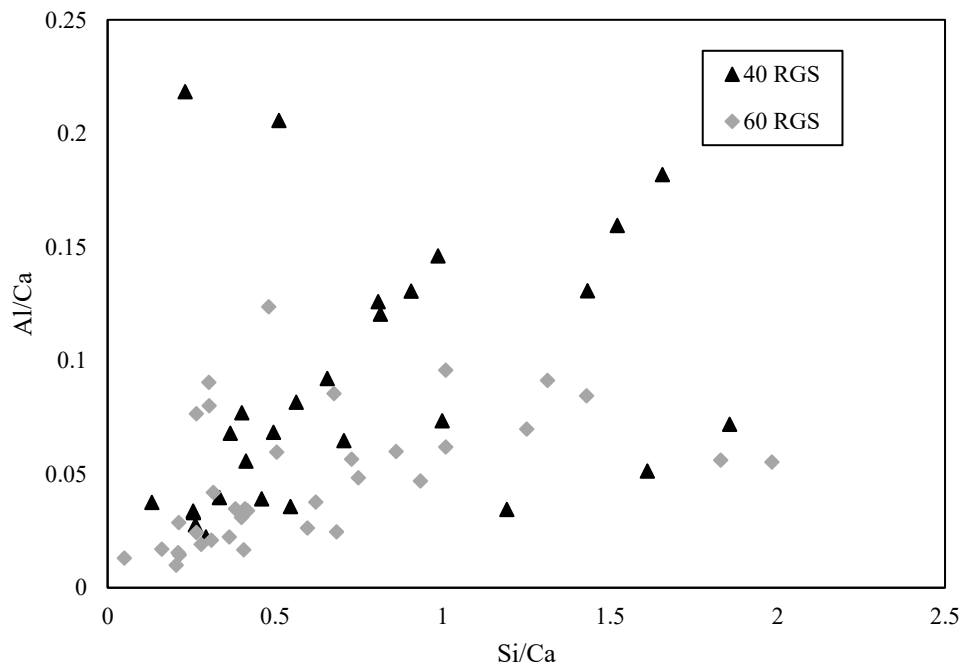


Figure 5.11 Si/Ca vs Al/Ca ratio in 40 RGS and 60 RGS (ASR) mortar

Table 5.4 shows the chemical composition of mortar samples obtained from EDS data plot. The amount of Si and Na was found to increase with the increase in glass sand quantity. Besides, the amount of K was variable due to the heterogeneous of aggregate. Control (0 RGS) mortar showed the highest (Na+K)/Si ratio. However, a noticeable decrease in (Na+K)/Si ratio was found in glass sand mortar compared with Control (0 RGS) mortar. It was found to decrease as the amount of natural sand replacement increased. Consequently, the decrease in ratios indicates low alkali content in the specimen. However, the ratio depended on the specific location analysed by SEM and EDS.

**Table 5.4 Average atomic composition of mortar samples measured by EDS**

Sample	Si	Na	K	(Na+K)/Si
Control	13.83	4.65	5.64	0.74
20 RGS	17.05	2.14	1.34	0.20
40 RGS	22.08	2.41	2.18	0.20
60 RGS	22.74	2.99	0.45	0.15

## 5.2.2 Microstructure of glass powder for RGP paste

### 5.2.2.1 Thermogravimetric analysis

In this study, TGA was conducted to determine the amount of  $\text{Ca(OH)}_2$ , which is produced in hydrated cement paste as a result of using glass powder as cement replacement. In the presence of moisture,  $\text{Ca(OH)}_2$  formed in cement hydration reacts with RGP and produces additional C-S-H. Consequently, a reduction is observed in  $\text{Ca(OH)}_2$  amounts in the cement paste. The lower amount of  $\text{Ca(OH)}_2$  indicates the pozzolanic reaction as  $\text{Ca(OH)}_2$  is consumed in the pozzolanic reaction to produce C-S-H gel. Higher amount of  $\text{Ca(OH)}_2$  indicates the lower pozzolanic reaction. Cement pastes with 10 RGP, 20 RGP, 30 RGP and 40 RGP were cast for one, seven,

28, 56 and 90 days. Control (RGP) with 100% general purpose (GP cement) without any glass powder content was cast to serve as a reference to evaluate the pozzolanic reactivity of glass powder.

The  $\text{Ca(OH)}_2$  content for Control (RGP) and RGP specimen was tested at one, seven, 28, 56 and 90 days (Figure 5.12). The control specimen had  $\text{Ca(OH)}_2$  content of 5.61% at one day.  $\text{Ca(OH)}_2$  content increased over time, for instance, 6.8% and 8.88% at seven and 28 days, respectively. The amount of  $\text{Ca(OH)}_2$  in the samples continued to increase for the first 28 days. The rapid hydration of  $\text{C}_3\text{S}$  is mainly responsible for this increase because approximately 70% of the  $\text{C}_3\text{S}$  in Portland cement will have reacted by 28 days (Taylor, 1997). Cement paste with 10 RGP showed  $\text{Ca(OH)}_2$  content higher than control specimen at one, seven and 28 days due to the substrate effect. However, cement paste with 20 RGP, 30 RGP and 40 RGP exhibited less  $\text{Ca(OH)}_2$  content compared with the control specimen and 10 RGP. This decrease was due to the reduction in  $\text{C}_3\text{S}$  and  $\text{C}_2\text{S}$  content as cement was replaced by 20%, 30% and 40% glass powder. However, there was no clear trend as RGP content increased up to seven days because the pozzolanic reaction was delayed compared with the cement hydration.

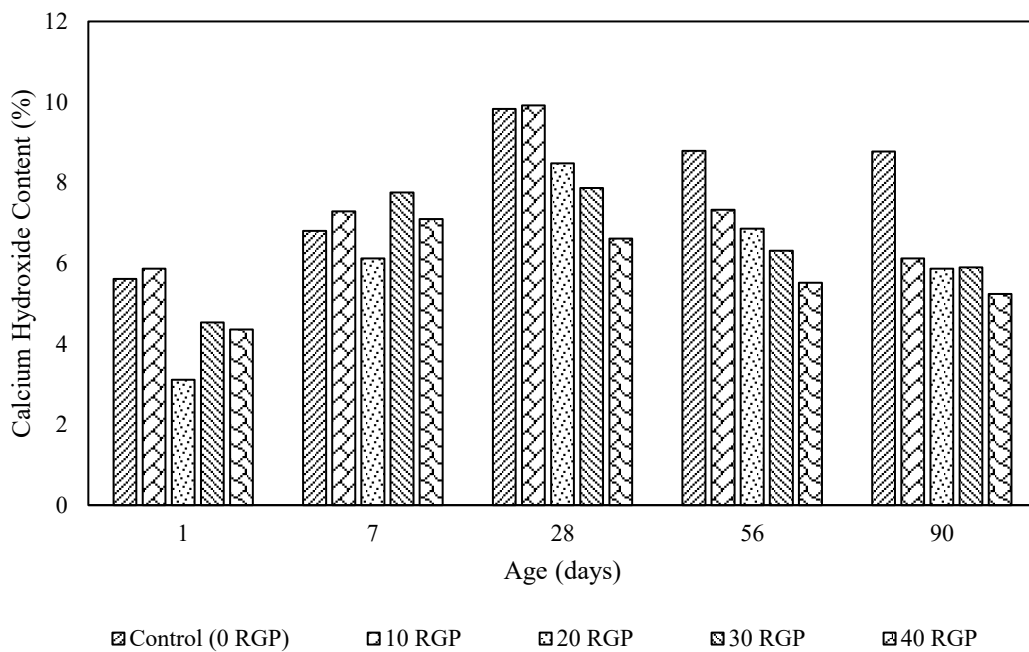


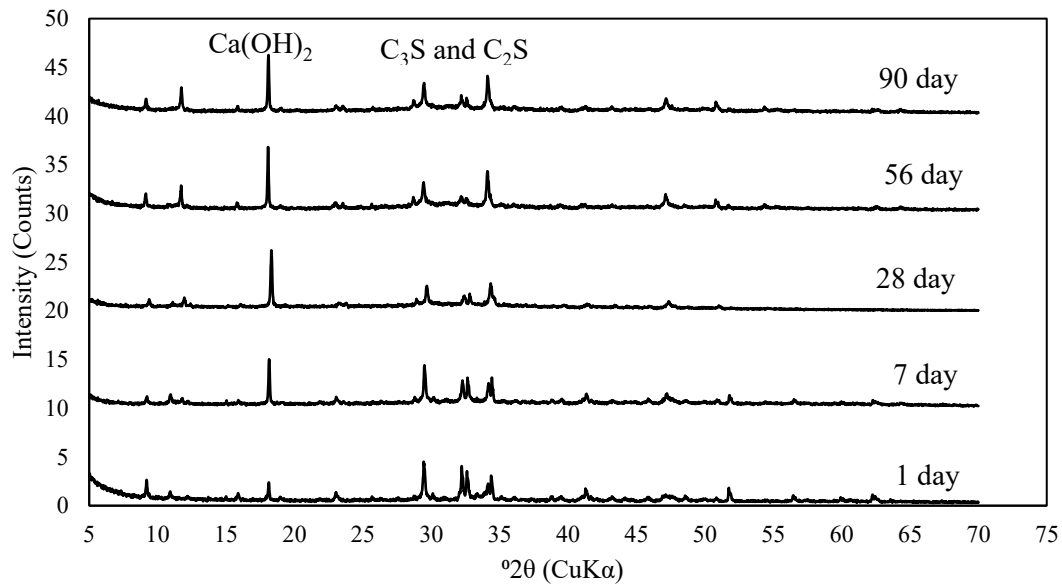
### **Figure 5.12 Calcium hydroxide content Control (0 RGP) and RGP pastes**

The pozzolanic material did not show its effects in the early days and hence became more prominent at later days. There is a noticeable trend at 28, 56 and 90 days that  $\text{Ca(OH)}_2$  content decreases as RGP replacement level increased. The control (RGP) specimen had almost similar  $\text{Ca(OH)}_2$  content at 56 and 90 days. As  $\text{Ca(OH)}_2$  content remained the same, no pozzolanic reaction was occurred in this specimen. However, 10 RGP showed a reduction in  $\text{Ca(OH)}_2$  content, 7.33% and 6.12% at 56 and 90 days, respectively.  $\text{Ca(OH)}_2$  formed during cement hydration slowly reacted with glass powder in the pozzolanic reaction to produce more C-S-H. 30 RGP and 40 RGP showed less reduction of  $\text{Ca(OH)}_2$  content compared with 10 RGP and 20 RGP. Slight reduction of  $\text{Ca(OH)}_2$  indicates the lower pozzolanic reaction.

#### **5.2.2.2 X-ray diffraction (XRD) results for RGP paste specimens**

XRD was carried out to identify  $\text{Ca(OH)}_2$  phase in cementitious system. The  $\text{Ca(OH)}_2$  quantity increases over time as more cement is hydrated. However, the amount of  $\text{Ca(OH)}_2$  reduces in the presence of glass powder in the cement paste. The lower amount of  $\text{Ca(OH)}_2$  indicates the pozzolanic reaction as  $\text{Ca(OH)}_2$  is consumed in the pozzolanic reaction to produce C-S-H gel. The XRD pattern of control (0 RGS) cement paste at seven, 28 and 90 days are shown in Figure 5.13. The peak in the  $2\theta$  region of  $18^\circ\text{C}$  was attributed to  $\text{Ca(OH)}_2$  in the control cement paste. The  $\text{Ca(OH)}_2$  observed in the X-ray diffraction pattern was pure hydration product, releasing from the hydration of cement. The peak intensity in the range of  $29\text{-}34^\circ\text{C}$  was indicated to  $\text{C}_3\text{S}$  and  $\text{C}_2\text{S}$ , the main composition of anhydrous cement particles.  $\text{C}_3\text{S}$  hydrates rapidly and contributes to early strength gain up to 28 days whereas  $\text{C}_2\text{S}$  hydrates slower than  $\text{C}_3\text{S}$  and was responsible for strength after the first 28 days. In the control cement paste, the peak at  $18^\circ\text{C}$  corresponding to  $\text{Ca(OH)}_2$  was found to increase gradually with time due to the hydration of  $\text{C}_3\text{S}$ . More  $\text{Ca(OH)}_2$  was found to be produced in the first 28 days, whereas the intensity of the

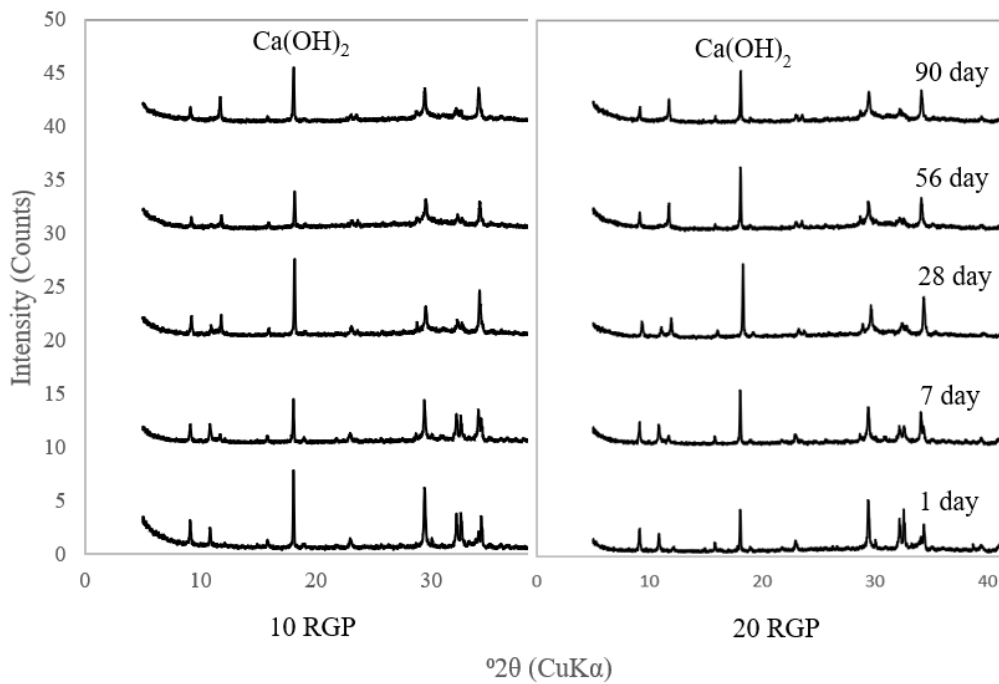
Ca(OH)<sub>2</sub> peak decreased slightly at 90 days. However, the peak corresponding to C<sub>3</sub>S and C<sub>2</sub>S appeared to decrease with time.



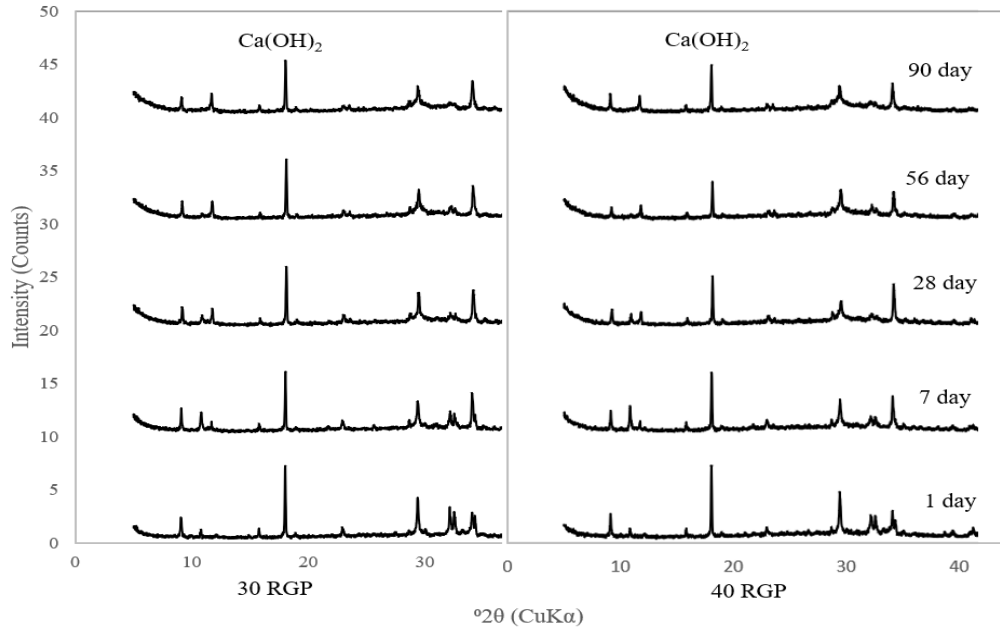
**Figure 5.13 XRD pattern of control (0 RGP) cement paste at 1, 7, 28, 56 and 90 days**

The qualitative analysis of the hardened cement paste containing 10 RGP, 20 RGP, 30 RGP and 40 RGP at seven, 28 and 90 days are shown in Figures 5.13 and 5.14. The addition of glass powder to the cement paste showed similar hydration phases throughout the XRD pattern compared with the control cement paste. No new phases were formed in the hydration of glass powder cement paste. The peak of Ca(OH)<sub>2</sub> was indicated to increase for 10 RGP cement paste up to 28 days of hydration. This increase was prominent compared with the control cement paste and quantitatively agreed with the Ca(OH)<sub>2</sub> content obtained from the thermogravimetric analysis (Figure 5.12). Ca(OH)<sub>2</sub> produced was increased at early stage due to an accelerating effect on the cement hydration. The presence of substrate surface of RGP in a cement paste allowed for a rapid precipitation of Ca(OH)<sub>2</sub> during the early stage of cement hydration (Afshinnia and Rangaraju, 2015a). The intensity of the Ca(OH)<sub>2</sub> peak decreased at 90 days compared with 28 days hydration. This reduction at 90 days represented the consumption of Ca(OH)<sub>2</sub> by the pozzolanic reaction. Ca(OH)<sub>2</sub> reacted with glass powder and produced more

C-S-H in the pozzolanic reaction. 20 RGP showed a similar XRD pattern compared with 10 RGP. The intensity of the peak was found to decrease gradually with an increase in glass powder addition to the cement paste. 40 RGP showed the lowest peak for CH at 90 days. This reduction in  $\text{Ca(OH)}_2$  can be attributed to both the pozzolanic reaction and the dilution effect. The dilution effects occurred due to less availability unreacted of cement in the glass cement paste, which supports the findings from the thermogravimetric analysis.



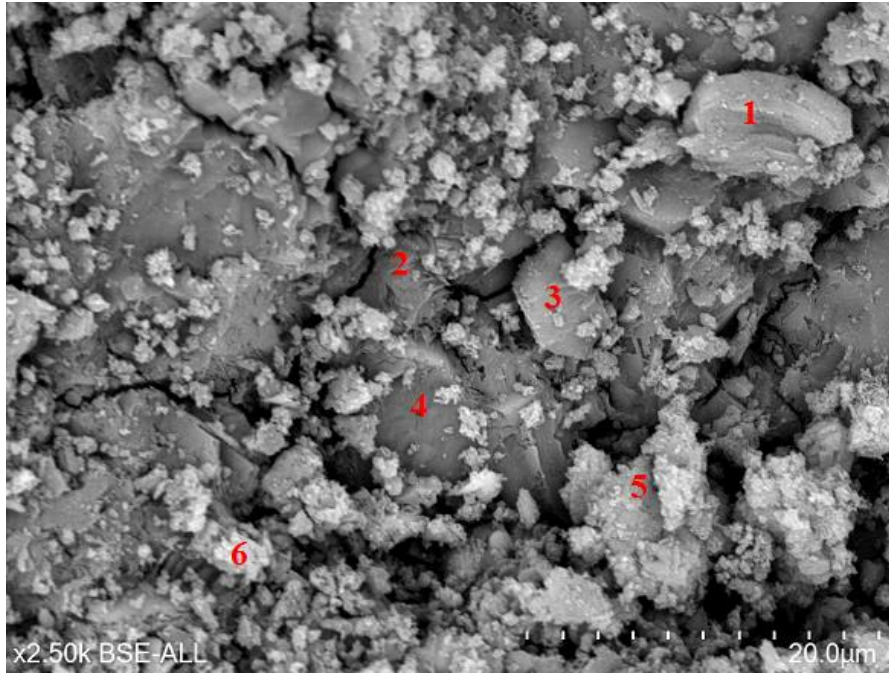
**Figure 5.14 XRD pattern of 10 RGP and 20 RGP cement paste at 1, 7, 28, 56 and 90 days**



**Figure 5.15 XRD pattern of 30 RGP and 40 RGP cement paste at one, seven, 28, 56 and 90 days**

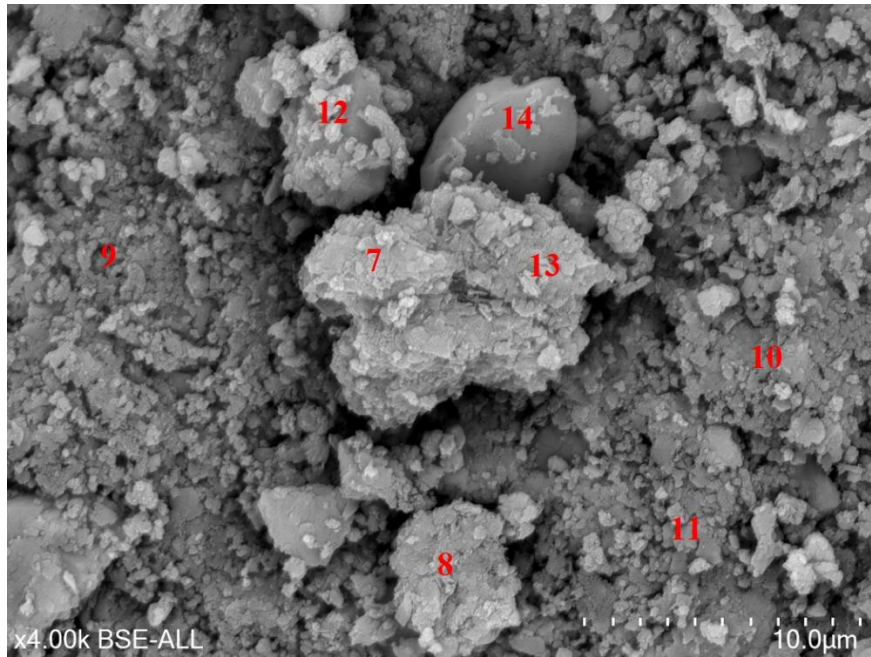
### 5.2.2.3 Scanning electron microscope results for RGP samples

Figure 5.16 shows the SEM microstructure of the Control (0 RGP) cement paste after 90 days of hydration. A hexagonal shape,  $\text{Ca(OH)}_2$ , was observed in the Control (0 RGP) cement paste. Some  $\text{Ca(OH)}_2$  detected in the microstructure analysis, which was the by-product of hydration reaction such as at point 1 and 2. However, some partially reacted  $\text{Ca(OH)}_2$  was also found surrounded by silica-rich product at Spectrum 3 and 4. The other hydration product, C-S-H, appeared to be dense and bright in the backscattered image (Spectrum 5 and 6). Ettringite needles were not observed in the cement paste. However, C-S-H found in the microstructure was intermixed with calcium aluminium silicate hydrates (C-A-S-H). Also, cracks were developed through porous areas such as air voids in the hydration product and observed on the surface of the hardened cement paste.



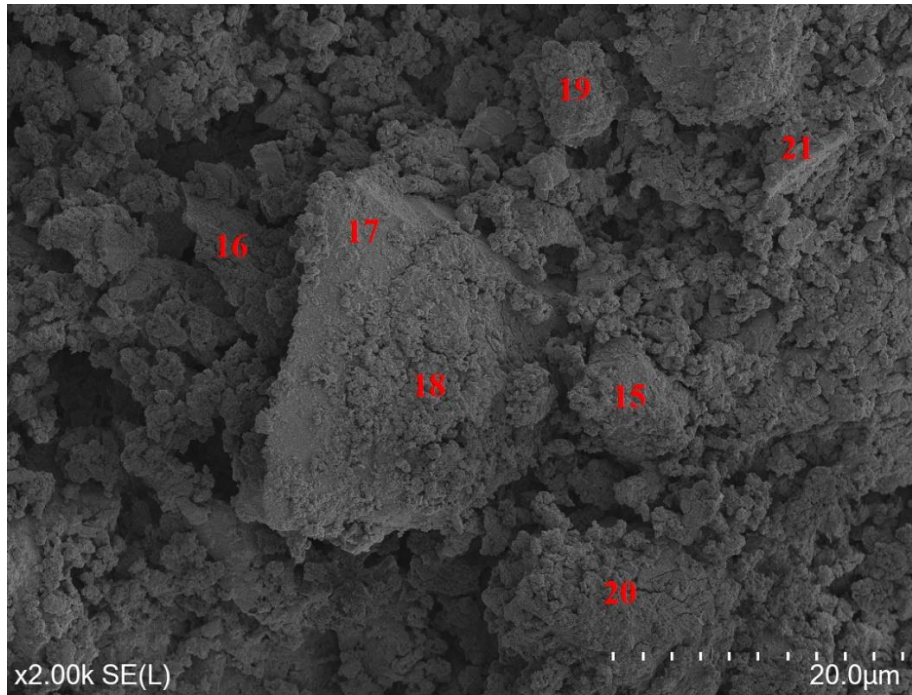
**Figure 5.16 SEM image of Control (0 RGP) cement paste at 90 days**

Figure 5.17 shows the microstructure of 10 RGP containing cement paste after 90 days of hydration. 10 RGP cement paste was covered with the formation of C-S-H and showed a dense microstructure compared with the control cement paste.  $\text{Ca(OH)}_2$  was no longer observed with identical hexagonal shape in the paste as  $\text{Ca(OH)}_2$  which indicates that  $\text{Ca(OH)}_2$  reacted with RGP and producing additional C-S-H in the microstructure at this ages (Spectrum 7, 8, 9, 10, 11, 12, 13). Some RGP was found covered with hydration products indicating formation of new C-S-H. A very few unreacted RGP were observed in the microstructure (Spectrum 14). However, some hydration products were visible on the surface of RGP. Ettringite was not found in acicular type in 10 RGP cement paste. But calcium aluminium silicate hydrates (C-A-S-H) enriched microstructure was found at Spectrum 8, 9, 10, 11 and 13.



**Figure 5.17 SEM image of 10 RGP cement paste at 90 days**

The microstructure of 20 RGP modified cement paste was shown in Figure 5.18. Some partially reacted glass powder was covered with the reaction product at Spectrum 15, 16. Large size unreacted glass powder (at Spectrum 17 and 18) (around  $20 \mu m$ ) was noticed in the middle of the microstructure and started to cover with hydration product. Apart from that, the presence of C-S-H was found at Spectrum 19, 20 and 21. C-S-H appeared intermixed with Na and Al at points 16 and 19. However, the microstructure was less dense compared with 10 RGP cement paste. The Si of formed C-S-H was partially substituted by Al to form calcium aluminium silicate hydrates (C-A-S-H). However,  $Ca(OH)_2$  was found less dense compared with control (0 RGP) cement paste.



**Figure 5.18 SEM image of 20 RGP cement paste at 90 days**

As shown in Figure 5.19 for 30 RGP, there are some visibly smooth particles which were attributed to unreacted glass powder particle in the microstructure (Spectrum 22, 23, 24, 25, 26 and 27). As 30% of cement was replaced with glass powder, inadequate cement paste was available in the mix to assist bonding within the mix. There was not adequate hydration reaction happening to produce  $\text{Ca}(\text{OH})_2$  necessary for the pozzolanic reaction of all RGP. Therefore, 30 RGP made the microstructure less adhesive between RGP and cement paste compared with 10 RGP and 20 RGP, which consequently formed the microscopic voids. However, RGP participated in the hydration and produced C-S-H, C-A-S-H and Na-S-H as shown in Spectrum 252, 259 and 272.  $\text{Ca}(\text{OH})_2$  was also observed with an identical hexagonal shape in the paste (Spectrum 268 and 270).  $\text{Ca}(\text{OH})_2$  can react with glass powder to produce C-S-H at the pozzolanic reaction.

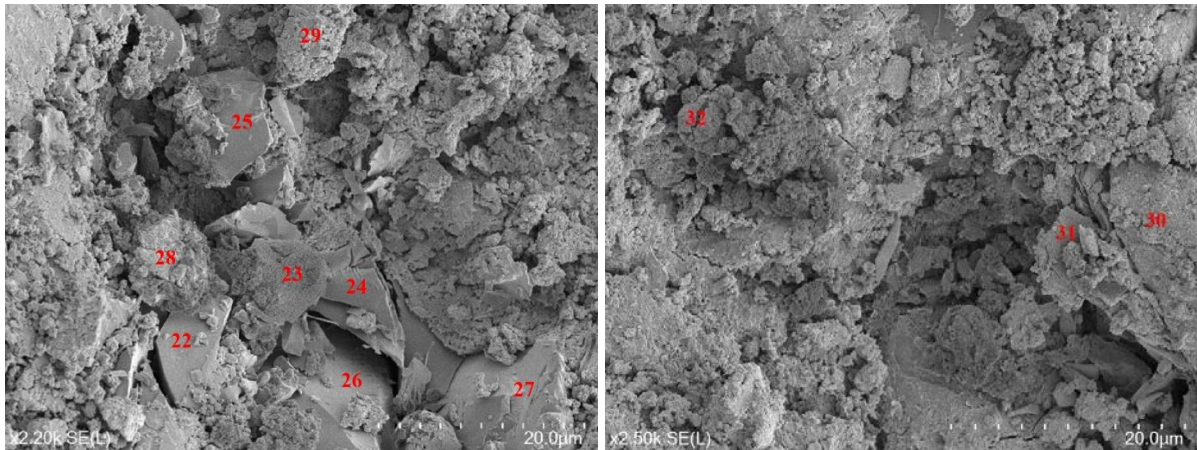


**Figure 5.19 SEM image of 30 RGP cement paste at 90 days**

Figure 5.20 shows that the quantity of RGP was prominent as RGP replaced 40% cement. Some 40 RGP appeared as large-sized particles with an angular and prismatic shape (Spectrum 33, 34 and 35). These large size glass powder particles remained embedded in the 40 RGP cement pastes even after 90 days of hydration (Spectrum 36, 37, 38 and 39). The large size glass powder showed relatively poor adhesion between the cement paste and RGP. Inadequate cement reduced the hydration reaction and hence the reduction in  $\text{Ca(OH)}_2$  which was required for pozzolanic reaction. Not all glass powder went through pozzolanic reaction in 40 RGP sample. A longer hydration duration is required to develop the pozzolanic reaction fully. The formation of C-S-H was found in the microstructure, as shown in Spectrum 40, 41, 42 and 43. However, the formation of C-S-H was less compared with other RGP replacement.

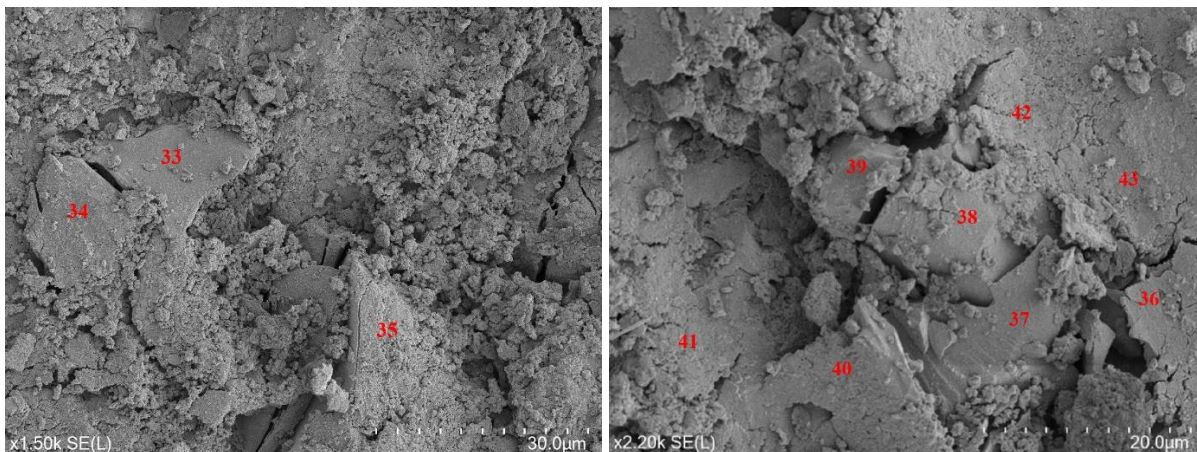


**Figure 5.20 SEM image of 40 RGP cement paste at 90 days**

#### **5.2.2.4 Energy-dispersive spectroscopy (EDS) results from RGP paste specimens**

EDS analysis was carried out to determine the chemical composition phases presented in Control (0 RGP) cement paste and glass powder modified (10 RGP, 20 RGP, 30 RGP, 40 RGP) cement paste. In general, the C-S-H phases are known as “jennite-like” with the high Ca/Si ratio (1.25-1.50). The C-S-H phases are known as “tobermorite-like” phases with the low Ca/Si ratio, for instance, (0.66-0.83). The jennite C-S-H phases have both Ca-O and Ca-OH bonds in the main calcium layer, while tobermorite C-S-H phases contain only Ca-O. The EDS data point with Si/Ca versus Al/Ca representations from the cement paste, and RGP cement paste are projected in a 2D scatter plot (Figure 5.21). EDS data point was analysed based on 50 randomly chosen points on the surface of the cement pastes. Ca(OH)<sub>2</sub> was located at (0, 0) on the scatter plot. For plain cement and alite, the typical CaO/SiO<sub>2</sub> molar ratio (Ca/Si) of C-S-H is within 1.50 to 2.00. The C-S-H that forms in blended systems has the CaO/SiO<sub>2</sub> molar ratio (Ca/Si) between 0.8 and 2.00 (Karen Scrivener, 2016). Figure 17 shows that the Ca/Si ratio of control cement paste was found within 0 to 2.5. Some EDS data point was located near the origin, which represented the formation of Ca(OH)<sub>2</sub> during hydration. The values of Si/Ca ratios described jennite-like structures with both Ca-O and Ca-OH bonds which supports the findings in the SEM analysis. However, Al was also found intermixed with hydration products.

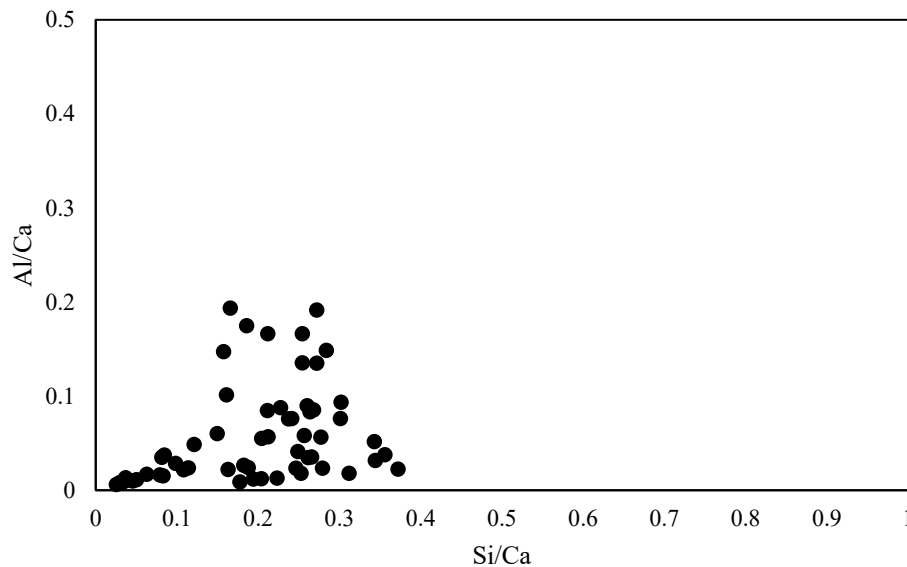


**Figure 5.21 2 D scatter plot of EDS analyses of Control (0 RGP) cement paste at 90 days**

The plot for 10 RGP and 20 RGP cement paste showed a similar distribution of Si/Ca vs Al/Ca ratios (Figure 5.22). However, the plot was found more scattered than the Control (0 RGP) cement paste. Si/Ca was found to be increased compared with control cement paste, for instance, from 0.4 to 0.5. It can be attributed to the increase in the silica content, contributed by the siliceous waste glass. The addition of waste glass powder in the cement paste reacted with  $\text{Ca(OH)}_2$  and produced outed C-S-H, which can make the microstructure confined. Consequently,  $\text{Ca(OH)}_2$  was found less dense compared with Control (0 RGP) cement paste as data cloud near origin corresponding to  $\text{Ca(OH)}_2$  was less dense. Besides, the chemical composition of those data points close to the origin typically represents compositions of early-stage hydration of C-S-H gels that form from  $\text{Ca(OH)}_2$ . The less amount of  $\text{Ca(OH)}_2$  indicates the pozzolanic reaction as  $\text{Ca(OH)}_2$  is consumed in the pozzolanic reaction to produce additional C-S-H gel. Intermixing occurred between  $\text{Ca(OH)}_2$  and C-S-H, as well as between Al and C-S-H appeared in 20 RGP and 20 RGP cement paste.

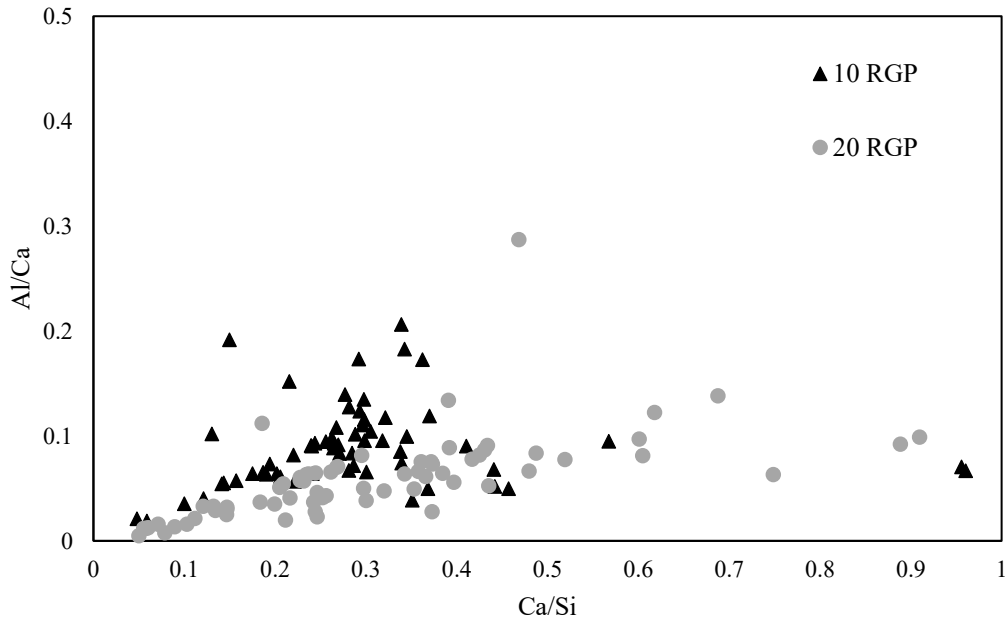


**Figure 5.22 2 D scatter plot of EDS analyses of 10 RGP and 20 RGP cement paste at 90 days**

2D scatter plot distribution was found similar for 30 RGP and 40 RGP. The plot showed a more scattered cloud of chemical composition compared with the control and 10 RGP cement paste. Figure 5.23 indicates a wide range of Si/Ca ratios in their chemical compositions. The Si/Ca was found to be further increased as the glass powder content increases. The amount of  $\text{Ca(OH)}_2$  was reduced as it took part in further hydration to produce C-S-H. For 30 RGP, Si/Ca vs Al/Ca was more prominent within 0.2 to 0.6 whereas 40 RGP showed between 0.3 and 0.6. The Ca/Si ratio of C-S-H in RGP cement paste was found to be lower as expected, which supports other results (Karen Scrivener, 2016). However, Si/Ca vs Al/Ca represented jennite-like structures. It can take a longer time to show a tobermorite-like phase due to delayed pozzolanic reaction.

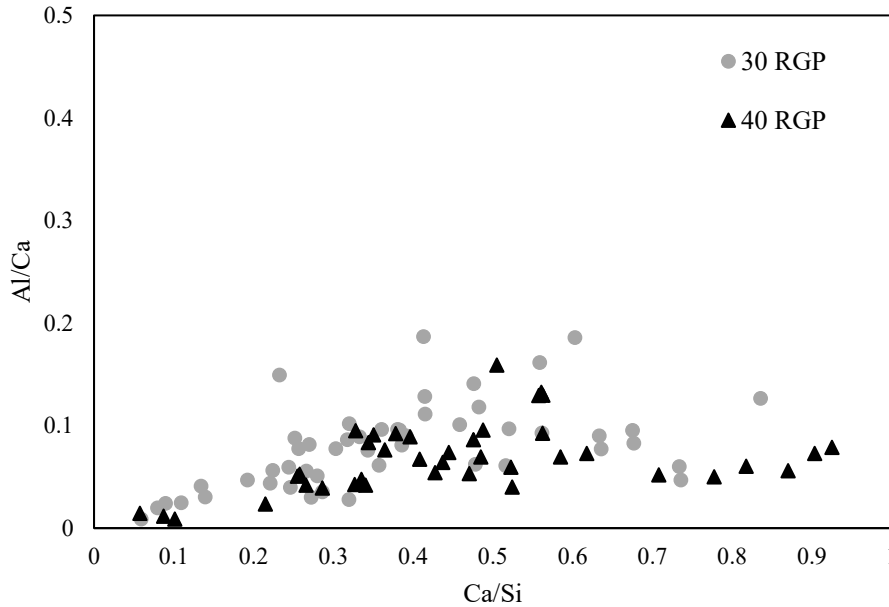


**Figure 5.23 2 D scatter plot of EDS analyses of 30 RGP and 40 RGP cement paste at 90 days**

### 5.3 Conclusion

This research studied the microstructure of glass sand mortar and glass powder cement paste.

For glass sand mortar, thermogravimetric analysis was carried out to quantify the amount of  $\text{Ca(OH)}_2$ .  $\text{Ca(OH)}_2$  content was found to decrease in 20, 40 and 60 RGS compared with control mortar. This reduction can be attributed to the consumption of  $\text{Ca(OH)}_2$  in the reaction with glass sand. As glass sand used in this research was smaller (3 mm), no internal cracks were found at the surface or inside the glass particles. The ASR expansion was not observed in the SEM microstructure for glass sand mortar samples. EDS results showed that 40 RGS and 60 RGS showed high Si/Ca ratio compared to Control (0 RGS) and 20 RGS. Reversely, in low Ca/Si ratio, finer RGS can react with  $\text{Ca(OH)}_2$  and produce C-S-H at later days.

For cement paste, thermogravimetric analysis showed that the pozzolanic material did not show its effects in early days and hence became more prominent later. There was a noticeable trend at 28, 56 and 90 days that  $\text{Ca(OH)}_2$  content decreases as RGP replacement level increased.

$\text{Ca(OH)}_2$  formed during cement hydration slowly reacts with glass powder in the pozzolanic reaction to produce more C-S-H. SEM result showed that 10 RGP cement paste was covered with the formation of C-S-H and showed dense microstructure compared to Control (0 RGP) cement paste.  $\text{Ca(OH)}_2$  was no longer observed with identical hexagonal shapes in the paste as  $\text{Ca(OH)}_2$  further reacted with RGP and formed additional C-S-H in the microstructure at 90 days. The addition of waste glass powder in the cement paste reacted with  $\text{Ca(OH)}_2$  and produced C-S-H, which can make the microstructure confined.

## Chapter 6: Environmental benefits of using recycled glass in concrete

Nafisa Tamanna, Rabin Tuladhar. “Environmental benefits of using recycled glass in concrete.” (In progress).

Life cycle assessment (LCA) is a recognised method of estimating and evaluating the environmental impacts associated with the entire life cycle of a product. In this research, a comprehensive LCA was conducted to quantify the environmental benefits of using recycled glass as a partial sand and cement replacement in concrete compared with the traditional concrete. The software tool SimaPro v.8.0 was used to assess and quantify environmental effects. Each material of concrete was assessed and multiplied their weight proportion with a specific weight ( $2400 \text{ kg/m}^3$ ) to achieve  $1 \text{ m}^3$  of concrete. The functional unit was selected as  $1 \text{ m}^3$  of concrete. The major environmental impact categories, such as global warming, ozone depletion, eutrophication, land use and fossil fuels were assessed. Sensitivity analysis and uncertainty analysis were performed in the LCA to consider the variation in the quality of data.

### 6.1 Methodology

The LCA was evaluated in accordance with the principals of framework (ISO 14040) (ISO14040, 2006) and requirements and guidelines (ISO 14044) (ISO14044, 2006). The assessment was carried out for three scenarios (Control concrete, RGS concrete and RGP concrete) and compared to quantify the environmental benefit. Cradle to gate LCA was conducted where the LCA scope was limited to the production of GP cement concrete, RGS concrete and RGP concrete. It does not take into account the environmental impact of construction processes, and demolition of the concrete structure after its service. It is

considered that the construction process and demolition process for all these three types of concrete will essentially be the same.

## **6.1.1 Goal, functional unit and system boundaries**

### **6.1.1.1 Goal and functional unit**

The goal of the LCA was to compare the overall environmental impact of conventional control concrete and concrete modified with recycled waste glass. The functional unit in this study was selected as 1  $m^3$  of concrete. The concrete mix design was designed for a characteristic strength of 32 *MPa* at 28 days. Each material of concrete was assessed and multiplied their weight proportion with a specific weight (2400  $kg/m^3$ ) to achieve 1  $m^3$  of concrete. Three different scenarios were assessed to evaluate the effect of using recycled glass in concrete.

**Scenario I:** Production of general purpose (GP) cement concrete with natural aggregates (control).

**Scenario II:** Recycled glass sand concrete (RGS concrete). Three concrete mixes containing RGS as coarse natural sand substitution at 20%, 40% and 60% (noted as 20 RGS, 40 RGS and 60 RGS, respectively) were assessed. For the LCA of 20 RGS concrete, it was assumed that remaining 80% of glass waste was landfilled. Similarly for the LCA of 40 RGS and 60 RGS concrete, 60% and 40% glass sand was assumed to be sent to landfill.

**Scenario III:** Recycled glass powder concrete (RGP concrete). Three concrete batches were analysed that corresponded to the replacement of cement with 10%, 20%, and 30% recycled glass powder, noted as 10 RGP, 20 RGP and 30 RGP, respectively. For the LCA of 10 RGP concrete, it was assumed that remaining 90% of glass waste was landfilled. Similarly for the LCA of 20 RGP and 30 RGP concrete, 80% and 70% glass waste was assumed to be sent to

landfill. To get crush waste glass to powder form, a pulverising process was required. The energy needed to pulverise 1 kg of glass sand is taken as 0.124 kWh as supplied by ALS.

Concrete mix supplied by Pioneer North Queensland (PNQ) Concrete (Tables 3.2 and 4.1) was used as the control mix in the study. Admixture used in this mix was a very small amount, consequently the contributions of admixture to the total environmental impacts would be very small. The environmental impacts of admixtures have been excluded from the comparison.

### **6.1.1.2 System boundaries**

Cradle to gate LCA was conducted where the system boundary included raw materials extraction of each material, processing, transportation and production of concrete. The environmental impact was limited to the production of GP cement concrete, RGS concrete and RGP concrete. The impact of end-of-life disposal of concrete was not included in the scope. The fundamental components of concrete include GP cement, coarse aggregate, fine aggregate (coarse and fine sand) and water. The complete environmental effect is the combination of individual materials for each type of concrete. Energy consumption and water use are included in the boundary.

In this research, LCA was carried out at three different boundary levels. The first boundary level was for conventional concrete production which included the details of raw material extraction and material production. The system boundary for the RGS involved waste glass collection, raw material extraction and material production. In the third level, the use of glass powder as cement replacement was described. This boundary level included waste glass collection, grinding to a powdered form, raw material extraction and material productions.

**GP cement concrete:** Figure 6.1 shows the flow diagram of the GP cement concrete production process and its system boundaries.

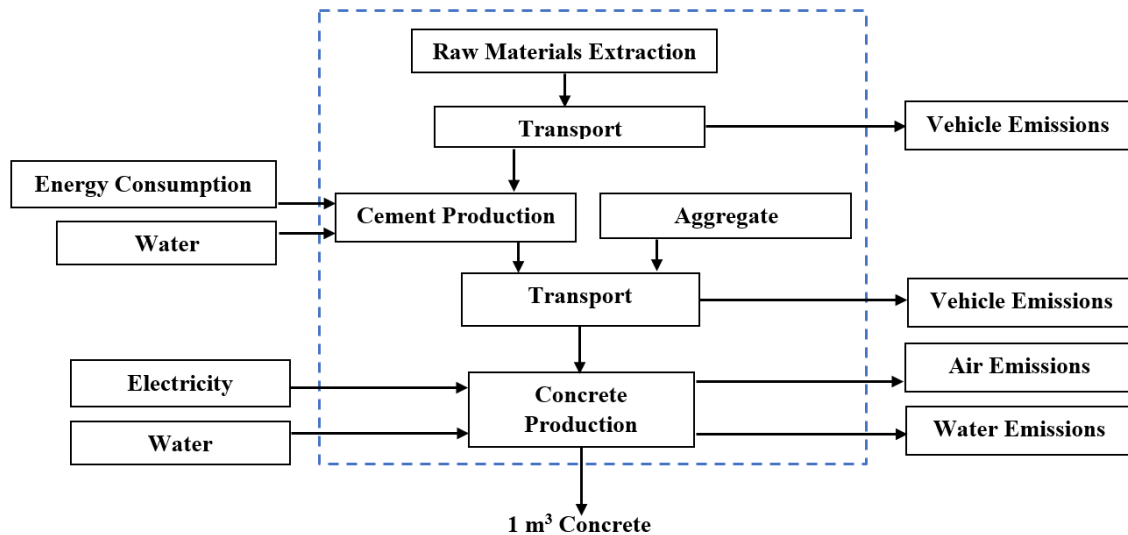


**Figure 6.1 System boundaries of conventional GP concrete**

**RGS concrete:** Mixed-coloured soda-lime glass supplied by the Cairns Regional Council was used in RGS concrete. All collected recyclable materials, which includes paper, cardboard, plastic bottles, aluminium cans and glass bottles were sorted and large items removed as they passed through the conveyor belt at the materials recovery facility (MRF) unit. Sorted glass items were then sent to a glass crushing facility. Glass crushing was done through an imploder, shearing unit and sanding unit. The fine glass particles of 3 mm were used in construction. Glass sorting and crushing to sand size required electricity which was considered in the assessment. Transport was included in this system boundary (Table 6.1). Figure 6.2 shows system boundaries of concrete modified with RGS as sand replacement.

**Table 6.1 Travel distance for each material**

<b>Materials</b>	<b>Distance (km)</b>
Cement	5.4
Gravel	21
Coarse sand	18
Fine sand	93

RGS	4.6
RGP	5.4

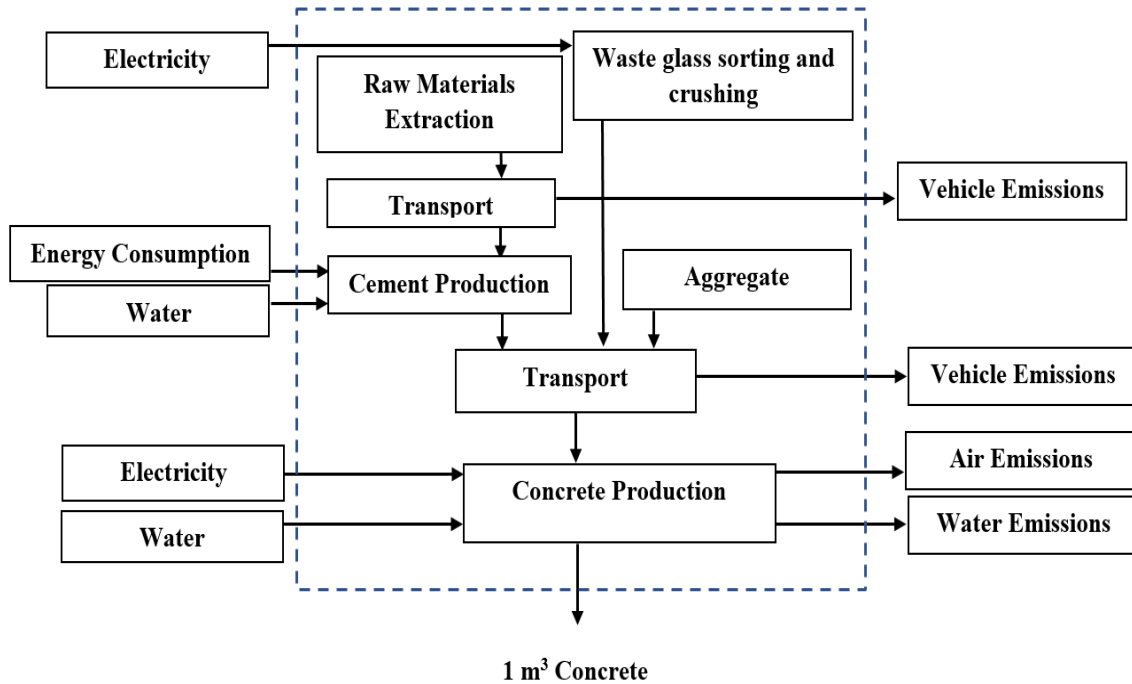


**Figure 6.2 System boundaries of concrete modified with RGS as sand replacement**

**RGP Concrete:** The 3 mm size glass particles were further pulverised to powder form (80% passing through 45  $\mu\text{m}$  sieve) at ALS Minerals Geochemistry-Townsville Laboratory. The energy required to pulverised 1 kg of glass sand is 0.124 kWh supplied by ALS. Transport was also included in this system boundary. Figure 6.3 shows the system boundaries of concrete modified with RGP as cement replacement.

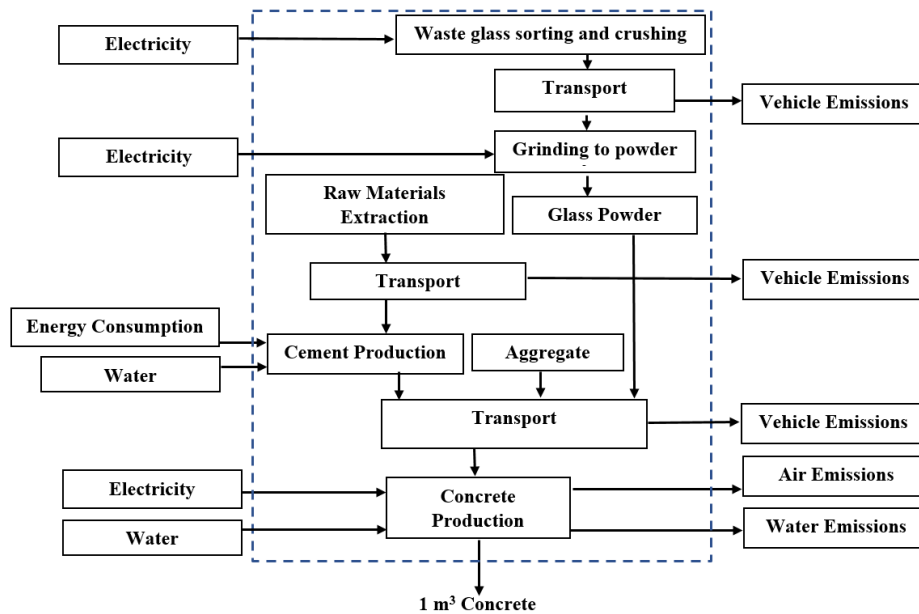


**Figure 6.3 System boundaries of concrete modified with RGP as cement replacement**

### 6.1.2 Life cycle inventory

The life cycle inventory data (LCI) used in this research was acquired from the inventory database: SimaPro 8.0 Australian LCA database (AusLCI, 2011); waste and recycling facilities (Cairns Regional Council); materials recovery facility (Townsville City Council) and scientific journal papers; materials recovery facility (MRF); glass pulverising plants (ALS Geochemistry-Townsville); concrete industries such as PNQ, and scientific publications. Since the LCI data used were obtained mainly from the Australian average LCA database, the variable may have uncertainty.

### 6.1.3 Life cycle impact assessment

The software tool SimaPro v.8.0 (PRé Consultant, Amersfoort, The Netherlands) was used to assess and quantify environmental effects based on inventory analysis. The analysis was conducted using the Australian database method, Australian indicator V3.00. The LCIA data of each process, including required raw materials, energy consumption, emission and landfill to produce 1  $m^3$  concrete was calculated and converted into environmental impact categories.

The assessment was carried out for three scenarios (control concrete, RGS concrete and RGP concrete) and compared to quantify the environmental benefit. Environmental impacts were assessed based on Australian conditions, water use, material consumption, fuel consumption, CO<sub>2</sub> equivalent and PO<sub>4</sub> equivalent during concrete production. Impact category, CO<sub>2</sub> equivalent represents the associated global warming potential, whereas PO<sub>4</sub> equivalent accounts for eutrophication. Eutrophication is a process in which a body of water becomes enriched with minerals and nutrients which stimulate the growth of aquatic plants, resulting in depletion of dissolved oxygen. The ozone layer keeps the earth protected from ultraviolet radiation emitted by the sun. However, its depletion increases cancer risks and other adverse effects.

#### **6.1.4 Sensitivity and uncertainty analysis**

Sensitivity analysis and uncertainty analysis were performed in the LCA to consider the variation in the quality of data. Sensitivity analysis was conducted to analyse the impact of variations on the LCA results with the changes in the key parameters used in this research. The sensitivity analysis aimed to assess the change of results due to the variation of input parameters, for instance, the change of cement, aggregate and transport distance over 1 m<sup>3</sup> concrete. The sensitivity analysis was carried out by changing each input parameter in the range of ±40%. Uncertainty analysis is the estimation of environmental impacts associated with LCI input data variance (Yin, 2015). Standard deviation is used to assess uncertainty data for each key parameter. Parameter uncertainty is found by developing the uncertainty of input parameter in a Monte Carlo approach, built-in SimaPro 8.0. Uncertainty analysis for each impact categories was calculated using this approach with 100 runs within a 95% confidence interval.

## **6.2 Results and discussion**

### **6.2.1 Recycled glass sand as sand replacement**

The life cycle impact categories associated with the production of 1  $m^3$  control concrete and concrete with RGS are shown in Figure 6.4. Global warming, ozone depletion, eutrophication and fossil fuels are the major environmental impact categories for RGS in concrete. The control concrete showed the highest global warming impact of about 356  $kg$   $CO_2$  equivalent. The use of RGS slightly improved environmental footprint of concrete. 20 RGS, 40 RGS and 60 RGS showed reduced global warming by 0.84%, 1.7% and 2.2%, respectively, compared with the control concrete. Fossil fuel was lower for RGS. The control concrete consumed 68.1  $kg$  oil equivalent. Use of 20 RGS, 40 RGS and 60 RGS reduced fossil fuel by 1%, 3% and 4%, respectively. The use of RGS also enhanced eutrophication. 60 RGS improved the most with 4% reduction in eutrophication, followed by 40 RGS with 2% and 20 RGS with 1%. The reduction of ozone layer depletion was found 5%, 9% and 14% for 20 RGS, 40 RGS and 60 RGS, respectively.

As can be seen in Figure 6.5, for all types of concrete, global warming occurred mostly due to cement, transport, gravel, landfill, sand, the energy required and water. Cement is the prime source of emissions in the control concrete and RGS concrete. Global warming due to cement remained constant, as the amount of cement in the mix design for control and RGS concrete were unchanged. The second dominant source was mainly due to the impact on landfill. The landfill was responsible for global warming of 10.99  $kg$   $CO_2$  equivalent for control concrete. The 20 RGS, 40 RGS and 60 RGS concrete reduced the landfill impact of 20%, 40% and 60%, respectively, compared with control concrete. Concrete was produced by replacing natural river sand with 20%, 40% and 60% of RGS as the waste glass which would otherwise be landfilled was reused in concrete. 20 RGS, 40 RGS and 60 RGS concrete reduced the global warming impact of 13.97%, 27.94% and 42.16%, which corresponded to natural sand. In contrast, the addition of RGS increased global warming impact slightly as the quantity of recycled glass

sand increased. However, transport distance had a slight effect on global warming due to transport of RGS.

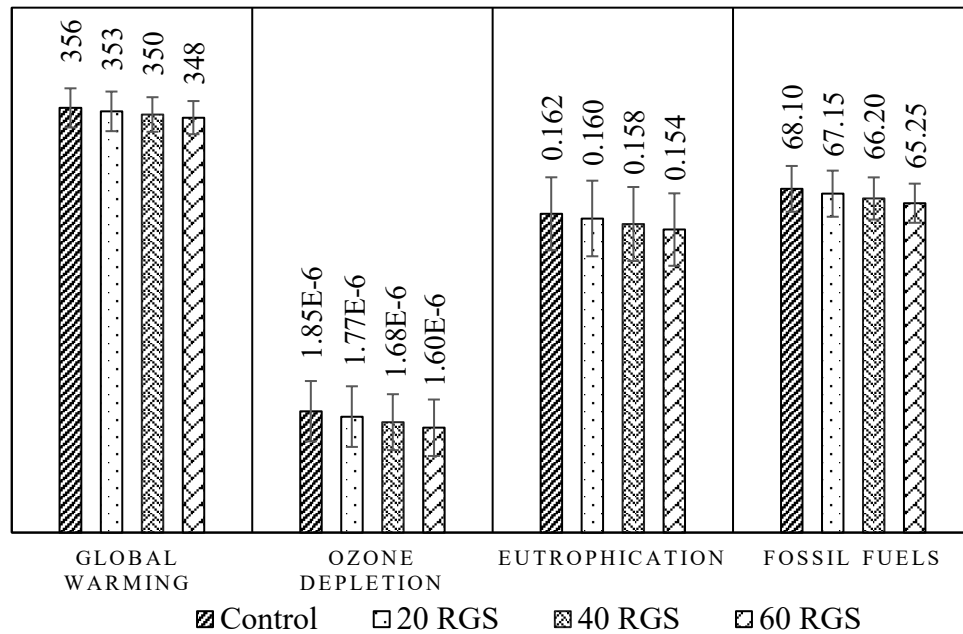


**Figure 6.4 Life cycle impact categories associated with 1 m<sup>3</sup> RGS concrete**

As can be seen in Figure 6.5, for all types of concrete, global warming occurred mostly due to cement, transport, gravel, landfill, sand, the energy required and water. Cement is the prime source of emissions in the control concrete and RGS concrete. Global warming due to cement remained constant, as the amount of cement in the mix design for control and RGS concrete were unchanged. The second dominant source was mainly due to the impact on landfill. The landfill was responsible for global warming of 10.99 kg CO<sub>2</sub> equivalent for control concrete. The 20 RGS, 40 RGS and 60 RGS concrete reduced the landfill impact of 20%, 40% and 60%, respectively, compared with control concrete. Concrete was produced by replacing natural river sand with 20%, 40% and 60% of RGS as the waste glass which would otherwise be landfilled was reused in concrete. 20 RGS, 40 RGS and 60 RGS concrete reduced the global warming impact of 13.97%, 27.94% and 42.16%, which corresponded to natural sand. In contrast, the

addition of RGS increased global warming impact slightly as the quantity of recycled glass sand increased. However, transport distance had a slight effect on global warming due to transport of RGS.

The impact of ozone layer depletion was found due to cement, landfill, transport, gravel, sand, the energy required and water. 20 RGS, 40 RGS and 60 RGS reduced ozone depletion of 5%, 9% and 14%, respectively, compared with control concrete. Similar to global warming, the control concrete showed the highest ozone depletion and cement was the most significant contributor. As can be seen in Figure 6.5, ozone layer depletion from landfill decreased with the increasing replacement level of natural sand by RGS.

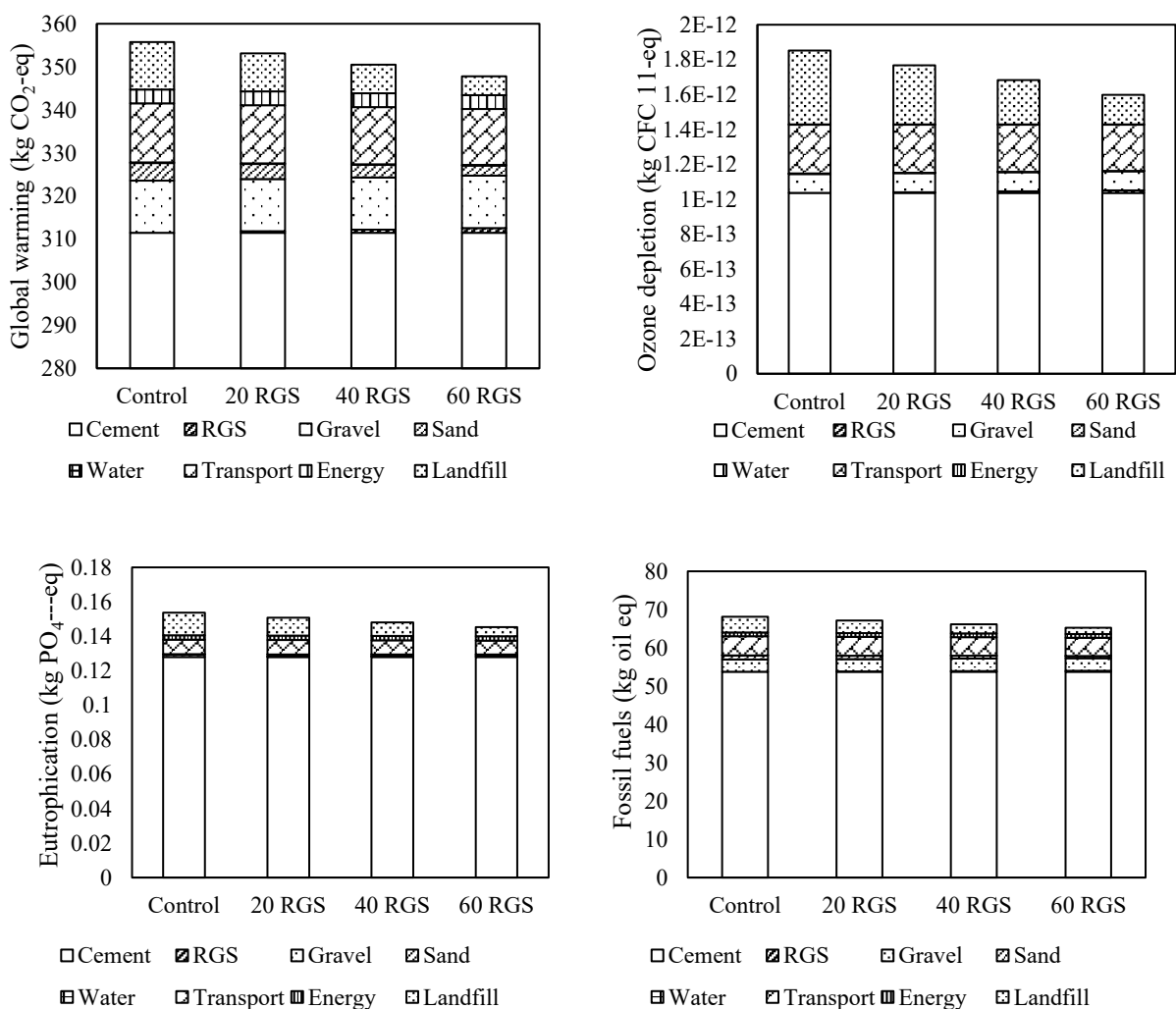


### **Figure 6.5 Major environmental impact categories for 1 m<sup>3</sup> concrete**

The use of RGS showed a negligible impact on eutrophication and fossils fuel consumption. 60 RGS slightly reduced 5% eutrophication and 4% fossils fuel consumption, compared with control concrete. Cement was responsible for a significant proportion of burden to the environment, for instance, cement released 78.86% and 78.96% PO<sub>4</sub> and oil, respectively for control concrete compared with the overall eutrophication and fossils fuel consumption. Emissions due to sand, RGS, water use, energy use were insignificant.

#### **6.2.1.1 Sensitivity analysis of RGS**

Sensitivity analysis was carried out to assess the sensitivity of the results stated in Section 6.2.1. The variation of key parameters used, including the change of cement, aggregate and transport distance was analysed for control concrete and concrete with RGS. The sensitivity analysis was conducted by the change of each variable in the range of  $\pm 40\%$ .

Figure 6.6 shows the relative change of global warming to the variation of cement, gravel, coarse aggregate, fine aggregate, 60 RGS and transport distance for control and 60 RGS concrete. The variation of cement was very sensitive in the range of  $\pm 40\%$ . Cement showed the highest relative change of about 18% and 36% for  $\pm 20\%$  and  $\pm 40\%$ , respectively. The other results were not sensitive to the change of gravel, coarse sand, fine sand and transport distance in the range of  $\pm 40\%$ . The associated environmental impact due to landfill was assessed as 100% recycled glass was going to landfill with no replacement of coarse sand.

In the sensitivity analysis, the variation of cement, gravel, fine sand did not have a major impact on global warming for 60 RGS concrete compared with control concrete. Coarse sand showed less sensitivity of global warming relative to control concrete as 60% coarse sand was being replaced by RGS (Figure 6.7). Only 40% RGS was sent to landfill, whereas 100% RGS was sent to landfill for control concrete. However, 60 RGS had a strong correlation with the change

of global warming. The associated environmental impact was found increased with (-20)% to (-40)% due to landfill effect. However, global warming corresponding to 60 RGS was reduced significantly in the range of +20% to +40%.

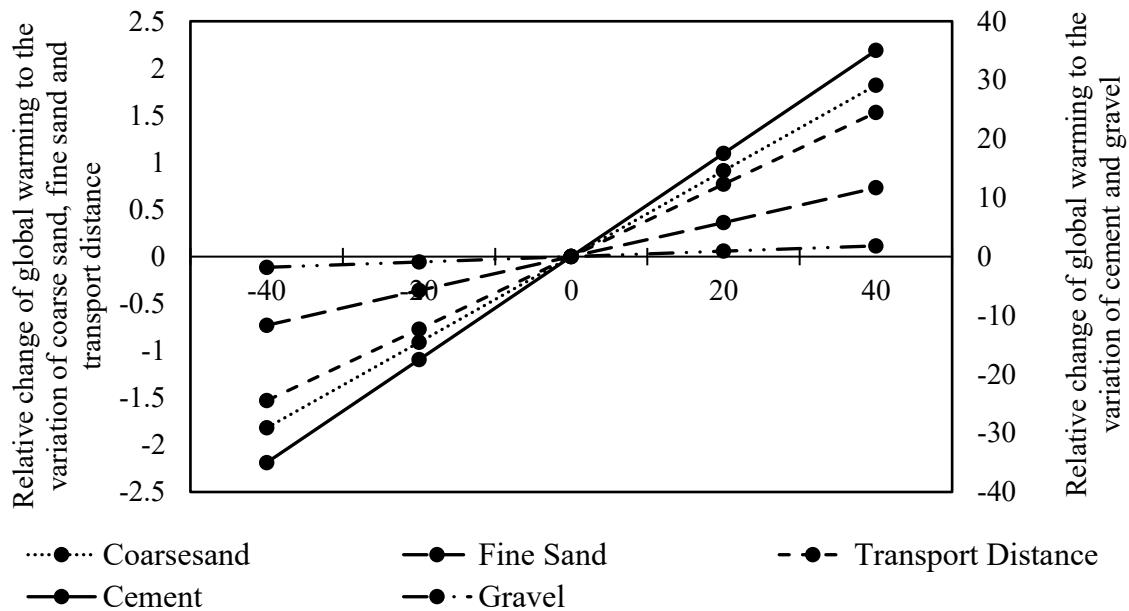


Figure 6.6 Relative change of global warming for control concrete

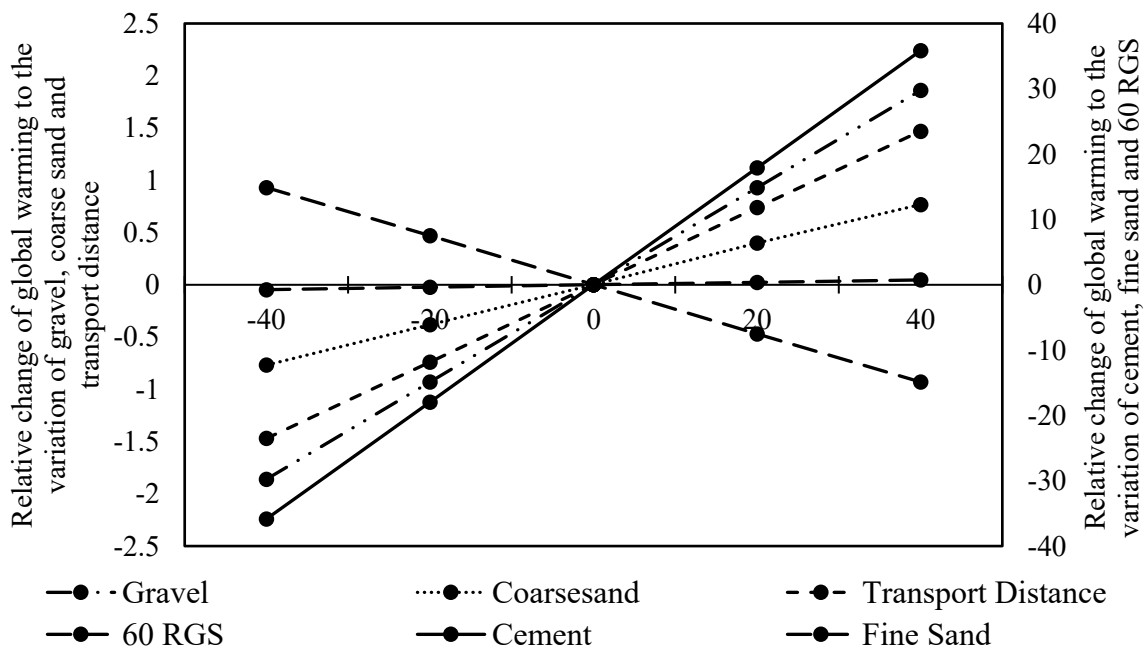
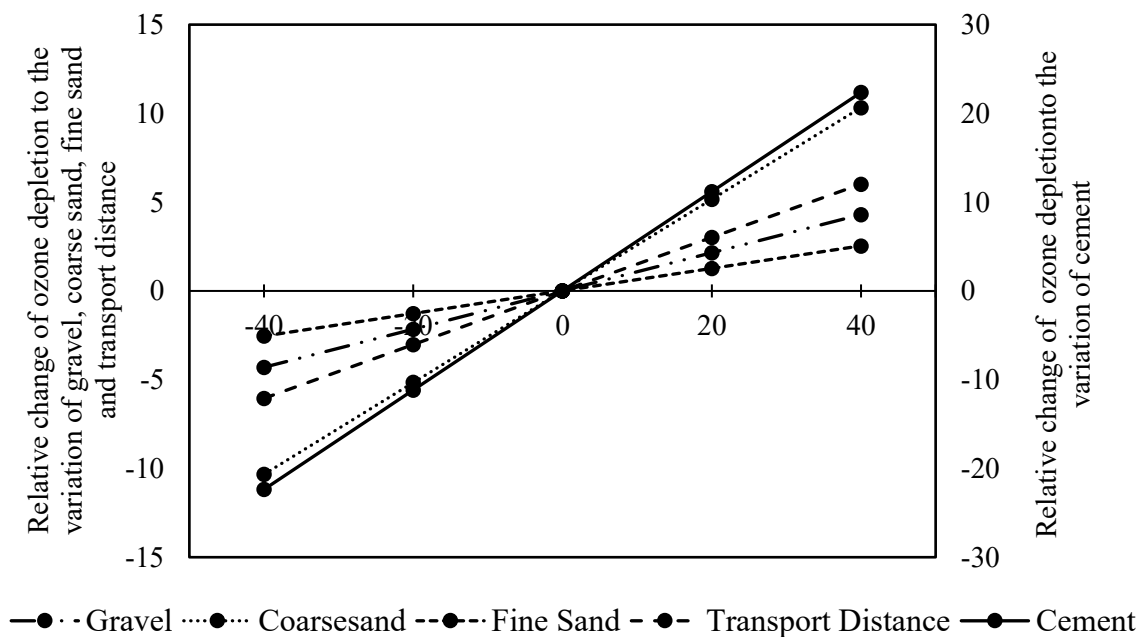
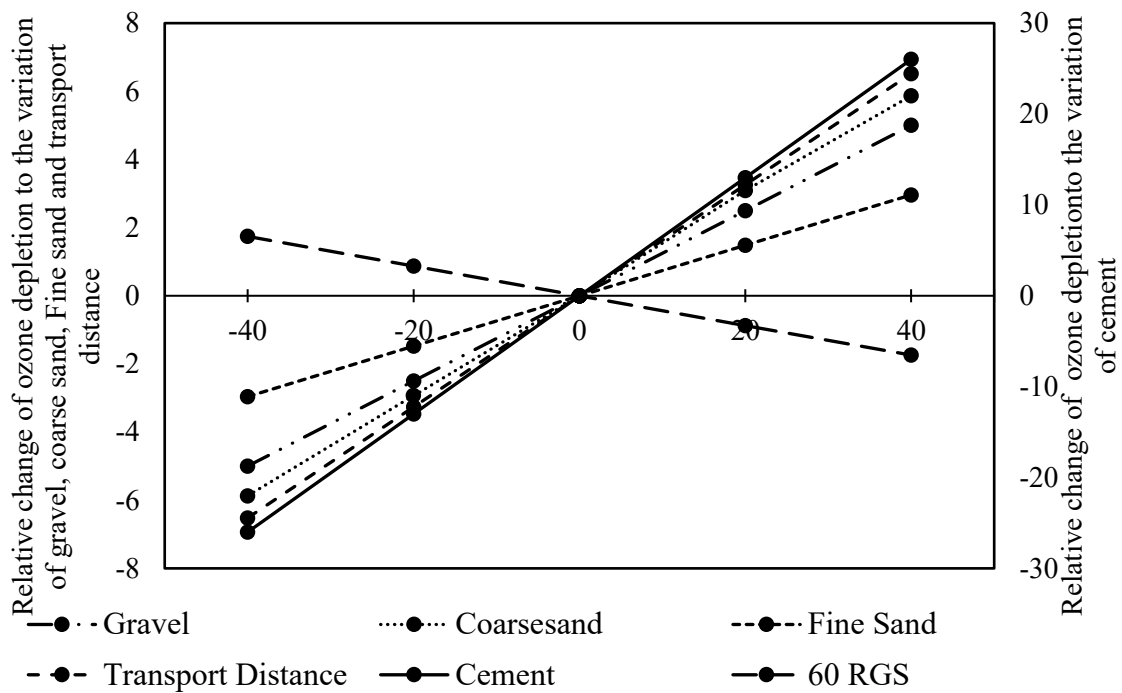


Figure 6.7 Relative change of global warming for control concrete

In ozone layer depletion, the change of cement, gravel and fine sand in 60 RGS concrete was 16% for both sensitivity analysis of  $\pm 20\%$  and  $\pm 40\%$ , compared with control concrete (Figures 6.8 and 6.9). The variation of transport distance in 60 RGS concrete had a slight impact, although 8% compared with control concrete. The sensitivity of coarse sand for control concrete was found to be  $\pm 5.2\%$  and  $\pm 10.3\%$  for  $\pm 20\%$  and  $\pm 40\%$ , respectively. Concrete with 60% RGS showed a sensitivity of coarse sand of  $\pm 3.1\%$  and  $\pm 5.9\%$ , which was 40% and 43% lower than control concrete. At higher glass sand replacement (60 RGS), the maximum glass sand (60%) was utilised in concrete which was sorted and crushed in the materials recovery facility. Moreover, 60 RGS was more sensible; for instance, 85% in ozone depletion relative to global warming.



**Figure 6.8 Relative change of ozone depletion for control concrete**



**Figure 6.9 Relative change of ozone depletion for 60 RGS concrete**

The change of 40% cement quantity in mix design resulted in a 32% variation in eutrophication in control concrete (Figure 6.10). However, the same 40% change in cement quantity caused the highest variation, albeit 1% in 60 RGS concrete (Figure 6.11). The difference of gravel, fine sand and transport distance showed slight variation in both control and 60 RGS concrete. In control concrete, about 3.8% variation was found for the change of 40% coarse sand quantity in the mix design. 60 RGS showed 1.72% change in results for the coarse sand variation of 40%. This reduction was due to the amount of coarse sand reduction, which was consequently reduced landfill impact corresponding to glass sand. RGS was less sensible compared to ozone depletion, however it showed more sensible compared to global warming.

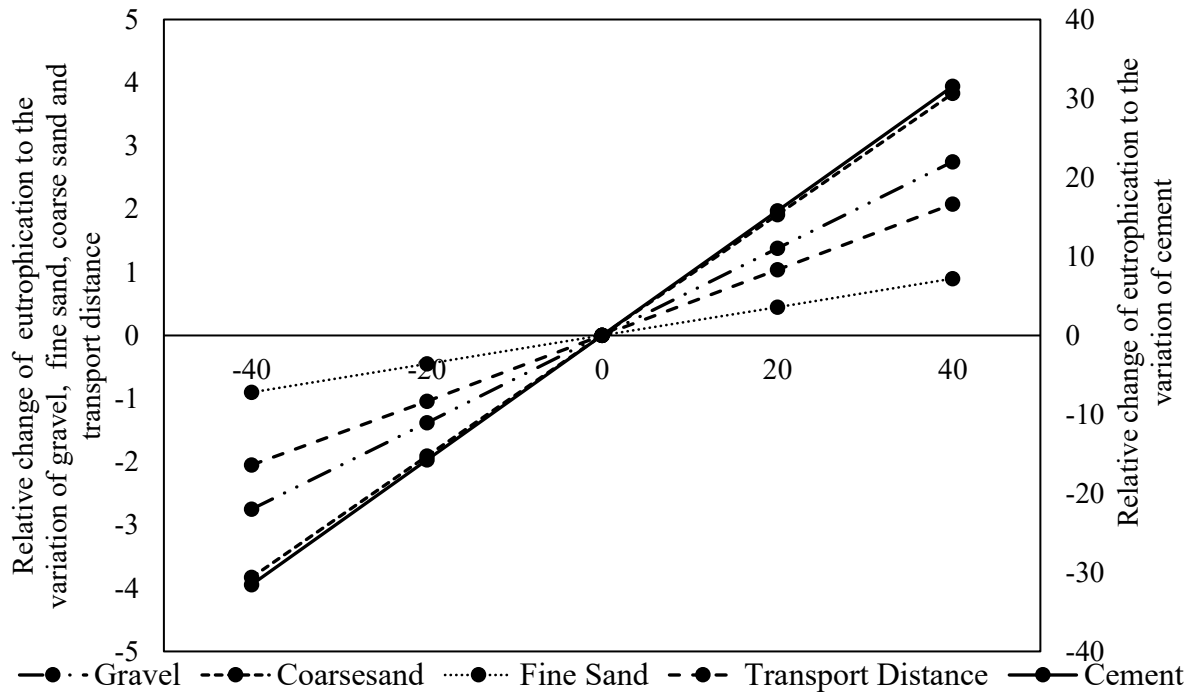


Figure 6.10 Relative change of eutrophication for control concrete

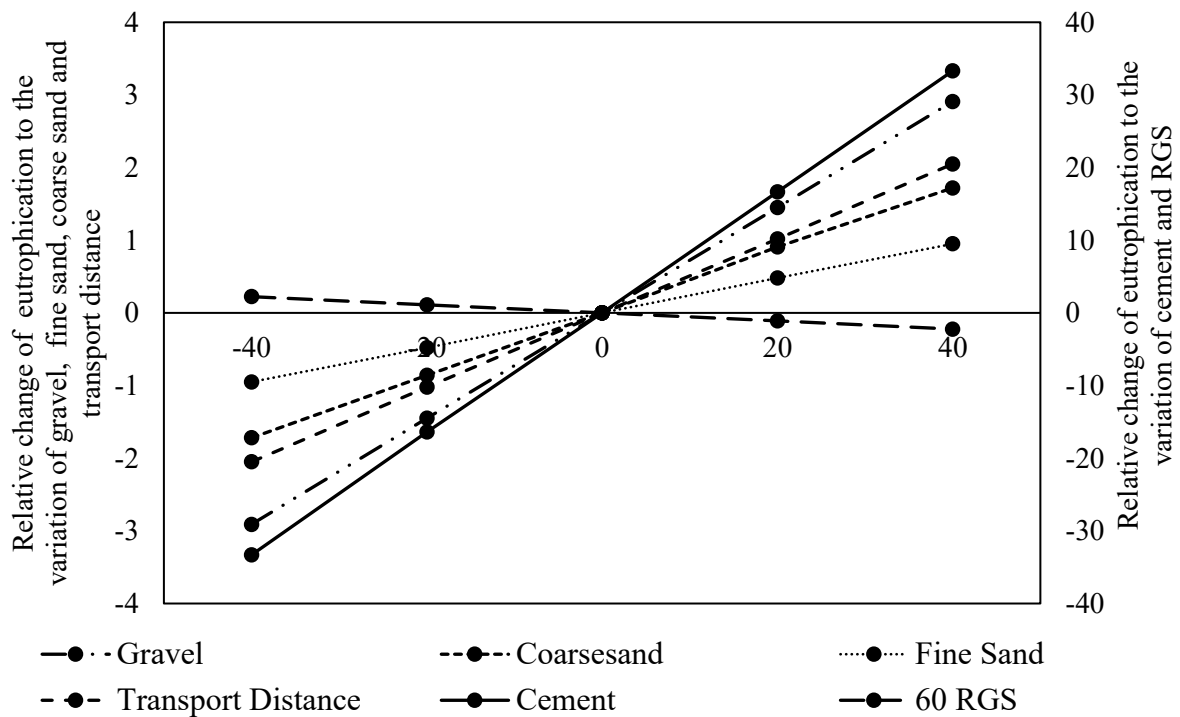
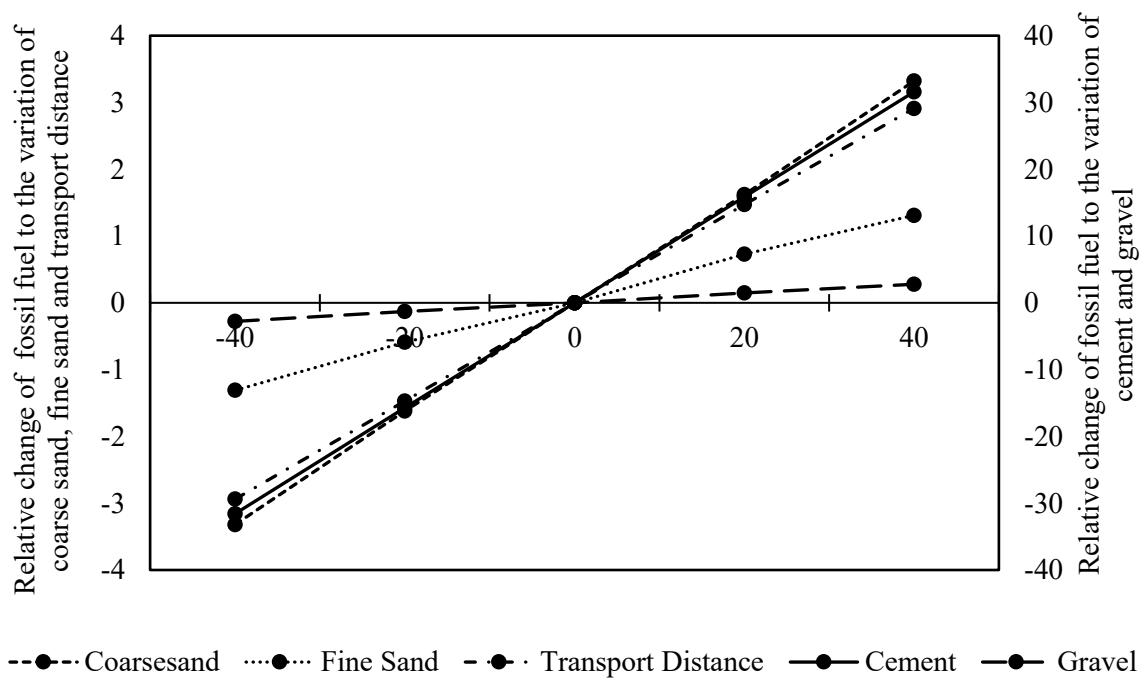
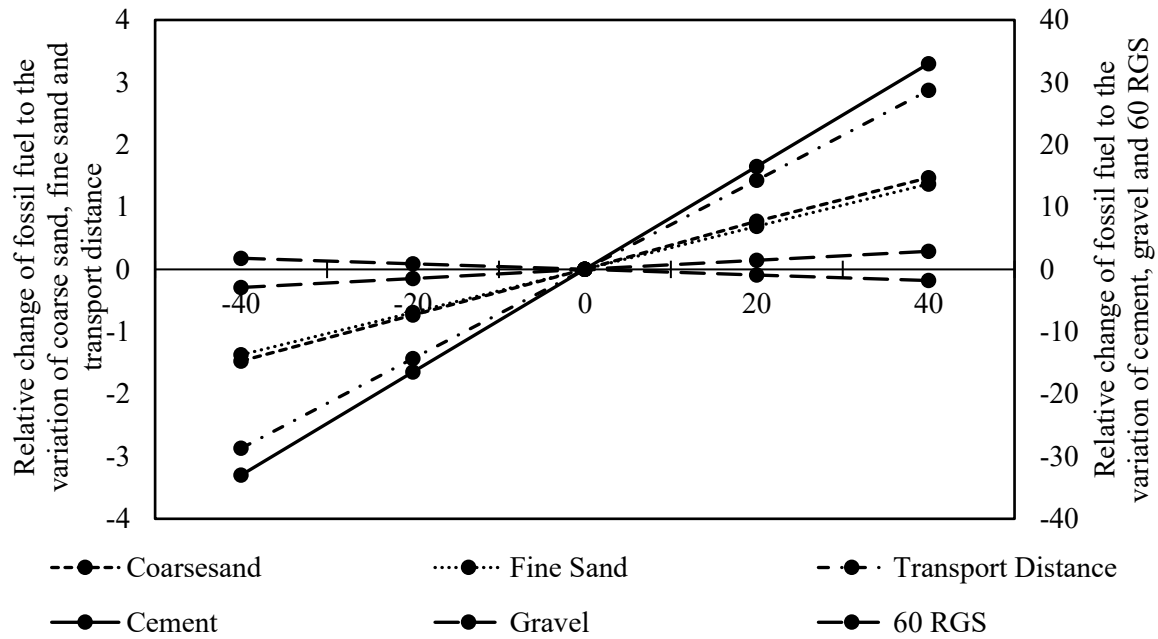


Figure 6.11 Relative change of eutrophication for 60 RGS concrete

The associated environmental impacts corresponding to fossil fuel to the variation of cement, gravel, coarse sand, fine sand and transport distance are shown in Figure 6.12 and 6.13. The variation of cement, gravel and fine sand in both control and 60 RGS concrete showed similar sensitivity to eutrophication. However, in control concrete, the change in transportation distance showed an increased variation of 40% compared with eutrophication. Increased in variation was also noticed in 60 RGS, compared with global warming and eutrophication. In contrast, a decrease in variation was found relative to ozone layer depletion.



**Figure 6.12 Relative change of fossil fuel for control concrete**



**Figure 6.13 Relative change of fossil fuel for 60 RGS concrete**

### 6.2.1.2 Uncertainty analysis of RGS

A comparison between 1  $m^3$  control concrete and 1  $m^3$  20 RGS concrete on the impact category is shown in Figure 6.14. A comparison was conducted by analysing the difference between two selections: for instance, control concrete minus 20 RGS concrete. As can be seen in Figure 6.14, 20 RGS concrete showed positive value, whereas control concrete presented negative values. The bar graph left of centre (negative values) represents the number of times the control concrete has a lower impact than 20 RGS concrete. In contrast, the bar at the right of centre or with positive values shows the probability of 20 RGS concrete having lower impacts than control concrete. 20 RGS concrete showed a lower effect on all impact categories compared with control concrete. For global warming, there was a 54% probability that 20 RGS concrete had a higher impact than control concrete, whereas control concrete had 46% change of having the global warming impact higher. 20 RGS concrete showed a lower impact on ozone depletion, eutrophication and fossil fuel with a probability of 95%, 68% and 63%, respectively.

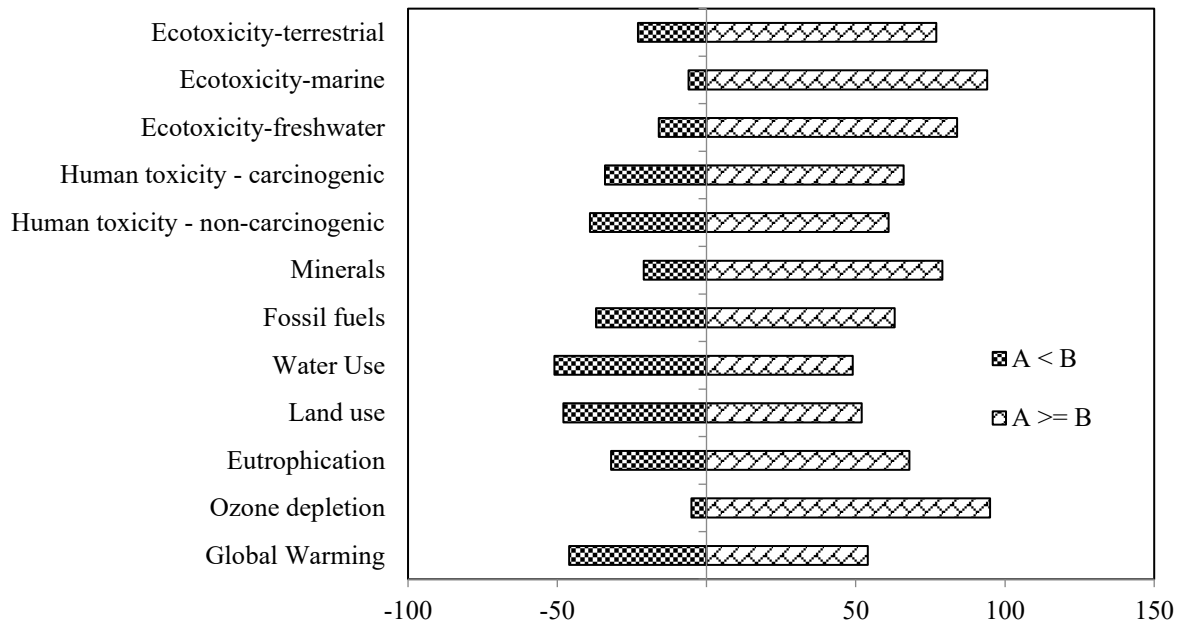


**Figure 6.14 Uncertainty analysis of 1m<sup>3</sup> control concrete (A) minus 1m<sup>3</sup> 20 RGS concrete (B)**

RGS quantity had a significant effect on each impact category as recycled glass sand quantity increased. The lower impact was found in each category for 40 RGS concrete and 60 RGS concrete (Figures 6.15 and 6.16, respectively). In the global warming impact category, control concrete had a probability of 46% to achieve lower impact compared with 40 RGS. However, 40 RGS concrete did not show uncertainty on ozone layer depletion and presented 100% of probability to show lower impact compared to control concrete. 60 RGS concrete also exhibited 100% lower impact compared with control concrete (Figure 6.16). Concrete with 60 RGS showed a lower impact on global warming, fossil fuel and eutrophication with a probability of 67%, 86% and 93%, respectively. Consequently, the probability reduced for control concrete as RGS quantity increased.

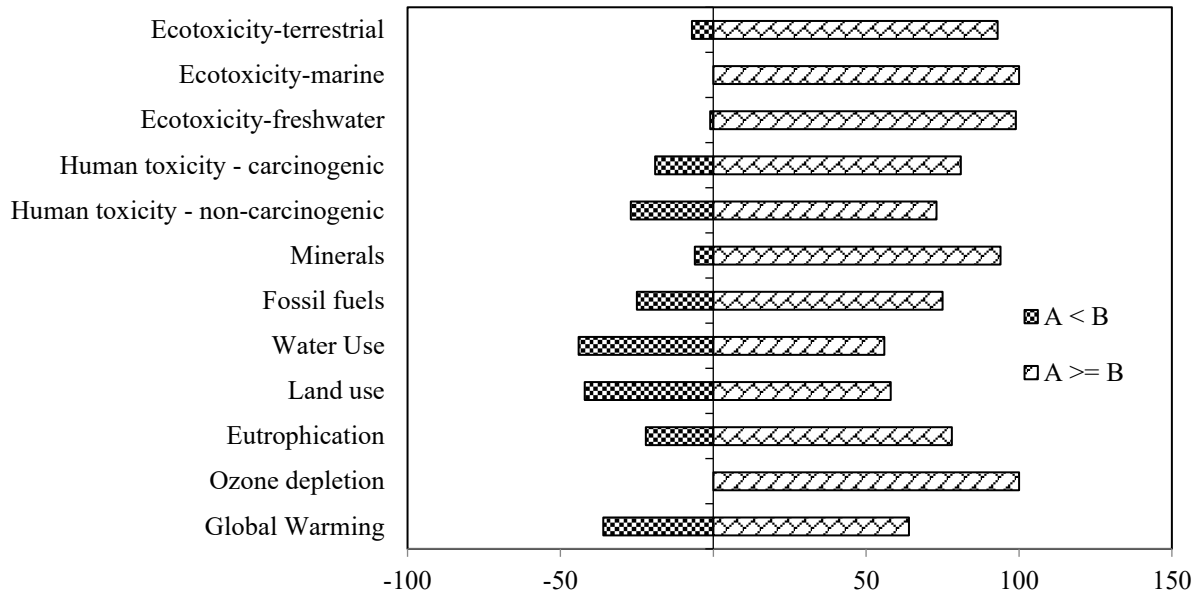


**Figure 6.15 Uncertainty analysis of 1 m<sup>3</sup> control concrete (A) minus 1 m<sup>3</sup> 40 RGS concrete (B)**

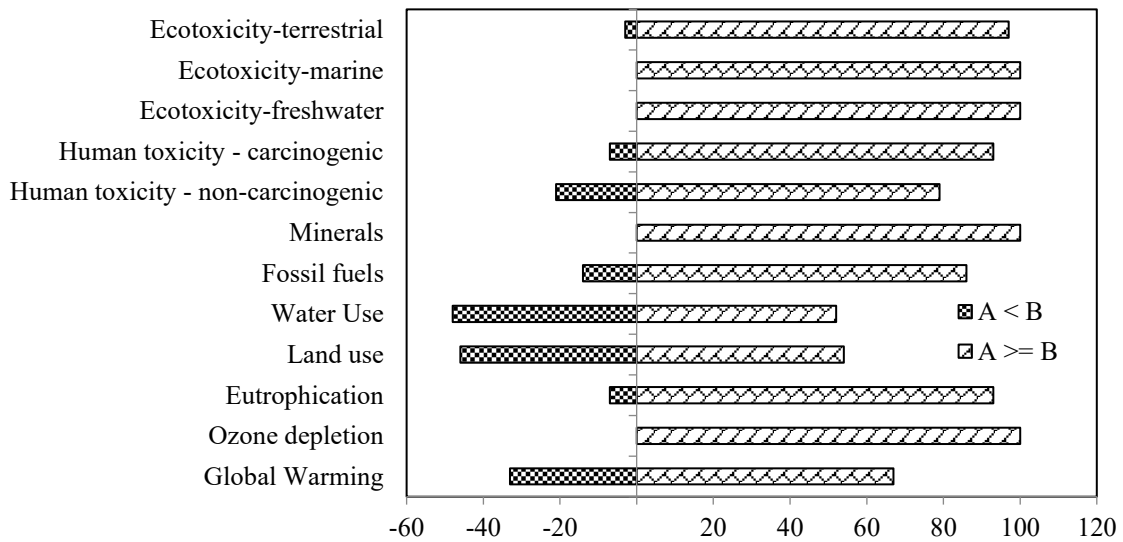


**Figure 6.16 Uncertainty analysis of 1 m<sup>3</sup> control concrete (A) minus 1 m<sup>3</sup> 60 RGS concrete (B)**

## 6.2.2 Recycled glass powder as cement replacement

Figure 6.17 shows 1  $m^3$  of control concrete presented the global warming potential of 351  $kg$   $CO_2$  equivalent, which showed the highest environmental footprint. As can be seen, the global warming potential correlated with RGP quantity. As the replacement level increased, RGP concrete reduced global warming potential. 10 RGP concrete released 323  $kg$   $CO_2$  equivalent to producing 1  $m^3$  concrete whereas 20 RGP and 30 RGP showed a global warming potential of 295  $kg$   $CO_2$  equivalent and 268  $kg$   $CO_2$  equivalent. The 30 RGP reduced the impact with 24%, followed by 20 RGP with 16% and 10 RGP with 8%.

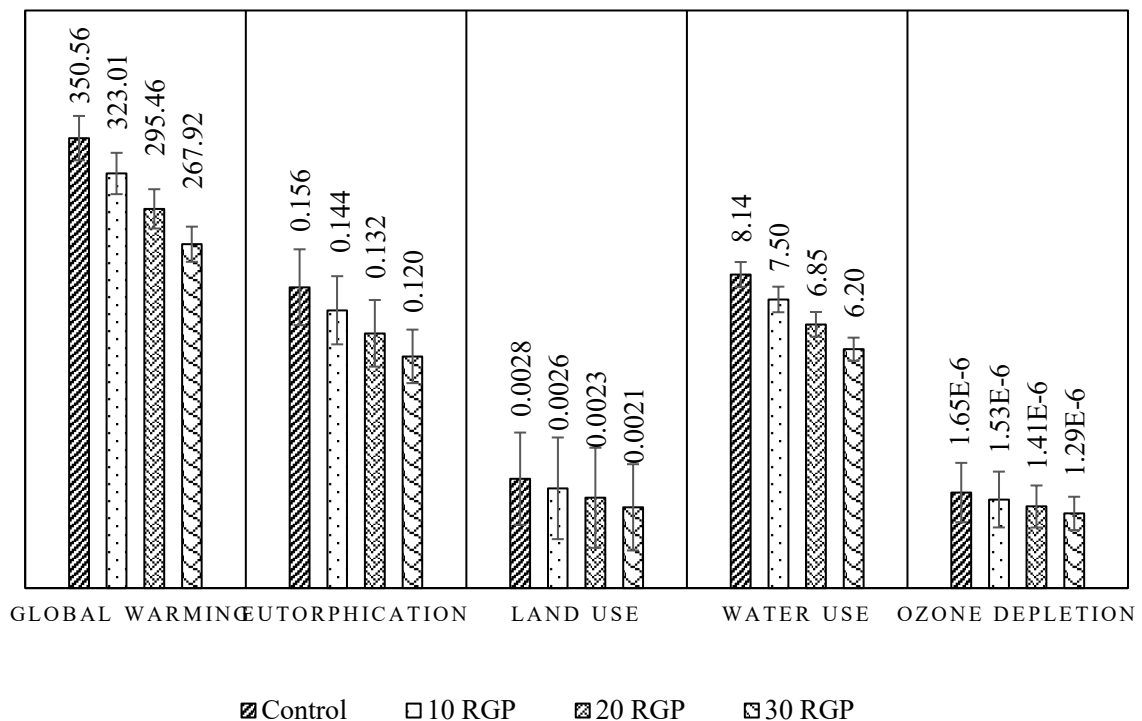


**Figure 6.17 life cycle impact categories associated with 1  $m^3$  RGP concrete**

Cement showed the highest contribution to the overall global warming impact of concrete (Figure 6.18). Cement produced 311  $kg$   $CO_2$ , which was 89% of the total global warming potential for control concrete. The global warming was reduced consequently as a part of cement was replaced by 10%, 20% and 30% RGP. 10 RGP, 20 RGP and 30 RGP emitted  $CO_2$  of 280  $kg$ , 249  $kg$  and 218  $kg$  respectively, which was in the range of benchmark concrete

products in Australia (Mohammadi and South, 2017). For supplementary cementitious materials, CO<sub>2</sub> emissions per cubic metre of concrete were in the range of 209-521 kg CO<sub>2</sub> equivalent (Mohammadi and South, 2017). RGP had an impact on global warming corresponding to electricity for glass sorting and crushing. Further electricity use for pulverising glass sand to powder form and transport distance was assessed. However, the use of RGP showed lower impact compared with cement. For instance, cement emitted about 31 kg CO<sub>2</sub> equivalent for every 10% replacement whereas, RGP emitted only about 4 kg CO<sub>2</sub> equivalent for every 10% addition. Transport and landfill showed negligible global warming potential.

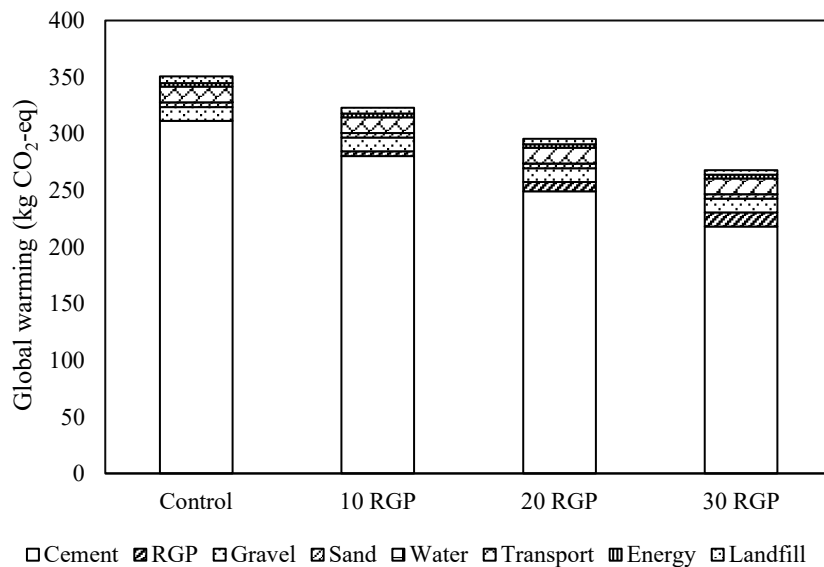


**Figure 6.18 Global warming potential of concrete with RGP**

Figure 6.19 shows the ozone layer depletion of control concrete and concrete with RGP. Concrete generated the lowest impact on ozone layer depletion among the fundamental damage categories. A large amount of ozone depletion was found for control concrete. Depletion tended to decrease with an increase in glass powder quantity in concrete. 10 RGP, 20 RGP and 30 RGP decreased 7% 15%, and 22% ozone layer depletion relative to control concrete. This decrease was mainly cement production, RGP, landfill and transportation. In the overall ozone

depletion category, 62% depletion occurred due to cement in control concrete. Cement replacement by RGP reduced ozone layer depletion of 2%, 4% and 7% of the control concrete. As cement quantity was reduced, the amount of RGP was increased and caused ozone layer depletion. However, this increase in depletion was insignificant compared with cement. Ozone layer depletion due to landfill was reduced as glass powder utilised in concrete mix.

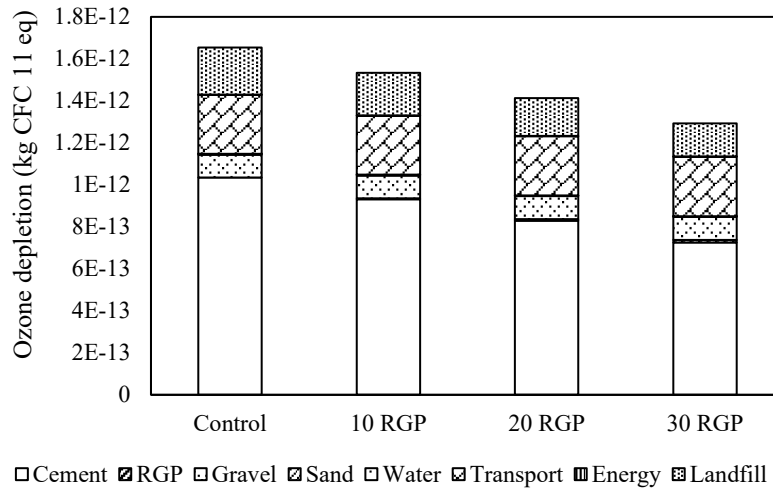


**Figure 6.19 Ozone depletion of concrete with RGP**

Another major damage category of control concrete and concrete with RGP was eutrophication (Figure 6.20). The use of RGP in concrete reduced the  $PO_4$  emission up to 23% for 30 RGP, followed by 15% for 20 RGP and 8% for 10 RGP. In eutrophication, about 82%  $PO_4$  emission was generated from cement, 6% from gravel, 5% from transport, 4% from landfill, and 3% from sand, water and electricity use. RGP as cement substitution reduced a significant amount of  $PO_4$  emission equivalent in terms of cement, RGP, transport and landfill. A reduction was attributed to the amount of RGP increased in concrete.

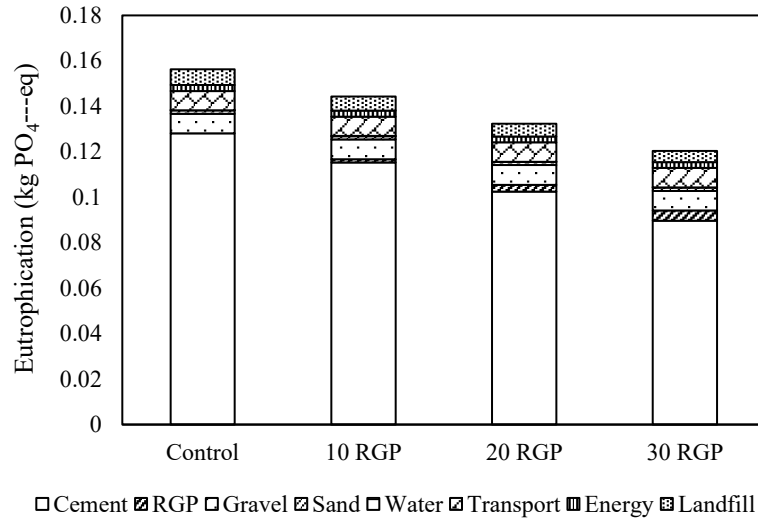


**Figure 6.20 Eutrophication of concrete with RGP**

Figure 6.21 shows the environmental impact due to land and water use caused by recycled glass concrete. Both land and water use tended to decrease with an increase in glass powder quantity in concrete to replace cement. There was a similar reduction in both land and water use for 10% glass powder addition in concrete, for instance, 9% and 8%, respectively, compared with control concrete. 20 RGP and 30 RGP reduced land use of 17% and 26% compared with control concrete, while 16% and 24% reduction was found for water use for 20 RGP and 30 RGP, respectively. Cement had the highest contribution to the land use and represented 94% of the total land use impact. The impact of cement reduced in 10 RGP, 20 RGP and 30 RGP, which was found to be 92%, 91% and 89% of the total land use, respectively. In water use, cement had a significant contribution, followed by gravel. Cement was responsible for 73-80% water use compared with the overall impact caused by water use. Landfill and transport distance showed negligible impact in both land and water use in concrete.

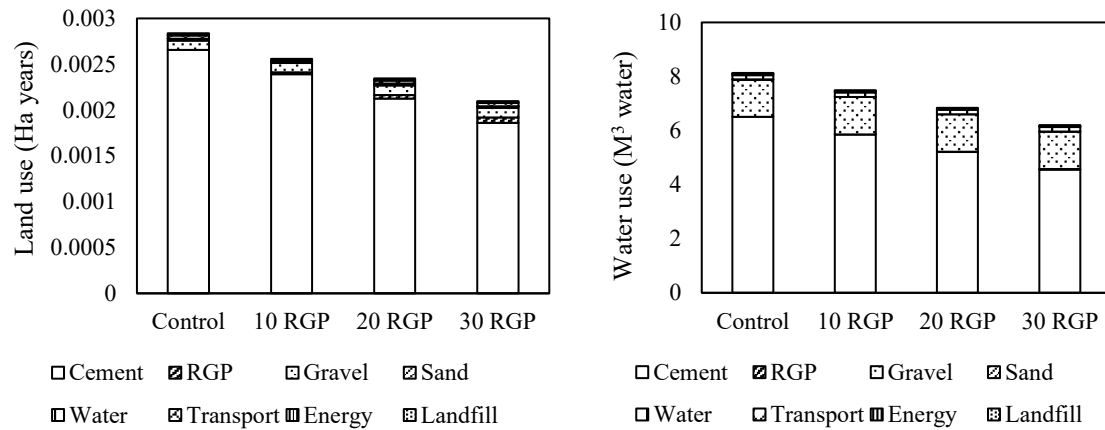


**Figure 6.21 Land and water use of concrete with RGP**

### 6.2.2.1 Sensitivity analysis of RGP

Sensitivity analysis was conducted to assess the variation of the results stated in Section 6.2.2. The variations of cement, aggregate and transport distance in mix design were analysed for control concrete and concrete with RGP. The sensitivity analysis was carried out by the change of each parameter in the range of  $\pm 40\%$ .

Figures 6.22 and 6.23 show the relative variation of global warming to the change of cement, coarse sand, fine sand and RGP in the mix design and as well as the change of transport distance for control concrete and RGP concrete. Cement is the most significant contributor in global warming and most sensitive to the change of its quantity. The change of 40% cement quantity in mix design resulted in a 36% variation in global warming in control concrete (Figure 6.22). Gravel, coarse sand, fine sand and transport distance showed a negligible difference in sensitivity analysis, for instance, 1.9%, 0.6%, 0.7%, and 1.5% variation with 40% change, respectively.

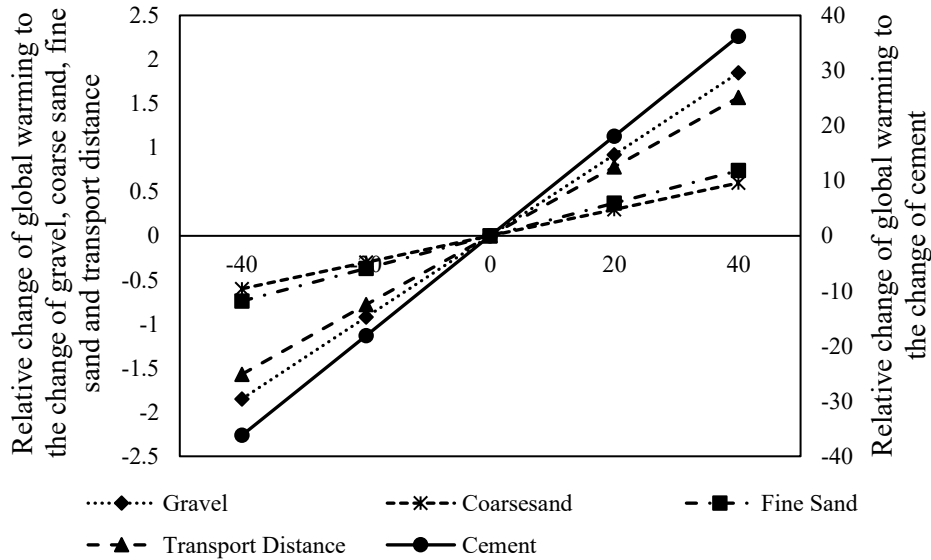


**Figure 6.22 Relative change of global warming for control concrete**

The sensitivity analysis of 30 RGP concrete showed a significant impact on global warming with a variation of 40%, compared with control concrete (Figure 6.23). Cement showed the highest variation of about 51% with the change of 40% cement quantity. The change in 40% cement amount caused 26% variation, which was 42% higher than control concrete. The gravel, coarse sand, fine sand and transport distance showed increased variation compared with control concrete. The change of 30 RGP quantity exhibited 6% and 12% variation with the change of 20% and 40%, respectively. This increased variation was due to sorting, crushing and pulverising of glass sand to glass powder.

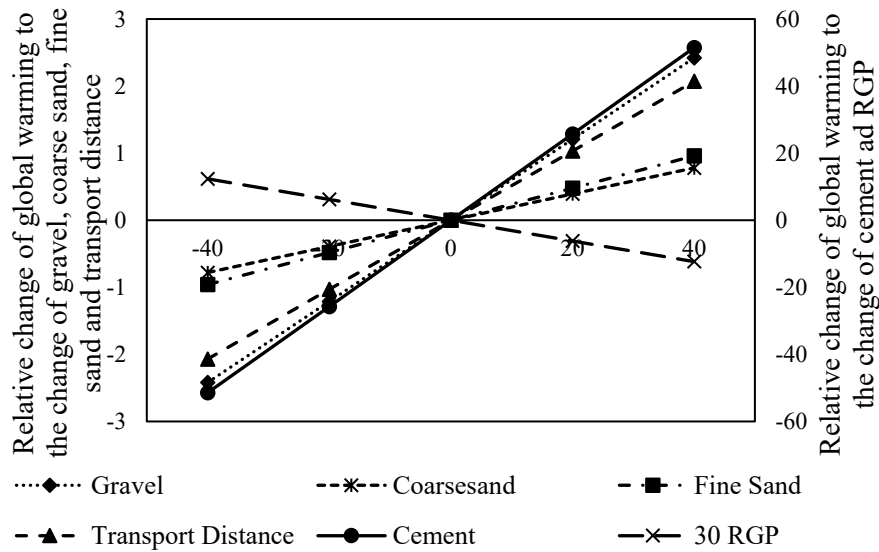


**Figure 6.23 Relative change of global warming for 30 RGP concrete**

In a sensitivity analysis of ozone depletion, cement showed the highest variation of about 31% in control concrete, whereas cement in 30 RGP concrete presented 39% variation due to 40% change in cement quantity (Figures 6.24 and 6.25). Sensitivity of coarse sand, fine sand, gravel and transport distance was found in the range of 1-5% in control concrete. In 30 RGP concrete, increased variation was found due to the change of gravel, transport distance and 30 RGP.

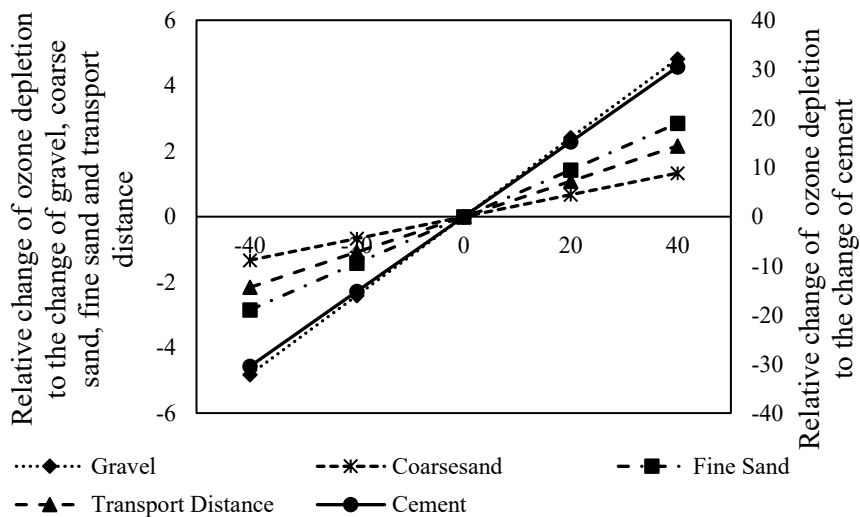


**Figure 6.24 Relative change of ozone depletion for control concrete**

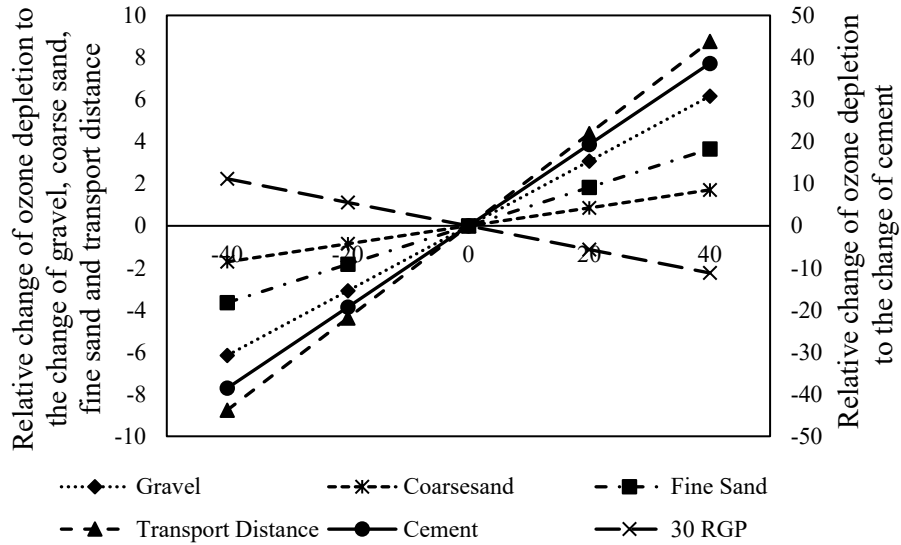


**Figure 6.25 Relative change of ozone depletion for 30 RGP concrete**

Similar to global warming and ozone depletion, cement showed the maximum variation in eutrophication in both control concrete and 30 RGP concrete (Figures 6.26 and 6.27). The change of 40% 30 RGP in mix design resulted in 12% variation in eutrophication, followed by gravel with 4%, transport distance with 3%, and fine and coarse sand with 1% as shown in Figure 6.20. Control concrete showed slightly less variation in all parameters.

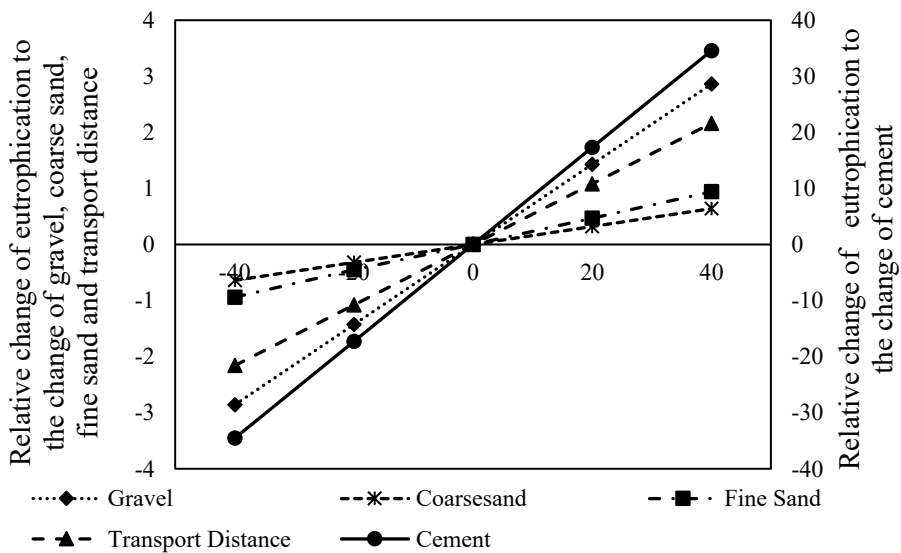


**Figure 6.26 Relative change of eutrophication for control concrete**

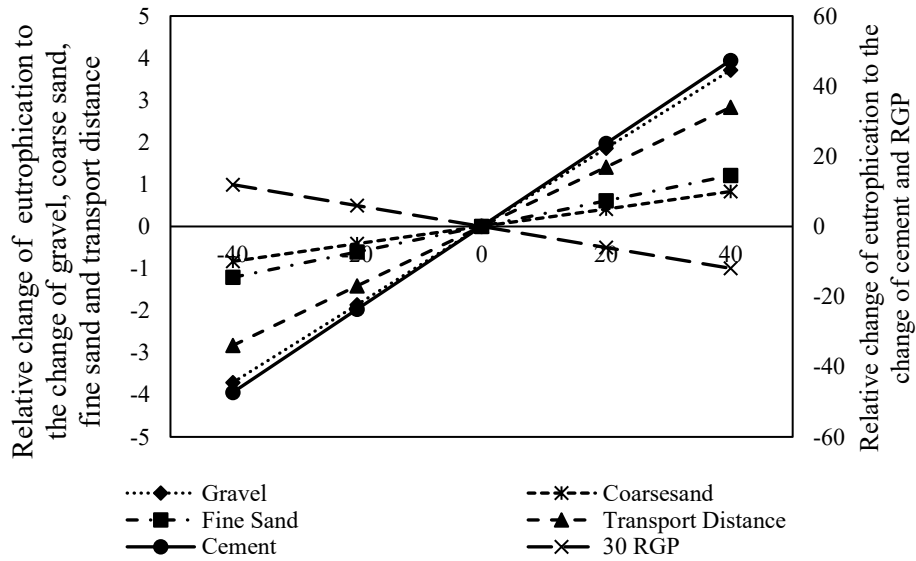


**Figure 6.27 Relative change of eutrophication for 30 RGP concrete**

As can be seen in Figure 6.28, land use showed the largest variation due to the variation of cement: 30% with the 20% change and 58% with the 40% variation of its volume. Cement was replaced by 30% RGP, which showed a 14% variation. Other parameters had a negligible variation, within 3% change due to 40% volume change. Water use displayed a similar trend in variation due to coarse sand, fine sand and transport distance. However, cement showed 43% variation, followed by 13% with 30 RGP and 9% with gravel.

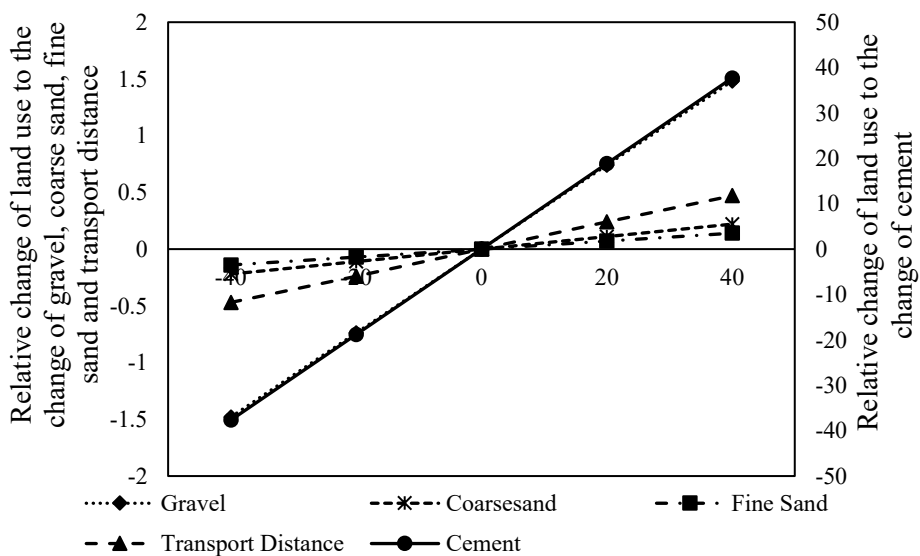


**Figure 6.28 Relative change of land use for control concrete**

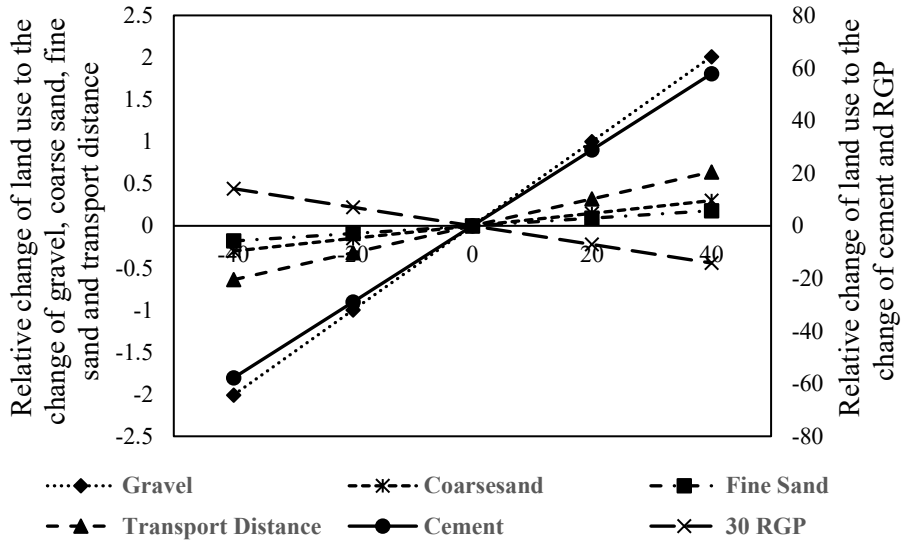


Figure 6.29 Relative change of land use for 30 RGP concrete

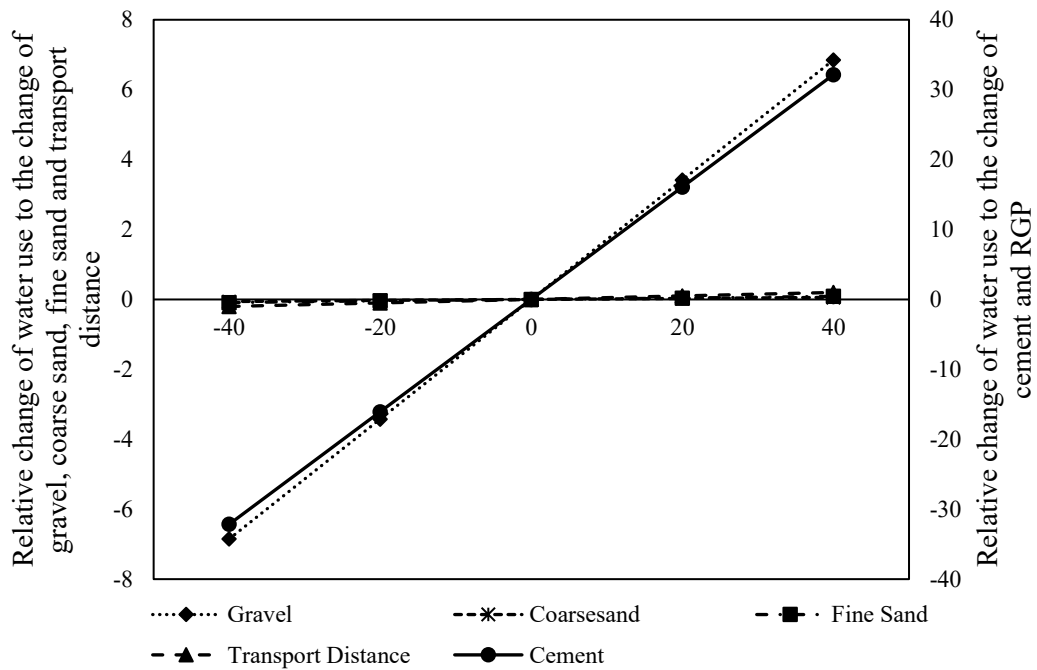
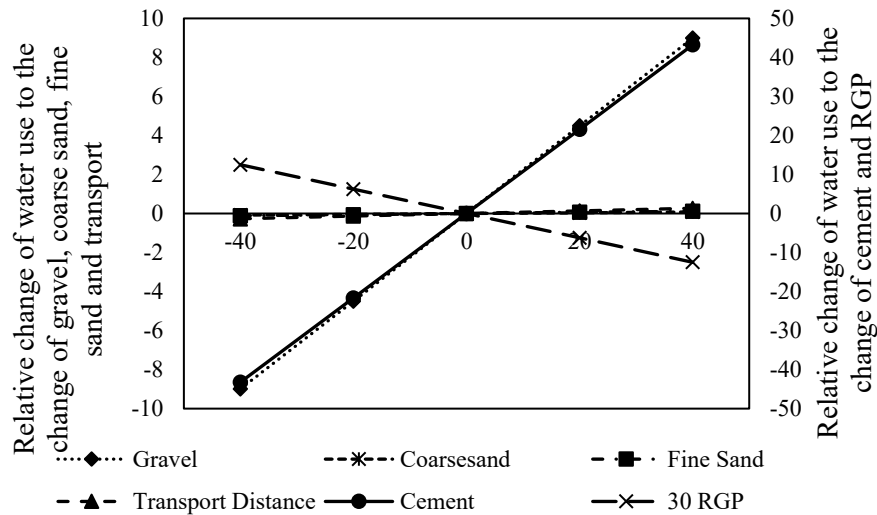


Figure 6.30 Relative change of water use for control concrete



**Figure 6.31 Relative change of water use for 30 RGP concrete**

### 6.2.2.2 Uncertainty analysis of RGP

Uncertainty analysis of  $1 m^3$  control concrete and  $1 m^3$  10 RGP concrete on the impact category is shown in Figure 6.32. The negative values on the bar graph represent the probability of control concrete to have lower impacts than RGP concrete. Similarly, a positive value shows the number of times RGP concrete has a lower effect over control concrete. RGP concrete had much lower uncertainty for significant impact categories, for example, greenhouse emissions, ozone layer depletion, eutrophication, fossil fuel, water use, land use and so on compared with RGS concrete. 10 RGP concrete had a higher probability of showing a lower impact on all impact categories. Control concrete had only 4% possibility on global warming, which indicated the certainty of 10 RGP concrete to be better on global warming. Besides, about 5%, and 4% chance found corresponding to ozone depletion and eutrophication, respectively. Land use and water use showed a similar probability for control concrete. The addition of RGP in concrete showed significant environmental benefit over control concrete. Figures 6.33 and 6.34 showed 100% of probability for all impact categories for both 20 RGP and 30 RGP concrete, meaning that the environmental benefit of RGP concrete was obvious over control concrete.

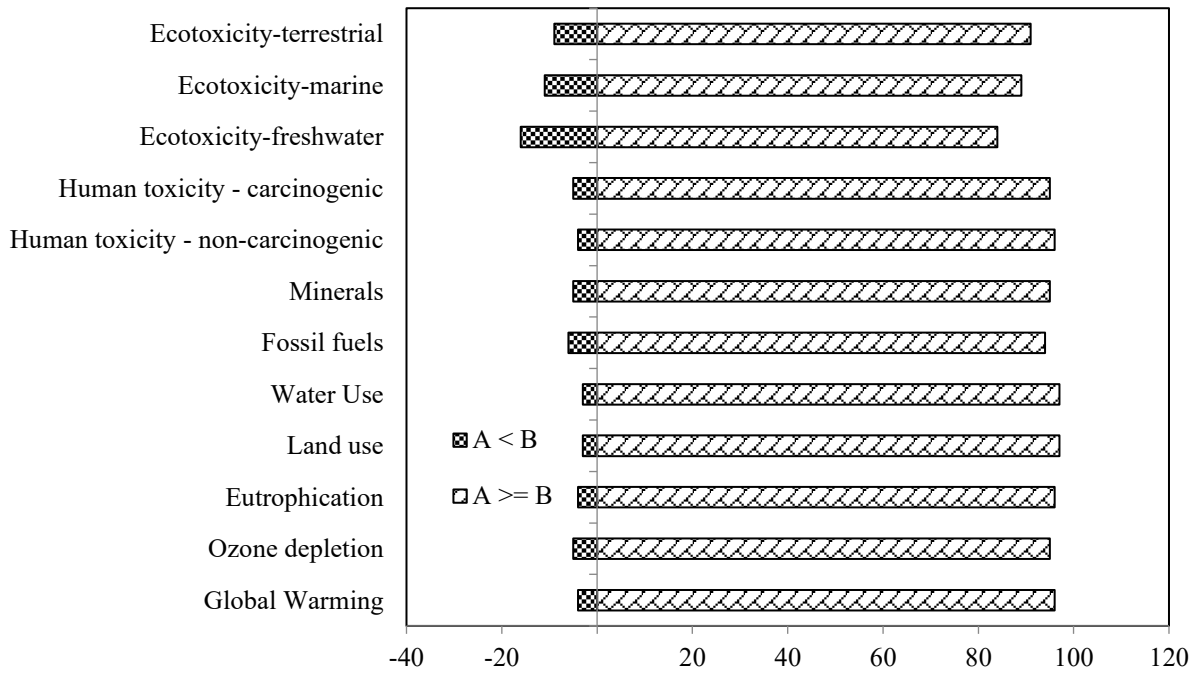


**Figure 6.32 Uncertainty analysis of 1 m<sup>3</sup> control concrete (cement) (A) minus 1 m<sup>3</sup> 10 RGP concrete (B)**

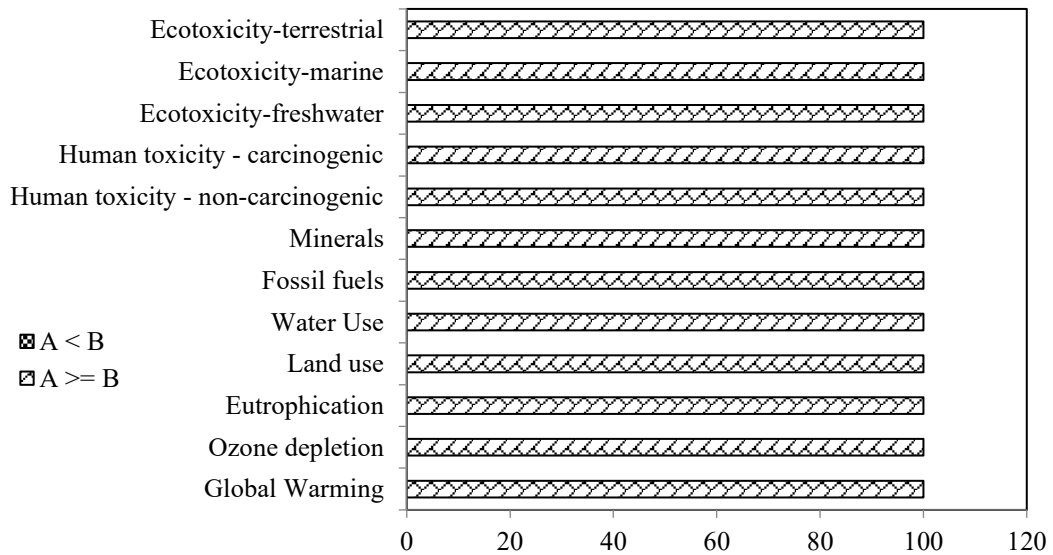


**Figure 6.33 Uncertainty analysis of 1 m<sup>3</sup> control concrete (cement) (A) minus 1 m<sup>3</sup> 20 RGP concrete (B)**

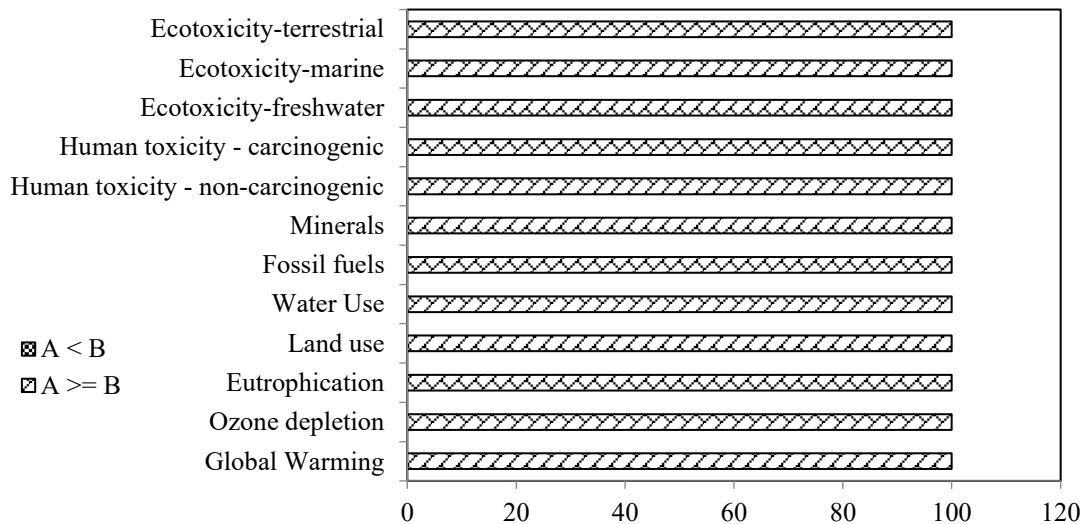


**Figure 6.34 Uncertainty analysis of 1 m<sup>3</sup> control concrete (cement) (A) minus 1 m<sup>3</sup> 30 RGP concrete (B)**

### 6.3 Conclusion

This research analysed the environmental benefits of using recycled glass to produce 1 m<sup>3</sup> concrete in the Australian context. Three different scenarios - control concrete, recycled glass sand concrete and recycled glass powder concrete – were assessed to evaluate the effect of using recycled glass in concrete using the software tool SimaPro 8.0. The use of RGS in concrete as a sand substitute did not have a high environmental footprint. However, 20 RGS, 40 RGS and 60 RGS reduced global warming of 0.84%, 1.7% and 2.2%, respectively, compared with control concrete. However, the global warming potential was correlated with RGP quantity. RGP concrete reduced global warming potential up to 24%, as the replacement level increased up to 60%. Cement exhibited the highest contribution to the overall global warming impact of concrete. The global warming was reduced consequently, as a part of cement was replaced by RGP. RGP concrete emitted CO<sub>2</sub> of 218-280 kg, which was in the range of benchmark concrete products in Australia. RGS concrete and RGP concrete can reduce up to 14% and 22% ozone layer depletion, respectively. Eutrophication was in the range of 0.120-0.162 kg PO<sub>4</sub>-eq per cubic meter of both RGS and RGP concrete. In a sensitivity

analysis, the variation of gravel, fine sand coarse sand and transport distance did not have a significant impact on different impact categories. Nevertheless, the variation of cement was very sensitive in the range of  $\pm 40\%$ . The addition of recycled glass as both sand and cement replacement had much lower uncertainty for significant impact categories. The outcome of this research can help towards sustainable development by reducing the consumption of sand and cement in concrete.

## **Chapter 7: Application of recycled waste glass sand in concrete footpath**

Low-risk infrastructure projects, for instance, concrete pedestrian and cyclist footpath was selected to demonstrate field application of RGS in concrete as a coarse sand replacement. This chapter presents the process of using RGS concrete in field trials. Concrete mix design was developed for the various ratios of glass sand used in the concrete footpath. A concrete slump test was conducted to assess the workability of RGS concrete. A compressive strength test was also carried out to evaluate the strength of RGS concrete.

### **7.1 Concrete footpath**

A footpath with a size of 108 *m* long and 2 *m* wide was cast at Progress Road, White Rock State School in Cairns, Queensland. For the trial basis, a total of four concrete batches were prepared, including a standard N class concrete (control), two concrete mixes containing RGS at 40% and 60% (denoted as RGS 40 and RGS 60, respectively) and one concrete mix with 40% RGS, TMR (Department of Transport and Main road) mix (RGS 40 – TMR) (Figure 7.1). A mixed-coloured soda-lime glass collected by the Cairns Regional Council was used in this study to produce RGS as a partial sand replacement in concrete with a target characteristic strength of 32 *MPa* at 28 days. Concrete mix design used in field trials is shown in Table 7.1.



**Figure 7.1 Crushed glass (3 mm size) at MRF site, Cairns**

**Table 7.1 Materials content for 1 m<sup>3</sup> of concrete mixture used in field trials**

Concrete Mix		RGS 40 - TMR	RGS 60	RGS 40	Control
Cementitious Materials	Cement Australia Townsville GP (kg/m <sup>3</sup> )	255	263	255	241
	Cement Australia Callide FA (kg/m <sup>3</sup> )	85	88	85	80
Coarse Aggregate	Edmonton Stone (10 mm) (kg/m <sup>3</sup> )	801	805	801	795
	Barron Coarse Sand (kg/m <sup>3</sup> )	0	0	0	487
Fine Aggregate	Tableland Fine Sand (kg/m <sup>3</sup> )	316	312	316	215
	Edmonton Fine Sand (kg/m <sup>3</sup> )	316	105	319	380
	Recycled Glass Sand (4 mm) (kg/m <sup>3</sup> )	405	600	405	0
Admixtures	SIKA Plastiment-45 (ml/100kg)	450	450	450	450
	SIKA Retarder-N (ml/100kg)	50-100	0	0	50-100
Water	Design Water (Litres)	156	156	156	155

Design W/C Ratio	0.45	0.45	0.46	0.49
------------------	------	------	------	------

Section of footpath casted with each RGS concrete mix was 30 m long, and a control mix was used for the remaining section of the footpath. The footpath was designed for a thickness of 100 mm with SL72 mesh consisting of 6.75 mm steel bars with 200 mm spacing (Figure 7.2). According to FNQROC (Far North Queensland Regional Organisation of Councils) standard drawing S1035-pathways/bikeways, expansion and contraction joints were placed at 15 m and 3 m centres, respectively for a 30 m long footpath.



**Figure 7.2 Reinforcing mesh for concrete footpath**

## **7.2 Concrete casting**

The RGS 40-TMR concrete of 30 m was poured on 11 January 2019 at 8am. Concrete had not set at 1pm on 11 January 2019. The footpath showed full depth penetration after five hours of pouring. However, the footpath was set at 3pm on 11 January 2019. Delayed footpath setting caused may be due to an adverse reaction between SIKA Retarder N and RGS. Presence of sugar in RGS can also be a reason for delayed concrete settings. RGS was sent to SGS Australia

Pty Ltd to test initial sugar content. Initial results revealed less than 25 mg/kg of carbohydrates as sugar. RGS sample was further sent to Sharp and Howells Pty Ltd to test the presence of sugar according to AS 1141.35 (AS1141.35,2007). Results did not show the presence of sugar in RGS, which is consistent with the test carried out at JCU, Townsville. RGS 60, RGS 40 and control concrete mix was poured at 7am, 8:30am and 2pm, respectively on 14 January 2019. All concrete was set in expected time as SIKA Retarder N was removed from the RGS 60 and RGS 40 concrete.

Figure 7.3 shows the formwork and reinforcement arrangement before the concrete pour. The ready-mix concrete was poured into the formwork directly (Figure 7.4). The fresh concrete mix was also poured into the cylinders for compressive strength (Figure 7.5). The manual screeding process of concrete mix was conducted to achieve the smooth surface of the footpath (Figure 7.6). Special care was taken to level the expansion joints and edge of the footpath (Figure 7.7). After finishing, SIKAFilm was used to cure the freshly poured concrete to reduce the evaporation rate of water in concrete (Figure 8). No issues arose during concrete casting and finishing. Figure 7.9 shows the freshly placed concrete footpath in the first stage. Figure 7.10 presents the hardened concrete (RGS 40 – TMR concrete) footpath at three days.



**Figure 7.3 Form work and reinforcement arrangement prior to concrete pour**



**Figure 7.4 Ready mix concrete pouring**



**Figure 7.5 Fresh concrete for compressive strength**



**Figure 7.6 Screeding of the concrete mix**



**Figure 7.7 Expansion joint**



**Figure 7.8 Curing of freshly placed concrete**



**Figure 7.9 Footpath in the fresh stage**



**Figure 7.10 RGS 40 – TMR concrete footpath**

## **7.3 Results and discussion**

### **7.3.1 Slump test**

A slump test (Figure 7.11) was conducted to determine the workability of fresh concrete mixes. The target slump was 80 *mm*, outlined by PNQ with a  $\pm 15$  *mm* permissible tolerance on slump according to AS 1379 Table 5.1 (AS1379.2007). The control concrete, RGS 40 - TMR, RGS 40 achieved the target slump however, RGS 60 exhibited slump 5mm above the permissible tolerance (Table 7.2). Increase in the slump observed was due to less water affinity of RGS, and hence, it appeared to be a wetted concrete mix. A little bleeding and segregation were noticed in the glass incorporated mixtures.



**Figure 7.11 Slump test**

**Table 7.2 Slump test results of control concrete and concrete using RGS**

Concrete Mix	RGS 40 - TMR	RGS 60	RGS 40	Control
Slump ( <i>mm</i> )	90	100	80	80

### 7.3.2 Compressive strength

Compressive strength results were collected from ETS Geotechnical and PNQ. The compressive strength was not obtained for control concrete at five days. However, RGS 40 showed the highest compressive strength (19 *MPa*) at five days. RGS 40 – TMR and RGS 60 concrete achieved 16.5 *MPa* and 14.5 *MPa*, respectively. Control concrete achieved the highest compressive strength (22.6 *MPa*) at seven days (Figure 7.12). RGS 40 obtained 96% of the control concrete, whereas RGS 40 – TMR and RGS 60 concrete achieved 79% and 73%, respectively. All concrete achieved the mean compressive strength of 16 *MPa* at seven days for N32 concrete as per AS 1379 Table 1.2 (AS1379, 2007). Control concrete and RGS 40 concrete achieved the characteristic strength of 32 *MPa* at 28 days. RGS 40 – TMR and RGS

60 did not achieve the target characteristic strength, however, obtained 84% and 76% of control concrete, respectively.

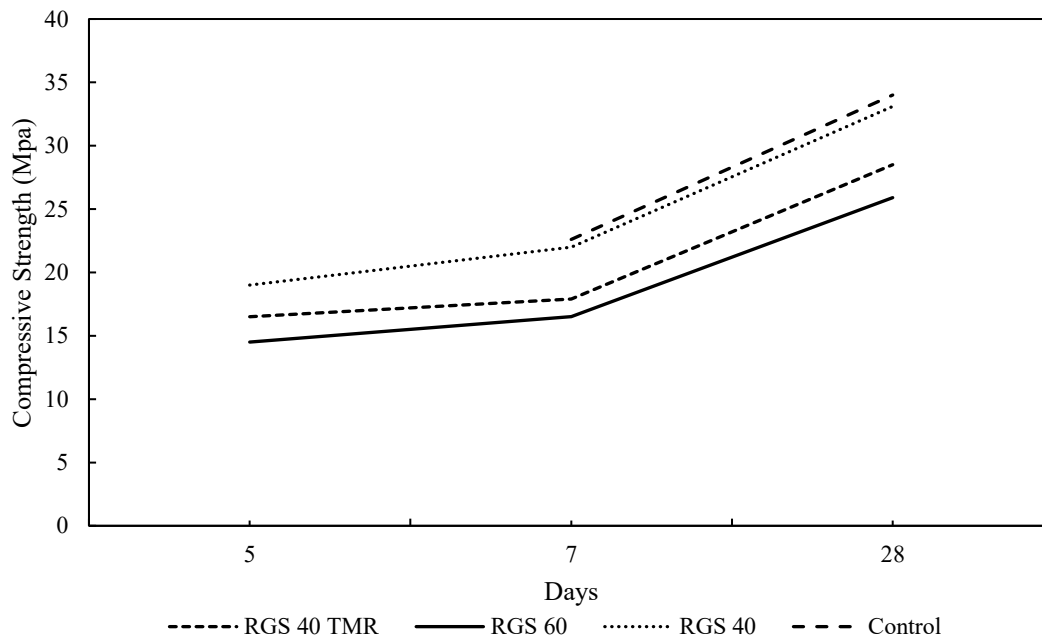


**Figure 7.12 Compressive strength of control concrete and concrete using RGS**

## 7.4 Conclusion

A footpath with a size of 108 m long X 2 m wide was cast at Progress Road, in Cairns, Queensland. A total of three concrete batches were prepared, including two concrete mixes containing RGS at 40% and 60% and one concrete mix with TMR 40% RGS. TMR 40% RGS showed delayed setting, however, glass sand did not show the presence of sugar. No adverse effect was noticed during pouring and finishing. The control concrete, RGS 40 - TMR, RGS 40 achieved the target slump; however, RGS 60 exhibited slump 5mm above the permissible tolerance due to less water affinity of RGS. Control concrete and RGS 40 concrete achieved the characteristic strength of 32 MPa at 28 days. RGS 40 – TMR and RGS 60 did not achieve the target characteristic strength, however, obtained 84% and 76% of control concrete, respectively. Therefore, the footpath has been used successfully for one year.

## **Chapter 8: Conclusion and recommendation**

### **8.1 Conclusions**

Several studies have been conducted on the use of waste glass in concrete. However, very limited field trials have been undertaken to observe the suitability of waste glass in concrete. The properties and performance of recycled glass sand depend upon the source and types of waste glass. The aim of this research has been to utilise recycled glass effectively as a partial replacement for the sand and cement in concrete. In this study, mixed-coloured soda-lime glass, collected by Cairns Regional Council, Australia, was used. A series of experimental study were conducted to investigate the influence of RGS and RGS concerning strength characteristics and durability properties and the following conclusions from this research are shown below:

1. A series of tests were conducted to determine the properties of the constituents, fresh concrete, and hardened concrete including its durability characteristics to investigate the suitability of using recycled waste glass sand (RGS) in concrete. Concrete was produced by replacing natural river sand with 20%, 40% and 60% of RGS. Target compressive strength was achieved by all concrete mixes in 28 days and most significantly, in seven days by control concrete and 20 RGS concrete. No adverse reduction in strength was noticed up to 60% replacement of natural sand with RGS. RGS concrete showed enhanced resistance to chloride-ion penetration up to 60%. 40 RGS exhibited the highest resistance to chloride ion penetration and made concrete less permeable. Besides, RGS addition significantly reduced expansion caused by the alkali-silica reaction. All mortar bar specimens exhibited expansion less than 0.1% at 21 days which is classified as non-reactive. The least ASR expansion was noticed for 40 RGS, followed by 60 RGS at 21 days. 40% is the optimum amount considering the field

application as well. The experimental results ascertain that the addition of RGS can be a good substitute for natural sand.

2. Concrete with recycled glass powder as a partial cement replacement in concrete with a target characteristic strength of 32 *MPa* at 28 days was assessed. Mechanical strength and durability properties of concrete with 10%, 20% and 30% of RGP as a partial cement replacement were tested and compared with typical concrete and fly ash blend concrete. The relative strength test of mortar was conducted to assess the reactivity of glass powder with the cement. RGP concrete showed an improvement in strength over time, like fly ash. RGP did not show significant strength gain at an early age due to the delay in pozzolanic reaction. However, 10 RGP concrete achieved the characteristic strength of 32MPa at 28 days. RGP showed a substantial strength development at 56 days. Using RGP significantly improved the resistance against chloride penetration with increasing glass powder content. Furthermore, 10 RGP also met the relative strength requirement as per Australian Standards requirement to be considered as a supplementary cementitious material.
3. Microstructural analysis was conducted to evaluate the influence on using recycled glass in mortar and cement paste, including thermogravimetric analysis, X-ray diffraction, scanning electron microscopy together with energy-dispersive spectroscopy. The mortar was prepared by replacing natural river sand with 20%, 40% and 60% of RGS, whereas cement paste was produced by replacing Portland cement with 10%, 20%, 30% and 40% of RGP.
  - For glass sand mortar, thermogravimetric analysis showed that  $\text{Ca(OH)}_2$  content was found to decrease in 20, 40 and 60 RGS compared with control mortar. The reduction of  $\text{Ca(OH)}_2$  indicates the pozzolanic reaction as  $\text{Ca(OH)}_2$  is consumed in the pozzolanic reaction to produce additional C-S-H gel. As glass sand used in this research was smaller

(3 mm), no internal cracks were found at the surface or inside the glass particles. The ASR expansion was not observed in the SEM microstructure for glass sand mortar samples. From EDS results, 40 RGS and 60 RGS showed high Si/Ca ratio compared to Control (0 RGS) and 20 RGS. Reversely, in low Ca/Si ratio, finer RGS can react with  $\text{Ca(OH)}_2$  and produce C-S-H at later days.  $\text{Ca(OH)}_2$  is consumed further reducing the potential of ASR reaction due to pozzolanic reaction.

- For cement paste, thermogravimetric analysis showed that the pozzolanic material did not show its effects in early days and hence became more prominent later. There was a noticeable trend at 28, 56 and 90 days that  $\text{Ca(OH)}_2$  content decreases as RGP replacement level increased.  $\text{Ca(OH)}_2$  formed during cement hydration slowly reacts with glass powder in the pozzolanic reaction to produce more C-S-H. SEM result showed that 10 RGP cement paste was covered with the formation of C-S-H and showed dense microstructure compared to Control (0 RGP) cement paste.  $\text{Ca(OH)}_2$  was no longer observed with identical hexagonal shapes in the paste as  $\text{Ca(OH)}_2$  further reacted with RGP and formed additional C-S-H in the microstructure at 90 days. The addition of waste glass powder in the cement paste reacted with  $\text{Ca(OH)}_2$  and produced C-S-H, which can make the microstructure confined.
4. The environmental benefits of using recycled glass to produce 1  $m^3$  concrete were assessed in the Australian context. Three different scenarios such as control concrete, recycled glass sand concrete and recycled glass powder concrete were evaluated using the software tool SimaPro 8.0 and Australian database method, Australian indicator V3.00. The use of RGS in concrete as a sand substitute did not have a high environmental footprint. However, global warming was reduced consequently, as a part of cement was replaced by RGP: for instance, 24% as the replacement level increased up to 60%. RGS concrete and RGP concrete can reduce ozone layer depletion up to

14% and 22%, respectively. Eutrophication was in the range of 0.120-0.162 *kg PO<sub>4</sub>-eq* per cubic metre of both RGS and RGP concrete. Compared with conventional concrete, both RGS and RGP concrete have a significant influence on reducing the environmental impact caused by concrete production.

5. To trial the use of concrete with RGS in field applications, a footpath 108 *m* long X 2 *m* wide was cast at Progress Road, White Rock State School in Cairns, Queensland. Concrete mix design was developed for a total of four concrete batches used in the concrete footpath. A concrete slump test and compressive strength test were carried out to assess the workability and strength of RGS concrete. A mixed-coloured soda-lime glass was used to produce RGS concrete with a target characteristic strength of 32 *MPa* at 28 days. Concrete with 40% RGS achieved the characteristic strength of 32 *MPa* at 28 days. The footpath has been used successfully for a year.

The successful application of using recycled glass in concrete not only can reduce sand dredging but also reduce the cement production along with the reduction of glass waste going into landfill sites. This research also aims to contribute towards sustainable development; therefore, it can be effectively used in industrial applications.

## **8.2 Recommendations**

The following recommendations for further development can be made based on the findings of this research.

1. Investigate the influence of drying shrinkage on the use of recycled glass in concrete.
2. Carry out microstructural analysis such as nuclear magnetic resonance spectroscopy, water absorption tests, and pore structure analysis to investigate the effect of hydration of glass cement-based systems.

3. The hydration of pozzolanic material gives a better result at later stages. Long-term investigation can be conducted to get more accurate information regarding hydration behaviour.
4. Investigate combined use of recycled glass sand and recycled glass powder in concrete.
5. Quantify economic life-cycle assessment on recycled glass in concrete and compare with conventional concrete.

## References

- ADAWAY, M. & WANG, Y. 2015. Recycled glass as a partial replacement for fine aggregate in structural concrete -Effects on compressive strength. *Electronic Journal of Structural Engineering* 14, 116-122.
- AFSHINNIA, K. & RANGARAJU, P. R. 2015a. Influence of fineness of ground recycled glass on mitigation of alkali-silica reaction in mortars. *Construction and Building Materials*, 81, 257-267.
- AFSHINNIA, K. & RANGARAJU, P. R. 2015b. Mitigating alkali-silica reaction in concrete: Effectiveness of ground glass powder from recycled glass. *Transportation Research Record*, 2508, 65-72.
- AFSHINNIA, K. & RANGARAJU, P. R. 2016. Impact of combined use of ground glass powder and crushed glass aggregate on selected properties of Portland cement concrete. *Construction and Building Materials*, 117, 263-272.
- AGGARWAL, Y. & SIDDIQUE, R. 2014. Microstructure and properties of concrete using bottom ash and waste foundry sand as partial replacement of fine aggregates. *Construction and Building Materials*, 54, 210-223.
- AL-QATAN, M. T., KASIM, E. A. & AHMED, S. M. 2011. A Study on Producing New Mortar Containing Mixture of Waste Limestone and Glass. *Cement and Concrete Composites*, 23, 654-661.
- AL-ZUBAIDI, A. B. & TABBAKH, A. A. A.-. 2016. Recycling Glass Powder and its Use as Cement Mortar Applications. *International Journal of Scientific & Engineering Research*, 7, 555-564.
- ALI, E. E. & AL-TERSAWY, S. H. 2012. Recycled glass as a partial replacement for fine aggregate in self compacting concrete. *Construction and Building Materials*, 35, 785-791.
- ALIABDO, A. A., ABD ELMOATY, A. E. M. & ABOSHAMA, A. Y. 2016. Utilization of waste glass powder in the production of cement and concrete. *Construction and Building Materials*, 124, 866-877.
- ALY, M., HASHMI, M. S. J., OLABI, A. G., MESSEIRY, M., ABADIR, E. F. & HUSSAIN, A. I. 2012. Effect of Colloidal Nano-Silica on the Mechanical and Physical Behaviour of Waste-Glass Cement Mortar. *Materials & Design*, 33, 127-135.
- AMIN, M. & ABU EL-HASSAN, K. 2015. Effect of using different types of nano materials on mechanical properties of high strength concrete. *Construction and Building Materials*, 80, 116-124.
- AN, J., KIM, S. S., NAM, B. H. & DURHAM, S. A. 2017. Effect of aggregate mineralogy and concrete microstructure on thermal expansion and strength properties of concrete. *Applied Sciences (Switzerland)*, 7, 1307.
- ANDREW, R. M. 2018. Global CO2 emissions from cement production. *Earth System Science Data*, 10, 195-217.
- AS1012.2 2014. Methods of Testing Concrete, Methos 2: Preparing Concrete Mixes in the Laboratory. *Australian Standards AS 1012.2*.
- AS1012.3.1 2014. Methods of Testing Concrete, Methos 3.2: Determination of Properties Related to the Consistency of Concrete- Slump Test. *Australian Standard AS 1012.3.1*.
- AS1012.8.1 2014. Methods of Testing Concrete, Method 8.1: Method for Making and Curing Concrete-Compression and Indirect Tensile Test Specimens. *Australian Standards AS 1012.8.1*.
- AS1012.9.1 2014. Methods of Testing Concrete, Method 9: Compressive Strength Tests- Concrete, Mortar and Grout Specimens. *Australian Standards AS 1012.9.1*.
- AS1012.10 2000. Methods of Testing Concrete, Method 10 Determination of Indirect Tensile Strength of Concrete Cylinders ( 'Brazil' or Splitting Test). *Australian Standard AS 1012.10*.
- AS1012.11 2014. Methods of Testing Concrete, Method 11: Determination of The Modulus of Rupture. *Australian Standards AS 1012.11*.
- AS1012.12.1 2014. Method of Testing Concrete, Method 12.1: Determination of Mass Per Unit Volume of Hardened Concrete- Rapid Measuring Method. *Australian Standards AS 1012.12.1*.

- AS1141.11.1 2009. Methods for Sampling and Testing Aggregates, Method 11.1: Particle Size Distribution- Sieving Method. *Australian Standard AS 1141.11.1*.
- AS1141.35 2007. Methods for Sampling and Testing Aggregates, Method 35: Sugar. *Australian Standards AS 1141.35*.
- AS1141.60.1 2014. Methods for Sampling and Testing Aggregates, Method 60.1: Potential Alkali-Silica Reactivity- Accelerated Mortar Bar Method. *Australian Standard AS 1141.60.1*.
- AS1379 2007. Specification and supply of concrete. *Australian Standard AS 1379*.
- AS2350.12 2006. Methods of Testing Portland, Blended and Masonry Cements, Method 12 : Preparation of a Standard Mortar and Moulding of Specimens. *Australian Standard AS 2350.12*.
- AS2701 2001. Methods of Sampling and Testing Mortar for Masonry Construction, Section 5: Method for Determination of Water Retention. *Australian Standard AS 2701*.
- AS2758.1 2014. Aggregates and Rock for Engineering Purposes. *Australian Standards AS 2758.1*.
- AS3582.1 2016. Supplementary Cementitious Materials, Part 1: Fly Ash. *Australian Standards AS 3582.1*.
- AS3583.6 2018. Methods of Test for Supplementary Cementitious Materials, Method 6 : Determination of Relative Water Requirement and Strength Index. *Australian Standards AS 3583.6*.
- AS/NZS2350.11 2006. Methods of Testing Portland, Blended and Masonry Cements, Method 11: Compressive Strength. *Australian Standard AS/ NZS 2350.11*.
- ASHISH, D. K. 2018. Feasibility of waste marble powder in concrete as partial substitution of cement and sand amalgam for sustainable growth. *Journal of Building Engineering*, 15, 236-242.
- ASTM C618 2014. Standard Specification for Coal Fly Ash and Raw or Calcined Natural Pozzolan for Use in Concrete. *ASTM C 618*. West Conshohocken, PA, USA: ASTM International.
- ASTM C1202 2012. Standard Test Method for Electrical Indication of Concrete's Ability to Resist Chloride Ion Penetration. *ASTM C1202*. West Conshohocken, PA, USA: ASTM International.
- AUSLCI 2011. The Australian Life Cycle Inventory Database Initiative.
- AVOSA, N. L. 2016. *Use of Recycled Glass as Partial Cement Replacement in Concrete*. Bachelor of Engineering, James Cook University.
- BAJAD, M. N., MODHERA, C. D. & DESAI, A. K. 2011. Studies on Workability of Concrete Containing Waste Glass Powder as Pozzolana. *International Journal of Engineering Research and Technology* 4, 435-442.
- BASHEER, L., KROPP, J. & CLELAND, D. J. 2001. Assessment of the durability of concrete from its permeation properties: a review. *Construction and Building Materials*, 15, 93-103.
- BATAYNEH, M., MARIE, I. & ASI, I. 2007. Use of selected waste materials in concrete mixes. *Waste Management*, 27, 1870-1876.
- BHAT, V. V. & RAO, N. B. 2014. Influence of Glass Powder on the Properties of Concrete. *International Journal of Engineering Trends and Technology* 16, 196-199.
- BIGNOZZI, M. C., SACCANI, A., BARBIERI, L. & LANCELLOTTI, I. 2015. Glass waste as supplementary cementing materials: The effects of glass chemical composition. *Cement and Concrete Composites*, 55, 45-52.
- BOEHLKE, J. 2018. The Effects of Improper Garbage Disposal. Sciencing.
- BORHAN, T. M. 2012. Properties of Glass Concrete Reinforced with Short Basalt Fibre. *Materials & Design*, 42, 265-271.
- CARSANA, M., FRASSONI, M. & BERTOLINI, L. 2014. Comparison of ground waste glass with other supplementary cementitious materials. *Cement and Concrete Composites*, 45, 39-45.
- CEMENT CONCRETE & AGGREGATE AUSTRALIA, C. 2009. Chloride Resistance of Concrete.
- CEMENT CONCRETE & AGGREGATES AUSTRALIA, C. 2010. Sustainable Concrete Materials.
- CHEN, C., HABERT, G., BOUZIDI, Y., JULLIEN, A. & VENTURA, A. 2010. LCA allocation procedure used as an incitative method for waste recycling: An application to mineral additions in concrete. *Resources, Conservation & Recycling*, 54, 1231-1240.

- CHEN, C. H., HUANG, R., WU, J. K. & YANG, C. C. 2006. Waste E-glass particles used in cementitious mixtures. *Cement and Concrete Research*, 36, 449-456.
- CORINALDESI, V., GNAPPI, G., MORICONI, G. & MONTENERO, A. 2005. Reuse of ground waste glass as aggregate for mortars. *Waste Management*, 25, 197-201.
- CORINALDESI, V., NARDINOCCHI, A. & DONNINI, J. 2016. Reuse of recycled glass in mortar manufacturing. *European Journal of Environmental and Civil Engineering*, 20, s140-12.
- CRC, C. R. C. 2016. Water and Waste Management.
- DE CASTRO, S. & DE BRITO, J. 2013. Evaluation of the durability of concrete made with crushed glass aggregates. *Journal of Cleaner Production*, 41, 7-14.
- DEGIRMENCI, N., YILMAZ, A. & CAKIR, O. A. 2011. Utilization of waste glass as sand replacement in cement mortar. *Indian Journal of Engineering and Materials Sciences*, 18, 303-308.
- DHIR, R. K., DYER, T. D. & TANG, M. C. 2009. Alkali-silica reaction in concrete containing glass. *Materials and Structures/Materiaux et Constructions*, 42, 1451-1462.
- DHIRENDRA, P., R.K., Y. & R., C. 2012. Strength Characteristics of Pre Cast Concrete Blocks Incorporating Waste Glass Powder. *ISCA Journal of Engineering Sciences*, 1, 68-70.
- DU, H. & GAO, H. J. Pozzolanic reaction of glass powder and its influences on concrete. 23rd Australian Conference on the Mechanics of Structures and Materials (ACMSM23), 2014 Byron Bay, Australia. S.T. Smith (Ed.), 267-272.
- DU, H. & TAN, K. H. 2013. Use of waste glass as sand in mortar: Part II - Alkali-silica reaction and mitigation methods. *Cement and Concrete Composites*, 35, 109-117.
- DU, H. & TAN, K. H. 2014a. Concrete with recycled glass as fine aggregates. *ACI Materials Journal*, 111, 47-57.
- DU, H. & TAN, K. H. 2014b. Effect of particle size on alkali-silica reaction in recycled glass mortars. *Construction and Building Materials*, 66, 275-285.
- DU, H. & TAN, K. H. 2017. Properties of high volume glass powder concrete. *Cement and Concrete Composites*, 75, 22-29.
- DUMITRU, I., SONG, T., CAPRAR, V., BROOKS, P. & MOSS, J. Incorporation of recycled glass for durable concrete. 2010 2010. 323-327.
- ENVIRONMENTAL PROTECTION AGENCY, E. 2010. Municipal Solid Waste (MSW) in the United States: facts and figures for 2010. USA.
- ENVIRONMENTAL PROTECTION AGENCY, E. 2015. Advancing sustainable materials management: 2013 fact sheet. . USA.
- EPA, Q. 2006. Queensland Used Glass Sourcing Study for Queensland Environmental Protection Agency.
- FEDERATION, C. I. 2013. Industry Report 2013. Australia.
- FEIZ, R., AMMENBERG, J., BAAS, L., EKLUND, M., HELGSTRAND, A., MARSHALL, R., INDUSTRIELL, M., LINKÖPINGS, U., TEKNISKA, H. & INSTITUTIONEN FÖR EKONOMISK OCH INDUSTRIELL, U. 2015. Improving the CO<sub>2</sub> performance of cement, part I: utilizing life-cycle assessment and key performance indicators to assess development within the cement industry. *Journal of Cleaner Production*, 98, 272-281.
- FISCHER, G., RAJABIPOUR, F. & MARAGHECHI, H. 2010. Investigating the Alkali-Silica Reaction of Recycled Glass Aggregates in Concrete Materials. *Journal of Materials in Civil Engineering*, 22, 1201-1208.
- FLOWER, D. J. M. & SANJAYAN, J. G. 2007. Green house gas emissions due to concrete manufacture. *The International Journal of Life Cycle Assessment*, 12, 282-288.
- FORUM, C. E. 2017. What is Supplementary Cementitious Materials (SCMs).
- GARTNER, E. 2004. Industrially interesting approaches to "low-CO<sub>2</sub>" cements. *Cement and Concrete Research*, 34, 1489-1498.
- GAUTAM, S. P., SRIVASTAVA VIKAS AND AGARWAL V. C. 2012. Use of glass wastes as fine aggregate in concrete. *Journal of Academia and Industrial Research*, 1, 320-322.

- GERSEKOWSKI, T. N. 2014. *The Design of an Optimum Mix for Steel Fibre Reinforced Concrete Bored Piers*. Bachelor of Engineering, James Cook University.
- GUNALAN, V. & KANAPATHY, P. S. G. 2013. *Performance of Using Waste Glass Powder In Concrete As Replacement Of Cement* [Online]. [Accessed 12 2].
- HASANBEIGI, A., PRICE, L., LU, H. & LAN, W. 2010. Analysis of energy-efficiency opportunities for the cement industry in Shandong Province, China: A case study of 16 cement plants. *Energy*, 35, 3461-3473.
- HEIDRICH, C., HINCZAK, I. & RYAN, B. 2005. SCM's potential to lower Australia's greenhouse gas emission profile, Iron and steel slag product.: Australain Slag Association onference, Sydney.
- HOU, X., STRUBLE, L. J. & KIRKPATRICK, R. J. 2004. Formation of ASR gel and the roles of C-S-H and portlandite. *Cement and Concrete Research*, 34, 1683-1696.
- HUNAG, L.-J., WANG, S.-Y. & WANG, H.-Y. 2015. A study of the durability of recycled green building materials in lightweight aggregate concrete. *Construction and Building Materials*, 96, 353-359.
- IDIR, R., CYR, M. & TAGNIT-HAMOU, A. 2010. Use of fine glass as ASR inhibitor in glass aggregate mortars. *Construction and Building Materials*, 24, 1309-1312.
- ILANGOVARA, R., MAHENDRANA, N. & NAGAMANIB, K. 2008. Strength and Durability Properties of Concrete Containing Quarry Rock Dust as Fine Aggregate. *ARPN Journal of Engineering and Applied Science*, 3, 20-26.
- ISLAM, G. M. S., RAHMAN, M. H. & KAZI, N. 2017. Waste glass powder as partial replacement of cement for sustainable concrete practice. *International Journal of Sustainable Built Environment*, 6, 37-44.
- ISMAIL, Z. Z. & AL-HASHMI, E. A. 2009. Recycling of waste glass as a partial replacement for fine aggregate in concrete. *Waste Management*, 29, 655-659.
- ISO14040 2006. Environmental Management – Life Cycle Assessment- Principles and Framework. *British Standards Institution*,. London, UK.
- ISO14044 2006. Environmental Management – Life Cycle Assessment- Requirements and Guidelines. *British Standards Institution*. London, UK.
- JANI, Y., HOGLAND, W., LINNÉUNIVERSITETET, INSTITUTIONEN FÖR BIOLOGI OCH, M. & FAKULTETEN FÖR HÄLSO- OCH, L. 2014. Waste glass in the production of cement and concrete – A review. *Journal of Environmental Chemical Engineering*, 2, 1767-1775.
- JIANG, M., CHEN, X., RAJABIPOUR, F. & HENDRICKSON, C. T. 2014. Comparative Life Cycle Assessment of Conventional, Glass Powder, and Alkali-Activated Slag Concrete and Mortar. *Journal of Infrastructure Systems*, 20, 4014020.
- JIMÉNEZ, C., BARRA, M., JOSA, A. & VALLS, S. 2015. LCA of recycled and conventional concretes designed using the Equivalent Mortar Volume and classic methods. *Construction and Building Materials*, 84, 245-252.
- JIN, W. 1998. *Alkali-silica reaction in concrete with glass aggregate: a chemo-physico-mechanical approach*. Doctor of Philosophy, Columbia University.
- JIN, W., MEYER, C. & BAXTER, S. 2000. Glascrete- Concrete with Glass Aggregate. *American Concrete Institute Material Journal*, 97, 208-213.
- JOHNSTON, C. D. 1974. Waste glass of coarse aggregate for concrete. *Journal of Testing and Evaluation* 2, 344-350.
- KAMALI, M. & GHAREMANINEZHAD, A. 2015. Effect of glass powders on the mechanical and durability properties of cementitious materials. *Construction and Building Materials*, 98, 407-416.
- KAMALI, M. & GHAREMANINEZHAD, A. 2016. An investigation into the hydration and microstructure of cement pastes modified with glass powders. *Construction and Building Materials*, 112, 915-924.
- KAREN SCRIVENER, R. S., AND BARBARA LOTHENBACH 2016. *A practical guide to microstructural analysis of cementitious materials*, Taylor & Francis Group.

- KEARSLEY, E. 2006. Aggregates in concrete by Mark Alexander and Sidney Mindess : book shelf. *Civil Engineering = Siviele Ingenieurswese*, 14, 28.
- KHASREEN, M. M., BANFILL, P. F. G. & MENZIES, G. F. 2009. Life-cycle assessment and the environmental impact of buildings: A review. *Sustainability*, 1, 674-701.
- KHATIB, J. M., NEGIM, E. M., SOHL, H. S. & CHILESHE, N. 2012. Glass Powder Utilisation in Concrete Production. *European Journal of Applied Sciences*, 4, 173-176.
- KHMIRI, A., SAMET, B. & CHAABOUNI, M. 2012. Assessment of the waste glass powder pozzolanic activity by different methods. *IJRRAS*, 10, 322-328.
- KIM, J., YI, C. & ZI, G. 2015. Waste glass sludge as a partial cement replacement in mortar. *Construction and Building Materials*, 75, 242-246.
- KISACIK, I. E. 2002. *Using Glass in Concrete, BS Thesis, Osmangazi University*. Bachelor of Science, Osmangazi University.
- LAM, C. S., POON, C. S. & CHAN, D. 2007. Enhancing the performance of pre-cast concrete blocks by incorporating waste glass – ASR consideration. *Cement and Concrete Composites*, 29, 616-625.
- LANDFIELD, A. H. & KARRA, V. 2000. Life cycle assessment of a rock crusher. *Resources, Conservation & Recycling*, 28, 207-217.
- LAWANIA, K., SARKER, P. & BISWAS, W. 2015. Global warming implications of the use of by-products and recycled materials in Western Australia's housing sector. *Materials*, 8, 6909-6925.
- LEA, F. M. & HEWLETT, P. C. 1998. *Lea's chemistry of cement and concrete*, London;New York;, Arnold.
- LEE, G., LING, T.-C., WONG, Y.-L. & POON, C.-S. 2011. Effects of crushed glass cullet sizes, casting methods and pozzolanic materials on ASR of concrete blocks. *Construction and Building Materials*, 25, 2611-2618.
- LEE, G., POON, C. S., WONG, Y. L. & LING, T. C. 2013. Effects of recycled fine glass aggregates on the properties of dry-mixed concrete blocks. *Construction and Building Materials*, 38, 638-643.
- LIMBACHIYA, M. C. 2009. Bulk engineering and durability properties of washed glass sand concrete. *Construction and Building Materials*, 23, 1078-1083.
- LING, T.-C. & POON, C.-S. 2011. Properties of architectural mortar prepared with recycled glass with different particle sizes. *Materials and Design*, 32, 2675-2684.
- LING, T.-C. & POON, C.-S. 2012. A comparative study on the feasible use of recycled beverage and CRT funnel glass as fine aggregate in cement mortar. *Journal of Cleaner Production*, 29-30, 46-52.
- LING, T.-C. & POON, C.-S. 2013. Effects of particle size of treated CRT funnel glass on properties of cement mortar. *Materials and Structures*, 46, 25-34.
- LING, T.-C., POON, C.-S. & KOU, S.-C. 2011. Feasibility of using recycled glass in architectural cement mortars. *Cement and Concrete Composites*, 33, 848-854.
- LU, J.-X., DUAN, Z.-H. & POON, C. S. 2017. Fresh properties of cement pastes or mortars incorporating waste glass powder and cullet. *Construction and Building Materials*, 131, 793-799.
- LU, J.-X. & POON, C. S. 2018. Use of waste glass in alkali activated cement mortar. *Construction and Building Materials*, 160, 399-407.
- MALIK, M. I., BASHIR, M., AHMAD, S., TARIQ, T. & CHOWDHARY, U. 2013. Study of concrete involving use of waste glass as partial replacement of fine aggregates. *IOSR Journal of Engineering (IOSRJEN)*, 3, 08-13.
- MARDANI-AGHABAGLOU, A., ANDIÇ-ÇAKIR, Ö. & RAMYAR, K. 2013. Freeze-thaw resistance and transport properties of high-volume fly ash roller compacted concrete designed by maximum density method. *Cement and Concrete Composites*, 37, 259-266.
- MARDANI-AGHABAGLOU, A., TUYAN, M. & RAMYAR, K. 2015. Mechanical and durability performance of concrete incorporating fine recycled concrete and glass aggregates. *Materials and Structures*, 48, 2629-2640.

- MATOS, A. M. & SOUSA-COUTINHO, J. 2012. Durability of mortar using waste glass powder as cement replacement. *Construction and Building Materials*, 36, 205-215.
- MEHTA, P. K. 1987. Natural Pozzolans: Supplementary Cementing Materials in Concrete. *CANMET Special Publication*, 86, 1-33.
- METWALLY, I. M. 2007. Investigations on the Performance of Concrete Made with Blended Finely Milled Waste Glass. *Advances in Structural Engineering*, 10, 47-53.
- MIRZAHOSSEINI, M. & RIDING, K. A. 2014. Effect of curing temperature and glass type on the pozzolanic reactivity of glass powder. *Cement and Concrete Research*, 58, 103-111.
- MOHAMMADI, J. & SOUTH, W. 2017. Life cycle assessment (LCA) of benchmark concrete products in Australia. *The International Journal of Life Cycle Assessment*, 22, 1588-1608.
- MOHAMMADINIA, A., WONG, Y. C., ARULRAJAH, A. & HORPIBULSUK, S. 2019. Strength evaluation of utilizing recycled plastic waste and recycled crushed glass in concrete footpaths. *Construction and Building Materials*, 197, 489-496.
- MUHAMMAD NAZRIN AKMAL, A. Z. M., K.; MAT YAHAYA, F.; MOHD HANAFI, H.; AND NUR AZZIMAH, Z. Utilization of fly ash as partial sand replacement in oil palm shell lightweight aggregate concrete. 2017 2017. 12003.
- NAPOLANO, L., MENNA, C., GRAZIANO, S. F., ASPRONE, D., D'AMORE, M., DE GENNARO, R. & DONDI, M. 2016. Environmental life cycle assessment of lightweight concrete to support recycled materials selection for sustainable design. *Construction and Building Materials*, 119, 370-384.
- NASSAR, R.-U.-D. & SOROUSHIAN, P. 2011. Field investigation of concrete incorporating milled waste glass. *Journal of Solid Waste Technology and Management*, 37, 307-319.
- NASSAR, R.-U.-D. & SOROUSHIAN, P. 2012. Strength and durability of recycled aggregate concrete containing milled glass as partial replacement for cement. *Construction and Building Materials*, 29, 368-377.
- NATIONAL ENVIRONMENTAL AGENCY, N. 2017. Waste Statistics and Overall Recycling. In: MANAGEMENT, W. (ed.). Singapore.
- NRRS, N. R. A. R. S. 2017. Paper packaging, Glass containers, Steel Cans and Aluminum Packaging.
- NWAUBANI, S. O. & POUTOS, K. I. 2013. The Influence of Waste Glass Powder Fineness on the Properties of Cement Mortars. *International Journal of Application or Innovation in Engineering & Management*, 2, 110-116.
- P.TURGUT & YAHLIZADE, E. S. 2009. Research into Concrete Blocks with Waste Glass. *International Journal of Civil and Environmental Engineering*, 3, 186-192.
- PARK, S.-B. & LEE, B.-C. 2004. Studies on expansion properties in mortar containing waste glass and fibers. *Cement and Concrete Research*, 34, 1145-1152.
- PATIL, D. M. & SANGLE, D. K. K. 2013. Experimental Investigation of Waste Glass Powder as Partial Replacement of Cement in Concrete. *International Journal of Advanced Technology in Civil Engineering*, 2, 112-117.
- PAUZI, N. N. M., JAMIL, M., HAMID, R., ABDIN, A. Z. & ZAIN, M. F. M. 2019. Influence of spherical and crushed waste Cathode-Ray Tube (CRT) glass on lead (Pb) leaching and mechanical properties of concrete. *Journal of Building Engineering*, 21, 421-428.
- PENACHO, P., BRITO, J. D. & ROSÁRIO VEIGA, M. 2014. Physico-mechanical and performance characterization of mortars incorporating fine glass waste aggregate. *Cement and Concrete Composites*, 50, 47-59.
- PEREIRA DE OLIVEIRA, L. A., CASTRO-GOMES, J. P. & SANTOS, P. Mechanical and Durability Properties of Concrete with Ground Waste Glass Sand. 11 DBMC International Conference on Durability of Building Materials and Components, 2008 Istanbul, Turkey.
- PETEK GURSEL, A., MASANET, E., HORVATH, A. & STADEL, A. 2014. Life-cycle inventory analysis of concrete production: A critical review. *Cement and Concrete Composites*, 51, 38-48.
- PIKE, R. G. & HUBBARD, D. 1957. Physicochemical studies of the destructive alkali-aggregate reaction in concrete. *Journal of Research of the National Bureau of Standards*, 59, 127-132.

- PILEGIS, M., GARDNER, D. & LARK, R. 2016. An investigation into the use of manufactured sand as a 100% replacement for fine aggregate in concrete. *Materials*, 9, 440.
- POLLEY, C., CRUZ, R. V. D. L. & CRAMER, S. M. 1998. Potential for Using Waste Glass in Portland Cement Concrete. *Journal of Materials in Civil Engineering*, 10, 210-219.
- PREZZI, M., MONTEIRO, P. J. M. & SPOSITO, G. 1997. The Alkali-Silica Reaction, Part I : Use of Double-Layer Theory to Explain Behaviour of Reaction-Product Gels. *American Concrete Institute Material Journal*, 94, 10-17.
- RAHMA, A., EL NABER, N. & ISSA ISMAIL, S. 2017. Effect of glass powder on the compression strength and the workability of concrete. *Cogent Engineering*, 4.
- RAJABIPOUR, F., GIANNINI, E., DUNANT, C., IDEKER, J. H. & THOMAS, M. D. A. 2015. Alkali-silica reaction: Current understanding of the reaction mechanisms and the knowledge gaps. *Cement and Concrete Research*, 76, 130-146.
- RITCHIE, M. 2016. States of Waste 2016 - Current and future Australian Trends. MRA Consulting Group.
- RUPASINGLE, M., NICOLAS, R. S., MENDIS, P. & SOFI, M. 2014. Analysing The Pozzolanic Reactivity of Nano-Silica in Cement Paste. *23rd Australian Conference on the Mechanics of Structures and Materials (ACMSM23)*, 131-136.
- SACCANI, A. & BIGNOZZI, M. C. 2010. ASR expansion behavior of recycled glass fine aggregates in concrete. *Cement and Concrete Research*, 40, 531-536.
- SAHA, A. K., KHAN, M. N. N., SARKER, P. K., SHAIKH, F. A. & PRAMANIK, A. 2018. The ASR mechanism of reactive aggregates in concrete and its mitigation by fly ash: A critical review. *Construction and Building Materials*, 171, 743-758.
- SCHWARZ, N., CAM, H. & NEITHALATH, N. 2008. Influence of a fine glass powder on the durability characteristics of concrete and its comparison to fly ash. *Cement and Concrete Composites*, 30, 486-496.
- SCMIDT, A. & SAIA, W. H. F. 1963. Alkali-aggregate reaction tests on glass used for exposed aggregate wall panel work. *Journal of the American Concrete Institute*, 60, 1235-1236.
- SERPA, D., SANTOS SILVA, A., DE BRITO, J., PONTES, J. & SOARES, D. 2013a. ASR of mortars containing glass. *Construction and Building Materials*, 47, 489-495.
- SERPA, D., SILVA, A. S., SOARES, D., SANTOS, M. B. & BRITO, J. D. 2013b. Behaviour of glass in cement-based materials: Its role on ASR. *Materials Science Forum*, 730-732, 415-420.
- SHAO, Y., LEFORT, T., MORAS, S. & RODRIGUEZ, D. 2000. Studies on concrete containing ground waste glass. *Cement and Concrete Research*, 30, 91-100.
- SHARIFI, Y., HOUSHIAR, M. & AGHEBATI, B. 2013. Recycled glass replacement as fine aggregate in self-compacting concrete. *Frontiers of Structural and Civil Engineering*, 7, 419-428.
- SHAYAN, A. & XU, A. 2004. Value-added utilisation of waste glass in concrete. *Cement and Concrete Research*, 34, 81-89.
- SHAYAN, A. & XU, A. 2006. Performance of glass powder as a pozzolanic material in concrete: A field trial on concrete slabs. *Cement and Concrete Research*, 36, 457-468.
- SHI, C., WU, Y., RIEFLER, C. & WANG, H. 2005. Characteristics and pozzolanic reactivity of glass powders. *Cement and Concrete Research*, 35, 987-993.
- SHI, C. & ZHENG, K. 2007. A review on the use of waste glasses in the production of cement and concrete. *Resources, Conservation & Recycling*, 52, 234-247.
- SHRUTHI, S., CHANDRAKALA, S. & NARAYANA, G. 2015. Partial Replacement of Cement in Concrete Using Waste Glass Powder and M-Sand as Fine Aggregate. *IJRET: International Journal of Research in Engineering and Technology*, 4, 133-138.
- SIVAKUGAN, N., GNANENDRAN, C. T., TULADHAR, R. & KANNAN, M. B. 2017. *Civil Engineering Materials*, Cengage Learning.
- SOBOLEV, K., TÜRKER, P., SOBOLEVA, S. & ISCIOGLU, G. 2007. Utilization of waste glass in ECO-cement: Strength properties and microstructural observations. *Waste Management*, 27, 971-976.

- SOLIMAN, N. A. & TAGNIT-HAMOU, A. 2016. Development of ultra-high-performance concrete using glass powder - Towards ecofriendly concrete. *Construction and Building Materials* 125, 600-612.
- SPRINCE, A., KORJAKINS, A. & PAKRASTINSH, L. Creep Behaviour of Concrete with Glass Waste Microfiller. Proceeding of the 8th International Scientific and Practical Conference, Environment.Technology. Resources, 2011. 125-131.
- STANDARDS, E. 2012. Fly ash for Concrete. Definition, Specifications and Conformity Criteria. *BS EN 450-1*.
- SURESH, D. & NAGARAJU, K. 2015. Ground Granulated Blast Slag (GGBS) in Concrete – A Review. *Ground Granulated Blast Slag (GGBS) in Concrete – A Review*, 12, 76-82.
- TAHA, B. & NOUNU, G. 2008. Properties of concrete contains mixed colour waste recycled glass as sand and cement replacement. *Construction and Building Materials*, 22, 713-720.
- TAHA, B. & NOUNU, G. 2009. Utilizing Waste Recycled Glass as Sand/Cement Replacement in Concrete. *Journal of Materials in Civil Engineering*, 21, 709-721.
- TAMANNA, N., SUTAN, N. M. & TULADHAR, R. The effect of waste glass powder on microstructural behaviour when used a partial cement replacement. 5th International fib Congress, 7-11 October 2018 2018 Melbourne, VIC, Australia.
- TAMANNA, N., SUTAN, N. M., TULADHAR, R., TEO, D. C. L. & YAKUB, I. 2016. Pozzolanic properties of glass powder in cement paste. *Journal of Civil Engineering, Science and Technology*, 7, 75-81.
- TAMANNA, N., TULADHAR, R., AVOSA, N. & SIVAKUGAN, S. 2017. The effect of using waste glass powder as cement replacement in concrete. *the 28th Biennial Conference of the Concrete Institute of Australia*. Adelaide, SA, Australia.
- TAN, K. H. & DU, H. 2013. Use of waste glass as sand in mortar: Part I – Fresh, mechanical and durability properties. *Cement and Concrete Composites*, 35, 109-117.
- TAYLOR, H. F. W. 1997. *Cement Chemistry*, Thomas Telford, London.
- TEJASWI, S. S., RAO, R. C., VIDYA, B. & RENUKA, J. 2015. Experimental Investigation of Waste Glass Powder as Partial Replacement of Cement and Sand in Concrete. *IUP Journal of Structural Engineering*, 8, 14.
- TERRO, M. J. 2006. Properties of concrete made with recycled crushed glass at elevated temperatures. *Building and Environment*, 41, 633-639.
- THOMAS, M. 2007. Optimizing the use of Fly Ash in Concrete. Portland Cement Association.
- TOPÇU, İ. B. & CANBAZ, M. 2004. Properties of concrete containing waste glass. *Cement and Concrete Research*, 34, 267-274.
- TORRES, A., BRANDT, J., LEAR, K. & LIU, J. G. 2017. A looming tragedy of the sand commons. *Science*, 357, 970-971.
- TUNCAN, M., KARASU, B. & YALCIN, M. The suitability for Using Glass and Fly ash in Portland Cement Concrete. The Proceedings of the Eleventh International Offshore and Polar Engineering Conference (ISOPE 2001), 2001 Stavanger, Norway. 146-152.
- TYLOR, H. F. W. 1997. *Cement Chemistry*, Thomas Telford.
- VAITKEVIČIUS, V., ŠERELIS, E. & HILBIG, H. 2014. The effect of glass powder on the microstructure of ultra high performance concrete. *Construction and Building Materials*, 68, 102-109.
- VICTORIA, S. 2014. *Fact Sheet- Market Summary-Recycled Glass* [Online]. [Accessed].
- VIEIRA, D. R., CALMON, J. L. & COELHO, F. Z. 2016. Life cycle assessment (LCA) applied to the manufacturing of common and ecological concrete: A review. *Construction and Building Materials*, 124, 656-666.
- VIJAYKUMAR, D. G., VISHALINY, M. H. & GOVINDARAJULU, D. D. 2013. Studies on Glass Powder as Partial Replacement of Cement in concrete production. *International Journal of Emerging Technology and Advanced Engineering*, 3, 153-156.
- WANG, H.-Y. 2009. A study of the effects of LCD glass sand on the properties of concrete. *Waste Management*, 29, 335-341.

- WANG, H.-Y., ZENG, H.-H. & WU, J.-Y. 2014. A study on the macro and micro properties of concrete with LCD glass. *Construction and Building Materials*, 50, 664-670.
- WANG, W.-C., WANG, H.-Y., CHEN, B.-T. & CHOU, H.-C. 2016. A study of the engineering properties of alkali-activated waste glass material (AAWGM). *Construction and Building Materials*, 112, 962-969.
- WORLD BUSINESS COUNCIL FOR SUSTAINABLE DEVELOPMENT, W. 2006. The Cement Sustainability Initiatives. *Recycling Concrete*.
- YILMAZ, B. & OLGUN, A. 2008. Studies on cement and mortar containing low-calcium fly ash, limestone, and dolomitic limestone. *Cement and Concrete Composites*, 30, 194-201.
- YIN, S. 2015. *Development of Recycled Polypropylene Plastic Fibres to Reinforce Concrete*. Doctor of Philosophy, James Cook University.
- YU, X., TAO, ZHONG, SONG, TIAN-YI, AND PAN, ZHU 2016. Performance of concrete made with steel slag and waste glass. *Construction and Building Materials*, 114, 737-746.
- YUKSEL, C., AHARI, R. S., AHARI, B. A. & RAMYAR, K. 2013. Evaluation of three test methods for determining the alkali-silica reactivity of glass aggregate. *Cement and Concrete Composites*, 38, 57-64.
- ZAPAŁA-SŁAWETA, J. 2017. The effect of meta-halloysite on alkali-aggregate reaction in concrete. *Materials and Structures*, 50, 1-12.
- ZHAO, H., POON, C. S. & LING, T. C. 2013. Utilizing recycled cathode ray tube funnel glass sand as river sand replacement in the high-density concrete. *Journal of Cleaner Production*, 51, 184-190.